

The background of the cover is a watercolor illustration. It features several large, stylized cells with blue and red centers and radiating blue lines, resembling bacteria or immune cells. There are also pink, multi-lobed shapes that look like flowers or larger cells. Yellow, rod-like structures are scattered throughout, and blue, wavy lines represent tissue layers or membranes. Small, three-lobed blue shapes are also present.

KARIN
DIJKMAN

*Exploring protective and
pathogenic immune responses
in the non-human primate
model of tuberculosis*

Exploring protective and pathogenic immune responses in the non-human primate model of tuberculosis

Karin Dijkman

Exploring protective and pathogenic immune responses in the non-human primate model of tuberculosis

Identificatie van beschermende en pathogene immuun responsen in het niet-humane primaten tuberculose model

(met een samenvatting in het Nederlands)

Proefschrift

ter verkrijging van de graad van doctor aan de Universiteit Utrecht op gezag van de rector magnificus, prof.dr. H.R.B.M. Kummeling, ingevolge het besluit van het college voor promoties

in het openbaar te verdedigen op
maandag 9 november 2020 des morgens te 11.00 uur

door

Karin Dijkman

geboren op 5 juli 1987 te Doetinchem

Promotor:

Prof. R. Bontrop

Copromotor

Dr. F.A.W. Verreck

Assessment Committee

Prof. R. van Crevel

Prof. C.A.C.M. van Els

Prof. D. Kaushal

Prof. T.H.M. Ottenhoff

Prof. V.P.M.G. Rutten

*“Courage is doing what you’re afraid to do.
There can be no courage unless you’re scared.”*

Eddie Rickenbacker

The research described in this thesis was performed at the TB research group, part of the department of Parasitology at the Biomedical Primate Research Centre, Rijswijk, the Netherlands.

Financial support for publication of this thesis was provided by the Biomedical Primate Research Centre and U-CyTech.

Cover design & chapter illustrations:	A. Straathof, www.alettestraathof.com
Lay-out:	F. van Hassel
Printed by:	Ridderprint BV
ISBN:	978-94-6375-871-0

© Karin Dijkman, 2020. No parts of this thesis may be reproduced.

Table of Contents

Chapter 1	Introduction	9
Chapter 2	Disparate tuberculosis disease development in macaque species is associated with innate immunity	45
Chapter 3	Prevention of tuberculosis infection and disease by local BCG in repeatedly exposed rhesus macaques	83
Chapter 4	Pulmonary vaccination with <i>M.tuberculosis</i> -derived MTBVAC induces immune responses correlating with prevention of TB infection	123
Chapter 5	Systemic and pulmonary C1q as biomarker of progressive disease in experimental non-human primate tuberculosis	153
Chapter 6	General discussion and future perspectives	177
Chapter 7	Appendices	197
	Abbreviations	198
	Nederlandse samenvatting	200
	Dankwoord	204
	Curriculum vitae	208
	List of publications	210





Introduction

Introduction

Tuberculosis (TB) is a disease as old as time. Literally. The ancient Egyptians, who invented the sundial, the first device to tell time, were also one of the first people known to suffer from tuberculosis. Molecular analysis of the earliest known Egyptian mummy has identified traces of deoxyribonucleic acid (DNA) originating from tuberculosis bacteria in various tissues¹, and skeletons of excavated mummies exhibit signs of tuberculosis of the spine (Pott's disease)². Throughout human history, tuberculosis has gone by many names, including the tongue-twister "pthisis", the sinister "white death" and, in Dutch, "de tering". In the 19th century it was even known as the "romantics disease", as it resulted in a pale complexion, much sought after by high society at that time. Regardless of which name it carries, over the centuries, tuberculosis has contributed to more deaths than any other infectious disease in history, with over 1 billion casualties in the last 200 years alone³. Even in our current age of advanced medical care and antibiotics, tuberculosis continues to kill approximately 1.5 million people annually⁴. This makes TB the deadliest of infectious diseases, killing a person about every 20 seconds. Additionally, roughly 10 million people annually develop active tuberculosis disease⁴. The lack of an effective vaccine, shortage of accurate diagnostics and rise of drug-resistant strains are factors that hamper the elimination of TB. Attempts to mitigate these problems are complicated by knowledge gaps pertaining to protective immunity, disease pathogenesis and diagnosis. This thesis, by modeling and investigating TB in non-human primates (NHPs), aims to address several of these gaps in our knowledge.

1. Tuberculosis

1.1 Causative Agents

1.1.1 *Mycobacterium tuberculosis*

TB is primarily caused by the pathogen *Mycobacterium tuberculosis* (*Mtb*), member of the *Mycobacterium tuberculosis* complex (MTBC), a group of slow growing, closely related bacilli, and of the larger *Mycobacterium* genus. Another well-known member of this genus is *Mycobacterium leprae*, the causative agent of leprosy. Although *M. tuberculosis* had been causing disease for centuries, the pathogen was only discovered in 1882 by Dr. Robert Koch. *Mtb* bacilli are rod-shaped, 2-4 μm in length, acid-fast and impervious to Gram staining.

Based on genomic differences, *Mycobacterium tuberculosis* can be subdivided in distinct lineages, which differ in aspects such as virulence and transmission. To date, 5 different lineages of *Mtb* are recognized; L1 to L4 and L7. Lineage 5 and 6 are used to subdivide *Mycobacterium africanum*, another human-adapted member of the MTBC. L2, 3 and 4, in which a genomic region called TbD1 is deleted, are referred to as evolutionary "modern" *Mtb*, as they diversified more recently compared to the



other lineages, which, accordingly, are referred to as “ancient”⁵. Of the different lineages, L2 and L4 are geographically the most widespread, with L2 being most prevalent in (east) Asia and Russia and L4 in Europe and the Americas. In contrast, L1, L3 and L7 are more restricted in distribution; L1 and L3 are mostly found in countries around the Indian Ocean and L7 is typically found in Ethiopia only⁶. Although epidemiological data is conflicting, *in vitro* studies have found differences between lineages that may influence disease presentation and spread (reviewed by Coscolla and co-workers⁷). For instance, *in vitro* infection with modern lineages (L2, L3 & L4) generally induced a lower inflammatory response compared to ancient lineages, and strains from L2 and L4 specifically showed a high replication potential *in vitro* and in mice, potentially underlying to more rapid disease progression and widespread distribution of these lineages^{8,9}. *Mtb* lineages can be subdivided further in numerous strains and clinical isolates.

A major concern for global health is the increase in tuberculosis caused by drug-resistant *Mtb* strains (DR-TB). Multidrug resistant (MDR) strains (resistant to isoniazid and rifampicin) and even extensively drug resistant (XDR) strains (exhibiting an additional resistance to any fluoroquinolone and at least one of the second-line, injectable drugs) are becoming more and more prevalent, particularly in Eastern Europe and Central Asia^{10,11}. The development of drug resistance is caused by a variety of factors, including prior anti-TB drug treatment, patient social factors and strain-inherent factors^{7,12}. MDR and XDR-TB present major challenges in treatment, as second-line TB drugs are generally less effective and present with major side effects (**Box 1**).

1.1.2 Other mycobacteria

Besides *Mycobacterium tuberculosis*, all other members of the MTBC and several non-tuberculous mycobacteria (NTM) can also cause tuberculosis disease in humans. Next to *Mtb*, tuberculosis in human often associates with *Mycobacterium africanum*, which can be responsible for up to 50% of TB cases in some West-African countries¹⁵.

While *Mycobacterium tuberculosis* and *Mycobacterium africanum* are predominantly found in humans, the other members of the MTBC are primarily present in animals or environmental sources (soil, water)¹⁶. They can be pathogenic in a wide range of animals, including voles, seals and cattle. Although these mycobacteria have evolved to propagate in animals, cases of human tuberculosis caused by these animal-adapted members of the MTBC have been reported¹⁷. *Mycobacterium bovis* especially, a pathogen that predominantly infects cattle, is responsible for up to approximately 25% of tuberculosis cases in certain African countries¹⁸. Close contact with infected animals or consumption of unpasteurized milk transmits the pathogen from animal to man.

Many other bacteria of the *Mycobacterium* genus can cause tuberculosis disease, especially in immune compromised individuals. Members of the *Mycobacterium avium* complex (MAC), a group of related bacteria that are commonly found in birds and cattle, can cause (pulmonary) tuberculosis disease in susceptible hosts¹⁹. The

Box 1. Tuberculosis treatment. Brief summary of the WHO guidelines for the treatment of drug-susceptible and MDR-TB and their major side effects^{13,14}.

WHO recommended treatment for drug-susceptible TB

	Duration	Adverse effects
Isoniazid	6 months	Hepatotoxicity, peripheral neuropathy, CNS toxicity
Rifampicin	6 months	Gastrointestinal toxicity
Pyrazinamide	8 weeks	Hepatotoxicity
Ethambutol	8 weeks	Ocular toxicity

WHO recommended treatment for MDR-TB

A 12-24 months regimen consisting of a combination of drugs listed below, depending on *Mtb* drug susceptibility and patient condition.

Group A: include all three medicines	Adverse effects
levofloxacin <i>OR</i> moxifloxacin	QT-prolongation
bedaquiline	Hepatitis, joint pain, headache
linezolid	Ocular toxicity, peripheral neuropathy, myelosuppression
Group B: Add one or both medicines	
clofazimine	QT-prolongation
cycloserine <i>OR</i> terizidone	Mental health issues, such as psychosis, depression or anxiety
Group C: Add to complete the regimen and when medicines from Groups A and B cannot be used	
ethambutol	Ocular toxicity
delamanid	Nausea, vomiting, dizziness, QT prolongation
pyrazinamide	Hepatotoxicity
imipenem–cilastatin <i>OR</i> meropenem	Seizures
amikacin <i>OR</i> streptomycin	Nephrotoxicity, ototoxicity
ethionamide <i>OR</i> prothionamide	Nausea, vomiting, hyperthyroidism
p-aminosalicylic acid	Gastrointestinal toxicity



aquatic *Mycobacterium marinum* has been described to cause granulomatous skin lesions as well as tenosynovitis in man²⁰, and is the leading causative agent of extrapulmonary disease among the NTM²¹. Animal-adapted species rarely transmit from man to man and are most commonly acquired from environmental sources.

1.2 Tuberculosis transmission

Typically, infection with *Mtb* is acquired through the inhalation of pathogen-containing aerosols, which are expelled by individuals with pulmonary tuberculosis. By coughing, shouting, sneezing or singing, *Mtb* containing respiratory secretions are dissociated from the airway and discharged from the lungs. Both patients with and without detectable *Mtb* in their sputum can generate these infectious aerosols²²⁻²⁴. Tuberculosis transmission is typically thought to occur in a household setting, where people often live closely together, but recent research has shown that the majority of infections are acquired outside of one's household²⁵. Locations with poor ventilation and a high density of individuals, such as schools, prisons and public transportation, make for ideal foci for tuberculosis spread²⁶⁻²⁸.

1.3 Tuberculosis disease presentation

After inhalation of tuberculosis-causing bacilli, several outcomes can occur, ranging from complete clearance of the infection to the development of active tuberculosis disease.

1.3.1 *M. tuberculosis* clearance

Inhalation of *Mtb* bacteria does not always result in successful infection. It is possible for an exposed individual to clear the infection, by means of an innate or adaptive immune response. Epidemiological studies in high TB burden areas have described individuals that remain persistently negative on tuberculosis diagnostic tests²⁹⁻³², and thus appear to be resistant to *Mtb* infection. One might argue that these individuals, termed resisters, despite residing in a high burden area, might actually have never encountered *Mtb*. However, when profiling the immune responses of one of these cohorts in depth, these resisters were found to possess an adaptive *Mtb*-specific antibody response, indicating that these individuals were indeed exposed to *Mtb*³³. Additionally, it remains possible that *Mtb* could also be eliminated by cells of the innate immune system before the acquisition of an adaptive immune response³⁴. There is currently no reliable method to unambiguously identify resister individuals, as all available diagnostic tools either measure the adaptive immune response against *Mtb* or rely on detection of the pathogen in bodily fluids (see section **3. Diagnostics**).

When successful infection does occur, tuberculosis is typically divided in two clinically defined states; active (ATB, symptomatic, potentially transmissible) or latent TB infection (LTBI, a-symptomatic, non-transmissible)³⁵.

1.3.2 Latent TB infection

After establishment of infection, the majority of infected individuals go on to develop latent tuberculosis, whereby the pathogen is successfully contained by the immune system³⁶. By forming a structure called the granuloma, the pathogen is walled off from the surrounding, healthy tissue. The formation of a granuloma (or tubercle) is one of the defining characteristics of TB infection (**Box 2**). The World Health Organization (WHO) defines latent tuberculosis infection as a state of persistent immune response stimulation with *Mtb* antigens in absence of clinical symptoms of active TB. Despite this absence of symptoms, the latently infected individual does harbor replication-competent bacteria and is therefore at risk of developing active tuberculosis at any time (reactivation TB). Individuals with a latent tuberculosis can carry the infection unnoticed for decades³⁷.

Under the right circumstances, a latent TB infection can reactivate and progress to active disease. By mathematical modelling it has been estimated that approximately a quarter of the world's population carries a latent *Mtb* infection and is, thus, at risk of reactivation³⁸. This vast, persisting reservoir of recurring disease complicates the elimination of TB. Risk factors of reactivation of disease include, but are not limited to, infection with human immunodeficiency virus (HIV), silicosis, and treatment with immunosuppressive drugs such as tumor necrosis factor-alpha (TNF α)-antagonistic antibodies³⁹⁻⁴¹. Although there is evidence that LTBI protects from active tuberculosis disease upon subsequent exposure^{42,43}, this protection is not complete. Individuals with a latent TB infection are still at risk of acquiring a secondary TB infection, which may progress to active tuberculosis disease and be falsely labelled as reactivating TB⁴⁴.

Box 2. The granuloma

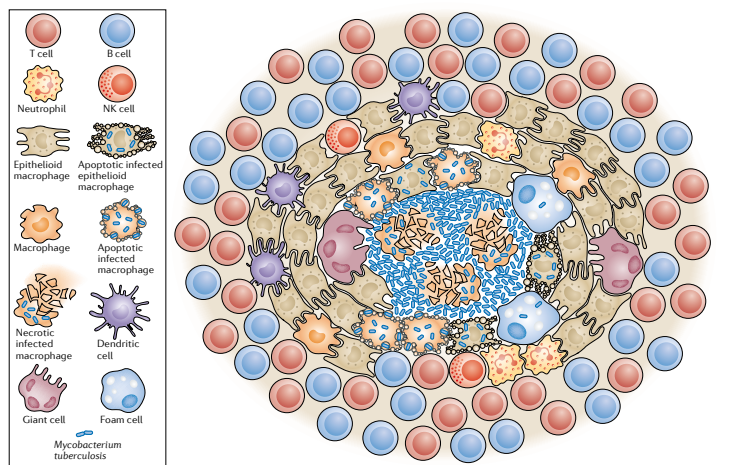


Image reproduced with permission from: Ramakrishnan, Nat. Rev. Immunology 201245



A granuloma is a structure consisting of immune cells which aggregate in an organized fashion, and, while not unique to tuberculosis, plays a very important role in the pathogenesis of *Mtb* infection. Historically, the granuloma was thought to be a solely host-protective response, “walling-of” the pathogen from healthy unaffected tissue. It has become clear, however, that, while it is possible for a granuloma to become sterile, granuloma formation might under certain conditions actually benefit the pathogen, providing a niche for bacterial replication^{45,46}.

After inhalation, *Mtb* is taken up by resident alveolar macrophages and translocates to the lung parenchyma. *Mtb* escapes elimination by interfering with the microbicidal effector functions of these cells and starts to replicate intracellularly, ultimately resulting in death of the infected cell. Newly recruited macrophages aggregate around the dying cell, phagocytose *Mtb*-infected cellular debris and become infected themselves. The dying macrophages produce chemokines, recruiting neutrophils, T-cells and other immune cells to the developing granuloma. While the granuloma matures, macrophages can differentiate into epithelioid cells, which are capable of forming a cuff by tight interactions with neighboring cells, further containing the bacilli, but also preventing T-cells from reaching *Mtb* infected macrophages. Eventually, the center of the granuloma starts to undergo caseous necrosis, resulting in the formation of caseum, a cheese-like material consisting of bacteria and cellular debris.

There is a large heterogeneity in granuloma fate, dependent on a multitude of factors such as cellular composition, bacterial load and host condition⁴⁷. For instance, a caseous granuloma can become calcified, typically indicative of a healing response. On the other hand, failure to control bacterial replication can lead to liquefaction of the caseum and the destruction of lung tissue, a phenomenon known as cavitation. When cavitating granulomas breach the airways, the *Mtb* infection is classified as open tuberculosis and the disease becomes contagious (see **1.2 Tuberculosis transmission**). The diversity in granuloma manifestation can be seen even within a single infected individual⁴⁸.

Granuloma formation involves complex interactions between pathogen and host, which have not yet been fully elucidated. A more complete understanding of the processes involved in beneficial and detrimental granuloma outcome could inform rational design of new vaccines and therapeutics.

1.3.3 Active TB

On average an estimated 5-10% of infected individuals^{42,49,50} go on to develop active tuberculosis disease, typically within 2 years after infection with the pathogen⁵¹. In the case of active tuberculosis disease, the immune system is unable to control pathogen replication, resulting in exacerbation of pathology and manifestation

of symptoms such as coughing, weight loss, night sweats and anemia. Unchecked pathogen replication can lead to failure of containment by the granuloma. As a consequence, bacteria can be released in the pulmonary space, where they can be coughed up and disseminated. This form of tuberculosis is known as “open tuberculosis”. Without timely and appropriate treatment, active TB disease poses a major threat to the health of the patient as well as its community. Risk of developing active TB is dependent on many conditions, such as age, immune status, rate of exposure and social-economic status⁵²⁻⁵⁵.

1.3.4 TB as a spectral disease

While tuberculosis is typically referred to by a binary classification, recent research has demonstrated large heterogeneity in what is defined as active or latent tuberculosis^{47,48}. These insights have led to a new understanding of tuberculosis as a spectrum of disease and the proposition of two additional clinical states between latent and active infection; incipient and subclinical disease^{56,57}. Typically, incipient TB is defined as the asymptomatic phase before active disease, where clinical symptoms as well as radiographic or microbiologic evidence of disease are absent, but progression to active TB disease is impending or ongoing. Subclinical disease is defined as a similar absence of clinical signs, but in combination with pathology or bacteria detectable by radiological or microbiological assays. However, some definitions of incipient TB do include the presence of these radiographic abnormalities or culture/smear positivity⁵⁷.

1.3.5 Extrapulmonary Tuberculosis

While pulmonary tuberculosis is the most prevalent form, TB can manifest itself in many different organs, such as the genital tract⁵⁸, the heart⁵⁹, but also skin⁶⁰ and bone tissue⁶¹.

Although representing only 1% of total tuberculosis cases, one of the most devastating and deadliest forms of extrapulmonary tuberculosis is central nervous system (CNS) TB, in which the infection is disseminated to the brain^{62,63}. The disease is typically initiated by the formation of a caseous granuloma in the meninges or cortex, which subsequently releases bacilli in the subarachnoid space (also known as a “Rich focus”)⁶⁴. CNS TB manifests itself primarily as tuberculosis meningitis (TBM) and to a lesser extent as granuloma formation in the grey or white matter, or tubercular encephalitis. Symptoms of TBM include fever, headaches and neck stiffness, and advanced stages can present with lethargy or even coma. Clinical presentation of cranial granulomas depends on their location and size^{65,66}. Both host and pathogen factors seem to play a role in the development of CNS TB. Children and HIV-infected individuals are especially at risk for developing meningeal TB^{62,67}, and it also seems that infection with Indo-Oceanic and East Asian (L1&2) *Mtb* lineages are more likely to cause meningeal TB compared to Euro-American *Mtb* lineages (L4)⁶⁸.



As for CNS TB, children and immunosuppressed individuals are also at increased risk of developing millitary TB; extensively disseminated tuberculosis disease with numerous, tiny granulomas (<5mm). Millitary TB often occurs in multiple organs simultaneously, resulting in an a-specific, heterogenous disease presentation, which hampers timely diagnosis⁶⁹. Due to difficulties in diagnosis in combination with extensive dissemination, millitary TB is associated with a high mortality rate.

2. Tuberculosis and the immune system

To understand tuberculosis, one must understand the role of the immune system in infection and disease. The immune system is critical in controlling *Mtb* infection in the host, however, at the same time it can cause collateral tissue damage, or even be exploited by *Mtb* for its survival. The interaction between *Mtb* and the immune system is complex, and especially our knowledge on the immune-mechanisms required for complete protection remains incomplete.

Our immune system is designed to recognize and eliminate harmful foreign agents. Invading pathogens are recognized by means of pattern recognition receptors (PRRs), expressed on innate immune cells, that bind pathogen-specific molecules, such as bacterial cell wall components or DNA. Typically, after recognition of an infectious agent, the innate immune system keeps the pathogen in check by deploying several antimicrobial effector functions, one of which is the recruitment of macrophages, which are capable of pathogen-removal through phagocytosis and subsequent eradication through fusion of the phagosomal compartment with acidic lysosomes. Simultaneously, a more potent adaptive immune response, its functional characteristics being dependent on the type of pathogen encountered, is primed by antigen-presenting cells (APC) and results in the eventual elimination of the invading pathogen, a downregulation of inflammatory responses to prevent excess damage and the establishment of immune memory. *Mtb* is notorious for its capacity to influence this cascade at many stages.

As the dominant resident innate immune cell of the lung, alveolar macrophages play a central role in tuberculosis immunity. They are among the first cells encountered by *Mtb* and are equipped with a range of effector mechanisms to eliminate infection, but can become hijacked by *Mtb* and converted into a vector for replication and dissemination⁷⁰⁻⁷². *Mtb* subsequently delays initiation of the adaptive immune response, by suppressing macrophage and neutrophil apoptosis and interfering with dendritic cell function⁷³⁻⁷⁵. In most individuals, the ensuing adaptive response is capable of controlling *Mtb* infection, as demonstrated by the relatively low incidence of disease in TB after infection, but not able to eliminate the pathogen, as evident by the vast amount of latently infected individuals.

2.1 Immune-mediated protection after *Mtb* infection

Which immune-mechanisms are important in protection from TB infection and disease can be inferred from observations in the clinic. Individuals with particular genetic defects in immune-signaling pathways, exhibit increased susceptibility to mycobacterial infections. Especially mutations abrogating the production or signaling-cascade of Interleukin(IL)-12, essential for the induction of an adaptive T-helper type 1 (Th1) response, and of Interferon- γ (IFN γ), an archetypical activator of macrophage effector functions, were found in association with disease caused by normally weakly pathogenic mycobacteria, and are therefore thought to be of critical importance in protection from *Mycobacterium tuberculosis* as well⁷⁶. The importance of the Th1-response in protection is further underpinned by the increased risk of TB development in individuals with a low CD4 T-cell count due to advanced HIV infection⁷⁷. Also Tumor Necrosis Factor- α (TNF α) was found to be necessary for mediating protection from TB, after the observation that treatment with TNF α -inhibitors led to increased risk of developing TB^{78,79}.

Our understanding of TB immunity is further informed by cohort-studies. Resisters, individuals frequently exposed to *Mtb* without evidence of infection, offer the opportunity to identify immune responses involved in resistance^{31,80}. A recent study described the presence of distinct *Mtb*-specific antibody responses of an enhanced avidity and non-IFN γ T-cell responses in these resisters compared with latently infected individuals³³. While not deemed essential for protection against intracellular bacteria, antibodies could contribute to protection from *Mtb* in a number of ways (reviewed in ⁸¹). In a cohort of TB case contacts, early clearance of *Mtb* was found to be associated with enhanced innate immunity in response to heterologous stimulation, a phenomenon known as trained innate immunity³⁴. Also by comparing the immune responses of latently infected individuals with ATB patients insights in protective immunity can be obtained. For instance, a multi-cohort study comparing actively and latently infected individuals identified a role for natural killer (NK) cells in *Mtb* infection control⁸².

In recent years, a plethora of new immune subsets and concepts, such as Donor Unrestricted T-cells (DURTs), Innate Lymphoid Cells (ILC) and γ/δ T-cells have been described and studied in the context of tuberculosis, but their exact role in protection and/or disease remains to be elucidated⁸³.

2.2 Immune evasion and manipulation by *Mtb*

While host-immunity is essential in control and protection, *Mtb* is capable of evading and exploiting it in myriad ways⁸⁴.

A notable example of immune-evasion is the capacity of *Mtb* to interfere with macrophage phagosome-lysosome fusion, and its ability to survive even if mature phagolysosomes are formed⁸⁵. This allows *Mtb* to persist and replicate inside the macrophage, effectively hiding from the immune system. The ways in which *Mtb* manipulates the immune system are numerous, but involve, amongst others, excess



production of the anti-inflammatory cytokine IL-10, suppressing effective anti-tuberculosis immunity^{86,87}, delaying T-cell priming and driving T-cells towards terminal differentiation, impairing their functionality^{88,89}.

Besides evading host immunity, *Mtb* also appears to take advantage of infection-induced immune responses. Rather than clearing the pathogen, monocytes and neutrophils recruited to the site of *Mtb* infection contribute to further dissemination of the infection⁹⁰. The observation that *Mtb* T-cell epitopes are under strong evolutionary selection, as evidenced by their hyper-conservation between MTBC members, may suggest that certain T-cell responses could be beneficial to the pathogen, potentially due to contributing to cavity formation which facilitates pathogen spread⁹¹.

So while some of the key players in anti-TB immunity have been identified, *Mtb* is capable of successfully circumventing these host immune responses. Our understanding of what is required for protective TB immunity remains incomplete and in need of further research to more effectively design immune-based prophylactic and therapeutic interventions.

3. Diagnostics

Timely and accurate diagnosis of (active) TB infection is not only essential in prevention of morbidity, but also for containment of pathogen-spread. *Mtb* infection can be diagnosed either by direct detection of the pathogen through microbiological and molecular assays or indirect assessment of pathogen-induced host pathology or immune responses. An individual suspect of tuberculosis may be tested by one or more of the diagnostic tools outlined below, and depending on where the patient falls within the spectrum of TB disease (see section **1.3 tuberculosis disease presentation**), it may test positive in one or more of these assays.

3.1 Diagnosis by microbiological assays

Direct detection of *Mtb* by microbiological assays is currently the only way to diagnose active pulmonary tuberculosis. At the moment, there are three predominant microbiological diagnostic tools: smear-microscopy, sputum culture or GeneXpert technology.

Sputum smear microscopy is a cost-effective and relatively quick method to detect *Mtb* in the sputum of individuals suspect of active pulmonary TB. Sputum is treated with acid-fast dyes and visually assessed for the presence of mycobacteria. While this method is the primary method of diagnosing active TB in resource-limited settings, it has a low sensitivity of detection⁹². Especially children and HIV-infected individuals with active TB often are smear-negative and require further testing to rule out active pulmonary TB^{93,94}.

Conventional or automated culture of sputum on media selective for tuberculosis is another cost-effective way to diagnose active TB. By further subculture with antibiotics added to the culture media, the drug-susceptibility of the infectious strain can be assessed. Culturing requires a lower bacterial load to yield a positive result and, thus, is more sensitive compared to microscopy-based detection³⁵. However, since *Mtb* is a slow growing pathogen, it can take up to 3 to 6 weeks to make a definitive diagnosis, thereby delaying the initiation of treatment. Besides sputum, other bodily fluids such as cerebrospinal fluid (CSF), bronchoalveolar as well as gastric lavages and tissue biopsies can be cultured for the presence of *Mtb*.

Finally, by means of automated GeneXpert MTB/RIF technology, sputum or other fluids are probed for the presence of mycobacterial DNA⁹⁵. Like smear-microscopy, this method is relatively quick (<1 day) but is more sensitive, especially in individuals with MDR-TB or HIV-TB co-infection⁹⁶. Furthermore, it has the additional advantage of being able to identify rifampicin-resistant *Mtb* strains, which informs on the subsequent drug-treatment regime. Cartridges that can detect resistance to antibiotics other than rifampicin are under development⁹⁷. The WHO now recommends the use of GeneXpert MTB/RIF technology as a first-line diagnostic for pulmonary TB in adults and children⁹⁸. Although relatively easy to use, the method requires expensive infrastructure and a constant source of electricity, hampering its implementation to lower levels of the health system particularly in endemic regions.

Several other assays that rely on the detection of pathogen-derived factors are endorsed by the WHO, notable examples include line-probe assays to detect drug-resistance in smear or culture positive samples and the lateral flow lipoarabinomannan (LF-LAM) assay, which detects mycobacterial cell wall derived lipoarabinomannan (LAM) in urine, and is used specifically to diagnose HIV-infected individuals with a low CD4 T-cell count⁹⁹.

3.2 Diagnosis by imaging technologies

Diagnosis of TB by imaging has a long history, starting with the use of chest X-ray in the early 20th century for disease management in sanatoria and hospitals, and active case-finding by mobile X-ray units. The formation of cavitating granulomas, pleural thickening and lymph node enlargement, typical of pulmonary TB pathology, all appear as abnormalities on a chest X-ray. Due to its poor specificity in diagnosing TB and challenges in implementation in developing countries, chest X-ray has suffered a decline in use during the late 20th century¹⁰⁰. However, recent advances in the field of radiography, such as the development of digital radiography and portable systems for field use, have led to the reappraisal of the chest X-ray as a sensitive modality to diagnose pulmonary TB and it is now recognized by the WHO as an essential tool to end the TB pandemic¹⁰¹. Confirmation by microbiological assays remains a prerequisite for a definitive diagnosis of active tuberculosis.

More modern imaging modalities such as magnetic resonance imaging (MRI) or Computed Tomography (CT), either or not combined with positron emission tomography (PET), all have a role in the diagnosis of the various forms of tuberculosis.



In the case of CNS-TB, MRI is deemed most suited for pathology imaging, while CT is the modality of choice for the evaluation of pulmonary and abdominal TB¹⁰². Both imaging modalities offer a better resolution than conventional X-ray by the benefit of visualizing the pathology in a three-dimensional fashion. While CT and MRI are primarily used to provide anatomical information, PET imaging provides functional information depending on the tracer used. Active tuberculous lesions have a high glucose uptake and can thus be visualized and tracked over time by 18F-fluorodeoxyglucose (FDG) PET-CT imaging. Imaging provides the opportunity to monitor a patient's response to chemotherapy or diagnose incipient/subclinical TB¹⁰³.

3.3 Diagnosis by immunological assays

Rather than testing for the presence of *Mtb*, immunological assays rely on the detection of immune responses induced by the pathogen. Immune-based assays are typically used to diagnose latent tuberculosis, and currently comprise two different methods: Tuberculin Skin Tests (TST) and Interferon- γ Release Assays (IGRA).

After his discovery of the *M.tuberculosis* bacilli, Robert Koch went on to develop what is now known as Old Tuberculin (OT), a heat-concentrated filtrate from broth-grown *Mtb*. Koch's tuberculin was originally presented as a cure for TB, but failed to deliver on that promise. However, in the early 1900s Clemens von Pirquet demonstrated its applicability as a diagnostic tool for (latent) TB infection by cutaneous injection¹⁰⁴, laying the foundation for what is now known as the Tuberculin Skin Test (TST). Over the years the TST has been refined, moving from OT to the use of a *Mtb* Purified Protein Derivate (PPD), resulting in higher specificity and less adverse reactions. Historically, various forms of the skin test have been in use, however nowadays the Mantoux test, based on intradermal injection of PPD, is the most widely used variant.

The TST allows to establish if there is a delayed-type hypersensitivity (DTH) reaction to *Mtb* antigens. Prior exposure to *Mtb* will have sensitized T-cells, which upon injection of PPD migrate to the injection site. This results in redness and swelling, which is typically assessed after 48 to 72 hours by visual inspection and palpation. The TST has several advantages, especially in low resource settings, being a low-cost assay not dependent on hardware or laboratory access. Disadvantages include low sensitivity, suppression of DTH at high-burden infection conditions, susceptibility to inter-reader variability and the need for the patient to return to the clinic for readout of the TST. Also, *Mtb* PPD contains antigens also found in NTM as well as the *M. bovis*-derived tuberculosis vaccine Bacillus Calmette Guerin (BCG). Therefore, in certain conditions, a positive TST may be the result of prior BCG vaccination or NTM exposure rather than *Mtb* infection¹⁰⁵.

In an effort to improve specificity of TSTs, blood-based Interferon- γ Release Assays (IGRAs) employing *Mtb*-specific antigens have been developed¹⁰⁶. As the name suggests, IGRAs measure the production of Interferon- γ (IFN- γ) by T-cells sensitized by prior *Mtb* exposure, in response to stimulation with antigen. There are

two commercially available IGRAs licensed for the diagnosis of active TB or LTBI; the QuantiFERON-TB assay and the T-SPOT.TB assay. The QuantiFERON assay involves in-tube incubation of peripheral whole blood with a set of *Mtb*-specific peptides, covering the Early Secretory Antigen 6 (ESAT-6) and Culture Filtrate Protein 10 (CFP-10), after which plasma IFN- γ levels are determined by an Enzyme-Linked ImmunoSorbent Assay (ELISA) and compared to cut-off for positivity. The T-SPOT.TB assay requires the isolation of Peripheral Blood Mononuclear Cells (PBMC) from whole blood, which are subsequently incubated with ESAT-6 & CFP-10 peptides in an Enzyme-Linked Immunospot (EliSPOT) assay after which the number of IFN- γ -producing T-cells are counted and compared to a predefined threshold.

The WHO recommends the use of either a TST or IGRA in the diagnosis of LTBI, depending on patient and resource conditions¹⁰⁷. However, formally, positivity in either the TST or IGRA is indicative of *Mtb* exposure only, as it cannot discern between exposure and ongoing *Mtb* infection. Another major limitation of immune-based assays is their limited sensitivity in immunocompromised individuals such as patients with a low CD4 T-cell count as a result of advanced HIV infection, or in the elderly who are at increased risk of a false negative result due to immune senescence.

4. Vaccines

An efficacious TB vaccination strategy is of the utmost importance for a number of reasons. Primarily, vaccine-mediated prevention of TB infection or disease can break the transmission cycle of *Mtb*. With the current state of TB diagnostics, as described in the **Diagnostics** section, TB is typically diagnosed well after establishment of infection. This delays initiation of treatment and increases risk of dissemination. Prevention of disease by vaccination would mitigate these issues. An effective vaccine would also circumvent the increasing incidence of drug-resistance exhibited by *Mtb* strains and diminish the need for prolonged TB chemotherapy, which comes with severe side effects (see **Box 1**).

To date, the only licensed prophylactic TB vaccine available is Bacillus Calmette Guerin (BCG), a live-attenuated vaccine derived from *Mycobacterium bovis*. In the early 1900's Calmette and Guérin cultured a *Mycobacterium bovis* isolate on a mixture of potato slices and bile for more than 200 passages, which took over 13 years. This passaging resulted in attenuation of the pathogen, to the point that it no longer caused disease in guinea pigs and could protect calves from natural infection with *M.bovis*¹⁰⁸. BCG was subsequently deployed for the first time in man in 1921, where it was administered orally to infants. The route of administration was later changed to intradermal injection. Over the years, BCG has dramatically reduced TB-related mortality in children, protecting them from severe forms of pediatric tuberculosis such as CNS or millitary TB¹⁰⁹. By means of a-specific bystander immunity, also known as "trained immunity", it also protects neonates from non-tuberculous causes of death¹¹⁰. Unfortunately, the efficacy of BCG in protecting adults from



pulmonary TB is notoriously variable, with reported efficacies ranging from 0-80%¹¹¹. The underlying reasons for this variability remain largely unknown, though greater efficacy seems associated with increased distance from the equator¹¹¹. Notwithstanding its efficacy against childhood TB, BCG on its own appears ineffective in controlling the ongoing tuberculosis epidemic, and new tuberculosis vaccines complementing or replacing BCG are urgently needed. Over the last decades several candidate vaccines have been under development, employing a variety of strategies to elicit protection^{112,113}.

4.1 Definitions of protection

Vaccine mediated protection with the purpose of controlling the ongoing tuberculosis epidemic can be approached in a number of ways. The two main strategies are preventing the development of active TB disease (Prevention of Disease, PoD), and therefore pathogen spread, or preventing *Mtb* infection (Prevention of Infection, Pol) altogether.

Modeling studies suggest that a PoD vaccine preventing the development of active tuberculosis in previously exposed individuals would have the greatest impact on the TB epidemic¹¹⁴, as it would both hamper transmission of the pathogen and greatly reduce TB morbidity and mortality. PoD vaccines could also be employed prophylactically. Unfortunately, PoD vaccine trials are logistically challenging due to the relatively low rate of disease progression in exposed/infected individuals.

Prevention of infection (Pol) vaccination aims to inhibit acquisition of *Mtb* infection, thereby also preventing the development of TB disease. While Pol vaccination is modelled as less impactful compared to PoD vaccination¹¹⁴, evidence of individuals resistant to TB infection suggests that it is possible to harness the immune system to prevent infection. Especially in high-transmission settings, a Pol vaccine would contribute significantly to reduction of TB morbidity and mortality¹¹⁵. Pol vaccine trials have the added benefit of requiring less participants and shorter follow-up time than PoD trials, with the potential of accelerated identification of efficacious candidate vaccines and correlates of protection, which could be translated into PoD vaccine design. Signals of protection after revaccination with BCG or H4: IC31 observed in the first reported clinical Pol trial, demonstrate the value of such trials¹¹⁶.

As antibiotics-treated TB patients are at increased risk of *Mtb* reinfection¹¹⁷, a vaccine that would prevent recurrence (PoR) of TB would benefit the millions of individuals that underwent TB treatment. Like Pol trials, PoR trials would require smaller sample sizes due to the increased incidence of study endpoints. Similarly, therapeutic vaccination could potentially complement TB chemotherapy, increasing efficacy and/or shortening treatment duration, which reduces the risk of severe side effects.

Ideally, a new TB vaccine would be applicable in all scenarios described above while being safe and efficacious in all individuals. However, due to the multifaceted nature of TB and the people afflicted, a “one size fits all” vaccine approach seems unlikely to achieve.

4.2 Harnessing the immune system for protection through vaccination

Vaccination aims to protect an individual from disease by eliciting long lasting, protective humoral or cellular adaptive immune responses. To induce the desired adaptive responses, vaccines target and modulate APCs, which prime and shape adaptive immunity, with a combination of pathogen-specific antigens and immunomodulatory agents. Through ligation of specific pathogen recognition receptors, either by administration of attenuated or dead pathogen or specific adjuvants, the vaccine-induced immune responses can be directed towards specific response types (e.g. Th1 cells, cytotoxic T-cells, antibody producing B-cells). Ultimately, vaccination will lead to a population of pathogen-specific memory T- and B-cells, which are capable of responding rapidly and effectively when encountering the pathogen in question.

When considering vaccine-mediated protection in the context of TB, especially cellular immune responses are thought to be of importance, as *M. tuberculosis* is thought to be able to avoid the antimicrobial effects of antibodies at the intracellular stage of its lifecycle. Therefore, most vaccination strategies under development so far have aimed to induce an *Mtb*-specific T-cell response, consisting of CD4+ T-cells producing IFN γ and TNF α , deemed essential for protection (see section **2. Tuberculosis and the immune system**), in combination with IL-2, required for T-cell maintenance and proliferation. Especially T-cells producing all three cytokines are considered to be of importance^{89,118}. However, it has become apparent from a recent clinical trial that establishing a peripheral, antigen-specific Th1 response is not enough to convey protection¹¹⁹. Additionally, human and animal studies, including the work described in this thesis, have identified other immune subsets involved in vaccine-mediated protection, such as IL17A producing T-cells (Th17) and NK cells, and, collectively, these observations have led to a re-evaluation of the requirements for protection^{120,121}. Unfortunately, under which conditions the different immune-mechanisms implicated lead to protection from TB remains unknown and reliable correlates of vaccine-mediated protection are lacking. Considering the heterogenous nature of *Mtb*, its human host and TB disease presentation, a single, universal mechanism of vaccine-mediated protection might not apply.

4.3 Vaccine administration

Another element to consider in TB vaccine development is the route of vaccine administration. The primary port of entry of *Mtb* is the lung, but current vaccine strategies under development predominantly rely on parenteral immunization, inducing primarily systemic immune responses which need to be recruited to the lung during infection. Mucosal vaccination on the other hand, is capable of eliciting immune-responses at or recruiting “pre-primed” parental responses to the site of infection, poised to respond rapidly to invading pathogens¹²². It has the added benefit of being needle-free, reducing fear and pain associated with vaccination by injection. Data from animal studies, including work described in this thesis, has shown that by adjusting the route of BCG delivery from the skin to the pulmonary mucosa,



significantly better protection can be achieved¹²³⁻¹²⁵. Whether mucosal routes of administration are similarly immunogenic in humans is currently under investigation^{126,127}.

4.4 Tuberculosis vaccines under development

A range of tuberculosis vaccines are currently in various stages of development. These vaccines can be categorized based on their properties (live attenuated, whole cell inactivated or subunit) and intended type of protection (Pol, PoD, PoR or therapeutic, see above). The latter categories are not mutually exclusive, a Pol vaccine for instance could also display efficacy in preventing recurrence. **Box 3** lists a number of notable TB vaccines currently under development.

4.4.1 Live attenuated vaccines

Live attenuated TB vaccines utilize mycobacteria that, by rational design, are weakened to such an extent that they no longer cause disease upon administration, while still being capable of inducing protective immune responses. The use of the complete mycobacteria results in a broad antigenic response, including antibodies against cell wall components. Most of the live attenuated vaccines under development are aimed as a replacement of BCG, also a live attenuated vaccine, though revaccination with BCG itself has gained renewed interest after encouraging results in a recent clinical trial¹¹⁶. Live attenuated TB vaccines that are being evaluated in clinical trials are MTBVAC^{128,129} and VPM1002¹³⁰, with many more under development^{131,132}.

4.4.2 Whole cell inactivated vaccines

While live attenuated vaccines induce robust immune responses, they remain replication-competent and therefore potentially dangerous for immunocompromised individuals. Whole cell inactivated vaccines, created by inactivation of live mycobacteria through chemical or physical means, circumvent that danger. As these vaccines still consist of the complete pathogen, they induce a similarly broad immune response as live attenuated vaccines, although at a lower magnitude. DAR-901¹³³ and *Mycobacterium indicus pranii* (MIP)^{134,135} are examples of whole cell inactivated vaccines under clinical evaluation.

4.4.3 Subunit vaccines

Subunit vaccines are made up of one or more pathogen-specific antigens (proteins, fusion-proteins or synthetic long peptides) that, upon administration, induce a protective immune response. To increase immunogenicity, antigens are typically formulated with an adjuvant or expressed by a viral vector, which also allows to specifically induce the type of immune response expected to mediate protection. The advantage of subunit vaccines is the possibility to rationally select vaccine antigens and combining proteins that are expressed by *Mtb* under different *in vivo* conditions, such as nutrient starvation^{136,137}. This offers the possibility to tailor vaccines to specific target populations or, in theory, design a universally applicable vaccine. Subunit vaccines currently under clinical evaluation are H4:IC31¹¹⁶ and M72:AS01E¹³⁸.

Box 3. Notable examples of different TB vaccination strategies under development. Sources:^{112,139,140} and literature cited in section 4.4

Live attenuated	Development stage	Application	Description	Proposed mode of action
BCG revaccination	Phase 2	Pol	Attenuated <i>Mycobacterium bovis</i>	Boosting of BCG induced immune responses
MTBVAC	Phase 2	Pol, PoD	<i>M.tuberculosis</i> PhoP and Fad26 deletion mutant.	Induction of immune responses of increased antigenic breadth
VPM1002	Phase 3	Pol, PoD, PoR, therapeutic	Recombinant BCG, expressing listeriolysin while lacking ureC.	Superior immunogenicity due to cytosolic antigen release
Inactivated whole cell				
MIP	Phase 3	therapeutic	Heat inactivated <i>Mycobacterium indicus pranii</i>	Enhanced early Th1 responses and late balancing of regulatory and Th1 immunity
RUTI	Phase 2	PoD, therapeutic	Detoxified, fragmented <i>M.tuberculosis</i>	Polyantigenic cellular and humoral immune responses
DAR-901	Phase 2	Pol, PoD	Heat inactivated <i>M. obuense</i>	Induction of Th1 immune responses and lymphoproliferation
Submit Adjuvanted protein				
M72	Phase 2	PoD	Fusion protein of Rv1196 & Rv0125, formulated in AS01E adjuvant	Polyfunctional Th1 responses, NK-cell IFN γ production
H4 / H56 : IC31	Phase 2	Pol, PoD, therapeutic	Fusion protein of Ag85B & TB10.4 (H4) or Ag85B, Rv2660 & ESA16 (H56) formulated in IC31 adjuvant	Induction of polyfunctional Th1 responses
ID93/GLA-SE	Phase 2	Pol, PoD, therapeutic	Fusion protein of Rv2608, Rv3619, Rv3620c & R1813, formulated in GLA-SE adjuvant	Polyfunctional Th1 responses and antigen-specific immunoglobulins
Virally vectored				
MVA85A	Phase 1		Aerosol administration of modified vaccinia Ankara virus expressing Ag85A	Antigen-specific Th1 immune responses in the lung
Ad5Ag85A	Phase 1		Replication deficient adenovirus expressing Ag85A	Induction of antigen-specific Th1 immune responses
ChAdOx1.85A	Phase 1		Replication deficient chimpanzee adenovirus expressing Ag85A	Induction of antigen-specific Th1 & cytotoxic T-cells
RhCMV-TB	Preliminary		Rhesus cytomegalovirus expressing different <i>Mtb</i> proteins	Induction and maintenance of <i>Mtb</i> -specific effector memory responses



Though TB vaccine development has made substantial progress in the recent years, the development of a more efficacious tuberculosis vaccine is hampered by our incomplete understanding of protective immunity. Therefore, to select the most promising candidates for efficacy evaluation in the field, initial screening in relevant model systems of TB remains necessary.

5. Animal models of tuberculosis

As discussed above, the elimination of TB is hampered by large gaps in our knowledge pertaining, amongst others, to protective immunity, disease progression and diagnostics. While progress is being made with *in silico* and *in vitro* modeling of immune system dynamics and tuberculosis pathogenesis^{141,142}, animal models remain indispensable in addressing these knowledge gaps, as no other model system can replicate the complexity of *Mtb* host-pathogen interactions. Amongst others, animal models have informed us on genetic determinants of disease susceptibility, the potential of host-directed therapies and the interaction between TB and comorbidities like diabetes, influenza and HIV.

To date, no animal model can completely replicate the immense diversity displayed by human tuberculosis disease manifestation, but aspects of disease can be recapitulated in individual models. Therefore, choosing an animal model that is fit for purpose to the research questions under investigation is essential. Tuberculosis can be modelled in a range of animal species, ranging from typical laboratory animals such as zebrafish and mice to more uncommon species such as goats and cattle (**Box 4**). A selection of the available model species and their features will be discussed in more detail below.

Box 4. The many hosts of Mycobacteria

Mycobacteria can infect and cause disease in a wide range of organisms, a variety of which are utilized in *in vivo* tuberculosis research. Besides mice, other rodent species classically used in laboratory research, such as Guinea pigs (*Cavia porcellus*)¹⁴³, rabbits (*Oryctolagus cuniculus*)¹⁴⁴ and rats (*Rattus norvegicus*)¹⁴⁵, are all applied in preclinical tuberculosis research, each recapitulating different aspects of TB disease development, such as cavitory lesions in rabbits and lymph node involvement in guinea pigs^{146,147}. Also invertebrate organisms, such as the fruit fly (*Drosophila melanogaster*)¹⁴⁸, *Dictyostellum* amoeba¹⁴⁹, and *Galleria mellonella* larvae¹⁵⁰, are amenable to infection with mycobacteria and provide the opportunity to study specific aspects of host-pathogen interactions in a more inexpensive manner. As *M. bovis* infection in cattle remains a pressing economical animal health problem, experimental mycobacterial infection of larger animal species, such as cattle

(*Bos taurus*), domestic goats (*Capra hircus*) and deer (*Odocoileus virginianus*) has been carried out mainly from a veterinary point of view¹⁵¹. Experimental TB models in badgers (*Meles meles*)¹⁵² and ferrets (*Mustela furo*)¹⁵³, both natural hosts of *Mycobacterium bovis*, have also been established from a veterinary perspective. Nevertheless, insights gained from the field of veterinary medicine can also benefit the clinic and vice versa, an integrative approach known as the One Health concept¹⁵⁴. Each animal model features properties useful in preclinical TB research, like a high genetic diversity or educated immune system, as well as limitations, such as a lack of immunological reagents or high costs. It is important to be aware of these properties when selecting animal models to address new research questions.

5.1 The zebrafish model of TB

Despite having gills rather than lungs, zebrafish (*Danio rerio*) and zebrafish embryos as model systems for tuberculosis have contributed to important insights in TB pathogenesis¹⁵⁵. Their small size and high reproductive efficiency make them a very cost-effective model-species, and the translucent skin of larval and embryonic stages offers the possibility to track fluorescently labelled bacteria or cell subsets by means of real-time imaging techniques¹⁵⁶. As the zebrafish adaptive immune system starts to develop after 4 days and takes several weeks to mature, zebrafish embryos can be used to study the effect of the innate immune system in isolation^{156,157}. Most often, zebrafish are used to study more fundamental aspects of TB, such as early bacterial dissemination and granuloma development^{90,158}, but they can also be applied in the screening of new therapeutic compounds¹⁵⁹ or vaccine efficacy testing^{160,161}. Typically, *Mycobacterium marinum*, rather than *Mtb*, is used as the pathogenic agent¹⁶². Infection can be established by various means, for instance by injection in the yolk sac or the peritoneum, and depends on the desired disease phenotype and research question to be addressed¹⁶³. By varying the strain and dose of bacilli administered, either an acute or chronic infection can be established^{164,165}. However, of the animal models in use, the zebrafish is the least phylogenetically related to humans, and therefore has limited face validity.

5.2 Modelling TB in mice

Of the animal models available, the mouse (*Mus musculus*) is the most commonly used animal species in laboratory research, including TB. The mouse offers a range of advantages, such as the availability of numerous knock-outs and transgenic strains, a plethora of immunological reagents and comparatively low costs of housing. A high degree of homology exists between the human and mouse genome, which makes it a powerful model to investigate the mechanistic contribution of individual genes to disease progression and protection by means of genetic modification^{166,167}. Additionally, the mouse model is extensively used as the initial model for the



preclinical evaluation of TB vaccine and drug efficacy^{168,169}. *Mtb* infection in mice can be established in many ways, including intravenous injection, intranasal administration or aerosol exposure. Mice are considered to be fairly resistant to tuberculosis; administering relatively low doses of the pathogen (~50 CFU) will result in establishment of infection but also relatively long survival times (>1 year). Higher doses are applied when rapid, fulminant disease development is desired, facilitating a relatively fast readout of efficacy signals. There is however considerable variability in resistance to *Mtb* infection between different mouse strains¹⁷⁰. Due to the wide range of mouse strains available, with or without genetic modifications, there are also large differences in TB disease presentation between the different strains¹⁷¹, which is further influenced by *Mtb* strain, dose and method of infection applied^{168,172,173}.

While the mouse is the most widely applied animal species in TB research, it does have some significant drawbacks. The majority of the research performed utilizes inbred mice strains, which do not capture the genetic diversity as present in human patient populations, hampering extrapolation of results. Additionally, from birth, mice are housed under specific-pathogen-free (SPF) conditions, and, while reducing intraexperimental variance, as a consequence, mice lack an educated immune system, likely influencing vaccine and pathogen immunity^{174,175}. And lastly, while granuloma formation in mice exhibits certain features of human granuloma development, it fails to recapitulate key elements, such as the development of the whole spectrum of necrotic, fibrotic or cavitating granulomas, and lacks the circumscribed structure classically observed in human granulomas^{171,173}. In an effort to address these issues new mouse models are continuously being developed. The Collaborative Cross¹⁷⁶ and Diversity Outbred¹⁷⁷ models were designed to display more genetic diversity, and indeed as a whole these models develop a spectrum of TB disease and can be used to identify genetic mechanisms of disease susceptibility and vaccine efficacy^{178,179}. Likewise, certain congenic or genetically modified strains, such as the C3HeB/Fej mouse, that more closely mimic necrotizing granuloma pathology as seen in humans have been developed¹⁸⁰.

5.3 Modeling TB in the non-human primate.

Non-human primates are often considered the most relevant animal models for tuberculosis, recapitulating not only aspects of TB disease development but also crucial human-host features, such as a high genetic diversity and an educated immune system caused by environmental pathogen exposure. Due to ethical and cost considerations, non-human primates are typically applied in translational tuberculosis research, such as vaccine efficacy testing, but have also provided important insights in more fundamental aspects of TB pathogenesis^{181,182}.

While a variety of NHPs are susceptible to infection with *Mtb*, three species frequently used in TB research will be discussed in more detail below; the cynomolgus macaque (*Macaca fascicularis*), the rhesus macaque (*Macaca mulatta*) and the common marmoset (*Callithrix jacchus*).

5.3.1 *The rhesus and cynomolgus macaque*

As attested by reports of TB outbreaks in macaque colonies, rhesus and cynomolgus monkeys are susceptible to natural infection with mycobacteria^{183,184}. After infection, macaques replicate many aspects of disease similar to human TB patients. As disease progresses, animals exhibit marked weight loss, anemia and systemic inflammation¹⁸⁵. Pathology mirrors TB in humans, including lymph node involvement, pneumonia and highly similar granuloma formation, with necrotizing, cavitating and calcified granulomas.

As an animal model for tuberculosis, rhesus macaques have been in use since the 1960s, when they were used for drug and BCG efficacy testing^{186,187}. They are highly susceptible for *Mtb* infection and disease, though the extent of disease is dependent on *Mtb* strain and dose¹⁸⁸. Interestingly, also rhesus macaque genotype appears to influence disease development and vaccine efficacy¹²⁴. Cynomolgus macaques were first described as a model for tuberculosis in 1996¹⁸⁹, where its relative resistance to TB disease was already noted. Despite a high similarity between cynomolgus and rhesus macaques, comparing the two species reveals notable differences in their subsequent immune-response and disease development. After low dose infection, cynomolgus macaques exhibit less pathology and bacterial load compared to rhesus macaques^{190,191}. Also, in approximately 50% of cynomolgus low dose infection results in the development of LTBI, as characterized by sustained absence of clinical disease parameters and bacteria in bronchoalveolar or gastric lavage. Latent TB in rhesus macaques is only observed after infection with low-virulence strains^{192,193}. In both species latent tuberculosis can be reactivated, by either co-infection with (simian) immunodeficiency virus (SIV) or immunosuppression^{194,195}. An exception to the resistant phenotype of cynomolgus macaques is the Mauritian cynomolgus macaque. Mauritian cynomolgus macaques descend from a small founder population and, as a consequence, exhibit limited genetic diversity. As a result, these animals appear to be as susceptible to TB disease as rhesus macaques^{190,196}.

Infection of macaques is most often established by pulmonary administration of the pathogen, either through instillation or aerosolization. Historically, a wide dose-range of *Mtb* has been used to establish infection (3-1000 CFU).

As mentioned, in addition to *Mtb*, macaques are also susceptible to infection with SIV, and are therefore ideal to model HIV-TB coinfection with the purpose of investigating the safety and efficacy of new attenuated vaccines as well as mechanisms of reactivation¹⁹⁷⁻¹⁹⁹.

5.3.2 *The common marmoset*

The common marmoset is a small, neotropical non-human primate species that, although not used widely, offers several advantages for TB research. Like macaques, marmosets are housed under non-SPF conditions, resulting in an experienced immune system, and are genetically diverse. The marmoset has the added advantage of giving birth to bone-marrow chimeric twins or triplets, which provides the



opportunity for adoptive transfer experiments, and their small size makes them easier to house and handle. Compared to the macaque species described above, marmosets are extremely susceptible to *Mtb* infection and disease; aerosol administration of doses as low as 1 CFU of *Mtb* Erdman leads to the rapid development of fulminant disease²⁰⁰. Pathology development in the marmoset mimics human disease and includes the presence of necrotizing and cavitating lesions²⁰¹. The marmoset is particularly suited for TB drug research; due to their small size smaller amounts of the compound under investigation are required.

6. This thesis

The research described in this thesis aims to address knowledge gaps in tuberculosis pathogenesis, vaccine-mediated protection and TB diagnostics through modelling of tuberculosis in macaques. Simultaneously, we set out to further refine the macaque model of tuberculosis, towards a low dose infection model and the read-out of prevention of infection in addition to prevention of disease.

As rhesus and cynomolgus macaques differ in disease development after experimental TB infection¹⁹⁰, we wanted to investigate whether the two species would also differ in their susceptibility to infection, by applying a dose-escalation study design. This simultaneously allowed us to pinpoint an *Mtb* dose applicable in future low dose challenge studies. Capitalizing on the known difference in disease development between the two species, we profiled peripheral and pulmonary immune responses, both innate and adaptive, at various time-points after infection, to identify responses associated with development of, and resistance to TB disease (**Chapter 2**).

After identifying a limiting infectious dose²⁰² of 1 CFU *Mtb* in the study described in **Chapter 2**, we designed an infectious challenge study where BCG vaccinated rhesus macaques were exposed multiple times to this limiting infectious dose, which enabled read out of prevention of infection in addition to measuring prevention of disease. BCG vaccination was applied either through the skin, the standard route of administration, or through the pulmonary mucosa, known to improve vaccine efficacy¹²⁴. Systemic and pulmonary immune responses were assessed after vaccination and challenge, to identify vaccine-induced correlates of protection (**Chapter 3**).

Building upon superior protection conferred by mucosal BCG and the immune correlates of this protection, as identified in **Chapter 3**, we evaluated whether pulmonary administration of a novel candidate tuberculosis vaccine, MTBVAC, also induced these responses. Compared to BCG, MTBVAC has the advantage of expressing and inducing recognition of a wider range of *Mtb*-specific antigens, which can be linked to increased protection²⁰³. In addition to profiling of these immune correlates, we characterized vaccine-induced cellular and humoral immune response more in depth. We assessed the expression of tissue-

residency and mucosal homing markers on antigen-specific T-cells, as well as the capacity of vaccine-induced antibodies to bind live *Mtb* and facilitate pathogen phagocytosis (**Chapter 4**).

In **Chapter 5**, the kinetics of complement component C1q, a new candidate biomarker of active tuberculosis disease, are investigated in various NHP tuberculosis studies with differential disease outcomes. After evaluation of this marker in human cohort studies²⁰⁴, we here back-translate and measure the time-line of C1q upregulation after experimental infection, both in serum as well as BAL fluid. The possibility to correlate C1q levels with TB disease levels allows for the strengthening of the association of C1q with disease progression.

Finally, in **Chapter 6** an overarching discussion of the work described in this thesis is provided, as well as future perspectives for the use of NHPs in tuberculosis research.



References

1. Donoghue, H.D., et al. Tuberculosis in Dr Granville's mummy: a molecular re-examination of the earliest known Egyptian mummy to be scientifically examined and given a medical diagnosis. *Proc Biol Sci* **277**, 51-56 (2010).
2. Crubezy, E., et al. Identification of Mycobacterium DNA in an Egyptian Pott's disease of 5,400 years old. *C R Acad Sci III* **321**, 941-951 (1998).
3. Paulson, T. Epidemiology: A mortal foe. *Nature* **502**, S2-3 (2013).
4. Geneva: World Health Organization. Global tuberculosis report 2019.
5. Brosch, R., et al. A new evolutionary scenario for the Mycobacterium tuberculosis complex. *Proceedings of the National Academy of Sciences of the United States of America* **99**, 3684-3689 (2002).
6. Gagneux, S. Ecology and evolution of Mycobacterium tuberculosis. *Nature reviews. Microbiology* **16**, 202-213 (2018).
7. Coscolla, M. & Gagneux, S. Consequences of genomic diversity in Mycobacterium tuberculosis. *Seminars in immunology* **26**, 431-444 (2014).
8. Portevin, D., Gagneux, S., Comas, I. & Young, D. Human macrophage responses to clinical isolates from the Mycobacterium tuberculosis complex discriminate between ancient and modern lineages. *PLoS pathogens* **7**, e1001307 (2011).
9. Reiling, N., et al. Clade-specific virulence patterns of Mycobacterium tuberculosis complex strains in human primary macrophages and aerogenically infected mice. *mBio* **4**(2013).
10. Glaziou, P., Sismanidis, C., Floyd, K. & Raviglione, M. Global epidemiology of tuberculosis. *Cold Spring Harbor perspectives in medicine* **5**, a017798 (2014).
11. Shah, N.S., et al. Worldwide emergence of extensively drug-resistant tuberculosis. *Emerg Infect Dis* **13**, 380-387 (2007).
12. Dalton, T., et al. Prevalence of and risk factors for resistance to second-line drugs in people with multidrug-resistant tuberculosis in eight countries: a prospective cohort study. *Lancet* **380**, 1406-1417 (2012).
13. Guidelines for treatment of drug-susceptible tuberculosis and patient care, 2017 update. Geneva: World Health Organization. (2017).
14. WHO consolidated guidelines on drug-resistant tuberculosis treatment. Geneva: World Health Organization. (2019).
15. de Jong, B.C., Antonio, M. & Gagneux, S. Mycobacterium africanum--review of an important cause of human tuberculosis in West Africa. *PLoS Negl Trop Dis* **4**, e744 (2010).
16. Falkinham, J.O., 3rd. Surrounded by mycobacteria: nontuberculous mycobacteria in the human environment. *Journal of applied microbiology* **107**, 356-367 (2009).
17. Malone, K.M. & Gordon, S.V. Mycobacterium tuberculosis Complex Members Adapted to Wild and Domestic Animals. in *Strain Variation in the Mycobacterium tuberculosis Complex: Its Role in Biology, Epidemiology and Control* (ed. Gagneux, S.) 135-154 (Springer International Publishing, Cham, 2017).
18. Muller, B., et al. Zoonotic Mycobacterium bovis-induced tuberculosis in humans. *Emerg Infect Dis* **19**, 899-908 (2013).
19. Daley, C.L. Mycobacterium avium Complex Disease. *Microbiology spectrum* **5**(2017).
20. Johnson, M.G. & Stout, J.E. Twenty-eight cases of Mycobacterium marinum infection: retrospective case series and literature review. *Infection* **43**, 655-662 (2015).
21. Aubry, A., Mougari, F., Reibel, F. & Cambau, E. Mycobacterium marinum. *Microbiology spectrum* **5**(2017).
22. Fennelly, K.P., et al. Variability of infectious aerosols produced during coughing by patients with pulmonary tuberculosis. *American journal of respiratory and critical care medicine* **186**, 450-457 (2012).

23. Behr, M.A., *et al.* Transmission of *Mycobacterium tuberculosis* from patients smear-negative for acid-fast bacilli. *Lancet* **353**, 444-449 (1999).
24. Turner, R.D. & Bothamley, G.H. Cough and the transmission of tuberculosis. *The Journal of infectious diseases* **211**, 1367-1372 (2015).
25. Andrews, J.R., Morrow, C., Walensky, R.P. & Wood, R. Integrating social contact and environmental data in evaluating tuberculosis transmission in a South African township. *The Journal of infectious diseases* **210**, 597-603 (2014).
26. Andrews, J.R., Morrow, C. & Wood, R. Modeling the role of public transportation in sustaining tuberculosis transmission in South Africa. *Am J Epidemiol* **177**, 556-561 (2013).
27. Telisingshe, L., *et al.* High tuberculosis prevalence in a South African prison: the need for routine tuberculosis screening. *PLoS one* **9**, e87262 (2014).
28. Churchyard, G., *et al.* What We Know About Tuberculosis Transmission: An Overview. *The Journal of infectious diseases* **216**, S629-s635 (2017).
29. Stein, C.M., *et al.* Resistance and Susceptibility to *Mycobacterium tuberculosis* Infection and Disease in Tuberculosis Households in Kampala, Uganda. *Am J Epidemiol* **187**, 1477-1489 (2018).
30. Buchwald, U.K., *et al.* Broad adaptive immune responses to *M. tuberculosis* antigens precede TST conversion in tuberculosis exposed household contacts in a TB-endemic setting. *PLoS one* **9**, e116268 (2014).
31. Simmons, J.D., *et al.* Immunological mechanisms of human resistance to persistent *Mycobacterium tuberculosis* infection. *Nature reviews. Immunology* **18**, 575-589 (2018).
32. Verrall, A.J., *et al.* Early Clearance of *Mycobacterium tuberculosis*: The INFECT Case Contact Cohort Study in Indonesia. *The Journal of infectious diseases* (2019).
33. Lu, L.L., *et al.* IFN-gamma-independent immune markers of *Mycobacterium tuberculosis* exposure. *Nature medicine* **25**, 977-987 (2019).
34. Verrall, A.J., *et al.* Early clearance of *Mycobacterium tuberculosis* is associated with increased innate immune responses. *The Journal of infectious diseases* (2019).
35. Diagnostic Standards and Classification of Tuberculosis in Adults and Children. This official statement of the American Thoracic Society and the Centers for Disease Control and Prevention was adopted by the ATS Board of Directors, July 1999. This statement was endorsed by the Council of the Infectious Disease Society of America, September 1999. *American journal of respiratory and critical care medicine* **161**, 1376-1395 (2000).
36. Getahun, H., Matteelli, A., Chaisson, R.E. & Raviglione, M. Latent *Mycobacterium tuberculosis* infection. *The New England journal of medicine* **372**, 2127-2135 (2015).
37. Lillebaek, T., *et al.* Molecular evidence of endogenous reactivation of *Mycobacterium tuberculosis* after 33 years of latent infection. *The Journal of infectious diseases* **185**, 401-404 (2002).
38. Houben, R.M. & Dodd, P.J. The Global Burden of Latent Tuberculosis Infection: A Re-estimation Using Mathematical Modelling. *PLoS medicine* **13**, e1002152 (2016).
39. Ai, J.W., Ruan, Q.L., Liu, Q.H. & Zhang, W.H. Updates on the risk factors for latent tuberculosis reactivation and their managements. *Emerging microbes & infections* **5**, e10 (2016).
40. Elbek, O., *et al.* Increased risk of tuberculosis in patients treated with antitumor necrosis factor alpha. *Clinical rheumatology* **28**, 421-426 (2009).
41. Corbett, E.L., *et al.* HIV infection and silicosis: the impact of two potent risk factors on the incidence of mycobacterial disease in South African miners. *AIDS (London, England)* **14**, 2759-2768 (2000).
42. Andrews, J.R., *et al.* Risk of progression to active tuberculosis following reinfection with *Mycobacterium tuberculosis*. *Clinical infectious diseases : an official publication of the Infectious Diseases Society of America* **54**, 784-791 (2012).
43. Cadena, A.M., *et al.* Concurrent infection with *Mycobacterium tuberculosis* confers robust protection against secondary infection in macaques. *PLoS pathogens* **14**, e1007305 (2018).



44. Chiang, C.Y. & Riley, L.W. Exogenous reinfection in tuberculosis. *The Lancet. Infectious diseases* **5**, 629-636 (2005).
45. Ramakrishnan, L. Revisiting the role of the granuloma in tuberculosis. *Nature reviews. Immunology* **12**, 352-366 (2012).
46. Davis, J.M. & Ramakrishnan, L. The role of the granuloma in expansion and dissemination of early tuberculous infection. *Cell* **136**, 37-49 (2009).
47. Cadena, A.M., Fortune, S.M. & Flynn, J.L. Heterogeneity in tuberculosis. *Nature reviews. Immunology* **17**, 691-702 (2017).
48. Barry, C.E., 3rd, et al. The spectrum of latent tuberculosis: rethinking the biology and intervention strategies. *Nature reviews. Microbiology* **7**, 845-855 (2009).
49. Sutherland, I., Svandova, E. & Radhakrishna, S. The development of clinical tuberculosis following infection with tubercle bacilli. I. A theoretical model for the development of clinical tuberculosis following infection, linking from data on the risk of tuberculous infection and the incidence of clinical tuberculosis in the Netherlands. *Tubercle* **63**, 255-268 (1982).
50. Sloot, R., Schim van der Loeff, M.F., Kouw, P.M. & Borgdorff, M.W. Risk of tuberculosis after recent exposure. A 10-year follow-up study of contacts in Amsterdam. *American journal of respiratory and critical care medicine* **190**, 1044-1052 (2014).
51. Behr, M.A., Edelstein, P.H. & Ramakrishnan, L. Revisiting the timetable of tuberculosis. *Bmj* **362**, k2738 (2018).
52. Scordo, J.M., et al. The human lung mucosa drives differential Mycobacterium tuberculosis infection outcome in the alveolar epithelium. *Mucosal immunology* (2019).
53. Ackley, S.F., et al. Multiple exposures, reinfection and risk of progression to active tuberculosis. *R Soc Open Sci* **6**, 180999 (2019).
54. Harries, A.D., Lawn, S.D., Getahun, H., Zachariah, R. & Havlir, D.V. HIV and tuberculosis--science and implementation to turn the tide and reduce deaths. *J Int AIDS Soc* **15**, 17396-17396 (2012).
55. Ortblad, K.F., Salomon, J.A., Barnighausen, T. & Atun, R. Stopping tuberculosis: a biosocial model for sustainable development. *Lancet* **386**, 2354-2362 (2015).
56. Drain, P.K., et al. Incipient and Subclinical Tuberculosis: a Clinical Review of Early Stages and Progression of Infection. *Clinical microbiology reviews* **31**(2018).
57. Achkar, J.M. & Jenny-Avital, E.R. Incipient and subclinical tuberculosis: defining early disease states in the context of host immune response. *The Journal of infectious diseases* **204** Suppl 4, S1179-1186 (2011).
58. Figueiredo, A.A., Lucon, A.M. & Srougi, M. Urogenital Tuberculosis. *Microbiology spectrum* **5**(2017).
59. Mutyaba, A.K. & Ntsekhe, M. Tuberculosis and the Heart. *Cardiol Clin* **35**, 135-144 (2017).
60. Hill, M.K. & Sanders, C.V. Cutaneous Tuberculosis. *Microbiology spectrum* **5**(2017).
61. Dunn, R.N. & Ben Husien, M. Spinal tuberculosis: review of current management. *Bone Joint J* **100-b**, 425-431 (2018).
62. van Well, G.T., et al. Twenty years of pediatric tuberculous meningitis: a retrospective cohort study in the western cape of South Africa. *Pediatrics* **123**, e1-8 (2009).
63. Rock, R.B., Olin, M., Baker, C.A., Molitor, T.W. & Peterson, P.K. Central nervous system tuberculosis: pathogenesis and clinical aspects. *Clinical microbiology reviews* **21**, 243-261, table of contents (2008).
64. Donald, P.R., Schaaf, H.S. & Schoeman, J.F. Tuberculous meningitis and miliary tuberculosis: the Rich focus revisited. *The Journal of infection* **50**, 193-195 (2005).
65. DeLance, A.R., et al. Tuberculoma of the central nervous system. *Journal of clinical neuroscience : official journal of the Neurosurgical Society of Australasia* **20**, 1333-1341 (2013).
66. Thwaites, G.E., van Toorn, R. & Schoeman, J. Tuberculous meningitis: more questions, still too few answers. *The Lancet. Neurology* **12**, 999-1010 (2013).

67. Berenguer, J., et al. Tuberculous meningitis in patients infected with the human immunodeficiency virus. *The New England journal of medicine* **326**, 668-672 (1992).
68. Caws, M., et al. The influence of host and bacterial genotype on the development of disseminated disease with *Mycobacterium tuberculosis*. *PLoS pathogens* **4**, e1000034 (2008).
69. Sharma, S.K. & Mohan, A. Miliary Tuberculosis. *Microbiology spectrum* **5**(2017).
70. Bruns, H. & Stenger, S. New insights into the interaction of *Mycobacterium tuberculosis* and human macrophages. *Future microbiology* **9**, 327-341 (2014).
71. McClean, C.M. & Tobin, D.M. Macrophage form, function, and phenotype in mycobacterial infection: lessons from tuberculosis and other diseases. *Pathog Dis* **74**(2016).
72. Liu, P.T. & Modlin, R.L. Human macrophage host defense against *Mycobacterium tuberculosis*. *Current opinion in immunology* **20**, 371-376 (2008).
73. Blomgran, R., Desvignes, L., Briken, V. & Ernst, J.D. *Mycobacterium tuberculosis* inhibits neutrophil apoptosis, leading to delayed activation of naive CD4 T cells. *Cell host & microbe* **11**, 81-90 (2012).
74. Wolf, A.J., et al. *Mycobacterium tuberculosis* infects dendritic cells with high frequency and impairs their function in vivo. *Journal of immunology (Baltimore, Md. : 1950)* **179**, 2509-2519 (2007).
75. Hinchey, J., et al. Enhanced priming of adaptive immunity by a proapoptotic mutant of *Mycobacterium tuberculosis*. *The Journal of clinical investigation* **117**, 2279-2288 (2007).
76. Ottenhoff, T.H., Verreck, F.A., Hoeve, M.A. & van de Vosse, E. Control of human host immunity to mycobacteria. *Tuberculosis (Edinburgh, Scotland)* **85**, 53-64 (2005).
77. Bell, L.C.K. & Noursadeghi, M. Pathogenesis of HIV-1 and *Mycobacterium tuberculosis* co-infection. *Nature reviews. Microbiology* **16**, 80-90 (2018).
78. Solovic, I., et al. The risk of tuberculosis related to tumour necrosis factor antagonist therapies: a TBNET consensus statement. *The European respiratory journal* **36**, 1185-1206 (2010).
79. Ai, J.W., et al. The Risk of Tuberculosis in Patients with Rheumatoid Arthritis Treated with Tumor Necrosis Factor-alpha Antagonist: A Metaanalysis of Both Randomized Controlled Trials and Registry/Cohort Studies. *J Rheumatol* **42**, 2229-2237 (2015).
80. Meermeier, E.W. & Lewinsohn, D.M. Early clearance versus control: what is the meaning of a negative tuberculin skin test or interferon-gamma release assay following exposure to *Mycobacterium tuberculosis*? *FT1000Research* **7**(2018).
81. Lu, L.L., et al. A Functional Role for Antibodies in Tuberculosis. *Cell* **167**, 433-443.e414 (2016).
82. Roy Chowdhury, R., et al. A multi-cohort study of the immune factors associated with *M. tuberculosis* infection outcomes. *Nature* **560**, 644-648 (2018).
83. Lewinsohn, D.M. & Lewinsohn, D.A. New Concepts in Tuberculosis Host Defense. *Clin Chest Med* **40**, 703-719 (2019).
84. Goldberg, M.F., Saini, N.K. & Porcelli, S.A. Evasion of Innate and Adaptive Immunity by *Mycobacterium tuberculosis*. *Microbiology spectrum* **2**(2014).
85. Ehrh, S. & Schnappinger, D. Mycobacterial survival strategies in the phagosome: defence against host stresses. *Cellular microbiology* **11**, 1170-1178 (2009).
86. Almeida, A.S., et al. Tuberculosis is associated with a down-modulatory lung immune response that impairs Th1-type immunity. *Journal of immunology (Baltimore, Md. : 1950)* **183**, 718-731 (2009).
87. Redford, P.S., Murray, P.J. & O'Garra, A. The role of IL-10 in immune regulation during *M. tuberculosis* infection. *Mucosal immunology* **4**, 261-270 (2011).
88. Mogueche, A.O., et al. Antigen Availability Shapes T Cell Differentiation and Function during Tuberculosis. *Cell host & microbe* **21**, 695-706.e695 (2017).
89. Day, C.L., et al. Functional capacity of *Mycobacterium tuberculosis*-specific T cell responses in humans is associated with mycobacterial load. *Journal of immunology (Baltimore, Md. : 1950)* **187**, 2222-2232 (2011).



90. Clay, H., et al. Dichotomous role of the macrophage in early *Mycobacterium marinum* infection of the zebrafish. *Cell host & microbe* **2**, 29-39 (2007).
91. Comas, I., et al. Human T cell epitopes of *Mycobacterium tuberculosis* are evolutionarily hyperconserved. *Nature genetics* **42**, 498-503 (2010).
92. Steingart, K.R., et al. Fluorescence versus conventional sputum smear microscopy for tuberculosis: a systematic review. *The Lancet. Infectious diseases* **6**, 570-581 (2006).
93. Getahun, H., Harrington, M., O'Brien, R. & Nunn, P. Diagnosis of smear-negative pulmonary tuberculosis in people with HIV infection or AIDS in resource-constrained settings: informing urgent policy changes. *Lancet* **369**, 2042-2049 (2007).
94. Kunkel, A., et al. Smear positivity in paediatric and adult tuberculosis: systematic review and meta-analysis. *BMC infectious diseases* **16**, 282 (2016).
95. Boehme, C.C., et al. Rapid molecular detection of tuberculosis and rifampin resistance. *The New England journal of medicine* **363**, 1005-1015 (2010).
96. Horne, D.J., et al. Xpert MTB/RIF and Xpert MTB/RIF Ultra for pulmonary tuberculosis and rifampicin resistance in adults. *Cochrane Database Syst Rev* **6**, Cd009593 (2019).
97. Xie, Y.L., et al. Evaluation of a Rapid Molecular Drug-Susceptibility Test for Tuberculosis. *The New England journal of medicine* **377**, 1043-1054 (2017).
98. Xpert MTB/RIF assay for the diagnosis of pulmonary and extrapulmonary TB in adults and children. Geneva; World Health Organization. (2013).
99. Peter, J.G., et al. Effect on mortality of point-of-care, urine-based lipoarabinomannan testing to guide tuberculosis treatment initiation in HIV-positive hospital inpatients: a pragmatic, parallel-group, multicountry, open-label, randomised controlled trial. *Lancet* **387**, 1187-1197 (2016).
100. Miller, C., Lonroth, K., Sotgiu, G. & Migliori, G.B. The long and winding road of chest radiography for tuberculosis detection. *The European respiratory journal* **49**(2017).
101. Chest radiography in tuberculosis detection; summary of current WHO recommendations and guidance on programmatic approaches. Geneva: World Health Organization. (2016).
102. Skoura, E., Zumla, A. & Bomanji, J. Imaging in tuberculosis. *International journal of infectious diseases : IJID : official publication of the International Society for Infectious Diseases* **32**, 87-93 (2015).
103. Ankrah, A.O., et al. Tuberculosis. *Semin Nucl Med* **48**, 108-130 (2018).
104. VON PIRQUET, C. FREQUENCY OF TUBERCULOSIS IN CHILDHOOD. *Jama* **LII**, 675-678 (1909).
105. Farhat, M., Greenaway, C., Pai, M. & Menzies, D. False-positive tuberculin skin tests: what is the absolute effect of BCG and non-tuberculous mycobacteria? *The international journal of tuberculosis and lung disease : the official journal of the International Union against Tuberculosis and Lung Disease* **10**, 1192-1204 (2006).
106. Pai, M. & Behr, M. Latent *Mycobacterium tuberculosis* Infection and Interferon-Gamma Release Assays. *Microbiology spectrum* **4**(2016).
107. Latent tuberculosis infection: updated and consolidated guidelines for programmatic management. Geneva: World Health Organization. (2018).
108. Calmette, A. Preventive Vaccination Against Tuberculosis with BCG. *Proc R Soc Med* **24**, 1481-1490 (1931).
109. Trunz, B.B., Fine, P. & Dye, C. Effect of BCG vaccination on childhood tuberculous meningitis and military tuberculosis worldwide: a meta-analysis and assessment of cost-effectiveness. *Lancet* **367**, 1173-1180 (2006).
110. Aaby, P., et al. Randomized trial of BCG vaccination at birth to low-birth-weight children: beneficial nonspecific effects in the neonatal period? *The Journal of infectious diseases* **204**, 245-252 (2011).

111. Mangtani, P., et al. Protection by BCG vaccine against tuberculosis: a systematic review of randomized controlled trials. *Clinical infectious diseases : an official publication of the Infectious Diseases Society of America* **58**, 470-480 (2014).
112. Andersen, P. & Scriba, T.J. Moving tuberculosis vaccines from theory to practice. *Nature reviews. Immunology* **19**, 550-562 (2019).
113. Sable, S.B., Posey, J.E. & Scriba, T.J. Tuberculosis Vaccine Development: Progress in Clinical Evaluation. *Clinical microbiology reviews* **33**(2019).
114. Knight, G.M., et al. Impact and cost-effectiveness of new tuberculosis vaccines in low- and middle-income countries. *Proceedings of the National Academy of Sciences of the United States of America* **111**, 15520-15525 (2014).
115. Hawn, T.R., et al. Tuberculosis vaccines and prevention of infection. *Microbiology and molecular biology reviews* : *MMBR* **78**, 650-671 (2014).
116. Nemes, E., et al. Prevention of M. tuberculosis infection with H4:IC31 Vaccine or BCG Revaccination. *The New England journal of medicine* **379**, 138-149 (2018).
117. Verver, S., et al. Rate of reinfection tuberculosis after successful treatment is higher than rate of new tuberculosis. *American journal of respiratory and critical care medicine* **171**, 1430-1435 (2005).
118. Darrah, P.A., et al. Multifunctional TH1 cells define a correlate of vaccine-mediated protection against *Leishmania major*. *Nature medicine* **13**, 843-850 (2007).
119. Tameris, M.D., et al. Safety and efficacy of MVA85A, a new tuberculosis vaccine, in infants previously vaccinated with BCG: a randomised, placebo-controlled phase 2b trial. *Lancet* **381**, 1021-1028 (2013).
120. McShane, H. Insights and challenges in tuberculosis vaccine development. *The Lancet. Respiratory medicine* (2019).
121. Khader, S.A., et al. Targeting innate immunity for tuberculosis vaccination. *The Journal of clinical investigation* **129**, 3482-3491 (2019).
122. Tchilian, E.Z., et al. Simultaneous immunization against tuberculosis. *PLoS one* **6**, e27477 (2011).
123. Aguilo, N., et al. Pulmonary but Not Subcutaneous Delivery of BCG Vaccine Confers Protection to Tuberculosis-Susceptible Mice by an Interleukin 17-Dependent Mechanism. *The Journal of infectious diseases* **213**, 831-839 (2016).
124. Verreck, F.A.W., et al. Variable BCG efficacy in rhesus populations: Pulmonary BCG provides protection where standard intra-dermal vaccination fails. *Tuberculosis (Edinburgh, Scotland)* **104**, 46-57 (2017).
125. Chen, L., Wang, J., Zganiacz, A. & Xing, Z. Single intranasal mucosal *Mycobacterium bovis* BCG vaccination confers improved protection compared to subcutaneous vaccination against pulmonary tuberculosis. *Infection and immunity* **72**, 238-246 (2004).
126. Hoft, D.F., et al. PO and ID BCG vaccination in humans induce distinct mucosal and systemic immune responses and CD4(+) T cell transcriptomal molecular signatures. *Mucosal immunology* **11**, 486-495 (2018).
127. Davids, M., et al. A Human Lung Challenge Model to Evaluate the Safety and Immunogenicity of PPD and Live BCG. *American journal of respiratory and critical care medicine* (2019).
128. Arbues, A., et al. Construction, characterization and preclinical evaluation of MTBVAC, the first live-attenuated M. tuberculosis-based vaccine to enter clinical trials. *Vaccine* **31**, 4867-4873 (2013).
129. Marinova, D., Gonzalo-Asensio, J., Aguilo, N. & Martin, C. MTBVAC from discovery to clinical trials in tuberculosis-endemic countries. *Expert review of vaccines* **16**, 565-576 (2017).
130. Kaufmann, S.H., et al. The BCG replacement vaccine VPM1002: from drawing board to clinical trial. *Expert review of vaccines* **13**, 619-630 (2014).
131. Scriba, T.J., et al. Vaccination Against Tuberculosis With Whole-Cell Mycobacterial Vaccines. *The Journal of infectious diseases* **214**, 659-664 (2016).



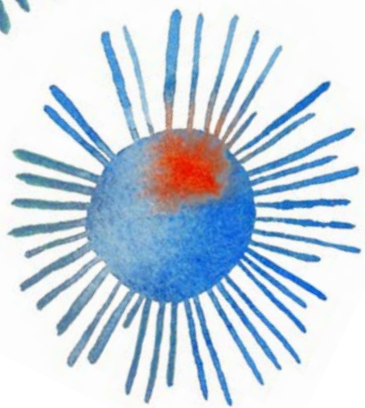
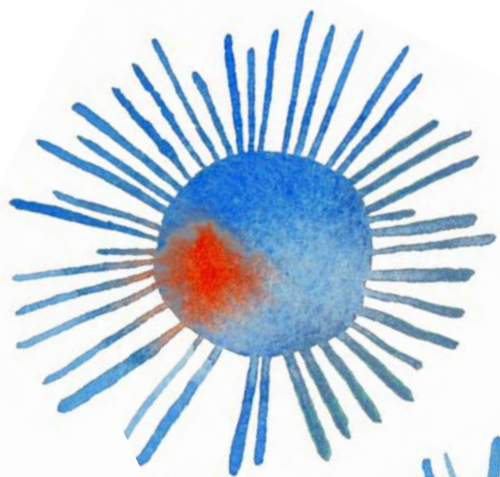
132. Nieuwenhuizen, N.E. & Kaufmann, S.H.E. Next-Generation Vaccines Based on Bacille Calmette-Guerin. *Front Immunol* **9**, 121 (2018).
133. von Reyn, C.F., *et al.* Safety and immunogenicity of an inactivated whole cell tuberculosis vaccine booster in adults primed with BCG: A randomized, controlled trial of DAR-901. *PLoS one* **12**, e0175215 (2017).
134. Sharma, S.K., *et al.* Efficacy and Safety of Mycobacterium indicus pranii as an adjunct therapy in Category II pulmonary tuberculosis in a randomized trial. *Sci Rep* **7**, 3354 (2017).
135. Mayosi, B.M., *et al.* Prednisolone and Mycobacterium indicus pranii in tuberculous pericarditis. *The New England journal of medicine* **371**, 1121-1130 (2014).
136. Voskuil, M.I., *et al.* Inhibition of Respiration by Nitric Oxide Induces a Mycobacterium tuberculosis Dormancy Program. *The Journal of experimental medicine* **198**, 705-713 (2003).
137. Commandeur, S., *et al.* An Unbiased Genome-Wide Mycobacterium tuberculosis Gene Expression Approach To Discover Antigens Targeted by Human T Cells Expressed during Pulmonary Infection. *The Journal of Immunology* **190**, 1659 (2013).
138. Tait, D.R., *et al.* Final Analysis of a Trial of M72/AS01E Vaccine to Prevent Tuberculosis. *New England Journal of Medicine* (2019).
139. Hansen, S.G., *et al.* Prevention of tuberculosis in rhesus macaques by a cytomegalovirus-based vaccine. *Nature medicine* **24**, 130-143 (2018).
140. Pipeline of TB vaccines. October 2019. *Tuberculosis Vaccine Initiative (TBVI)* (<https://www.tbvi.eu/what-we-do/pipeline-of-vaccines/>).
141. Gibson, S.E.R., Harrison, J. & Cox, J.A.G. Modelling a Silent Epidemic: A Review of the In Vitro Models of Latent Tuberculosis. *Pathogens (Basel, Switzerland)* **7**(2018).
142. Pennisi, M., *et al.* Predicting the artificial immunity induced by RUTI(R) vaccine against tuberculosis using universal immune system simulator (UISS). *BMC Bioinformatics* **20**, 504 (2019).
143. Clark, S., Hall, Y. & Williams, A. Animal models of tuberculosis: Guinea pigs. *Cold Spring Harbor perspectives in medicine* **5**, a018572 (2014).
144. Manabe, Y.C., *et al.* The aerosol rabbit model of TB latency, reactivation and immune reconstitution inflammatory syndrome. *Tuberculosis (Edinburgh, Scotland)* **88**, 187-196 (2008).
145. Sugawara, I., Yamada, H. & Mizuno, S. Pathological and immunological profiles of rat tuberculosis. *Int J Exp Pathol* **85**, 125-134 (2004).
146. Basaraba, R.J., *et al.* Lymphadenitis as a major element of disease in the guinea pig model of tuberculosis. *Tuberculosis (Edinburgh, Scotland)* **86**, 386-394 (2006).
147. Nedeltchev, G.G., *et al.* Extrapulmonary dissemination of Mycobacterium bovis but not Mycobacterium tuberculosis in a bronchoscopic rabbit model of cavitary tuberculosis. *Infection and immunity* **77**, 598-603 (2009).
148. Dionne, M.S., Ghori, N. & Schneider, D.S. Drosophila melanogaster is a genetically tractable model host for Mycobacterium marinum. *Infection and immunity* **71**, 3540-3550 (2003).
149. Solomon, J.M., Leung, G.S. & Isberg, R.R. Intracellular replication of Mycobacterium marinum within Dictyostelium discoideum: efficient replication in the absence of host coronin. *Infection and immunity* **71**, 3578-3586 (2003).
150. Li, Y., *et al.* Galleria mellonella - a novel infection model for the Mycobacterium tuberculosis complex. *Virulence* **9**, 1126-1137 (2018).
151. Buddle, B.M., Vordermeier, H.M. & Hewinson, R.G. Experimental Infection Models of Tuberculosis in Domestic Livestock. *Microbiology spectrum* **4**(2016).
152. Corner, L.A., *et al.* Experimental tuberculosis in the European badger (Meles meles) after endobronchial inoculation of Mycobacterium bovis: I. Pathology and bacteriology. *Res Vet Sci* **83**, 53-62 (2007).
153. McCallan, L., *et al.* A New Experimental Infection Model in Ferrets Based on Aerosolised Mycobacterium bovis. *Vet Med Int* **2011**, 981410-981410 (2011).

154. Van Rhijn, I., Godfroid, J., Michel, A. & Rutten, V. Bovine tuberculosis as a model for human tuberculosis: advantages over small animal models. *Microbes Infect* **10**, 711-715 (2008).
155. van Leeuwen, L.M., van der Sar, A.M. & Bitter, W. Animal models of tuberculosis: zebrafish. *Cold Spring Harbor perspectives in medicine* **5**, a018580 (2014).
156. Davis, J.M., et al. Real-time visualization of mycobacterium-macrophage interactions leading to initiation of granuloma formation in zebrafish embryos. *Immunity* **17**, 693-702 (2002).
157. Torraca, V., Masud, S., Spaink, H.P. & Meijer, A.H. Macrophage-pathogen interactions in infectious diseases: new therapeutic insights from the zebrafish host model. *Dis Model Mech* **7**, 785-797 (2014).
158. Ramakrishnan, L. Looking within the zebrafish to understand the tuberculous granuloma. *Advances in experimental medicine and biology* **783**, 251-266 (2013).
159. Carvalho, R., et al. A high-throughput screen for tuberculosis progression. *PLoS one* **6**, e16779 (2011).
160. Oksanen, K.E., et al. An adult zebrafish model for preclinical tuberculosis vaccine development. *Vaccine* **31**, 5202-5209 (2013).
161. Rivalde, M.A., et al. Control of mycobacteriosis in zebrafish (*Danio rerio*) mucosally vaccinated with heat-inactivated *Mycobacterium bovis*. *Vaccine* (2018).
162. Tobin, D.M. & Ramakrishnan, L. Comparative pathogenesis of *Mycobacterium marinum* and *Mycobacterium tuberculosis*. *Cellular microbiology* **10**, 1027-1039 (2008).
163. Meijer, A.H. Protection and pathology in TB: learning from the zebrafish model. *Seminars in immunopathology* **38**, 261-273 (2016).
164. Swaim, L.E., et al. *Mycobacterium marinum* infection of adult zebrafish causes caseating granulomatous tuberculosis and is moderated by adaptive immunity. *Infection and immunity* **74**, 6108-6117 (2006).
165. van der Sar, A.M., et al. *Mycobacterium marinum* strains can be divided into two distinct types based on genetic diversity and virulence. *Infection and immunity* **72**, 6306-6312 (2004).
166. Bucsan, A.N., Mehra, S., Khader, S.A. & Kaushal, D. The current state of animal models and genomic approaches towards identifying and validating molecular determinants of *Mycobacterium tuberculosis* infection and tuberculosis disease. *Pathog Dis* **77**(2019).
167. Cooper, A.M. Mouse model of tuberculosis. *Cold Spring Harbor perspectives in medicine* **5**, a018556 (2014).
168. De Groote, M.A., et al. Comparative studies evaluating mouse models used for efficacy testing of experimental drugs against *Mycobacterium tuberculosis*. *Antimicrob Agents Chemother* **55**, 1237-1247 (2011).
169. Cardona, P.J. & Williams, A. Experimental animal modelling for TB vaccine development. *International journal of infectious diseases : IJID : official publication of the International Society for Infectious Diseases* **56**, 268-273 (2017).
170. Medina, E. & North, R.J. Resistance ranking of some common inbred mouse strains to *Mycobacterium tuberculosis* and relationship to major histocompatibility complex haplotype and *Nramp1* genotype. *Immunology* **93**, 270-274 (1998).
171. Kramnik, I. & Beamer, G. Mouse models of human TB pathology: roles in the analysis of necrosis and the development of host-directed therapies. *Seminars in immunopathology* **38**, 221-237 (2016).
172. Verma, S., et al. Transmission phenotype of *Mycobacterium tuberculosis* strains is mechanistically linked to induction of distinct pulmonary pathology. *PLoS pathogens* **15**, e1007613 (2019).
173. Flynn, J.L. Lessons from experimental *Mycobacterium tuberculosis* infections. *Microbes Infect* **8**, 1179-1188 (2006).
174. Young, S.L., et al. Environmental strains of *Mycobacterium avium* interfere with immune responses associated with *Mycobacterium bovis* BCG vaccination. *Infection and immunity* **75**, 2833-2840 (2007).



175. Beura, L.K., *et al.* Normalizing the environment recapitulates adult human immune traits in laboratory mice. *Nature* **532**, 512-516 (2016).
176. Noll, K.E., Ferris, M.T. & Heise, M.T. The Collaborative Cross: A Systems Genetics Resource for Studying Host-Pathogen Interactions. *Cell host & microbe* **25**, 484-498 (2019).
177. Churchill, G.A., Gatti, D.M., Munger, S.C. & Svenson, K.L. The Diversity Outbred mouse population. *Mamm Genome* **23**, 713-718 (2012).
178. Smith, C.M., *et al.* Tuberculosis Susceptibility and Vaccine Protection Are Independently Controlled by Host Genotype. *mBio* **7**, e01516-01516 (2016).
179. Niazi, M.K., *et al.* Lung necrosis and neutrophils reflect common pathways of susceptibility to *Mycobacterium tuberculosis* in genetically diverse, immune-competent mice. *Dis Model Mech* **8**, 1141-1153 (2015).
180. Harper, J., *et al.* Mouse model of necrotic tuberculosis granulomas develops hypoxic lesions. *The Journal of infectious diseases* **205**, 595-602 (2012).
181. Foreman, T.W., Mehra, S., Lackner, A.A. & Kaushal, D. Translational Research in the Nonhuman Primate Model of Tuberculosis. *Ilar j* **58**, 151-159 (2017).
182. Pena, J.C. & Ho, W.Z. Monkey models of tuberculosis: lessons learned. *Infection and immunity* **83**, 852-862 (2015).
183. Panarella, M.L. & Bimes, R.S. A naturally occurring outbreak of tuberculosis in a group of imported cynomolgus monkeys (*Macaca fascicularis*). *Journal of the American Association for Laboratory Animal Science : JAALAS* **49**, 221-225 (2010).
184. Matz-Rensing, K., *et al.* Outbreak of Tuberculosis in a Colony of Rhesus Monkeys (*Macaca mulatta*) after Possible Indirect Contact with a Human TB Patient. *Journal of comparative pathology* **153**, 81-91 (2015).
185. Verreck, F.A., *et al.* MVA.85A boosting of BCG and an attenuated, *phoP* deficient M. tuberculosis vaccine both show protective efficacy against tuberculosis in rhesus macaques. *PloS one* **4**, e5264 (2009).
186. Schmidt, L.H. Studies on the antituberculous activity of ethambutol in monkeys. *Ann N Y Acad Sci* **135**, 747-758 (1966).
187. Barclay, W.R., Anacker, R.L., Brehmer, W., Leif, W. & Ribi, E. Aerosol-Induced Tuberculosis in Subhuman Primates and the Course of the Disease After Intravenous BCG Vaccination. *Infection and immunity* **2**, 574-582 (1970).
188. Scanga, C.A. & Flynn, J.L. Modeling tuberculosis in nonhuman primates. *Cold Spring Harbor perspectives in medicine* **4**, a018564 (2014).
189. Walsh, G.P., *et al.* The Philippine cynomolgus monkey (*Macaca fascicularis*) provides a new nonhuman primate model of tuberculosis that resembles human disease. *Nature medicine* **2**, 430-436 (1996).
190. Maiello, P., *et al.* Rhesus macaques are more susceptible to progressive tuberculosis than cynomolgus macaques: A quantitative comparison. *Infection and immunity* (2017).
191. Sharpe, S., *et al.* Ultra low dose aerosol challenge with *Mycobacterium tuberculosis* leads to divergent outcomes in rhesus and cynomolgus macaques. *Tuberculosis (Edinburgh, Scotland)* **96**, 1-12 (2016).
192. Capuano, S.V., 3rd, *et al.* Experimental *Mycobacterium tuberculosis* infection of cynomolgus macaques closely resembles the various manifestations of human M. tuberculosis infection. *Infection and immunity* **71**, 5831-5844 (2003).
193. Mehra, S., *et al.* Reactivation of latent tuberculosis in rhesus macaques by coinfection with simian immunodeficiency virus. *Journal of medical primatology* **40**, 233-243 (2011).
194. Diedrich, C.R., *et al.* Reactivation of latent tuberculosis in cynomolgus macaques infected with SIV is associated with early peripheral T cell depletion and not virus load. *PloS one* **5**, e9611 (2010).

195. Lin, P.L., *et al.* The multistage vaccine H56 boosts the effects of BCG to protect cynomolgus macaques against active tuberculosis and reactivation of latent Mycobacterium tuberculosis infection. *The Journal of clinical investigation* **122**, 303-314 (2012).
196. Sharpe, S.A., *et al.* An aerosol challenge model of tuberculosis in Mauritian cynomolgus macaques. *PLoS one* **12**, e0171906 (2017).
197. Safi, H., *et al.* Spectrum of manifestations of Mycobacterium tuberculosis infection in primates infected with SIV. *AIDS research and human retroviruses* **19**, 585-595 (2003).
198. Bucsan, A.N., *et al.* Mechanisms of reactivation of latent tuberculosis infection due to SIV coinfection. *The Journal of clinical investigation* (2019).
199. Jensen, K., *et al.* A recombinant attenuated Mycobacterium tuberculosis vaccine strain is safe in immunosuppressed simian immunodeficiency virus-infected infant macaques. *Clinical and vaccine immunology : CVI* **19**, 1170-1181 (2012).
200. Cadena, A.M., *et al.* Very Low Doses of Mycobacterium tuberculosis Yield Diverse Host Outcomes in Common Marmosets (*Callithrix jacchus*). *Comparative medicine* **66**, 412-419 (2016).
201. Via, L.E., *et al.* Differential virulence and disease progression following Mycobacterium tuberculosis complex infection of the common marmoset (*Callithrix jacchus*). *Infection and immunity* **81**, 2909-2919 (2013).
202. Roederer, M. Parsimonious Determination of the Optimal Infectious Dose of a Pathogen for Nonhuman Primate Models. *PLoS pathogens* **11**, e1005100 (2015).
203. Aguilo, N., *et al.* Reactogenicity to major tuberculosis antigens absent in BCG is linked to improved protection against Mycobacterium tuberculosis. *Nature communications* **8**, 16085 (2017).
204. Lubbers, R., *et al.* Complement Component C1q as Serum Biomarker to Detect Active Tuberculosis. *Front Immunol* **9**, 2427 (2018).



Disparate tuberculosis disease development in macaque species is associated with innate immunity



Karin Dijkman¹, Richard A.W. Vervenne¹, Claudia C. Sombroek¹, Charelle Boot¹, Sam O. Hofman¹, Krista E. van Meijgaarden², Tom H.M. Ottenhoff², Clemens H.M. Kocken¹, Krista G. Haanstra¹, Michel P.M. Vierboom¹, Frank A.W. Verreck¹.

¹ from the TB research group, department of Parasitology, Biomedical Primate Research Centre (BPRC), Rijswijk the Netherlands

² from the department of Infectious Diseases, Leiden University Medical Centre (LUMC), Leiden, the Netherlands

Published in Frontiers of Immunology, 1 November 2019

Abstract

While tuberculosis continues to afflict mankind, the immunological mechanisms underlying TB disease development are still incompletely understood. Advanced preclinical models for TB research include both rhesus and cynomolgus macaques (*Macaca mulatta* and *Macaca fascicularis*, respectively), with rhesus typically being more susceptible to acute progressive TB disease than cynomolgus macaques. To determine which immune mechanisms are responsible for this dissimilar disease development, we profiled a broad range of innate and adaptive responses, both local and peripheral, following experimental pulmonary *Mtb* infection of both species. While T-cell and antibody responses appeared indistinguishable, we identified anti-inflammatory skewing of peripheral monocytes in rhesus and a more prominent local pro-inflammatory cytokine release profile in cynomolgus macaques associated with divergent TB disease outcome. Importantly, these differences were detectable both before and early after infection. This work shows that inflammatory and innate immune status prior to and at early stages after infection, critically affects outcome of TB infection.

Introduction

Tuberculosis (TB), primarily caused by infection with *Mycobacterium tuberculosis* (*Mtb*) or one of the related *Mtb*-complex species, remains the leading cause of death from a single infectious agent. Annually, over 1.5 million individuals die of tuberculosis and an estimated 10 million people develop TB disease¹. Although it is assumed that some individuals are able to resist *Mtb* infection upfront, typically, successful infection can lead to acute progressive disease. The majority of infected individuals however, will control the invading *Mycobacterium* to an extent where there is no overt disease manifestation. Although it is appreciated that within an asymptomatic individual *Mtb* infection is dynamic rather than static, and that asymptomatic infection could be further differentiated into distinctive states²⁻⁴, the majority of asymptotically infected individuals establish a condition that can be referred to as latent TB infection (LTBI). By estimation, approximately a quarter of the world's population carries a latent *Mtb* infection⁵.

Disease manifestation after *Mtb* infection is diverse, as are the dynamics of the underlying host-pathogen interactions. There is a growing range of cellular and molecular host defense and inflammatory signaling associated with anti-mycobacterial immunity and TB pathogenesis, which, therefore, is likely to affect the outcome of *Mtb* infection^{3,6-8}. Despite the increasing knowledge base, we are still unable to accurately diagnose and predict who is at risk of developing TB disease and who will be able to control infection. Classically, T-lymphocyte derived IFN γ is recognized as an essential component of an effective antimycobacterial response and is harnessed in TB diagnostics in *Mtb*-specific IFN γ Release Assays (IGRA). Likewise, TNF α and its



receptor mediated signaling are known as a critical component of effective anti-*Mtb* immunity, while recently we and others have found evidence of a possible role of IL17A in protection from TB infection and disease⁹⁻¹¹. However, it is becoming increasingly clear that (peripheral) adaptive T-cell immune analysis on its own is likely to be insufficient to provide sufficiently accurate correlates of protective immunity against TB^{3,6-8}. Rather, a comprehensive temporal and spatial analysis of innate in addition to adaptive host response characteristics might allow identification of factors that differentiate between those at risk of active disease versus individuals that will develop TB disease tolerance¹².

While animal models play an important role in the preclinical research and development process of new TB vaccines and therapies, they also provide great opportunity for studying immune correlates and disease mechanisms. Macaque (*Macaca spp.*) models of TB in particular recapitulate many key aspects of TB disease in humans¹³⁻¹⁵. Cynomolgus macaques (*M. fascicularis*) and rhesus macaques (*M. mulatta*) are both used to study *Mtb* infection, but, while phylogenetically closely related, they differ significantly in their response to mycobacterial infection. In an earlier report it was shown that, in a high-dose *Mtb* challenge experiment, the efficacy of Bacillus Calmette-Guerin (BCG) vaccination differed between the two species, with vaccination conferring better protection to cynomolgus macaques¹⁶. Subsequently, the reduced susceptibility to the development of TB-associated pathology after experimental *Mtb* infection of cynomolgus macaques compared to rhesus macaques was further established^{17,18}. Furthermore, latent TB infection, which in these animals is characterized by sustained absence of clinical disease parameters and bacteria in bronchoalveolar or gastric lavage, occurs in approximately half of cynomolgus macaques upon low dose infection with 25 to 50 colony forming units (CFU) of *Mtb*¹⁹. Development of LTBI in rhesus macaques, however, has not been reported yet. A notable exception to these findings is the Mauritian cynomolgus macaque, a genetically distinct population of cynomolgus macaques with limited major histocompatibility complex (MHC) diversity, which appear to be equally susceptible to TB disease as rhesus macaques^{18,20}.

The difference in TB disease susceptibility between rhesus and cynomolgus macaques has been well-described and, yet, the host response mechanisms that determine this differential outcome of *Mtb* infection are poorly understood. To the best of our knowledge, only two studies compared rhesus and cynomolgus macaques head-to-head for their susceptibility to disease after *Mtb* challenge^{17,18}. In one of these studies a comparative immune analysis between the two species was reported, which however, was limited to a reduced IFN γ response signal from peripheral blood mononuclear cells (PBMC) in association with reduced TB disease severity. Furthermore, it remains unresolved if there is a difference in susceptibility to *Mtb* infection as well.

In the study reported here, we sought to identify the minimal infectious dose²¹ for either of the species, while simultaneously profiling both peripheral as well as local adaptive and innate immune responses, to identify responses associated with and

possibly predicting differential susceptibility to TB disease. We show comparable time and dose response dynamics to infectious *Mtb* challenge and corroborate the differential disease susceptibility between the two species. Most importantly, our immune analysis shows that rhesus macaques display anti-inflammatory monocyte skewing in the periphery, while cynomolgus macaques show a higher production of inflammatory cytokines locally, prior to and early after *Mtb* exposure.

This suggests that early orchestration of pro-and anti-inflammatory innate responses are underlying the distinctive TB disease development between cynomolgus and rhesus macaques after low dose *Mtb* infection, providing important insights in immune correlates of susceptibility to TB disease as well as mechanisms of early control of *Mtb* infection.

Results

Infection take after repeated exposure to increasing doses of *Mtb*

Cynomolgus and rhesus macaques present with differential susceptibility to pathology after *Mtb* infection. To investigate if the two species also differ in susceptibility to infection, we designed a dose-escalation study. Animals (n=10 per species) were exposed to increasing doses of *Mtb* strain Erdman K01 by endobronchial installation and monitored for success of infectious challenge at regular intervals. By study design, challenge events were planned at 4 weeks intervals and whether infectious challenge was successful was monitored 3 weeks after each *Mtb* instillation (based on previous *Mtb* challenge studies²²). As a surrogate for successful infection, hereafter referred to as infection-take, we used a negative to positive conversion in an Interferon Gamma Release Assay (IGRA), in this case a NHP-specific IFN γ ELISPOT lab test to be specific. The threshold for IGRA conversion was set at the average pre-infection response to *Mtb* Purified Protein Derivate (PPD) or ESAT6-CFP10 fusion-protein plus three times the standard deviation (in this case, 50 spots per million cells). When no infection-take was observed 3 weeks after challenge, by study design, animals were exposed to a 5-fold increased dose of *Mtb* the following week (**Figure 1a**). At the same time, another ELISPOT was performed at that point, again, to monitor (delayed) infection-take. Exposure to *Mtb* was repeated until all animals had an established infection. When ≥ 5 animals IGRA converted after a given dose of *Mtb*, that cohort was divided in two and sacrificed either 6 or 12 weeks after infection, to compare “early” versus “late” stage pathology and immunology.

The initial challenge dose was set at less than a single colony forming unit (CFU) of *Mtb* per dose (on average) to ensure we would capture a condition at which infection-take was a matter of chance. After administration of a calculated average of 0.2 CFU, none of the animals showed conversion to IGRA positivity (**Figure 1b**). After the subsequent, increased challenge with a calculated average of 1.3 CFU of *Mtb*, IGRA conversion occurred in half of the animals of both species at 3 weeks post-challenge. One week later, an additional 3 rhesus macaques and 1 cynomolgus

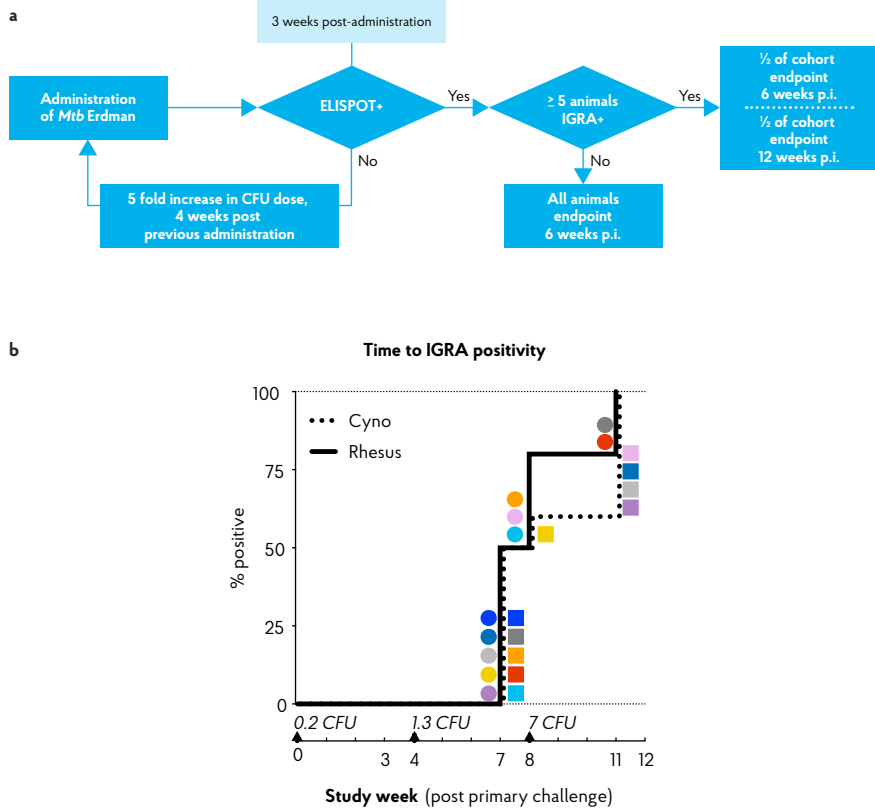












Figure 1. *Mtb* dose escalation challenge in cynomolgus and rhesus macaques. **a**) Schematic representation of the minimal *Mtb* dose-finding strategy applied in this study. Rhesus and cynomolgus macaques, $n=10$ each, were endobronchially challenged with an initial dose of 0.2 CFU of *Mtb* strain Erdman, after which infection take was determined by means of an *Mtb* specific IFN γ ELISPOT. Non-infected (read: IGRA-) animals were challenged with an increasing dose of *Mtb* until ELISPOT-positivity was obtained. ELISPOT-positive animals were randomly assigned and sacrificed either at 6 ($n=6$ per species) or 12 weeks ($n=4$ per species) after infectious *Mtb* exposure. **b**) Kaplan-Meier curve depicting the rate of IFN γ ELISPOT positivity/IGRA conversion. *Mtb* challenge events are indicated by triangles along the x-axis, accompanied by the calculated (extrapolated) challenge dose, verified by quality control plating. Squares represent individual cynomolgus macaques, circles represent individual rhesus macaques. Colour coding per individual, as defined in Table 1, is consistently applied throughout.

macaque converted to IGRA+. In accordance with the study design, these latter animals had received the next dose of 7 CFU of *Mtb* at that time point. Thus, these four animals are formally considered to be “superinfected”. Additionally, one IGRA+ cynomolgus macaque reverted to become IGRA- (C9, dark grey). As this transient IGRA+ animal had met the pre-defined criteria for infection, it was treated as such for the remainder of the study and, therefore, did not receive additional doses of *Mtb*. All remaining IGRA- animals (2 rhesus and 4 cynomolgus) became IGRA+ after the third exposure event to 7 CFU of *Mtb*. An overview of the infectious dose and time of IGRA conversion per animal is given in **Table 1**. With the exception of the one reverting cynomolgus macaque (C9, dark grey) all animals remained IGRA+ from their conversion time point onward. Statistical analysis of the rate of IGRA conversion revealed no significant difference in conversion dynamics between cynomolgus and rhesus macaques. Although sample size (n=10 per species) was limited, the data suggest that both species are similarly susceptible to *Mtb* infection, as measured by IGRA conversion.

	Cynomolgus									
Animal identifier	C.1	C.2	C.3	C.4	C.5	C.6	C.7	C.8	C.9	C.10
Symbol										
Infectious dose	7	1	7	1	1	7	7	1	1	1
IGRA+ at week	11	8	11	7	7	11	11	7	7	7
Superinfected	-	+	-	-	-	-	-	-	-	-
Sacrificed at week	12	6	12	6	12	6	6	6	12	6











	Rhesus									
Animal identifier	R.1	R.2	R.3	R.4	R.5	R.6	R.7	R.8	R.9	R.10
Symbol										
Infectious dose	1	1	1	1	7	1	1	1	7	1
IGRA+ at week	7	7	7	8	11	7	8	8	11	7
Superinfected	-	-	-	+	-	-	+	+	-	-
Sacrificed at week	6	6	6	6	12	12	6	6	12	12

Table 1. Infection characteristics after dose-escalation *Mtb* administration for each individual. Overview of infectious challenge dose in CFU that led to IGRA conversion, week of IGRA conversion, occurrence of superinfection and time to sacrifice for each individual animal. Infectious dose given as number of CFU, “+” indicates superinfected animals



Tuberculosis disease and bacterial load after low dose *Mtb* challenge

By study design, endpoint of post-infection follow-up was set at 6 weeks (n=6/species) or 12 weeks (n=4/species) after the challenge that resulted in IGRA conversion. This approach enabled host response profiling at an “early” and “later” time point (see **Table 1** for time of sacrifice for each animal). For data analysis, the animals “superinfected” with 7 CFU were kept in the same arm of study design and analysis as the animals that converted after 7 CFU. At endpoint, macroscopic TB pathology in lungs, lung draining lymph nodes and extra-thoracic organs was scored by using a predefined, arbitrary scoring algorithm based on lesion size, appearance and frequency.

Quantification revealed a significantly higher level of pathology in the lungs of rhesus as compared to cynomolgus monkeys, both in the primary targeted lung lobe, the site of endobronchial instillation, as well as in the secondary lung lobes as a measure of intrapulmonary dissemination (**Figure 2a & 2b**). This species difference in lung pathology was already apparent 6 weeks after infection ($p=0.013$ for primary lobe pathology, **Supplemental Figure 1a**). While median lung pathology scores appeared higher 12 weeks post-infection compared to 6 weeks post-infection in both species, group sizes were too small to establish statistical significance of this increase. Interestingly, pathology of lung draining lymph nodes did not differ between the two species (**Figure 2c**). Extra-thoracic pathology was observed in an equal number of rhesus and cynomolgus macaques (5 versus 5, **Figure 2d**), and primarily affected liver and spleen. When present, cynomolgus monkeys generally exhibited more severe extra-thoracic pathology. The different infectious doses (1.3 versus 7 CFU), regardless of species, were not found to be associated with pathology levels.

Mtb tissue burden was quantified by plating homogenates of specific lesions sampled from the primary, targeted lung lobe, the remainder of the primary lobe, the pooled secondary lobes, and the lung draining lymph nodes. When assessing *Mtb* burden in granulomas isolated from the targeted lung lobe, we did not detect a difference in CFU between the two species (**Figure 2e**), as described previously¹⁸. However, bacterial burden in the remainder of the primary lobe as well as the secondary lung lobes trended to be lower in the cynomolgus macaques compared to the rhesus macaques, in accordance with the extent of observed lung pathology (**Figure 2f & 2g**). CFU counts from lung draining lymph nodes did not differ between groups (**Figure 2h**). The cynomolgus macaque that was transiently IGRA+ (C9, dark grey) had no detectable pathology nor CFU in the organs analyzed. Whether this animal was not infected or cleared the infection at a very early stage remains unclear. Consequently, this animal was excluded from the downstream immune analyses.

In addition to pathology and bacterial burden, we measured several clinical parameters associated with progressive TB disease in NHP. No marked weight loss was observed in either group (**Supplemental Figure 1b**), with the exception of one rhesus macaque, which also reached a humane endpoint due to relatively severe disease development (R8, orange). Furthermore, over time, neither the mean corpuscular hemoglobin (MCH) and C-reactive protein (CRP) levels, as markers of

infection-associated anemia or systemic inflammation, respectively, nor the monocyte/lymphocyte ratio²³, showed any difference between the two species (**Supplemental Figure 1c-e**). This lack of differences in clinical features of experimental TB disease is in accordance with the low challenge dose and the relatively short follow-up time post-infection in this experiment.

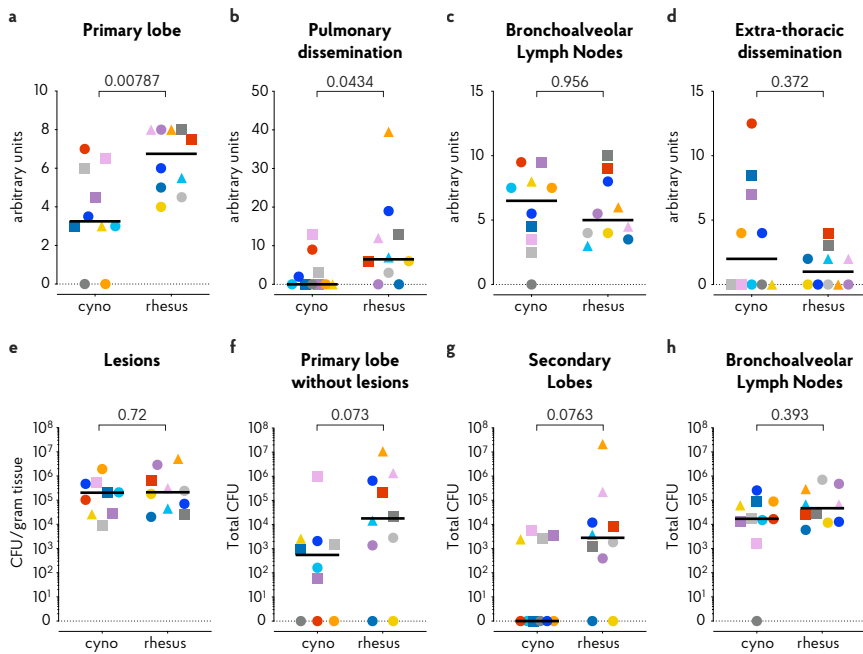


Figure 2. Cynomolgus macaques exhibit less pulmonary tuberculosis disease after low dose *Mtb* infection. **a-d)** Post-mortem scores of gross *Mtb* pathology in **a)** the primary targeted lung lobe, targeted when challenging with *Mtb*, **b)** all other lung lobes, as pulmonary dissemination, **c)** the lung-draining lymph nodes and **d)** the extra-thoracic organs as extra-thoracic dissemination. **e-h)** Quantification of bacterial load in homogenates **e)** of individually collected and pooled lesions from the primary lobe, **f)** of the remainder of the primary lung lobe (after collection of individual lesions), **g)** of pooled secondary lung lobes and **h)** of lung draining lymph nodes. Circles represent animals that IGRA converted 3 weeks after 1.3 CFU challenge, squares represent animals that IGRA converted 3 weeks after 7 CFU challenge, and triangles represent animals that IGRA converted 4 weeks after 1.3 CFU challenge and received another 7 CFU of *Mtb* one week later. N=10 per group, except for figure **e)**, where n=9 cynomolgus macaques, as one animal did not yield any macroscopic lesions. Horizontal lines indicate group medians. Significance of differences between species was determined by two sided Mann-Whitney testing. Colour coding per individual, as defined in Table 1, is consistently applied throughout.



***In vitro* mycobacterial growth control after *Mtb* infection**

After low dose *Mtb* infection cynomolgus macaques display a reduced amount of lung pathology and a lower mycobacterial load compared to rhesus monkeys. To investigate whether control of bacterial replication could underlie this milder disease phenotype, we employed a mycobacterial growth inhibition assay (MGIA)²⁴. PBMCs from both species, isolated pre-infection, 6 weeks post-infection and, where applicable, 12 weeks after infection, were co-cultured for 96 hours with BCG and subsequently transferred to Mycobacterial Growth Indicator Tubes (MGITs), as detailed in ²⁵, to compare the rates of mycobacterial outgrowth. As observed previously in humans with PBMCs from recently *Mtb* infected versus uninfected humans²⁶, BCG outgrowth was significantly reduced after incubation with cells obtained post-*Mtb* infection in comparison to cells obtained from the same animals pre-infection (**Figure 3a**). However, when comparing the outgrowth between species no differences between the two groups were found (**Figure 3b**). Thus, the reduced pathological involvement and bacterial tissue burden observed in cynomolgus compared to rhesus macaques is not reflected in differential bacterial outgrowth control as measured by PBMC-based MGIA.

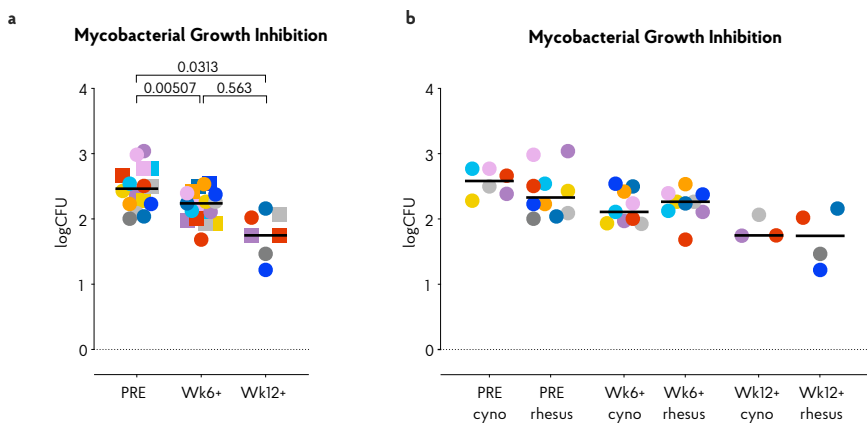


Figure 3. Mycobacterial growth inhibition capacity increases after *Mtb* infection but does not differ between species. A mycobacterial growth inhibition assay (MGIA) was used to determine the potential of rhesus and cynomolgus PBMC to control mycobacterial growth after infection. Data are depicted relative to individual IGRA conversion time points, for **a**) rhesus and cynomolgus together, or **b**) for each of the two species separately. Number of animals per time point varied due to sample availability. Horizontal lines indicate group medians. In **a**); squares represent cynomolgus samples, circles represent rhesus samples. Two-sided Mann-Whitney testing was used to determine significance of differences between groups. Colour coding per individual, as defined in Table 1, is consistently applied throughout.

Local and peripheral T-cell responses after low dose *Mtb* challenge.

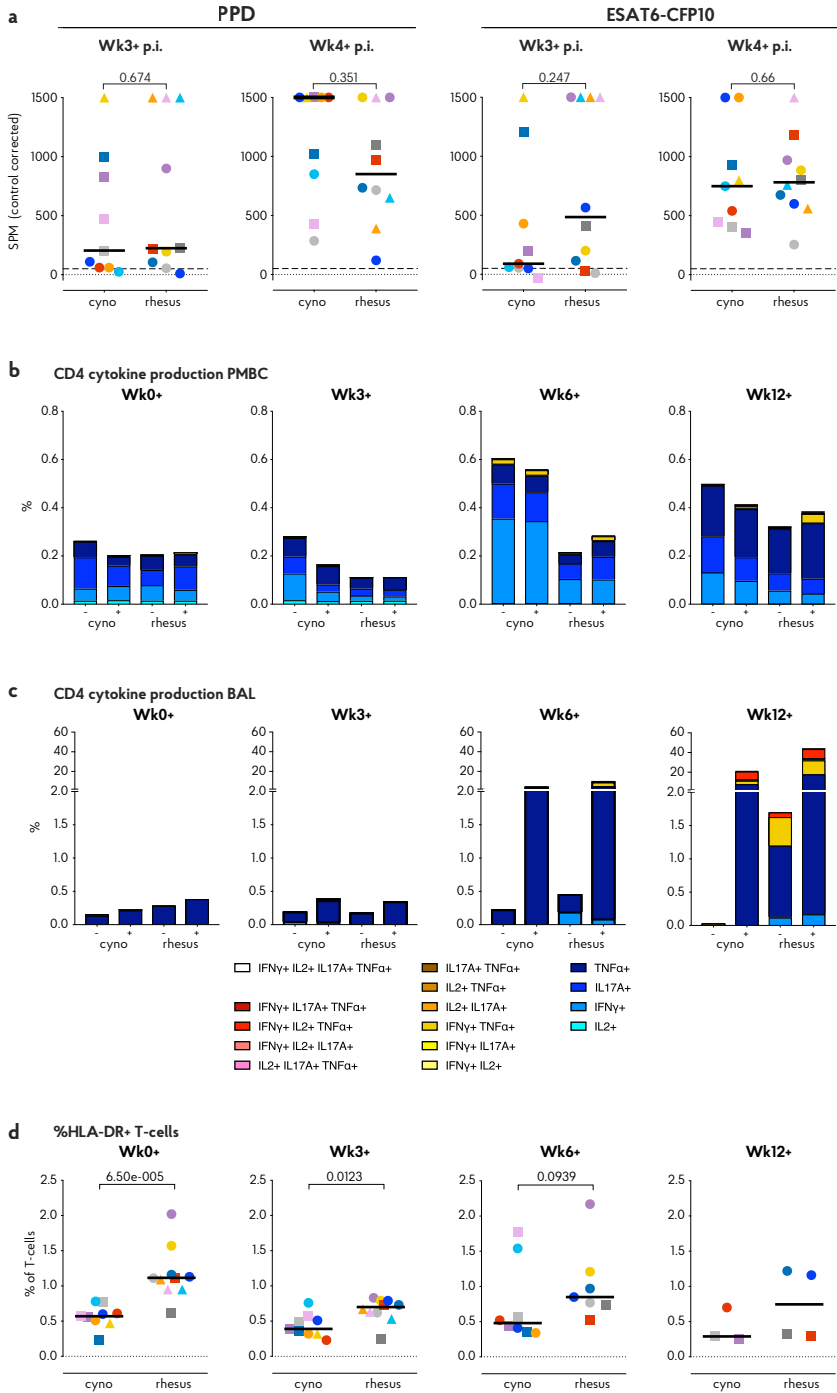
In an effort to identify potential immune correlates associated with the difference in disease development between the two species, we profiled peripheral as well as local adaptive immune responses at various timepoints after *Mtb* infection-take (as measured by IGRA conversion). Consequently, all data are aligned to the moment of each individual's time point of infection-take.

Beyond assessment of IGRA conversion, quantification of the IFN γ ELISPOT responses measured 3 and 4 weeks after infection revealed no differences in the capacity of PBMCs of rhesus and cynomolgus macaques to produce IFN γ in response to either PPD or ESAT6-CFP10 stimulation (**Figure 4a**).

PPD-specific production of IFN γ , TNF α , IL2 and IL17A by peripheral CD4+ T-cells was assessed by flow-cytometry. Over time, low dose *Mtb* infection appeared to induce little detectable PPD-specific, peripheral cytokine production in either species, and there were no appreciable differences in frequencies or polyfunctionality observed between the two species (**Figure 4b** and **Supplemental Figure 2a**). Transient elevation of background cytokine production was observed in cynomolgus macaques, which remains unexplained, especially since it occurs in the absence of an appreciable induction of PPD-specific responses, but may reflect some systemic increase in the activation status of CD4+ T lymphocytes in the blood.

Profiling of the local response by BAL cell analysis revealed the induction of substantial frequencies of PPD-specific cytokine+ CD4+ T-cells from 6 weeks post-infection onward, with on average strongest response signals at 12 weeks post-infection (**Figure 4c** and **Supplemental Figure 2b**). Despite marginal differences occasionally, also for the local CD4 T-cell response in the bronchoalveolar space, it appeared that neither magnitude nor phenotype seemed to be associated with the differential pathology levels between rhesus and cynomolgus macaques. Due to a technical error CD8+ T-cells in BAL samples were not stained directly. However, analysis of CD4 negative CD3+ cells, which contain the unstained CD8+ T-cells, again, revealed no significant differences in cytokine production between two species (data not shown). At later timepoints cynomolgus macaques trended towards lower T-cell responses in the lung, potentially reflecting reduced T-cell priming due to lower antigenic load.

Figure 4. T lymphocyte cytokine responses do not associate with the differential disease outcome between species. **a)** The IFN γ ELISPOT response to PPD and ESAT6-CFP10 recall stimulation *in vitro*, 3 or 4 weeks post-*Mtb* infection take (p.i.; median of triplicates per animal). **b)** Median frequency of cytokine producing CD4+ T-cell subsets in PBMC, and **c)** in BAL, both after overnight stimulation with culture medium as a control (-) or *Mtb*-derived PPD (+). **d)** Frequencies of circulating HLA-DR+ T-cells. Data are aligned to the moment of each individual's time point of infection take. Number of animals per time point varies due to sample availability. Horizontal lines indicate group medians in **a)** and **d)**; dashed lines in **a)** mark the cut-off value for positivity in the ELISPOT assay. P-values of possible differences between species was determined by two-sided Mann-Whitney testing. Colour coding per individual, as defined in Table 1, is consistently applied throughout. ►



Intriguingly, we did observe a higher frequency of circulating HLA-DR+ T-cells, a known correlate of an increased TB disease risk in man²⁷, in rhesus compared to cynomolgus macaques at the moment of and early after *Mtb* infection (**Figure 4d**).

Collectively, peripheral as well as local *Mtb*-specific Th1 and Th17 responses, within the limits of our analyses, appeared not to be implicated in the differential disease susceptibility observed between rhesus and cynomolgus macaques.

Post-*Mtb* infection humoral immune responses in the lung and periphery

We subsequently investigated if the humoral arm of the adaptive immune response was associated with the difference in TB manifestation between the species, as *Mtb*-specific antibodies can potentially contribute to mycobacterial infection control in various ways^{28,29}. The *Mtb*-specific antibody response was assessed both peripherally and locally by measuring *Mtb* whole cell lysate (WCL) specific IgM, IgA and IgG in serum and BAL fluid collected over the course of the infection.

Prior to infection with *Mtb*, rhesus macaques showed a trend towards higher levels of *Mtb*-reactive serum IgM, though not IgA or IgG (**Figure 5a-c**). After *Mtb* infection, the serum antibody responses to *Mtb* were increased in some, but not all animals and serum IgM levels were higher in rhesus monkeys compared to cynomolgus macaques, although this difference just failed to reach statistical significance. No species-related differences were apparent in the magnitude of the *Mtb*-specific IgA and IgG response after *Mtb* infection (**Figure 5b-c**).

Locally, again, higher *Mtb*-specific IgM levels prior to infection were observed in rhesus macaques (**Figure 5d**), while no differences were observed in *Mtb*-specific IgA and IgG responses (**Figure 5e-f**). Like in serum, *Mtb*-specific antibody-levels in BAL seemed to increase in some but not all animals over the course of *Mtb* infection. The magnitude of the local antibody responses during *Mtb* infection does not significantly differ between the species at any time point.

Peripheral monocyte phenotype after *Mtb* infection

As our adaptive T cell and humoral response analysis revealed no overt differences between rhesus versus cynomolgus macaques, we next investigated if a differential innate immune response could be underlying the disparate disease susceptibility between the species. We stimulated whole blood with *Mtb* WCL and assessed cytokine production by different Antigen Presenting Cell (APC) subsets by flow cytometry. *Mtb* WCL contains the full range of Pathogen Associated Molecular Patterns (PAMPs) of *Mtb* and therefore should activate several of the Pathogen Recognition Receptors (PRRs) of the innate immune system. We profiled production of three key cytokines, TNF α , IL12 and IL8, in monocytes and DC subsets before and at 3, 6 and 12 weeks after infection.

In the DC subsets, differentiated by CD11c, CD1c and CD16 expression, we could not identify any differences in cytokine positivity (data not shown). However, in the CD14+ monocyte population we found dissimilar frequencies of cytokine producing monocytes between rhesus and cynomolgus macaques. Early after infection (Wk3+),

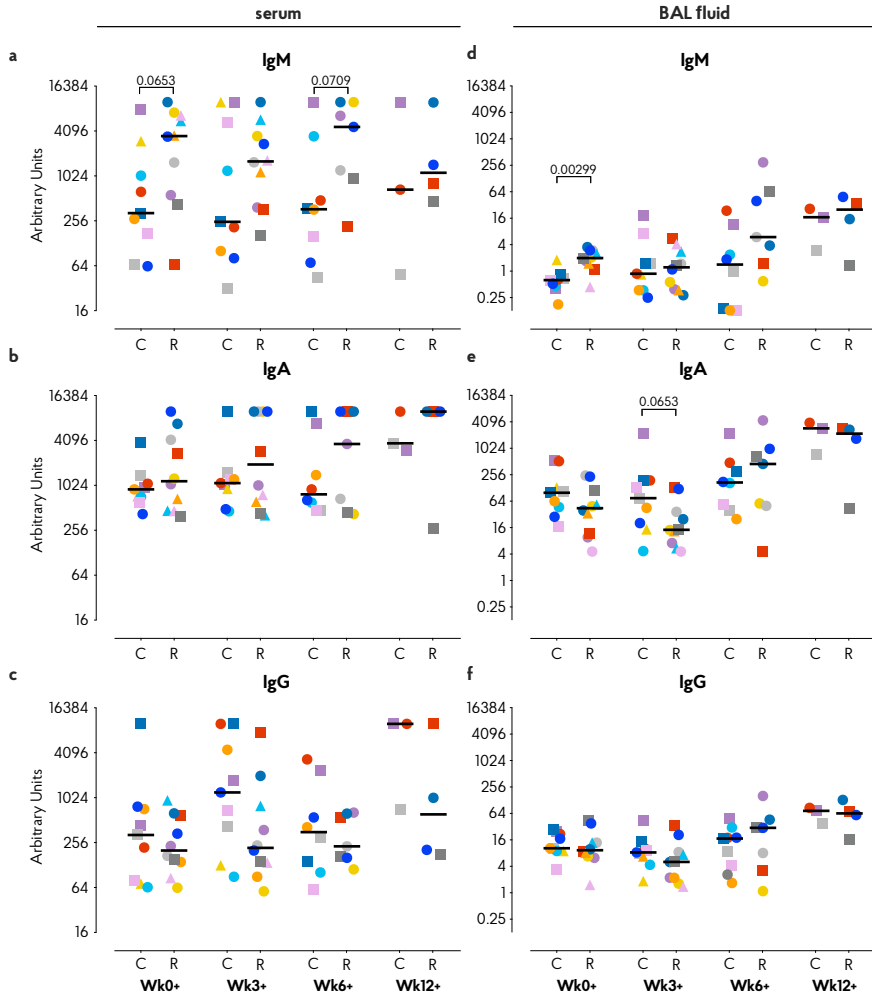
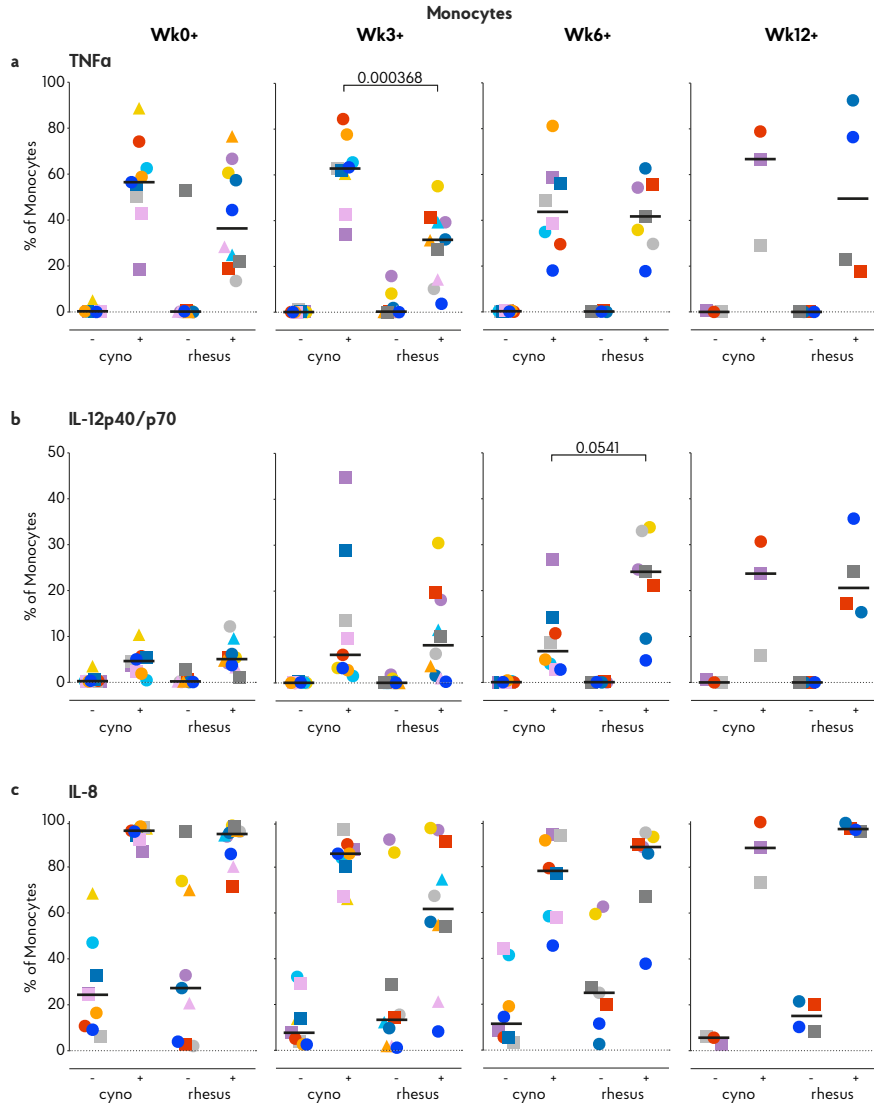


Figure 5. Antigen-specific antibody levels after *Mtb* infection. Measurement of *Mtb*-specific IgM **a****d**), IgA **b****e**) and IgG **c****f**) antibody response in serum (**a-c**) and BAL fluid **d-e**) prior to and after *Mtb* infection of cynomolgus (“C”) and rhesus macaques (“R”). Antibody levels are plotted as arbitrary units, determined by standardization against a reference sample. Data are aligned to the moment of each individual’s time point of infection take. Number of animals per time point varies due to sample availability. Horizontal lines indicate group medians. Significance of group differences was determined by two-sided Mann-Whitney test. Colour coding per individual, as defined in Table 1, is consistently applied throughout.

TNF α producing monocytes were found to be more frequent in peripheral blood of cynomolgus macaques, and the frequency of TNF α positive monocytes at this time point correlated negatively with the amount of lung pathology (Spearman's rho = -0.5507, p = 0.0145). This difference was no longer observed at 6 weeks after *Mtb* infection (**Figure 6a**). At this timepoint the frequency of IL12p40/p70 positive monocytes however, was higher in rhesus macaques compared to cynomolgus macaques (**Figure 6b**). The frequency of IL12 producing monocytes in response to *Mtb* WCL stimulation increased over the course of the infection. Overall, frequencies of IL8 positive monocytes were high after stimulation with *Mtb* WCL, but never differed between species at any week post-infection (**Figure 6c**).

Monocytes display functional plasticity and are able to act in a pro- as well as an anti-inflammatory manner depending on environmental stimuli. Previously, anti-inflammatory CD16 $^{+}$ monocytes expressing CD163 and Mer Tyrosine Kinase (MerTK) were found to be expanded after *Mtb* exposure and associated with disease severity in man as well as macaques³⁰. Prompted by the differences in monocyte cytokine production we profiled the expression of these markers on circulating CD16 $^{+}$ monocytes of both species. When assessing the *ex vivo* frequencies of CD163 $^{+}$ and MerTK $^{+}$ double positive CD16 $^{+}$ monocytes we found that already at baseline rhesus macaques had significantly higher frequencies of MerTK $^{+}$ CD163 $^{+}$ CD16 $^{+}$ monocytes, which were however markedly decreased from 3 weeks post-infection onward (**Figure 6d**). Analysis of CD163 $^{+}$ and MerTK $^{+}$ CD16 $^{+}$ monocytes separately (**Figure 6e&f**), showed that primarily the frequencies of MerTK $^{+}$ CD16 $^{+}$ monocytes were decreased. Frequencies of circulating CD163 $^{+}$ CD16 $^{+}$ monocytes, regardless of MerTK expression, remained higher in rhesus macaques up until week 3 post-infection. Statistical analysis revealed a positive correlation between the frequency of CD163 $^{+}$ monocytes at baseline and the amount of lung pathology (Spearman's rho = 0.4548, p = 0.0504). Taken, together, these data show a more potent pro-inflammatory APC signature in cynomolgus macaques before and/or early after *Mtb* infection compared to rhesus macaques.

In addition to their capacity to produce antibodies, B-cells can also function as antigen presenting cells. Atypical, CD11c $^{+}$ expressing B-cells in particular have been described as potent APCs and were also found to be upregulated after TB infection^{31,32}. We therefore compared the frequencies of circulating CD11c $^{+}$ B-cells between two species before and after *Mtb* infection. Interestingly, a significantly larger portion of the B-cells of cynomolgus macaques displayed this atypical phenotype, as characterized by CD11c expression (**Figure 6g**). This difference was maintained up to 3 weeks post-infection, after which the frequency of atypical B-cells in rhesus macaques starts to increase, reminiscent of what is seen in humans with TB disease. Therefore, while the post-*Mtb* antibody response did not notably differ between the species (**Figure 4**), B-cells in their capacity as APCs might influence disease outcome in NHPs.



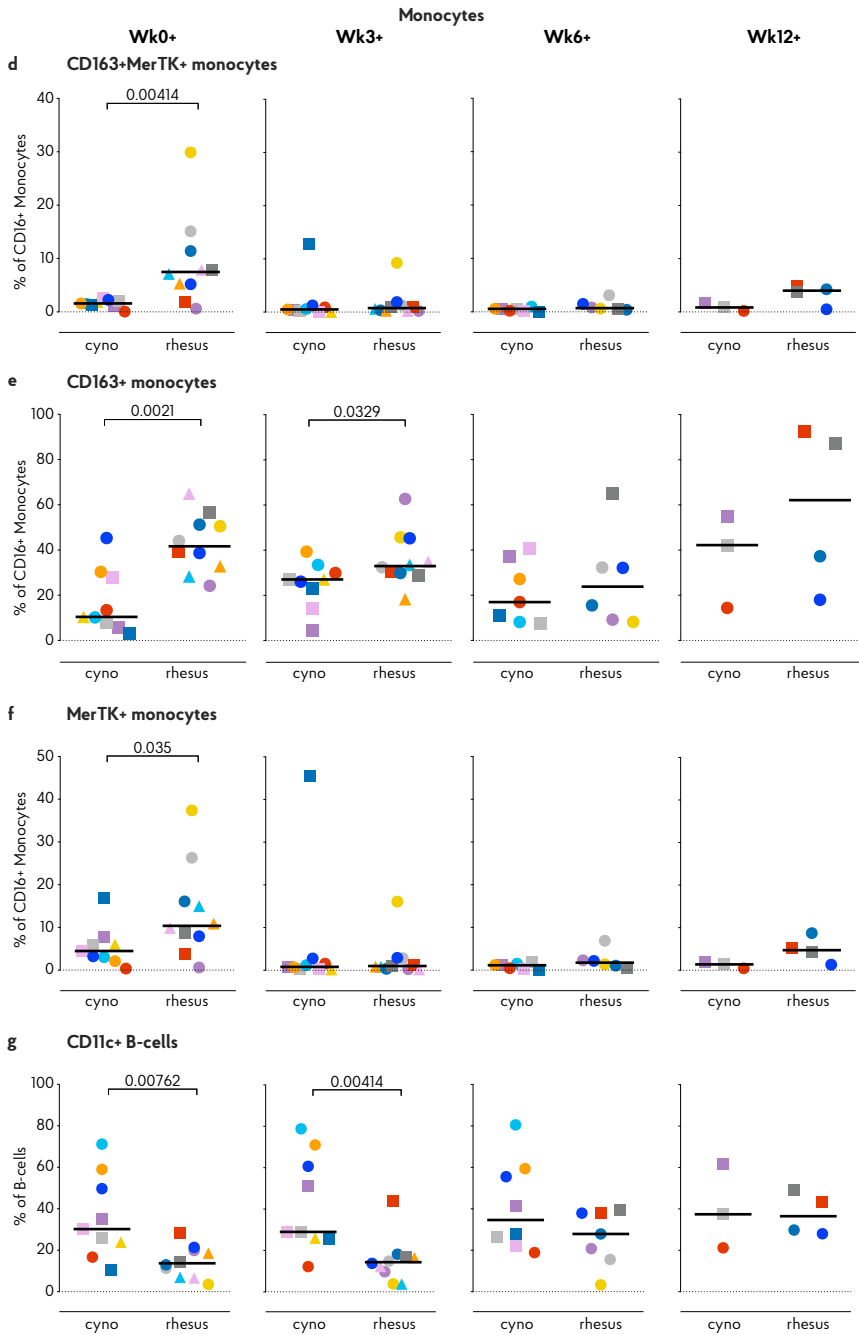


Figure 6 continued.



Local innate cytokine production in response to *Mtb*

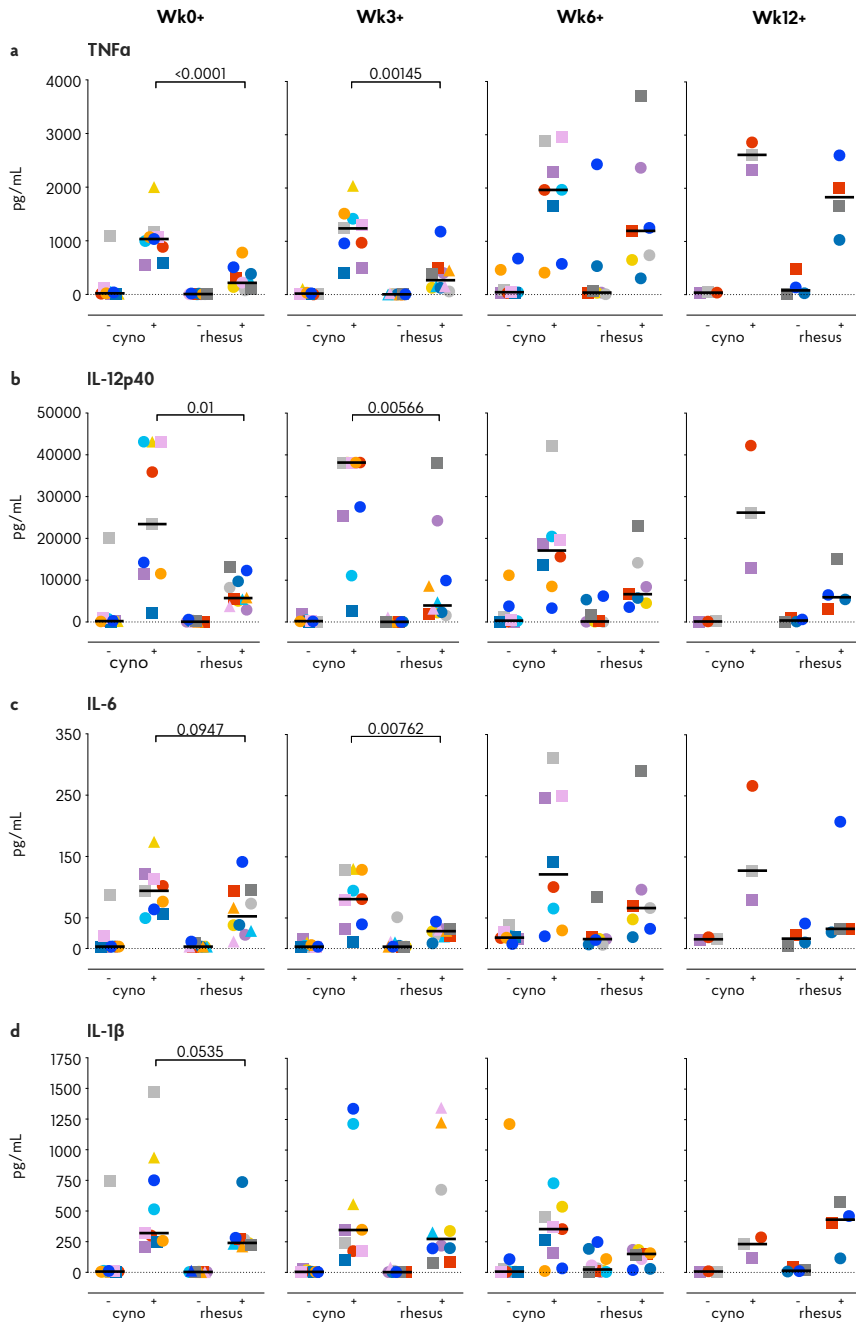
In the face of aerogenic *Mtb* infection, the first immune cell encountered by the bacteria is likely to be the alveolar macrophage, the most predominant cell-type lining the pulmonary mucosa³³. These local macrophages are likely to play a critical role in determining the fate of invading *Mtb*. However, due to high auto-fluorescence flow cytometric analysis of alveolar macrophages is challenging. Therefore, to assess possible species differences in the local innate immune response, we stimulated the total of unfractionated cells obtained from BAL with *Mtb* WCL and assessed cytokine production before and after *Mtb* infection by means of a multiplex Luminex assay.

Interestingly, in response to *Mtb* WCL stimulation, TNF α , IL6, IL12p40 and IL1 β were produced to a significantly higher extent by BAL cells of cynomolgus macaques already prior to infection (**Figure 7a-d**), concordant to the pro-inflammatory profile of circulating monocytes in cynomolgus macaques. Early after infection, TNF α , IL6 and IL12p40, but not IL1 β , remained present at significantly higher levels in BAL cell supernatants from cynomolgus macaques. At later time-points differences in cytokine production between the two species could no longer be observed.

Thus, the local inflammatory response observed at the moment of and shortly after *Mtb* infection in cynomolgus macaques seems to provide a milieu that supports constraint of *Mtb*-associated pathology.

Discussion

Rhesus and cynomolgus macaques are known to differ in their susceptibility to TB disease after *Mtb* challenge, with rhesus monkeys generally exhibiting more severe TB pathology compared to cynomolgus macaques^{17,18}. Here, we demonstrate that the two species do not differ in their susceptibility to *Mtb* infection, as measured by IGRA conversion, and that administration of a single colony forming unit of *Mtb* Erdman is sufficient to establish infection in both rhesus and cynomolgus macaques. Exposure to 1 CFU resulted in infection of 50% - 80% of macaques as defined by the induction of an antigen-specific IFN γ secretion response (IGRA conversion). Based on this finding we have recently defined for the first time in NHP⁹ a repeated limiting dose challenge model for the readout of preclinical vaccine efficacy not only by signals of prevention of disease but also by signals of prevention of infection. As the current study demonstrates that both species are equally susceptible to *Mtb* infection and corroborates the distinct difference in TB disease susceptibility between the two species^{17,18}, it also reveals differential immune response profiles that associate with and potentially underlie the differences in TB pathogenesis. Cynomolgus macaques exhibited a stronger local pro-inflammatory response than rhesus monkeys, while rhesus macaques displayed a more anti-inflammatory peripheral monocyte phenotype. Of note, the majority of the differential immune responses were observed already prior to or early after *Mtb* infection.





As both the pathogenesis and immune responses after *Mtb* infection closely resemble the spectrum of TB manifestation in man, we can consider both rhesus and cynomolgus macaques as highly relevant model species for TB research. When assessing prophylactic or therapeutic interventions rhesus macaques may be the more stringent and practical model, considering the rapid disease progression in this species. Cynomolgus macaques on the other hand would be more appropriate when investigating chronic TB manifestations or when evaluating therapies targeted to latently TB infected individuals.

In search of immune-mechanisms associated with the differential disease susceptibility between the two macaque species, we extensively profiled the adaptive immune responses known to be critically involved in anti-*Mtb* immunity. We extended our analysis beyond the conventional IFN γ ³⁴ response by measuring TNF α , IL2 and IL17a producing T-cells as well, both in the periphery as well as at the site of the infection at various time points after infection. Peripherally, we observed little induction of *Mtb*-specific cytokine responses in either species. Profiling of the T-cell response in BAL after *Mtb* infection revealed the induction of robust T-cell responses locally, as observed previously⁹. However, these responses did not discriminate between rhesus and cynomolgus macaques and therefore did not correlate with their differential disease susceptibility. Despite a non-significant difference in pre-infection IgM, but not IgA or IgG, levels, we also did not find the magnitude of the peripheral or local antibody-response to *Mtb* to differ between the species.

Within the limits of our analyses this study fails to show any significant difference in adaptive immune response parameters, but rather points to more upstream and very early immune cascades that seemingly impact on the disparate outcome of infection in cynomolgus versus rhesus macaques.

When assessing innate immune responses in both species we found responses in the monocyte compartment in particular to be associated with differential disease outcome after low dose *Mtb* infection. Monocytes and macrophages, alveolar macrophages in particular, are considered to be the typical target cell for *Mtb* infection, where the bacterium, by interfering with macrophage effector function, can proliferate and persist³⁵. Perturbation of the monocyte compartment in TB patients has been associated with expansion of a suppressive, CD16+, non-classical monocyte population exhibiting an anti-inflammatory phenotype, characterized by the expression of CD163 and MerTK^{30,36}. These CD16+CD163+MerTK+ monocytes were found to be more permissive to mycobacterial growth. In rhesus macaques, we

- ◀ **Figure 7. Local innate cytokine production at the time of or early after *Mtb* infection is more prominent in cynomolgus macaques.** Production of a) TNF α , b) IL6, c) IL12p40 and d) IL1 β by BAL cells after overnight stimulation with culture medium (-) or *Mtb* whole cell lysate (+). Data are aligned to the moment of each individual's time point of infection take. Number of animals per time point varies due to sample availability. Horizontal lines indicate group medians. Significance of group differences was determined by two-sided Mann-Whitney test. Colour coding per individual, as defined in Table 1, is consistently applied throughout.

found greater levels of circulating CD163⁺CD16⁺ monocytes prior to and early after *Mtb* infection. Furthermore, the frequency of circulating monocytes expressing MerTK, a negative regulator of T-cell responses³⁷, was found to be higher in rhesus macaques prior to *Mtb* infection. Although no difference in T-lymphocyte effector populations could be found in the present study, the increased frequency of MerTK⁺ monocytes in rhesus macaques could affect a T-cell population beyond the (detection-)limits of the analyses performed and samples profiled in this study. Intriguingly, in addition to the distinct monocyte response between the species, we also found a population of atypical, CD11c expressing B-cells, described as potent APCs, to be more frequent in cynomolgus macaques. While B-cell depletion in cynomolgus macaques did not have an unequivocal effect on *Mtb* infection and disease, granulomas of B-cell depleted monkeys tended to contain more bacilli³⁸. The finding that, in individuals with active TB, B-cells display a dysfunctional phenotype and significantly impact *Mtb*-specific T-cell responses further points to a role for B-cells in the protective immunity against TB³².

Of note, TNF α production by innate immune cells, both peripherally and locally, was found to be higher in the more disease-resistant cynomolgus macaques early after *Mtb* exposure. TNF α has been identified as a crucial component in the anti-mycobacterial immune response, playing a role in, amongst others, granuloma formation and APC activation³⁹. The importance of TNF α is maybe best emphasized by the observation that patients receiving anti-TNF α treatment are at an increased risk of disseminating reactivation TB⁴⁰. Interestingly, in mice myeloid derived TNF α specifically was required for early control of *Mtb* replication, while T-cell derived TNF α was necessary for control of chronic TB infection⁴¹.

In addition to TNF α , proinflammatory IL1 β , IL6 and IL12p40 were found to be secreted to a greater extent by (non-purified) total BAL cells from cynomolgus macaques, all cytokines which have been implied previously to have a protective effect after *Mtb* infection. Knock-out studies in mice have demonstrated that IL1 β is critical in host resistance to *Mtb* (reviewed in⁴²) while in a Malawi cohort of pulmonary TB patients impaired IL1 β (and TNF α) production in response to heat killed *Mtb* was associated with poor infection outcome⁴³. The IL12 cytokine family has similarly been described as a critical mediator of anti-*Mtb* resistance (reviewed in^{44,45}). Interestingly, IL12p40 may contribute to protection not only by initiation and maintenance of a Th1 and Th17 response but also potentially by mediating activation of dendritic cells⁴⁶. The role of IL6 in anti-tuberculosis immunity is less well-defined, but a number of studies suggest a role for IL6 in *Mtb* control^{42,47,48}.

In our analysis, standard correlation analysis identified the frequency of CD163⁺ monocytes at baseline and the frequency of TNF α ⁺ monocytes at 3 weeks post-infection only as statistical correlates of TB pathology. As TB disease pathogenesis is multifactorial and complex, an unbiased, multivariate analysis might be more suited to identify a protective versus pathogenic immune signature, however the low number of samples in this study hampers such an analysis. Furthermore, sampling at even earlier timepoints, ranging from hours to several days after *Mtb* infection, would



be required to further detail the role of early innate immune responses in infection outcome. Purification of specific myeloid subsets (e.g. alveolar macrophages) would add to unravelling such cascades. Taken together, the pro-inflammatory immune environment present at the mucosal surfaces at the moment of, or early after infection in cynomolgus macaques is likely to facilitate a more favorable disease outcome.

Interestingly, some of the differential innate immune responses between the two species were observed before exposure to *Mtb*. This suggests that underlying factors inherent to the species, such as differences in genetics, may be responsible for the observed differences in immune responses⁴⁹. Alternatively, as cynomolgus and rhesus are typically bred separately, disparate exposure to environmental factors also may have shaped the diverging immune response to *Mtb*⁵⁰. A well-known manifestation of this phenomenon is trained immunity, which was not specifically addressed in this study but would be of interest for further research^{26,51}. In that regard, the difference in pre-infection IgM response observed between the two species might be a result of differential exposure to non-tuberculous mycobacteria (NTM), even though all animals were screened negative for NTM-specific cellular immune responses prior to the start of the study. Lastly, another underlying factor influencing *Mtb* infection and disease susceptibility might be a dissimilar gut or pulmonary microbiome composition between the species⁵²⁻⁵⁴. Further research will be required to unravel the possible mechanisms that connect nature and/or nurture with the early innate and pro-inflammatory immune response profiles in the context of the reduced susceptibility to TB disease displayed by cynomolgus macaques.

In conclusion, our study corroborates the differential phenotype between rhesus and cynomolgus macaques observed after *Mtb* infection, and points to early innate rather than adaptive immunity as a potential cause for this difference. These results provide novel leads for correlates of risk of developing TB disease after infection as well as clues for further research to identify the underlying mechanisms that result in these disparate immune responses between the two macaque species.

Acknowledgements

We thank drs. Jeffrey Bajramovic and Jan Langermans for manuscript review. We thank the BPRC's animal and veterinary care teams and the clinical lab and pathology personnel for their excellent expert contributions to this study. We thank Kees Franken from the Ottenhoff lab at the Leiden University Medical Centre for providing us with recombinant ESAT6-CFP10 fusion protein. The following reagents were obtained through the NIH Biodefense and Emerging Infections Research Resources Repository, NIAID, NIH: *Mycobacterium tuberculosis*, Strain Erdman K01 (TMC107), NR-15404 and *Mycobacterium tuberculosis*, Strain HN878, Whole Cell Lysate, NR-14824. This work was performed under the TBVI governed TBVAC.2020 network programme for advancing TB vaccine candidates from early discovery through preclinical and into early clinical development, supported by the European

Commission under the Horizon.2020 programme, grant agreement no. 643381. Prof. Tom Ottenhoff is supported by an NWO-TOP grant and grants from the European Commission (Horizon.2020 TBVAC.2020; FP7 ADITEC; FP7 TRANSVAC2). TB team management was supported by a grant from the Bill & Melinda Gates Foundation, OPP1130668.

Material and Methods

Ethics, animals and handling

All housing and animal care procedures took place at the Biomedical Primate Research Centre (BPRC) in Rijswijk, the Netherlands, and were in compliance with European directive 2010/63/EU, as well as the “Standard for Humane Care and Use of Laboratory Animals by Foreign Institutions” provided by the Department of Health and Human Services of the US National Institutes of Health (NIH, identification number A5539-01). The BPRC is accredited by the American Association for Accreditation of Laboratory Animal Care (AAALAC). Before the start of the study ethical approval was obtained from the independent animal ethics committee (in Dutch: Dierexperimentencommissie, DEC) as well as BPRC’s institutional animal welfare body (in Dutch: Instantie voor Dierwelzijn, IvD). The study protocol was registered under DEC accession no. 761subA.

Ten male, non-Mauritian cynomolgus macaques (*Macaca fascicularis*) and 10 male Indian-type rhesus macaques (*Macaca mulatta*) were selected from the in-house colonies. Selected animals were screened as being negative for prior exposure to mycobacteria by means of tuberculin skin testing with Old Tuberculin (Synbiotics Corporation, San Diego, CA) and an IFN γ ELISPOT against Purified Protein Derivative (PPD) from *Mycobacterium bovis*, *Mycobacterium avium* (both Fisher Scientific, USA) or *Mycobacterium tuberculosis* (Statens Serum Institute, Copenhagen, Denmark). Selected cynomolgus and rhesus macaques were matched in age (mean age \pm SD in years; 6.3 ± 0.69 versus 6.1 ± 0.61 respectively) but differed significantly in weight (mean weight \pm SD in kilograms; 7.6 ± 1.3 versus 10.7 ± 2.8 , $p = 0.0029$).

Throughout the experiment animals were socially housed (pair-wise) at biosafety level 3 and provided with enrichment in the form of food and non-food items on a daily basis. Diet was identical for both species. Animal welfare was monitored daily. Animal weight was recorded prior to each blood collection event. To limit possible discomfort due to severe TB disease humane endpoints were predefined prior to the start of the study. All animal handling and biosampling was performed under ketamine sedation (10 mg/kg, by intra-muscular injection). For endobronchial instillation ketamine (5mg/kg) was supplemented with intramuscular medetomidine (0.04 mg/kg) and an analgesic sprayed into the larynx. By the end of the infection phase or when reaching a humane endpoint, animals were euthanized by intravenous injection of pentobarbital (200 mg/kg) under ketamine sedation.



Standard hematology on EDTA blood was performed on a Sysmex 2000i system (Siemens). C-reactive protein serum levels were determined using a Cobas™ Integra400+ (Roche Diagnostics). All veterinary staff and clinical lab personnel were blinded to animal treatment.

***Mycobacterium tuberculosis* infection & monitoring of infection take**

Animals were challenged with increasing doses of *Mycobacterium tuberculosis* Erdman K01 strain (BEI Resource, VA, USA). Each *Mtb* challenge dose was delivered by endobronchial instillation of 3 mL inoculum, targeting the lower left lung lobe and all challenge events occurred in a single session within 2-3 hours from preparing the inoculum from a frozen *Mtb* stock, challenging all animals in random order. When applicable, all peripheral blood sampling and/or bronchoalveolar lavages were performed prior to administration of *Mtb*. For quality assurance and determination of final dose administered, serial dilutions from the inoculum preparation process of each challenge were plated on 7H10 Middlebrook plus PANTA antibiotic mixture plates (Tritium, the Netherlands). Doses reported in the Results section are the extrapolated doses calculated from the number of CFUs grown from the dilution closest to the inoculum (extrapolated doses administered: 0.2, 1.3 and 7 CFU).

Infection take was monitored by means of a non-human primate specific IFN γ ELISPOT (U-CyTech, the Netherlands) performed 3 and 4 weeks each after *Mtb* exposure. Assay was performed according to manufacturer's protocol. In brief, 200,000 PBMCs were incubated in triplicate for 24 hours with *Mtb*-derived Purified Protein Derivate (PPD, Statens Serum Institute, Denmark) or recombinant ESAT6-CFP10 fusion protein (provided by K. Franken from the Ottenhoff lab, Leiden University Medical Centre)^{34,55}, both at a final concentration of 5 μ g/mL. The following day cells were washed and transferred to anti-IFN γ coated membrane plates (Millipore). After 24 hours of incubation cells were discarded and membrane-bound IFN γ was visualized with biotinylated anti-IFN γ detector antibody, streptavidin-horseradish peroxidase conjugate and tetramethylbenzidine substrate. Spots were quantified using an automated reader (AELVIS, Hannover). The pre-infection response to both PPD and ESAT6-CFP10 of all animals was used to determine the threshold for conversion from negative to positive. Cut-off was set at the average medium control corrected pre-infection response plus 3x the standard deviation. This resulted in a cut-off value for positivity of 50 control corrected spots per million for PPD as well as ESAT6-CFP10. Animals were considered infected if either the PPD or ESAT6-CFP10 response reached the threshold for positivity.

Peripheral and local bio-sample collection and processing

Cells from the pulmonary mucosa were harvested by broncho-alveolar lavage (BAL), targeting the lower left lung lobe. Three volumes of 20 mL of prewarmed 0.9% saline solution were consecutively instilled and recovered. BALs were passed over a 100 μ m filter and cellular fraction was separated from fluid by centrifugation for 10 minutes at 400g. Supernatant was decanted and stored at -80°C pending

further analysis. Cell pellet was resuspended in RPMI supplemented with 10% fetal calf serum (FCS), glutamax and penicillin/streptomycin (from now on referred to as R10). Heparinized blood for immune monitoring, EDTA blood for standard haematology, and serum for clinical chemistry were all collected by venipuncture. Peripheral blood mononuclear cells (PBMCs) were obtained by density gradient centrifugation of heparinized blood. Because of a species difference in blood osmolality we used Lymphoprep lymphocyte separation medium (Axis-Shield, UK) for rhesus macaques and a Percoll solution (GE Healthcare, IL, USA) for cynomolgus macaques. After harvesting and washing cells were resuspended in R10 for downstream immunological assays. Serum tubes were centrifuged for 10 minutes at 1000g to harvest cell-free serum which was stored at -80°C pending further analysis. Serum and BAL fluid were filter-sterilized by centrifugation through 0.2 µm PVDF membrane plates (Fisher Scientific) before analysis.

Post-mortem tuberculosis pathology assessment

After euthanasia tuberculosis pathology was assessed by a semi-quantitative grading system (adapted from⁵⁶) based on lesion size, manifestation and frequency, and lymph node involvement. The thoracic cavity, including the heart, ribcage, vertebrae and diaphragm were all macroscopically scored for the presence of granulomas and pleural adhesions. Lungs were isolated and lobes were separated from the trachea. Subsequently, lung lobes were cut in 5mm thick slices and scored for the amount of pathology. The most affected lung lobe was designated as the primary lung lobe. From this lobe individual lesions were isolated, weighed and processed separately. The remainder of the primary lobe was mechanically homogenized. The remaining lung lobes were pooled and mechanically homogenized. Lung draining lymph nodes were isolated from the trachea and scored for size and extent of involvement. Axillar and inguinal lymph nodes were similarly assessed. Extra-thoracic organs such as the kidneys, spleen, pancreas and liver were macroscopically assessed for the presence of lesions. The summed score of all extra-thoracic organs was used as a measure of extra-thoracic dissemination.

Determination of bacterial load in tissue

After pathology assessment and initial homogenization lesions and lung lobes were further homogenized in GentleMACS C- and M-tubes (Miltenyi). Bronchoalveolar lymph nodes were first processed to a single cell suspension by straining over a 100 µm cell strainer (Greiner) and subsequently homogenized in GentleMACS M-tubes. All homogenates were frozen at -80° Celsius before quantification of bacterial counts. Thawed samples were 3-fold serially diluted and plated on 7H10 plates supplemented with PANTA antibiotic mixture (Tritium, the Netherlands). Plates were incubated at 37° Celsius for at least 3 weeks until Colony Forming Units (CFU) were observed. Plates were incubated for at least 6 weeks before scored as negative. CFUs were counted with a Scan4000 automated counting system (Interscience, France).



Mycobacterial Growth Inhibition Assay

Cryopreserved PBMCs were thawed and incubated with 10U/mL benzonase (Merck) in R10. After 2 hours cells were washed, taken up in RPMI supplemented with 10% inactivated pooled human serum and glutamax and counted. 1×10^6 PBMCs were co-cultured with 100 CFU BCG Pasteur (P3) for 4 days, in a final volume of 600 μ l, on a rotator at 37° Celsius, as described in ²⁶.

After 4 days, samples were transferred to Mycobacterial Growth Indicator Tubes (MGIT, Beckton Dickinson) supplemented with PANTA antibiotic mixture and OADC enrichment. Tubes were placed in a BACTEC960 system (Beckton Dickinson) and measured until Time to Positivity (TTP) was reached. Samples with a TTP <100 hours were considered to be contaminated and excluded from analysis.

To be able to convert TTP to CFU, serial dilutions of the BCG stock were plated on Middlebrook 7H10 plates to determine CFU, as well as added to MGIT tubes to determine TTP. Counted CFUs were converted to $10 \log$ CFU and a standard curve to convert TTP to \log CFU was generated by means of linear regression.

Flowcytometric analysis of local and peripheral immune subsets

Whole blood, PBMCs and BAL cells were profiled by flow cytometry to characterize monocyte phenotype and cytokine production by T-cells and Antigen Presenting Cells (APC, see **Supplemental Table 1** for overview of panels used).

T-cell cytokine production. Cryopreserved BAL cells and PBMCs were thawed in R10 containing 50U/mL benzonase. After washing cells were incubated with either medium or 5 μ g/mL PPD for 3 hours at 37° Celsius. GolgiPlug transport inhibitor (BD Biosciences) was added and incubated overnight. Cells were stained the subsequent day with the T-cell cytokine panel (**Supplemental Table 1**). PMA/ionomycin stimulated samples were taken along as technical/positive controls.

APC cytokine production. 200 μ l heparinized whole blood was incubated with medium or 25 μ g/mL *Mtb* H828 Whole Cell Lysate (BEI Resource, VA, USA) 37° Celsius for 3 hours and subsequently incubated overnight with Golgiplug transport inhibitor. Prior to staining with the APC cytokine panel (**Supplemental Table 1**) samples were treated with Pharm Lyse (BD Biosciences) to lyse red blood cells.

Pro- and anti-inflammatory monocyte phenotyping. 200 μ l heparinised whole blood was stained *ex vivo* with the monocyte phenotyping panel (**Supplemental Table 1**). After staining cells were treated with FACS Lyse (BD Biosciences) to lyse red blood cells.

After staining all samples were fixed overnight with 2% paraformaldehyde and measured on a 3 laser, 14 colour LSR-II flowcytometer (BD Biosciences). All analyses were performed with FlowJo software version 10 (Treestar). Any anomalies indicative of unstable signal acquisition were excluded using the time parameter. Representative gating strategies are depicted in **Supplemental Figure 3**.

Antibody ELISAs

Mtb-reactive antibody levels in serum and BAL were determined by Enzyme Linked ImmunoSorbent Assay (ELISA). In brief, 96-well plates were coated with 5 µg/mL *Mtb* HN828 Whole Cell lysate (BEI Resource, VA, USA) in PBS. After overnight blocking with 1% BSA, serial dilutions of BAL and serum samples were added and incubated for 2 hours at 37° Celsius. Bound antibodies were subsequently detected with horse radish peroxidase-conjugated anti-IgG (Rockland, PA, USA) in combination with tetramethylbenzidine substrate, alkaline phosphatase-conjugated anti-IgA (Fisher Scientific) or alkaline phosphatase-conjugated IgM (Sigma) with *para*-nitrophenylphosphate substrate for ELISA colour development. All samples were normalized to arbitrary units (AU) against a serial dilution of a positive reference sample included in all assays.

Multiplex cytokine assay

Cytokine production of BAL cells stimulated overnight with PPD (5 µg/mL) and *Mtb* WCL (25 µg/mL) was assessed by a custom Procartaplex Luminex kit (ThermoFisher Scientific, USA). Assays were performed according to manufacturer's protocol. In short: supernatants of stimulated cells were incubated with beads coated with cytokine-specific antibodies. Bound cytokines were visualized using biotin-coupled detection antibodies and PE-labelled streptavidin. Beads were acquired on a Bioplex 200 system and cytokine levels were calculated with Bioplex Manager software version 6.1 (both Biorad, CA, USA).

Statistics

Statistical analyses were performed using Graphpad Prism software version 7. Significance of differences between groups was calculated by two-sided Mann-Whitney testing. Paired observations within groups were analyzed by two-sided Wilcoxon signed-rank test. Unless indicated otherwise in the figure legends, statistical calculations are based on n=10 observations per treatment group.



References

1. Geneva: World Health Organization. Global tuberculosis report 2019.
2. Drain, P.K., *et al.* Incipient and Subclinical Tuberculosis: a Clinical Review of Early Stages and Progression of Infection. *Clinical microbiology reviews* **31**(2018).
3. Simmons, J.D., *et al.* Immunological mechanisms of human resistance to persistent *Mycobacterium tuberculosis* infection. *Nature reviews. Immunology* **18**, 575-589 (2018).
4. Barry, C.E., 3rd, *et al.* The spectrum of latent tuberculosis: rethinking the biology and intervention strategies. *Nature reviews. Microbiology* **7**, 845-855 (2009).
5. Houben, R.M. & Dodd, P.J. The Global Burden of Latent Tuberculosis Infection: A Re-estimation Using Mathematical Modelling. *PLoS medicine* **13**, e1002152 (2016).
6. Dorhoi, A. & Kaufmann, S.H. Pathology and immune reactivity: understanding multidimensionality in pulmonary tuberculosis. *Seminars in immunopathology* **38**, 153-166 (2016).
7. Jeyanathan, M., Yao, Y., Afkhami, S., Smail, F. & Xing, Z. New Tuberculosis Vaccine Strategies: Taking Aim at Un-Natural Immunity. *Trends in immunology* **39**, 419-433 (2018).
8. Roy Chowdhury, R., *et al.* A multi-cohort study of the immune factors associated with *M. tuberculosis* infection outcomes. *Nature* **560**, 644-648 (2018).
9. Dijkman, K., *et al.* Prevention of tuberculosis infection and disease by local BCG in repeatedly exposed rhesus macaques. *Nature medicine* (2019).
10. Scriba, T.J., *et al.* Sequential inflammatory processes define human progression from *M. tuberculosis* infection to tuberculosis disease. *PLoS pathogens* **13**, e1006687 (2017).
11. Aguilo, N., *et al.* Pulmonary but Not Subcutaneous Delivery of BCG Vaccine Confers Protection to Tuberculosis-Susceptible Mice by an Interleukin 17-Dependent Mechanism. *The Journal of infectious diseases* **213**, 831-839 (2016).
12. Divangahi, M., Khan, N. & Kaufmann, E. Beyond Killing *Mycobacterium tuberculosis*: Disease Tolerance. *Front Immunol* **9**, 2976 (2018).
13. Cardona, P.J. & Williams, A. Experimental animal modelling for TB vaccine development. *International journal of infectious diseases : IJID : official publication of the International Society for Infectious Diseases* **56**, 268-273 (2017).
14. Hunter, R.L., *et al.* Pathogenesis and Animal Models of Post-Primary (Bronchogenic) Tuberculosis, A Review. *Pathogens (Basel, Switzerland)* **7**(2018).
15. Laddy, D.J., *et al.* Toward Tuberculosis Vaccine Development: Recommendations for Nonhuman Primate Study Design. *Infection and immunity* **86**(2018).
16. Langermans, J.A., *et al.* Divergent effect of bacillus Calmette-Guerin (BCG) vaccination on *Mycobacterium tuberculosis* infection in highly related macaque species: implications for primate models in tuberculosis vaccine research. *Proceedings of the National Academy of Sciences of the United States of America* **98**, 11497-11502 (2001).
17. Sharpe, S., *et al.* Ultra low dose aerosol challenge with *Mycobacterium tuberculosis* leads to divergent outcomes in rhesus and cynomolgus macaques. *Tuberculosis (Edinburgh, Scotland)* **96**, 1-12 (2016).
18. Maiello, P., *et al.* Rhesus macaques are more susceptible to progressive tuberculosis than cynomolgus macaques: A quantitative comparison. *Infection and immunity* (2017).
19. Capuano, S.V., 3rd, *et al.* Experimental *Mycobacterium tuberculosis* infection of cynomolgus macaques closely resembles the various manifestations of human *M. tuberculosis* infection. *Infection and immunity* **71**, 5831-5844 (2003).
20. Sharpe, S.A., *et al.* An aerosol challenge model of tuberculosis in Mauritian cynomolgus macaques. *PLoS one* **12**, e0171906 (2017).
21. Roederer, M. Parsimonious Determination of the Optimal Infectious Dose of a Pathogen for Nonhuman Primate Models. *PLoS pathogens* **11**, e1005100 (2015).

22. Verreck, F.A.W., *et al.* Variable BCG efficacy in rhesus populations: Pulmonary BCG provides protection where standard intra-dermal vaccination fails. *Tuberculosis (Edinburgh, Scotland)* **104**, 46-57 (2017).
23. Naranbhai, V., *et al.* The association between the ratio of monocytes:lymphocytes at age 3 months and risk of tuberculosis (TB) in the first two years of life. *BMC medicine* **12**, 120 (2014).
24. Brennan, M.J., *et al.* The Cross-species Mycobacterial Growth Inhibition Assay (MGIA) Project 2010-2014. *Clinical and vaccine immunology : CVI* (2017).
25. Tanner, R., *et al.* Optimisation, harmonisation and standardisation of the direct mycobacterial growth inhibition assay using cryopreserved human peripheral blood mononuclear cells. *Journal of immunological methods* **469**, 1-10 (2019).
26. Joosten, S.A., *et al.* Mycobacterial growth inhibition is associated with trained innate immunity. *The Journal of clinical investigation* **128**, 1837-1851 (2018).
27. Fletcher, H.A., *et al.* T-cell activation is an immune correlate of risk in BCG vaccinated infants. *Nature communications* **7**, 11290 (2016).
28. Jacobs, A.J., Mongkolsapaya, J., Screation, G.R., McShane, H. & Wilkinson, R.J. Antibodies and tuberculosis. *Tuberculosis* **101**, 102-113 (2016).
29. Li, H. & Javid, B. Antibodies and tuberculosis: finally coming of age? *Nature reviews. Immunology* (2018).
30. Lastrucci, C., *et al.* Tuberculosis is associated with expansion of a motile, permissive and immunomodulatory CD16(+) monocyte population via the IL-10/STAT3 axis. *Cell research* **25**, 1333-1351 (2015).
31. Rubtsov, A.V., *et al.* CD11c-Expressing B Cells Are Located at the T Cell/B Cell Border in Spleen and Are Potent APCs. *Journal of immunology (Baltimore, Md. : 1950)* **195**, 71-79 (2015).
32. Joosten, S.A., *et al.* Patients with Tuberculosis Have a Dysfunctional Circulating B-Cell Compartment, Which Normalizes following Successful Treatment. *PLoS pathogens* **12**, e1005687 (2016).
33. Yu, Y.A., *et al.* Flow Cytometric Analysis of Myeloid Cells in Human Blood, Bronchoalveolar Lavage, and Lung Tissues. *Am J Respir Cell Mol Biol* (2015).
34. Coppola, M., *et al.* New Genome-Wide Algorithm Identifies Novel In-Vivo Expressed Mycobacterium Tuberculosis Antigens Inducing Human T-Cell Responses with Classical and Unconventional Cytokine Profiles. *Sci Rep* **6**, 37793 (2016).
35. Bruns, H. & Stenger, S. New insights into the interaction of Mycobacterium tuberculosis and human macrophages. *Future microbiology* **9**, 327-341 (2014).
36. Balboa, L., *et al.* Paradoxical role of CD16+CCR2+CCR5+ monocytes in tuberculosis: efficient APC in pleural effusion but also mark disease severity in blood. *Journal of leukocyte biology* **90**, 69-75 (2011).
37. Cabezon, R., *et al.* MERTK as negative regulator of human T cell activation. *Journal of leukocyte biology* **97**, 751-760 (2015).
38. Phuah, J., *et al.* Effects of B Cell Depletion on Early Mycobacterium tuberculosis Infection in Cynomolgus Macaques. *Infection and immunity* **84**, 1301-1311 (2016).
39. Lin, P.L., Plessner, H.L., Voitenok, N.N. & Flynn, J.L. Tumor necrosis factor and tuberculosis. *The journal of investigative dermatology. Symposium proceedings* **12**, 22-25 (2007).
40. Elbek, O., *et al.* Increased risk of tuberculosis in patients treated with antitumor necrosis factor alpha. *Clinical rheumatology* **28**, 421-426 (2009).
41. Allie, N., *et al.* Prominent role for T cell-derived tumour necrosis factor for sustained control of Mycobacterium tuberculosis infection. *Sci Rep* **3**, 1809 (2013).
42. Cooper, A.M., Mayer-Barber, K.D. & Sher, A. Role of innate cytokines in mycobacterial infection. *Mucosal immunology* **4**, 252-260 (2011).

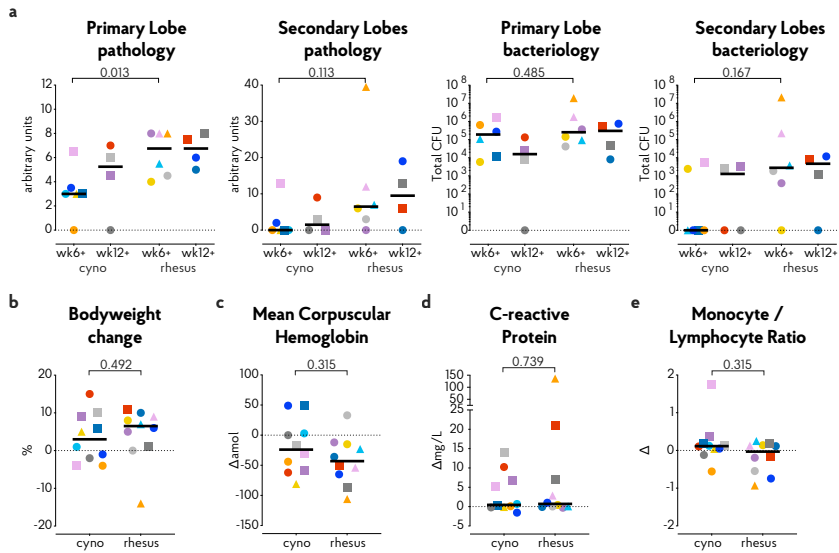
43. Waitt, C.J., *et al.* Monocyte unresponsiveness and impaired IL1beta, TNFalpha and IL7 production are associated with a poor outcome in Malawian adults with pulmonary tuberculosis. *BMC infectious diseases* **15**, 513 (2015).
44. Cooper, A.M., Solache, A. & Khader, S.A. Interleukin-12 and tuberculosis: an old story revisited. *Current opinion in immunology* **19**, 441-447 (2007).
45. Ottenhoff, T.H., *et al.* Genetics, cytokines and human infectious disease: lessons from weakly pathogenic mycobacteria and salmonellae. *Nature genetics* **32**, 97-105 (2002).
46. Cooper, A.M. & Khader, S.A. The role of cytokines in the initiation, expansion, and control of cellular immunity to tuberculosis. *Immunological reviews* **226**, 191-204 (2008).
47. Martinez, A.N., Mehra, S. & Kaushal, D. Role of interleukin 6 in innate immunity to Mycobacterium tuberculosis infection. *The Journal of infectious diseases* **207**, 1253-1261 (2013).
48. Ladel, C.H., *et al.* Lethal tuberculosis in interleukin-6-deficient mutant mice. *Infection and immunity* **65**, 4843-4849 (1997).
49. Yan, G., *et al.* Genome sequencing and comparison of two nonhuman primate animal models, the cynomolgus and Chinese rhesus macaques. *Nature Biotechnology* **29**, 1019 (2011).
50. MacGillivray, D.M. & Kollmann, T.R. The role of environmental factors in modulating immune responses in early life. *Frontiers in immunology* **5**, 434-434 (2014).
51. Netea, M.G., *et al.* Trained immunity: A program of innate immune memory in health and disease. *Science (New York, N.Y.)* **352**, aaf1098 (2016).
52. Dumas, A., *et al.* The Host Microbiota Contributes to Early Protection Against Lung Colonization by Mycobacterium tuberculosis. *Frontiers in immunology* **9**, 2656-2656 (2018).
53. Khan, N., *et al.* Alteration in the Gut Microbiota Provokes Susceptibility to Tuberculosis. *Front Immunol* **7**, 529 (2016).
54. Cadena, A.M., *et al.* Profiling the airway in the macaque model of tuberculosis reveals variable microbial dysbiosis and alteration of community structure. *Microbiome* **6**, 180 (2018).
55. Franken, K.L., *et al.* Purification of his-tagged proteins by immobilized chelate affinity chromatography: the benefits from the use of organic solvent. *Protein expression and purification* **18**, 95-99 (2000).
56. Lin, P.L., *et al.* Quantitative comparison of active and latent tuberculosis in the cynomolgus macaque model. *Infection and immunity* **77**, 4631-4642 (2009).



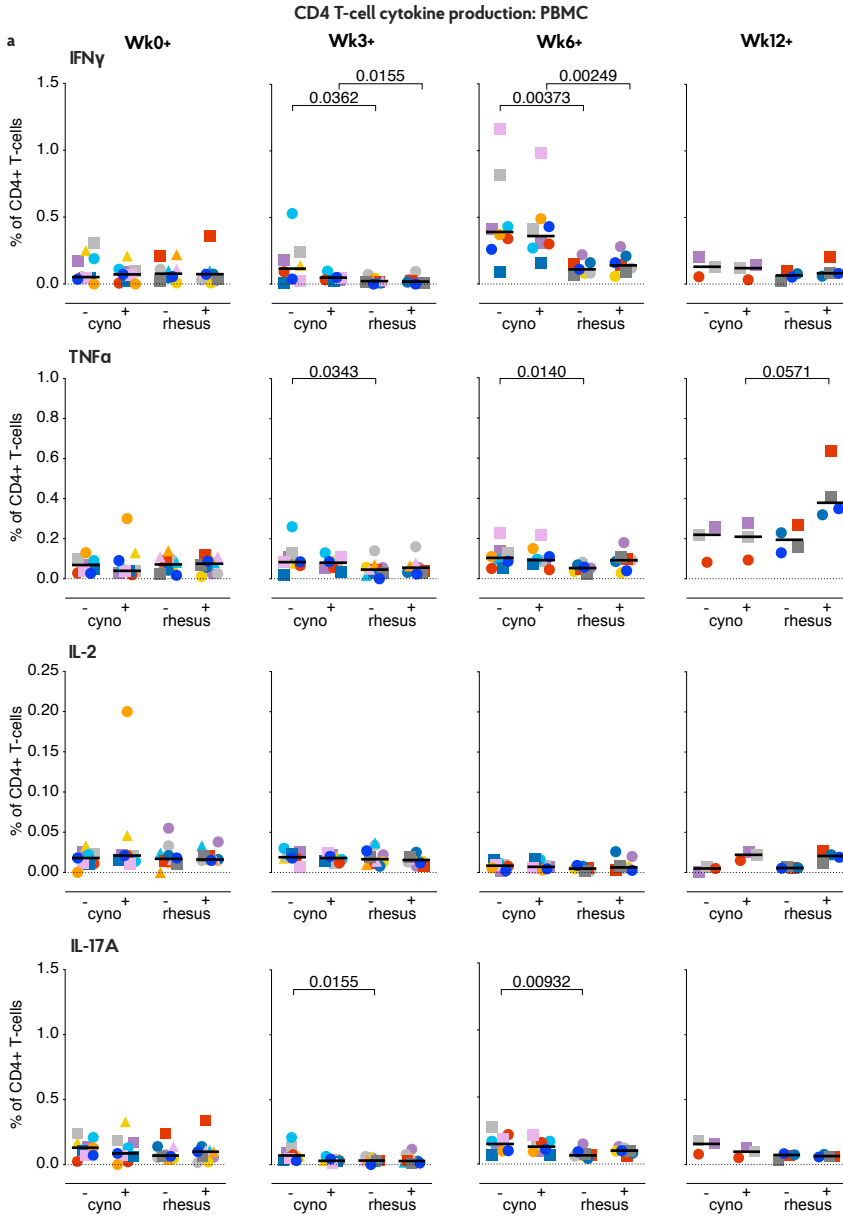
Supplemental data

T-cell Cytokine Panel			APC Cytokine Panel			Monocyte Phenotype Panel		
Marker	Clone	Manufacturer	Marker	Clone	Manufacturer	Marker	Clone	Manufacturer
VIVID Fixable viability stain		Thermo Fisher	VIVID Fixable viability stain		Thermo Fisher			
CD28	CD28.2	Beckman Coulter	CD123	7G3	Becton Dickinson	CD83	HB15A	Beckman Coulter
CD14	M5E3	Becton Dickinson	CD14	M5E3	Becton Dickinson	CD14	M5E3	Becton Dickinson
CD45	D058-1283	Becton Dickinson	CD16	3G8	Becton Dickinson	CD16	3G8	Becton Dickinson
CD3	SP34-2	Becton Dickinson	CD3	SP34-2	Becton Dickinson	CD86	FUN1	Becton Dickinson
CD4	L200	Becton Dickinson	HLA-DR	L243	Becton Dickinson	HLA-DR	L243	Becton Dickinson
CD8	SK-1	Becton Dickinson	CD8	SK-1	Becton Dickinson	CD163	GHI/61	Becton Dickinson
TNF	Mab11	Becton Dickinson	IL-8	G265-8	Becton Dickinson	MerTK	I25518	R&D systems
CD20	2H7	Biologend	TNF	Mab11	Becton Dickinson			
CD95	DX2	Biologend	CD20	2H7	Biologend			
PD-1	EH12.2H7	Biologend	CD11c	3.9	Biologend			
IL-2	MQ1-17H12	Biologend	IL12p40/70	C8.6	Miltenyi			
IFN γ	4S.B3	Biologend	CD66	TET2	Miltenyi			
CD25	4E3	Miltenyi	CD1c	L161	ThermoFisher			
CD127	ebioDR5	ThermoFisher						
IL-17A	ebio64DEC17	ThermoFisher						

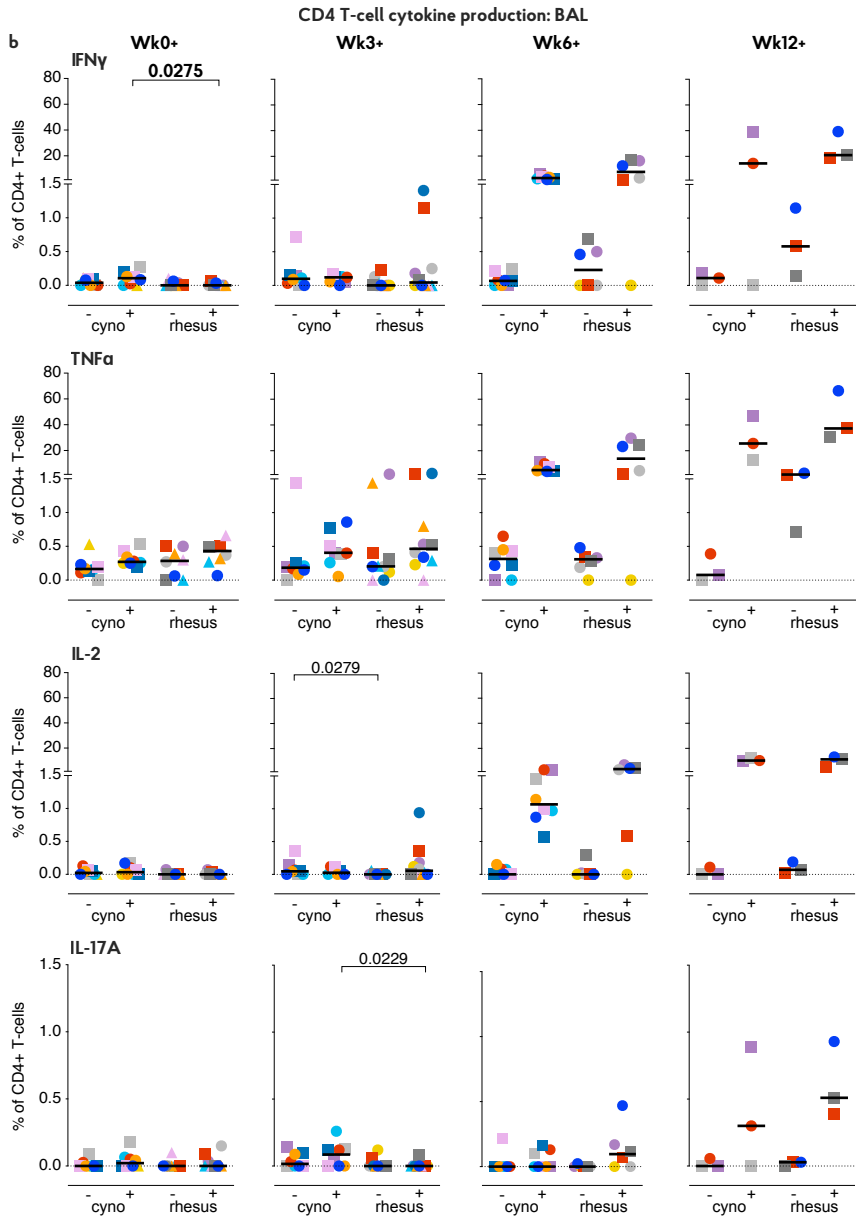
Supplemental Table 1: Antibodies used for flow cytometric analysis of BAL, PBMC and whole blood.



Supplemental Figure 1. Additional parameters of tuberculosis disease severity. a) Lung pathology plotted per species per time-to-endpoint. b-e) Change in b) bodyweight and c-e) haematological and serological parameters associated with tuberculosis disease over the course of the *Mtb* infection. Circles represent animals infected after administration of 1.3 CFU, squares represent animals infected after administration of 7 CFU and triangles indicate animals administered both 1.3 and 7 CFU of *Mtb*. N=10 animals per group. Horizontal lines indicate group medians. Two-sided Mann-Whitney testing was used to determine significance of differences between groups. Colour coding per individual, as defined in Table 1, is consistently applied throughout.

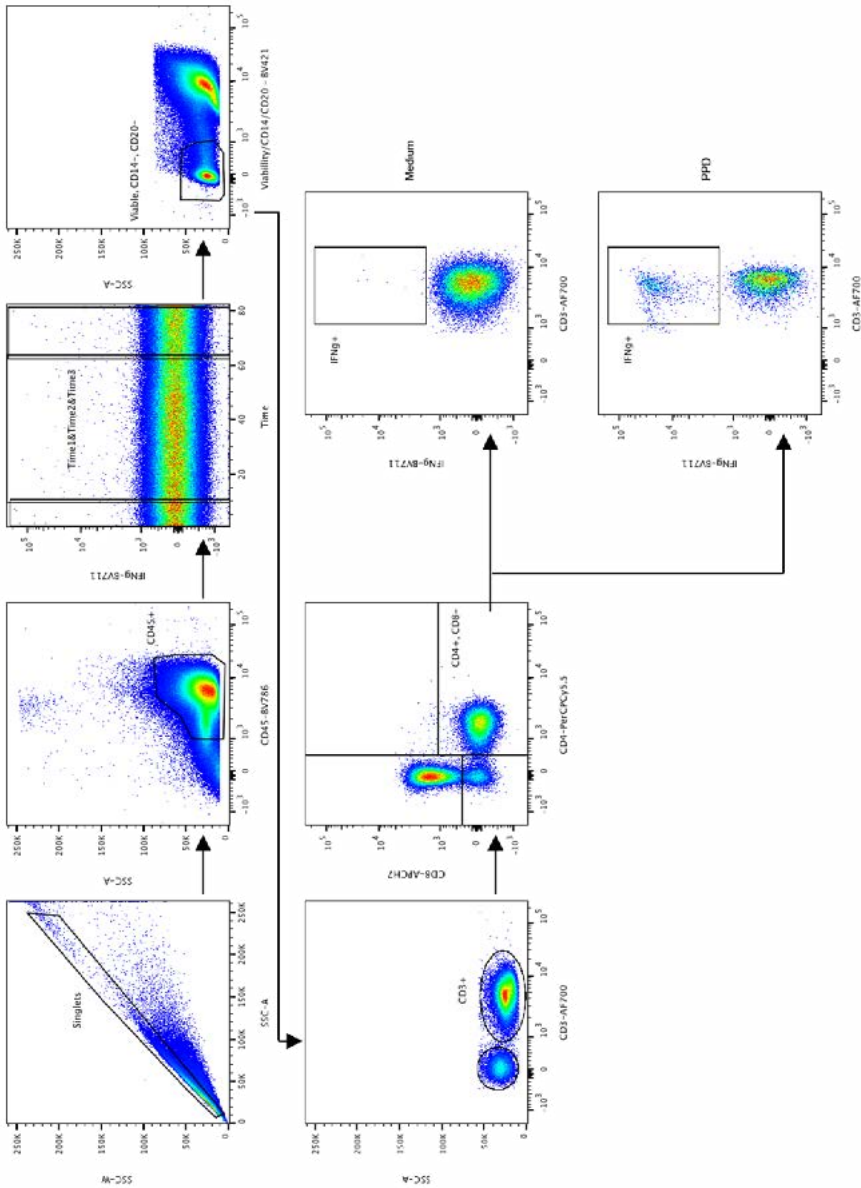


Supplemental Figure 2. Peripheral and local CD4 cytokine production. a) percentage CD4 T-cells in the periphery producing IFN γ , TNF α , IL2 or IL17A after overnight incubation with culture medium (-) or PPD (+) b) percentage CD4 T-cells at the pulmonary mucosa producing IFN γ , TNF α , IL2 or IL17A after overnight incubation with culture medium (-) or PPD (+) Data are aligned to the moment of each individual's time point of infection take. Number of animals per time point varies due to sample availability.

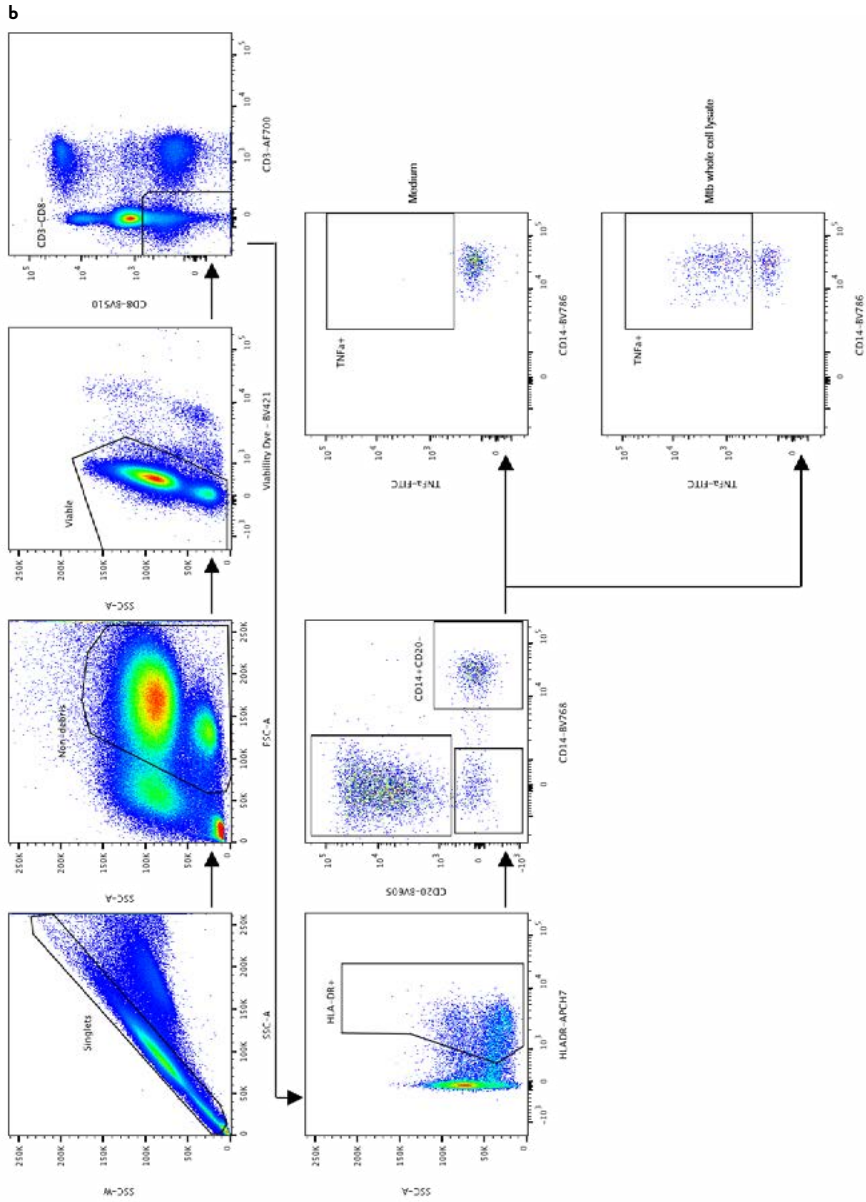


Supplemental Figure 2 continued. Circles represent animals infected after administration of 1.3 CFU, squares represent animals infected after administration of 7 CFU and triangles indicate animals administered both 1.3 and 7 CFU of *Mtb*. Horizontal lines indicate group medians. P-values of possible differences between species were determined by two-sided Mann-Whitney testing.

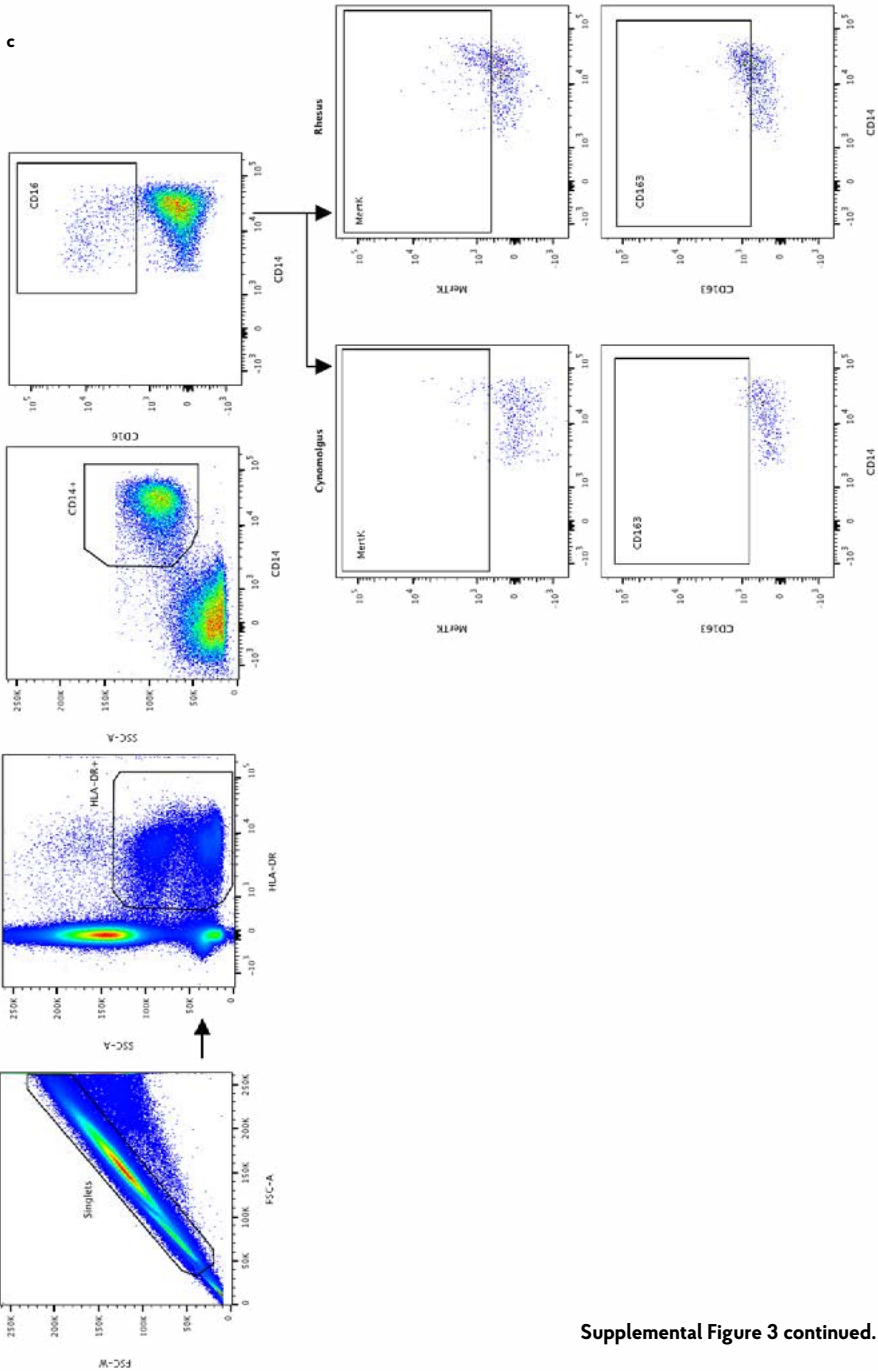
a



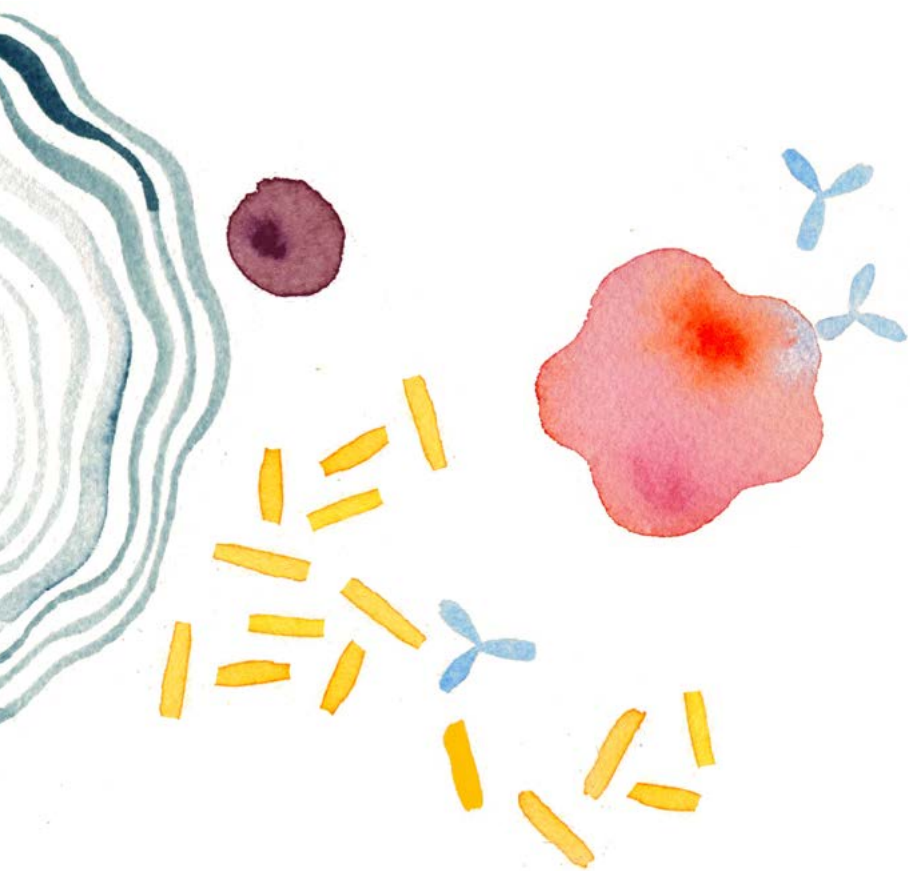
Supplemental Figure 3. Gating strategy applied for flow cytometric analysis of a) T-cells and b) & c) monocytes.



Supplemental Figure 3 continued.



Supplemental Figure 3 continued.



Prevention of tuberculosis infection and disease by local BCG in repeatedly exposed rhesus macaques



Karin Dijkman¹, Claudia C. Sombroek¹, Richard A.W. Vervenne¹, Sam O. Hofman¹, Charelle Boot¹, Edmond J. Remarque¹, Clemens H.M. Kocken¹, Tom H.M. Ottenhoff², Ivanela Kondova¹, Mohammed A. Khayum¹, Krista G. Haanstra¹, Michel P.M. Vierboom¹, Frank A.W. Verreck¹

¹ from the Biomedical Primate Research Centre (BPRC), Rijswijk, the Netherlands

² from the Dpt of Infectious Diseases, Leiden University Medical Centre (LUMC), Leiden, the Netherlands

Published in Nature Medicine, 2019 Feb; 25(2):255-262.

Tuberculosis (TB) remains the most deadly infectious disease¹, and the widely used Bacille Calmette-Guérin (BCG) vaccine fails to curb the epidemic. An improved vaccination strategy could provide a cost-effective intervention to break the transmission cycle and prevent anti-microbial resistance^{2,3}. Limited knowledge of host responses critically involved in protective immunity hampers development of improved TB vaccination regimens. Therefore, assessment of new strategies in preclinical models to select best candidates prior to clinical vaccine testing remains indispensable. We have previously established in rhesus macaques (*Macaca mulatta*) that pulmonary mucosal BCG delivery reduces TB disease where standard intradermal injection fails^{4,5}. Here, we show that pulmonary BCG prevents infection utilizing a novel repeated limiting dose (RLD) *Mycobacterium tuberculosis* (*Mtb*) challenge model and identify Th17A, IL10 and IgA as correlates of local protective immunity. These findings warrant further research into mucosal immunization strategies and their translation to clinical application to more effectively prevent the spread of TB.

Typically, in preclinical vaccine studies, animals are challenged by a single dose of *Mtb* that results in infection and disease in 100% of non-treated controls to demonstrate reduction of disease and/or bacterial burden by prior vaccination. However, whether such reduction after single dose challenge of a highly susceptible species like rhesus macaques is a good predictor of clinical vaccine performance, remains to be determined^{6,7}. Such single challenge may overwhelm or disregard relevant immunological cascades and mask the full potential of any investigational vaccine strategy⁸. Notably, repeated exposure to (expectedly) low amounts of *Mtb* in itself has immunological impact and may contribute to protection against clinical TB, as described in well-defined cases⁹. However, to our best knowledge, repeated exposure to limiting doses of *Mtb* to address efficacy by prevention of infection, as applied successfully in preclinical HIV vaccine research^{10,11}, has not been reported for TB vaccine studies in macaques. To investigate pulmonary BCG efficacy under RLD challenge conditions, healthy, adult, Indian-type rhesus macaques were stratified into three groups of n=8. Two were vaccinated with a standard (adult) human dose of BCG, either by endobronchial instillation (BCG.muc) or by standard intradermal injection (BCG). The third received endobronchial instillation of saline, serving as non-vaccinated controls (nv.ctrls). A study design schematic indicating (peripheral and local) sampling and RLD challenge time points is provided in **Figure 1a**. Thirteen weeks after vaccination, animals were inoculated 8 times at 1 week intervals with a predetermined, limiting dose of 1 CFU of *Mtb* Erdman (see **Extended Data 1a**) by endobronchial instillation into the lower left lung lobe.

Successful immunisation was verified in all vaccinees by elevated IFN γ production and proliferation of peripheral blood mononuclear cells (PBMC) stimulated *in vitro* with protein purified derivative (PPD) of *Mtb* (**Extended Data 2a&b**). Local cells harvested by bronchoalveolar lavage (BAL cells) proliferated to PPD, and BCG could be recovered from bronchoalveolar lavage fluid after mucosal vaccination only (**Extended Data 2c&d**).

During and after RLD challenge animals were monitored weekly for infection, utilizing *Mtb*-specific ESAT6-CFP10 protein stimulation and an ELISPOT-based IFN γ release assay (IGRA). The rate of IGRA-conversion of the standard BCG group was not significantly different from non-vaccinated controls ($p=0.2646$, **Figure 1b**). Mucosal BCG, however, significantly delayed IGRA conversion relative to nv.ctrls ($p = 0.0128$) as well as standard BCG ($p = 0.0184$). Notably, 3 out of 8 BCG.muc animals exhibited no IGRA-conversion at all.

The nv.ctrl group showed increasing IFN γ responses to PPD and to *Mtb*-specific ESAT6-CFP10 from 3 weeks after first inoculation onward (**Figure 1c&d**). After prior intradermal BCG the ESAT6-CFP10 response dynamic was comparable to the dynamic in non-vaccinated controls, but after BCG.muc *Mtb*-specific IFN γ production developed more slowly and was reduced (**Figure 1c&d**). When aligning individual *Mtb*-specific ELISPOT signals by IGRA conversion time point, BCG.muc IGRA converters showed the lowest IFN γ responses overall (**Figure 1e&f**). Once converted none of the animals reverted to become IGRA-negative again, except for 1 BCG.muc (dark blue) and 1 standard BCG animal (yellow), which both transiently reverted for 1 week.

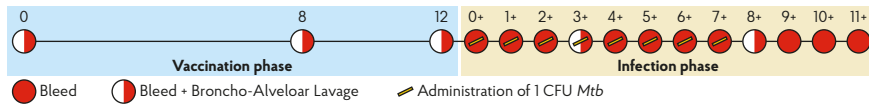
At study endpoint, 4 weeks after final challenge, animals were euthanised and macroscopic TB pathology was scored using a predefined algorithm, scoring size, appearance and frequency of lesions. One non-vaccinated control animal (grey) was culled at week 8 of the infection-phase as it had reached a humane endpoint by predefined criteria. Pulmonary BCG vaccination significantly reduced lung pathology in the primary targeted lung lobe (lower left), better than intradermal BCG treatment (**Figure 2a**). Both BCG vaccination strategies prevented dissemination to other lung lobes in all but one intradermally vaccinated animal (**Figure 2b**). Primary lung lobe pictures from animals representing median level pathology are depicted in **Extended Data 3a**. Histopathological evaluation of randomly sampled lesions of nv.ctrls and BCG animals showed granulomas in different developmental stages, displaying typical TB granuloma architecture. However, BCG.muc animals mostly showed minimal focal interstitial and intra-alveolar lympho-histiocytic cellular infiltrates admixed with prominent collagenous connective tissue and fibroblasts (**Extended Data 3b**).

Similar to the effect on pulmonary dissemination, both BCG administration routes significantly reduced dissemination to extra-thoracic organs (**Figure 2c**). However, only pulmonary BCG vaccination significantly reduced lung draining lymph node involvement (**Figure 2d** and **Extended Data 3a**).

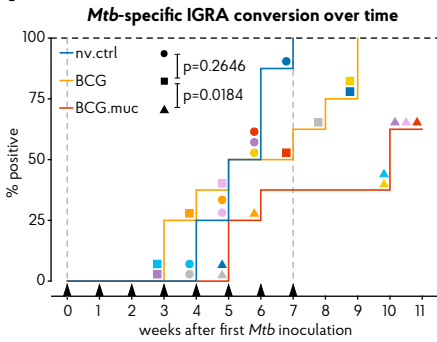


a

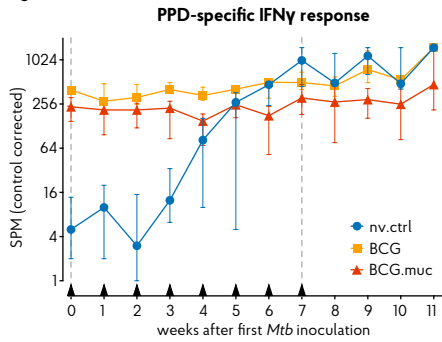
Study week:



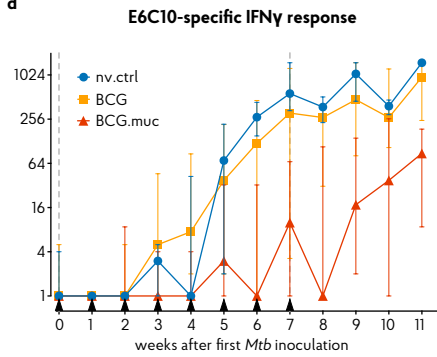
b



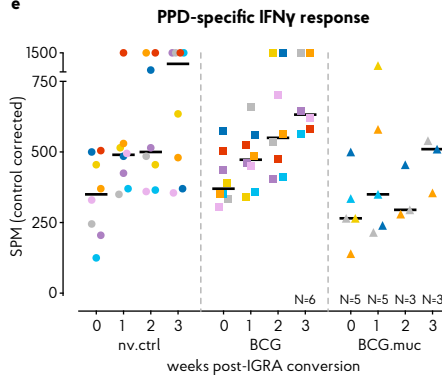
c



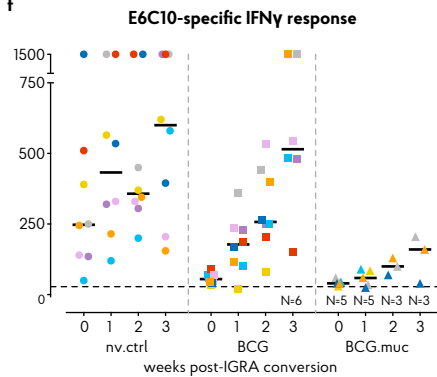
d



e



f



Altogether, no TB-associated pathology was observed in two BCG.muc vaccinated animals (light blue and pink), one of which had remained IGRA-negative (pink, **Supplemental Table 1**). The two other IGRA-negative BCG.muc animals (purple and red, **Supplemental Table 1**) showed a single lesion only, apparently not eliciting any detectable ESAT6-CFP10-specific IGRA response.

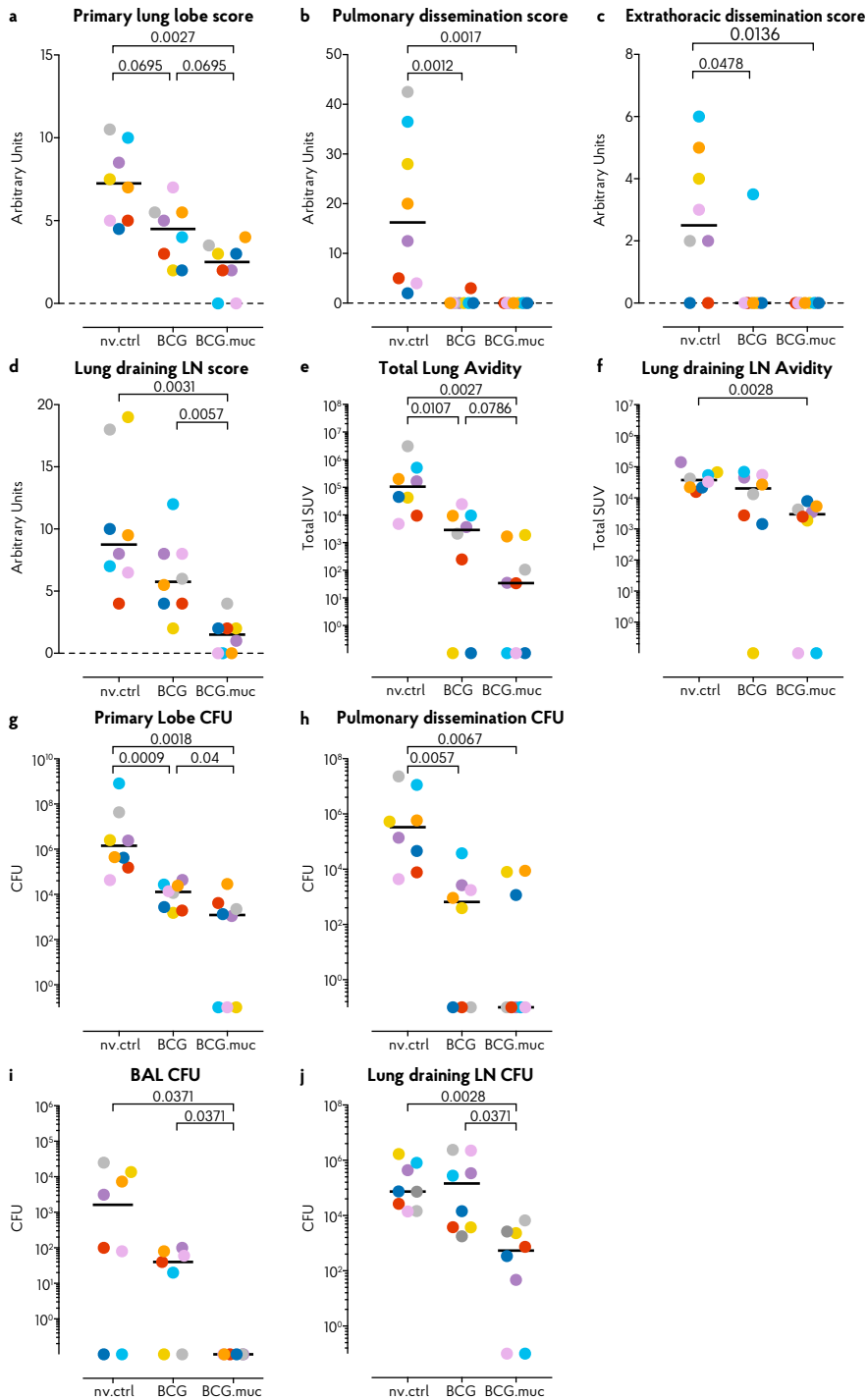
We recorded PET-CT images 1 week after final *Mtb* inoculation, using 18F-fluorodeoxyglucose (FDG) as a tracer of metabolic activity and inflammation¹². Qualitatively, the BCG.muc group revealed lowest levels of inflammation (**Extended Data 3a**). Upon quantification, standard uptake values (SUV) of total lung and lung draining lymph nodes were lowest in the BCG.muc group, although not significantly different from intradermal BCG (**Figure 2e&f**).

One week after final inoculation BAL fluid was plated to assess the presence of *Mtb*. *Mtb* was cultured from 6 nv.ctrl and 5 standard BCG animals (**Figure 2i**). In contrast, no culturable *Mtb* was retrieved from BCG.muc animals. Post-mortem, *Mtb* tissue burden was enumerated by plating homogenates of specific lesions and the primary lung lobe, pooled secondary lobes, and lung draining lymph nodes. Pulmonary BCG significantly reduced the bacterial load in the primary lung lobe as well as in the lung draining lymph nodes (**Figure 2g&j**), outperforming standard BCG. Both BCG vaccinated groups showed a significant reduction of *Mtb* CFU in the secondary lobes compared to nv.ctrls (**Figure 2h**). Thus, protective effects as assessed by bacterial burden and aforementioned pathology read-outs are similar. Altogether, 2 out of 8 BCG.muc animals (light blue and pink) showed no signs of infection or disease (**Figures 2a-j**). Tuberculosis infection and disease read-outs per individual are summarized in **Supplemental Table 1**.

Progressive tuberculosis infection in man as well as in NHPs induces wasting and perturbs haematology and clinical chemistry values^{13,14}. Body weight reduction at endpoint was present in only a small number of animals (**Extended Data 3c**). Changes in mean corpuscular haemoglobin and monocyte-lymphocyte ratio were least affected in the BCG.muc group (**Extended Data 3d&e**). Correspondingly, BCG.muc

- ◀ **Figure 1. Study design schematic & monitoring of TB infection by IFN γ release after repeated ultra-low dose (RLD) exposure to *Mtb*.** Comparing standard versus pulmonary mucosal BCG vaccination in a non-human primate experiment, addressing protective efficacy after repeated ultra-low dose challenge with *Mtb*. **a**) A schematic of the study design shows animal handling and sample collection over time. **b**) Kaplan-Meier curves show conversion of *Mtb*-specific IFN γ response per individual, based on a specific IFN γ ELISPOT assay using ESAT6-CFP10 fusion protein for *in vitro* recall stimulation upon RLD *Mtb* exposure. Triangles along the x-axis indicate the *Mtb* inoculation events. Survival curves (n=8 animals per group) were compared by Mantel-Cox test. **c**) Group medians (n=8 animals per group) of peripheral IFN γ ELISPOT responses to PPD and **d**) *Mtb*-specific ESAT6-CFP10 along the infection phase. In **c**) and **d**) group medians are based on antigen-specific, medium-control corrected SPM and plotted as group medians + interquartile range. Triangles along the x-axis indicate *Mtb* inoculation events. Individual IFN γ ELISPOT responses upon stimulation of PBMCs with **e**) PPD or **f**) ESAT6-CFP10 and aligned for IGRA conversion. In **e**) and **f**) horizontal lines indicate group medians, horizontal dashed line in **f**) indicates the cut-off value of 28 spots per million for positivity to ESAT6-CFP10. Colour coding per individual is consistent throughout (see also **Supplemental Table 1**).





animals were more protected from systemic inflammation as measured by changes in C-reactive protein and serum albumin (**Extended Data 3f&g**).

Whilst pulmonary mucosal BCG vaccination was superior over standard BCG, peripheral IFN γ production and proliferation post-vaccination were not different (**Extended Data 2a&b**). To identify correlates of superior BCG.muc vaccination, T-cell responses in blood and BAL were analysed by flow cytometry at week 8 post-vaccination, at about the peak of the peripheral IFN γ response (representative gating strategy is depicted in **Extended Data 4**). The proportion of PPD-specific IFN γ , IL2, TNF α and IL17A positive CD4 $^+$ T-cells was found to be considerably higher in BALs of pulmonary BCG vaccinated animals compared to standard BCG treated animals (for all: $p < 0.01$, **Figure 3a**), and accompanied by an increase in T-cell numbers in the BAL (**Extended Data 5a**). Intradermal BCG administration resulted in a more modest yet significant local cytokine response that lacks, however, an overt IL17A signal in contrast to pulmonary BCG. Only the latter induced an exclusive quadruple-cytokine-positive population, expressing IL17A in addition to IFN γ , IL2 and TNF α (**Figure 3g left panel and Extended Data 5b**). Additionally, local IFN γ^+ and TNF α^+ CD8 $^+$ T-cells were more frequent after mucosal BCG compared to intradermal BCG (**Figure 3b & 3h left panel**). In the periphery, the CD4 $^+$ T-cell response was comparable between both vaccinated groups (**Figure 3i left panel and Extended Data 5c**) and no vaccine-specific cytokine production was observed in peripheral CD8 $^+$ T-cells (**Figure 3j left panel and Extended Data 5d**).

BAL cells and PBMCs were similarly profiled 1 week after the final inoculation with *Mtb*. Locally, *Mtb* challenge induced substantial PPD-specific cytokine-positive CD4 $^+$ T cell frequencies in nv.ctrl and intradermal BCG vaccinated animals (**Figure 3c**) with an increase of T-cell numbers in BAL (**Extended Data 6a**). In all groups, CD4 $^+$ T-cells predominantly showed a polyfunctional cytokine profile (**Figure 3g middle panel and Extended Data 6b**). Most notably, however, prominent local IL17A $^+$ polyfunctional CD4 $^+$ T-cells remained an exclusive feature of BCG.muc animals (**Figure 3c and Extended Data 6b**) and, thus, appears specific to pulmonary BCG immunization and not pulmonary *Mtb* exposure or intradermal BCG priming.

- ◀ **Figure 2. Pulmonary mucosal BCG vaccination significantly reduces TB disease** Post-mortem evaluation of gross pathology and enumeration of bacterial load in specific tissues demonstrates improved efficacy of BCG.muc over standard BCG. Pathological involvement in arbitrary scores is plotted for **a**) the primary lung lobe, as targeted by endobronchial inoculation, **b**) for all other lung lobes, added up as a pulmonary dissemination score, **c**) for extra-thoracic organs, as a disseminating disease score, and **d**) for draining, hilar lymph node involvement. 18F-fluorodeoxyglucose (FDG) total standard uptake values for **e**) lung and **f**) lung draining lymph nodes 8 weeks into the infection phase. Bacterial counts are plotted for **g**) the primary, targeted lung lobe, **h**) the remaining, secondary lung lobes, **i**) BAL samples collected 1 week after final inoculation and **j**) the draining, hilar lymph nodes. For all figures $n=8$ animals per group, except for **i**) where one BCG and 2 BCG.muc BAL samples could not be interpreted due to contamination. Horizontal lines indicate group medians. Statistical significance of group differences is determined by two sided Mann-Whitney, adjusted for multiple comparisons. Holms adjusted p -values are depicted. Colour coding per individual is consistent throughout (see also **Supplemental Table 1**).



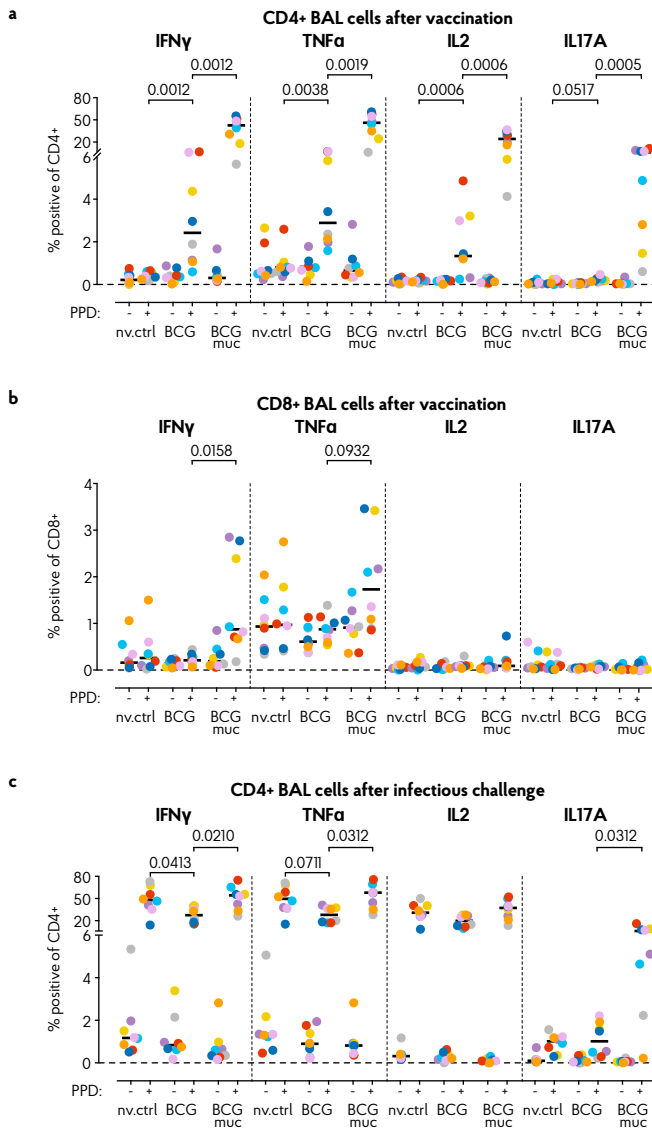


Figure 3. Flow cytometric analysis of the local immune response after BCG vaccination and RLD *Mtb* challenge. Characterisation of cytokine responses in T-cells in the lung **a-b**) 8 weeks after vaccination with BCG and **c-f**) 8 weeks after initial *Mtb* challenge. **a, c, e**) The percentage of total cytokine producing CD4+ and **b, d, f**) CD8+ T cells in BAL, is depicted from left to right for IFN γ , TNF α , IL2 and IL17A (n=8 animals per group). Stacked bar graphs of the multi-functional cytokine positive frequencies of **g**) BAL CD4+, **h**) BAL CD8+, **i**) peripheral CD4+ and **j**) peripheral CD8+ T-cells plotted by their group median values (n=8 animals per group, except for figure **i**) and **j**), middle and

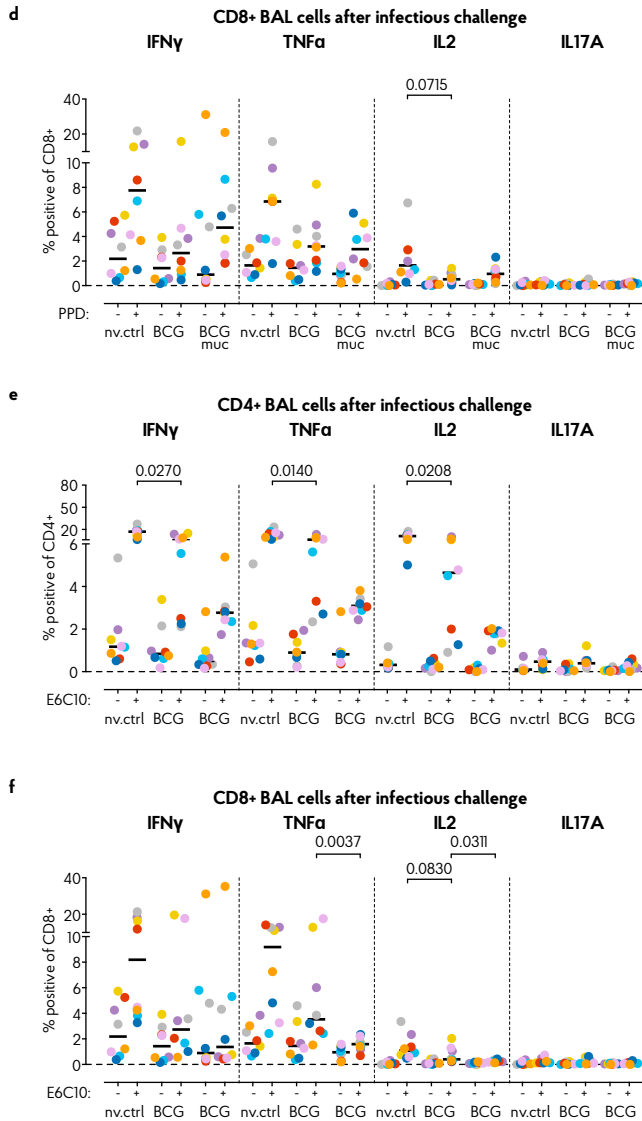


Figure 3 continued. right panels, where for the BCG.muc group n=6 and the BCG group n=7) after PPD stimulation post-vaccination (left) and post-challenge (middle), and ESAT6-CFP10 stimulation post-challenge (right). **a-d)** The symbol "+" indicates PPD or ESAT6-CFP10 stimulated samples, "-" indicates unstimulated, culture medium incubated samples as controls. **a-f)** Horizontal lines indicate group medians. Significance of group differences determined by two-sided Mann-Whitney test adjusted for multiple comparisons. Holms adjusted p-values are depicted. Colour coding per individual is consistent throughout (see also **Supplemental Table 1**).

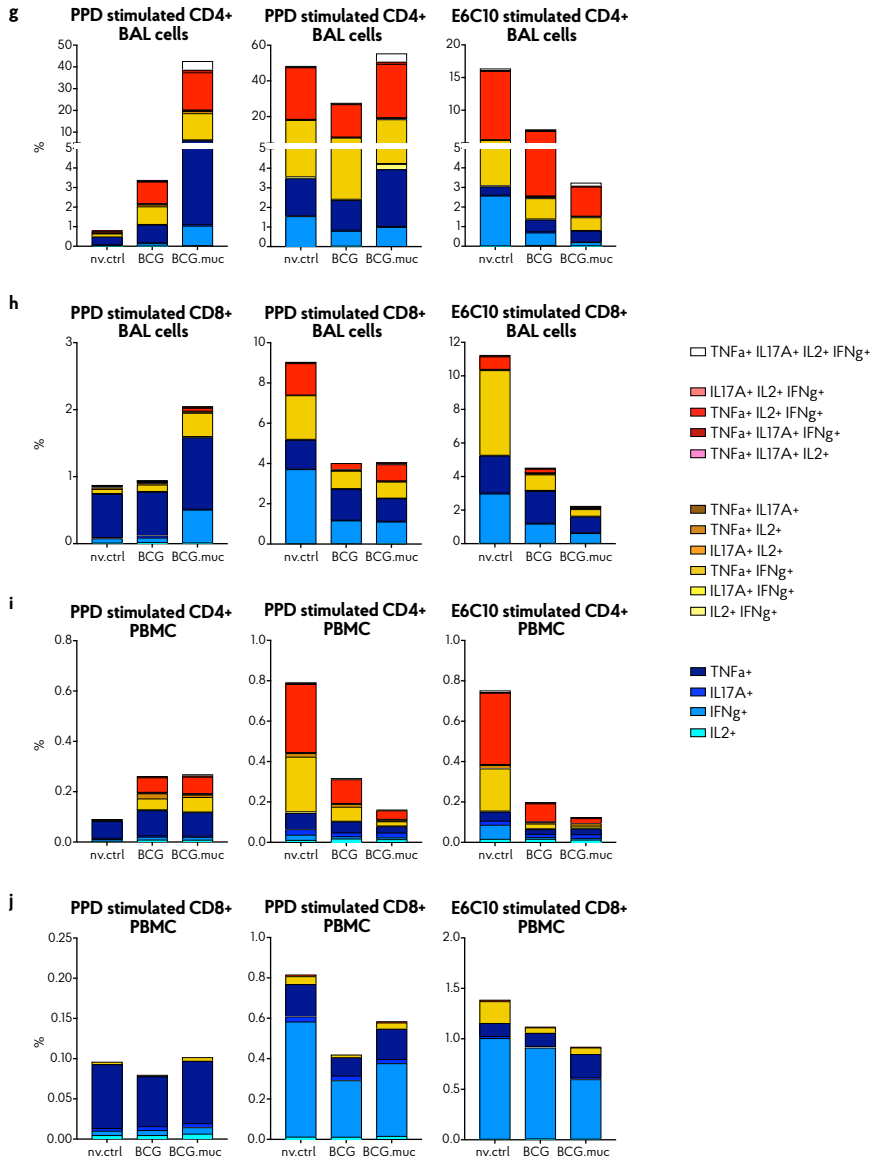


Figure 3 continued.

Beside PPD, BAL cells were stimulated with ESAT6-CFP10 to assess *de novo* *Mtb*-specific cytokine responses. In contrast to stimulation with PPD, frequencies of ESAT6-CFP10-specific cytokine-positive CD4⁺ T-cells were, on average, the lowest in the BCG.muc group (**Figure 3e and 3g right panel**), suggesting limited *Mtb*-specific priming corresponding with reduced *Mtb* tissue load in this group (**Figure 2g-j**). This finding corroborates that suppressed ESAT6-CFP10 responsiveness post-challenge is a marker of a protective vaccine effect. ESAT6-CFP10-stimulated CD4⁺ T-cells produced no or minimal IL17A, supporting the notion of its induction by pulmonary BCG exclusively. After *in vitro* stimulation with PPD or ESAT6-CFP10, pulmonary CD8⁺ T-cells were predominantly positive for IFN γ and TNF α (**Figure 3d,f & h middle and right panel**). Similar to CD4⁺ T-cells, frequencies of cytokine-positive CD8⁺ T-cells after ESAT6-CFP10 stimulation appeared highest in non-vaccinated controls.

In peripheral blood, non-vaccinated controls displayed the highest percentages of PPD and ESAT6-CFP10 specific cytokine-producing CD4⁺ and CD8⁺ T-cells (**Figure 3i and 3j middle and right panels**, and **Extended Data 6c&e and 6d&f**, respectively). Thus, peripheral T-cell cytokine production appears to be largely driven by *Mtb* burden.

Local T-cells from the lung were examined in more detail for the expression of other functional and phenotypic markers. Cytokine producing CD4⁺ T-cells predominantly express a central memory phenotype, as defined by CD28 and CD95 co-expression¹⁵, which is further skewed by vaccination (**Extended Data 5e**). After RLD challenge, this skewed phenotype remained slightly more prominent in vaccinees compared to nv.ctrls (**Extended Data 6g**). In BCG.muc animals, PD-1, which has been associated with a tissue-parenchyma phenotype^{16,17} and control of *Mtb* infection^{16,18,19}, was expressed at significantly higher level by polyfunctional IL17A⁺ CD4⁺ T-cells compared to triple-positive cells lacking IL17A (**Extended Data 5f**). This 'PD-1 high' phenotype was sustained post-challenge (**Extended Data 6h**). CD69, a marker of early activation as well as tissue memory^{20,21}, was not differentially expressed by CD4⁺ T-cells of the respective treatment groups post-vaccination (**Extended Data 5g**), but after RLD challenge was highest on CD4⁺ T-cells of the BCG.muc group. (**Extended Data 6i**). Although co-expression of PD-1 and CD69 was not assessed, the data are in agreement with the induction of a pulmonary IL17A⁺ CD4⁺ T-cell population after mucosal BCG vaccination expressing a parenchymal memory phenotype. Granzyme B expression in local CD8⁺ T-cells *ex vivo* was significantly increased with BCG.muc, though not significantly different from standard BCG vaccination (**Extended Data 5h**). After RLD challenge the pattern was reversed, with non-vaccinated controls displaying highest and BCG.muc the lowest frequency of granzyme B⁺ CD8⁺ T-cells (**Extended Data 6j**).

We also used a Luminex™ array to identify effector molecules associated with protective vaccination by measuring secretion levels from PPD and ESAT6-CFP10 stimulated PBMC and BAL cells (again, 8 weeks post-BCG and 1 week after final *Mtb* inoculation). For IFN γ , TNF α , IL2 and IL17A, secretion levels corresponded grossly to



what was observed by flow cytometry (**Extended Data 7a-d** for BAL, **7e-h** for PBMC), although peripheral TNF α secretion was higher after BCG.muc compared to standard BCG. Again, after vaccination, IL17A was detected in BAL cell supernatants from BCG.muc animals exclusively (although not ubiquitously) (**Extended Data 7d&h**).

Additionally, GM-CSF, IL6, granzyme B and IL10 were secreted by PPD-stimulated BAL cells of the BCG.muc group, whereas upon standard BCG only IL6 was detectable (**Figure 4a-d**). IL10 provided the most distinctive signal in terms of protective immunity, as after RLD *Mtb* challenge PPD-specific IL10 remained the highest in the BCG.muc group (**Figure 4d**). Post-vaccination, peripheral PPD-specific production of these cytokines did not differ between groups (**Extended Data 7i-l**). After RLD challenge, PBMC and BAL cells from nv.ctrls typically showed highest cytokine-secretion levels, with the exception of aforementioned local PPD-specific IL10.

Pulmonary BCG vaccination induced both a peripheral and a local proliferation response (**Extended Data 2b&c**). To assess the potential of vaccine-primed lymphocyte expansion after RLD *Mtb* challenge, we measured proliferation of BAL cells and PBMCs 1 week after the final challenge in comparison to pre-*Mtb* levels. After challenge, BAL cells exhibited very limited to no antigen-specific proliferation (**Figure 4e**), despite high local IL2 production measured by flow cytometry (**Figure 3c**). PBMCs, however, proliferated in response to both PPD and ESAT6-CFP10 (**Figure 4f**). PBMCs from nv.ctrls and intradermal BCG animals proliferated more strongly than those from BCG.muc animals, suggesting that peripheral exhaustion of T-cell expansion is not underlying the greater level of infection and disease in the former two.

We also investigated the possible contribution of PPD-specific immunoglobulins in BAL fluid and serum 8 weeks after vaccination (designated as pre-*Mtb*) and 1 week after the final *Mtb* challenge. Pulmonary but not intradermal BCG vaccination yielded significantly elevated PPD-specific antibodies including IgA in BAL fluid (**Figure 4g**). Upon RLD challenge, however, nv.ctrls and standard BCG vaccinees also showed high specific immunoglobulin signals (**Figure 4g**). Serum levels of PPD-specific immunoglobulin, but not IgA, were slightly higher in both BCG vaccinated groups compared to nv.ctrls (**Figure 4h**). After RLD *Mtb* challenge, both PPD-specific Ig and IgA serum levels increased slightly in the nv.ctrls but did not differ between groups.

To verify the differential immune responses after vaccination as immune correlates of successful vaccination we calculated Spearman's rho coefficients against time to IGRA conversion as well as pathology score and bacterial load of the primary lung lobe. Prognostically, responses 8 weeks post-vaccination from all BCG/BCG.muc vaccinees were included, assuming that mechanisms of protective immunity should not be different. Diagnostically, we analyzed the immune responses profiled 1 week after final inoculation, including results from all study subjects. Results are summarized in **Supplemental Table 2**.

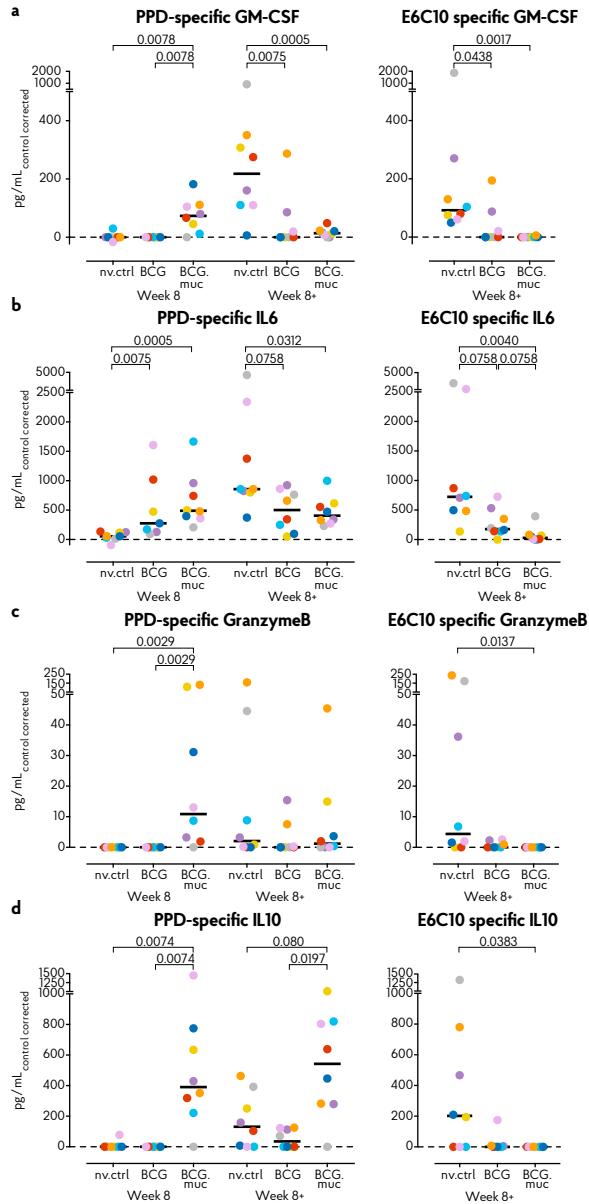


Figure 4. Post-BCG and post-*Mtb* cytokine profiles, proliferative and humoral immune responses. Production of **a)** GM-CSF, **b)** IL6, **c)** granzyme B and **d)** IL10 by BAL cells stimulated with PPD or ESAT6-CFP10 fusion protein 8 weeks after vaccination with BCG or 8 weeks after initial RLD challenge (Week 8+). All cytokines are plotted as culture medium control corrected values. PPD and ESAT6-CFP10 specific proliferation of **e)** BAL cells and **f)** PBMCs before and after *Mtb* challenge. Proliferation is depicted as stimulation index: the ratio of antigen- over medium control-stimulated values. Pan-Ig and IgA antibody response against PPD in **g)** BAL fluid and **h)** serum, 8 weeks after.

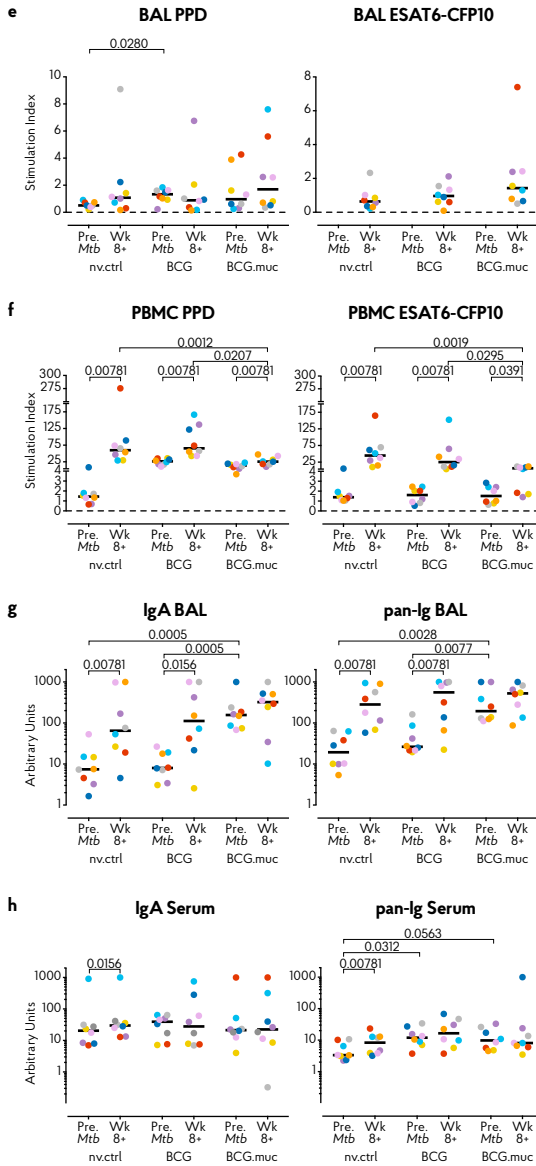


Figure 4 continued. BCG vaccination and 8 weeks after Mtb infection. Antibody levels are plotted as arbitrary units, determined by standardization against a reference sample. Horizontal lines indicate group medians, with n=8 animals per group for all graphs, except for **e**) where n=7 for the pre-infection nv.ctrl data. Significance of group differences was determined by two-sided Mann-Whitney test adjusted for multiple comparisons. Holms adjusted p-values are depicted. Within group comparisons performed by two-sided Wilcoxon signed-rank test. Colour coding per individual is consistent throughout (see also **Supplemental Table 1**).

Prognostically, the frequency of IFN γ +, TNF α +, IL2+ as well as IL17A+ CD4+ T-cells in BAL, but not in PBMC, correlate significantly with protective effects by either of the outcome measures. However, after infectious challenge, only the frequency of local IL17A+ CD4+ T-cells remains as a correlate of protection, while peripheral IFN γ +, TNF α + and IL2+ CD4+ T-cell frequencies correlate with TB disease. Local IFN γ + and TNF α + CD8+ T-cell frequencies after vaccination correlate with beneficial outcome. However, after challenge the correlation between these cytokine-positive CD8+ T-cell frequencies and a protective phenotype is no longer present. Regarding PPD-specific cytokine and effector molecule secretion from BAL cells post-vaccination, all correlate significantly or trend towards correlation with beneficial outcome. After infectious challenge, however, their secretion mainly appears to correlate with disease, except for IL17A and IL10. Regarding PBMCs, increased TNF α , GM-CSF and to a lesser extent IL6 post-vaccination correlate with beneficial outcome. Post-*Mtb*, however, increased secretion levels from PBMC, except for IL17A, appear as correlates of TB disease. Despite the fact that *Mtb*-specific antibodies have been associated with protection against TB in mouse studies and through mycobacterial growth assays in the presence of antibodies *in vitro*^{5, 22, 23, 24} we failed to demonstrate significant correlation of the quantitative level of antigen-specific immunoglobulins in BAL or serum with any of the infection and disease measures. The relative low number of subjects in this study hampers multivariate analyses to identify more complex signatures, for which further studies are warranted.

The findings from our study underpin that quantitative and qualitative characteristics of the immune response as well as aspects of temporal and spatial distribution are relevant to scrutinize when investigating protective immunity against TB. The cellular and molecular signals that prognostically correlate with beneficial outcome, i.e. delay in IGRA conversion and reduction of lung pathology and bacterial load, are found to correlate with poor outcome after infectious challenge, with the notable exception of local IL17A and IL10 response signals. A role of IL17A in protective TB immunity has been suggested previously by studies in mice^{5,25,26} and cynomolgus macaques²⁷, but appears ambiguous from TB patients (reviewed in²⁸⁻³⁰). Yet, Scriba *et al.* have reported early suppression of Th17 responses in progressors relative to *Mtb*-infected controls³¹. Although the cellular source of IL10 in this study remains unknown and co-expression with IL17A formally cannot be concluded, in mice Th17 cells have been reported to be able to co-express IL10 under the influence of TGF β and IL6³², the latter of which was produced in our study most prominently by stimulated BAL cells after BCG.muc vaccination. Importantly, IL10-expressing Th17 cells were reported to be enriched in the blood of latently infected individuals over active TB cases, who showed higher levels of pro-inflammatory IFN γ + Th17 cells lacking IL10³³. Despite the association of IL10 with immune evasion and long-term lung infection³⁴, the presence of both IL17A and IL10 in the pulmonary space upon *Mtb* challenge may provide an important signature of balanced inflammation and protective immunity.



This study also corroborates the efficacy of standard intradermal BCG in preventing dissemination of disease. The considerable LN involvement and lack of prevention of infection, however, highlight the shortcoming of the IFN γ + Th1 response induced by standard BCG³⁵.

For pulmonary mucosal vaccination we instilled BCG unilaterally by bronchoscope. Future studies should also interrogate a contralateral strategy to assess whether the protective phenotype against RLD infection extends beyond the vaccine-targeted lung lobe and consider more translatable mucosal administration approaches like aerosolisation³⁶. Also, the impact of viability, integrity and persistence of BCG on its efficacy needs to be addressed, as it is notable that the one BCG.muc vaccinee without culturable BCG from its BAL after vaccination displayed the weakest immunisation signals and among the highest infection and disease levels after challenge.

Prior exposure to *Mtb* has been associated with protection against clinical TB in well-defined cases and recently also in NHP^{9,37}. Paradoxically, in man³⁸ and rabbits³⁹ it was suggested that repeated exposure exacerbates disease. Neither of these phenomena can be inferred from this work because of study design and lack of appropriate historic controls. Our study conditions do concur with the notion that an ongoing, progressive *Mtb* infection in rhesus macaques does drive a cellular Th1 and a humoral response, yet, without any appreciable protective efficacy.

The present NHP study demonstrates that repeated *Mtb* challenge is feasible for (head-to-head comparative) vaccine screening toward improved efficacy over standard BCG. Most importantly, the immune signatures associated with protective pulmonary mucosal BCG vaccination provide important leads for further investigation and the development of improved prophylactic vaccination strategies to effectively fight TB.

Acknowledgements

We thank G. Koopman and R. Bontrop for manuscript review. We thank BPRC's animal and veterinary care teams and the clinical lab personnel for their excellent expert contributions to this study. We thank K. Franken from the Ottenhoff lab at the Leiden University Medical Centre for providing us with recombinant ESAT6-CFP10 fusion protein. We thank F. van Hassel for figure-editing assistance. The following reagent was obtained through the NIH Biodefense and Emerging Infections Research Resources Repository, NIAID, NIH: *Mycobacterium tuberculosis*, Strain Erdman K01 (TMC107), NR-15404. PET/CT infrastructure and TB team management was supported by a grant from the Bill & Melinda Gates Foundation, OPP1130668. This work was performed under the TBVI governed TBVAC.2020 network programme for advancing TB vaccine candidates from early discovery through preclinical and into early clinical development, supported by the European Commission under the Horizon.2020 programme, grant agreement no. 643381.

Materials & Methods

Ethics, animals and handling

Before the start of the study ethical approval was obtained from the independent animal ethics committee (in Dutch: Dierexperimentencommissie, DEC) as well as BPRC's institutional animal welfare body (in Dutch: Instantie voor Dierwelzijn, IvD). The study protocol was registered under DEC accession no. 761subB. All housing and animal care procedures took place at the Biomedical Primate Research Centre (BPRC) in Rijswijk, the Netherlands, and were in compliance with European directive 2010/63/EU, as well as the "Standard for Humane Care and Use of Laboratory Animals by Foreign Institutions" provided by the Department of Health and Human Services of the US National Institutes of Health (NIH, identification number A5539-01). The BPRC is accredited by the American Association for Accreditation of Laboratory Animal Care (AAALAC). Twenty-four healthy male Indian-type rhesus macaques (*Macaca mulatta*) from the in-house breeding colony were stratified into 3 groups of 8 animals each; treatment was randomly assigned to each of the groups. The study was powered to detect a reduction in lung pathology of 22 arbitrary units as a primary outcome, considering a power of 80% and an alpha of 0.05. Stratification was based on social indicators for pair-wise housing, age and body weight: (mean age \pm SD in years: nv.ctrls = 5.1 \pm 0.5, BCG = 5.6 \pm 1.3, BCG.muc = 5.7 \pm 1.6; mean weight \pm SD in kilograms: nv.ctrls = 9.0 \pm 1.8, BCG = 9.4 \pm 1.8, BCG.muc = 9.5 \pm 3.1). Throughout the experiment animals were socially housed (pair-wise) at biosafety level 3. Macaques were provided with enrichment in the form of food and non-food items on a daily basis and animal welfare was monitored daily. Animal weight was recorded prior to each blood collection event. Humane endpoints were predefined to limit possible discomfort. All animal handling and biosampling was performed under ketamine sedation (10 mg/kg, by intra-muscular injection). For endobronchial instillation ketamine (5mg/kg) was supplemented with intramuscular medetomidine (0.04 mg/kg) and an analgesic sprayed into the larynx. By the end of the infection phase or when reaching a humane endpoint, animals were euthanized by intravenous injection of pentobarbital (200 mg/kg) under ketamine sedation. All veterinary staff was blinded to treatment of individual animals.

BCG vaccination and repeated limiting dose *Mtb* challenge

Two of 3 groups were vaccinated with Bacillus Calmette Guérin strain Sofia (InterVax Ltd., Ontario). One group received a standard, adult human dose of 1.5-6.0 $\times 10^5$ CFU in 0.1 mL reconstituted vaccine in the skin (abbreviated as BCG). The other group received the same dose but in 10 mL of sterile saline solution by endobronchial instillation into the lower left lung lobe (abbreviated as BCG.muc). BCG, regardless of administration route, was prepared from a single pooled mix of freshly reconstituted vials immediately prior to vaccination. Vaccination was executed for all animals in a single session in random order within 2-3 hours from vaccine preparation. Limiting infectious dose of *Mtb* Erdman K01 strain was determined in a prior study: a calculated



average of 1.3 CFU resulted in an infection rate of 80%, as measured by IFN γ ELISPOT (**Extended Data 1a**). Animals were infected weekly for 8 consecutive weeks by endobronchial instillation, targeting the lower left lung lobe. All challenge events occurred in a single session within 2-3 hours from preparing the inoculum from a frozen *Mtb* stock, challenging all animals in random order. For quality assurance at each infection time point serial dilutions from the inoculum preparation process were plated on 7H10 Middlebrook plus PANTA antibiotic mixture plates. Average recovery of CFUs from the *Mtb* Erdman stock was 85% of the expected number of CFU (95%CI: 61%-109%, **Extended Data 1b**). When applicable, peripheral blood sampling and/or bronchoalveolar lavage was performed prior to infectious challenge.

Bio-sample collection and processing

Cells from the pulmonary mucosa were recovered at specific time points by broncho-alveolar lavage (BAL), targeting the lower left lung lobe. Three volumes of 20 mL of prewarmed 0.9% saline solution were consecutively instilled and recovered. BAL fluid was harvested by centrifugation of BAL samples for 10 minutes at 400g after 100 μ m filtration. Supernatant was subsequently decanted and stored at -80°C pending further analysis. The BAL cell pellet was taken up in RPMI supplemented with 10% fetal calf serum (FCS), glutamax and penicillin/streptomycin (from now on referred to as R10) and used in downstream assays freshly. Heparinised blood for immune monitoring, EDTA blood for standard haematology, and serum for clinical chemistry were all collected by venepuncture. Peripheral blood mononuclear cells (PBMCs) were obtained by density gradient centrifugation with Lymphoprep lymphocyte separation medium (Axis-Shield, UK) and resuspended in R10 for downstream immunological assays. Serum tubes were spun for 10 minutes at 1000g to harvest cell-free serum. Serum and BAL fluid were filter-sterilized by centrifugation through 0.2 μ m PVDF membrane plates (Fisher Scientific) before analysis.

PET/CT image acquisition and analysis

All PET/CT scans were acquired on anesthetized macaques in a biosafety level 3 imaging suite using a hybrid preclinical MultiScan LFER 150 PET/CT scanner (Mediso Medical Imaging Systems, Budapest, Hungary) having 320 μ m slice thickness for CT and 800 μ m slice thickness for PET. PET/CT image analyses were performed using Osirix MD viewer, an open source image analysis software. Total lung [18 F]FDG uptake was measured by first segmenting the lung on CT image using a region grow ROI tool (-1024 to -300HU) of Osirix¹². This segmented ROI was then copied on the co-registered PET image to extract lung. Within this extracted PET lung, region grow ROIs were drawn on every granuloma (2.3 to 100 SUV) and data was exported as standardized uptake value (SUV) within these ROIs¹². To measure the activity in the lymph nodes, co-registered PET/CT images were used to localise individual lymph nodes. All PET-CT acquisition and analysis was performed in a blinded fashion.

Post-mortem pathology assessment.

After euthanasia tuberculosis pathology was quantified using a semi-quantitative grading system (adapted from⁴⁰) based on lesion size, manifestation and frequency, and lymph node involvement. The thoracic cavity, including the heart, ribcage, vertebrae and diaphragm were all macroscopically scored for the presence of granulomas and pleural adhesions. Lungs were isolated and lobes were separated from the trachea. Subsequently, lung lobes were cut in 5mm thick slices prior to pathology scoring. Granulomas were collected and immersed in 4% neutral-buffered formalin for histological analysis. Lung draining lymph nodes were isolated, photographed and scored for size and extent of involvement. Axillar and inguinal lymph nodes were similarly assessed but not found to be affected in any animal. Extra-thoracic organs such as kidneys, spleen, pancreas and liver were macroscopically assessed for the presence of lesions. Any affected tissue was collected and immersed in 4% neutral-buffered formalin for histological analysis.

Determination of bacterial load in tissue

After pathology assessment and sampling for histopathology lung lobes were minced and homogenized in GentleMACS C- and M-tubes (Miltenyi). The primary targeted lung lobe was processed separately from other lung lobes to assess intrapulmonary bacterial dissemination. Bronchoalveolar lymph nodes were first processed to a single cell suspension by straining over a 100 µm cell strainer (Greiner) and then homogenized in GentleMACS M-tubes. All homogenates were frozen at -80° Celsius before enumeration of bacterial counts from serial homogenate dilutions on 7H10 Middlebrook agar plates, supplemented with PANTA antibiotic mix and 2-thiophenecarboxylic acid hydride (TCH) (Tritium, the Netherlands). Plates were incubated at 37° Celsius at least for 3 weeks until Colony Forming Units (CFU) were observed. Plates were incubated for at least 6 weeks before scored as negative. CFUs were counted with a Scan4000 automated counting system (Interscience, France). Persistence of BCG in the lungs was determined by parallel plating of lung homogenates on 7H10 Middlebrook agar plates, supplemented with PANTA only. Colonies that grew on plates without TCH but not with TCH were collected and processed for isolation of mycobacterial DNA and genotyping by specific PCR to confirm the nature of *Mtb*. Briefly, bacteria were first incubated with lysozyme mix (20 mg/mL lysozyme; 20 mM Tris-HCl (pH 8.0); 2 mM EDTA; 1.2% Triton) and incubated at 37 ° Celsius for 60 minutes. Subsequently, proteinase K and carrier RNA were added and samples were incubated at 56° Celsius for another 30 minutes. After 15 minutes of heat-inactivation at 95° Celsius DNA was isolated with the QIAmp DNA Mini Kit according to manufacturer's protocol. Colony identity was determined amplifying the RD1 region by PCR, as described previously⁴¹.



Hematology and clinical chemistry

Standard hematology on EDTA blood was performed on a Sysmex 2000i system (Siemens). Serum C-reactive protein and Albumin levels were determined using a Cobas™ Integra400+ (Roche Diagnostics). Clinical lab personnel were blinded to animal treatment.

IFN γ ELISPOT

Non-human primate specific IFN γ ELISPOT (U-CyTech, the Netherlands) was performed according to manufacturer's protocol on PBMCs at specific time points along the study. Briefly, 200,000 PBMCs were incubated in triplicate for 24 hours with *Mtb*-derived Purified Protein Derivate (PPD, Statens Serum Institute, Denmark) or recombinant ESAT6-CFP10 fusion protein (provided by Kees Franken from the Ottenhoff lab, Leiden University Medical Centre)^{42,43}, both at a final concentration of 5 μ g/mL. The next day, supernatant was harvested and stored, and cells were washed and transferred to anti-IFN γ coated membrane plates (Millipore). After another 24 hours of incubation cells were discarded and membrane-bound IFN γ was visualized using a biotinylated anti-IFN γ detector antibody, streptavidin-horseradish peroxidase conjugate and tetramethylbenzidine substrate. Spots were quantified using an automated reader (AELVIS, Hannover). The pre-infection response to ESAT6-CFP10 of all animals was used to determine the threshold for conversion from negative to positive, which was set at the average control corrected pre-infection response plus 3x the standard deviation. This resulted in a cut-off value for positivity of 28 control corrected spots per million.

Proliferation assays

Proliferation of PBMCs and BAL cells was determined by tritium-labelled thymidine (³H-thymidine) incorporation after antigen-specific stimulation in vitro. Cells were seeded at 100,000 cells/well in triplicate (PBMCs) or at 200,000 cells/well in single wells (BAL cells) in 96-well round-bottom microtiter plates. Samples were stimulated with 5 μ g/mL PPD or ESAT6-CFP10, or concanavalin A as positive control. After 72 hours supernatant was harvested and 0.5 μ Ci ³H-thymidine was added and cells were incubated for 18-24 hours before harvesting cells on glass-fiber filter plates (PerkinElmer). After drying, MicroScint-E scintillation fluid (PerkinElmer) was added to the wells and activity was measured on a TopCount (PerkinElmer) scintillation counter.

Flowcytometry

Cell type-specific immune responses post-vaccination and post-infection were determined by flowcytometric analyses of PBMCs and BAL cells. Cells were profiled either *ex vivo* or after overnight incubation with or without PPD and in the presence of GolgiPlug transport inhibitor (BD Biosciences, added 3-4 hours after start of incubation) with combinations of antibodies listed in **Supplemental Table 3**. PMA/ionomycin stimulated samples were taken along as technical/positive controls.

Stained samples were fixed overnight with 2% paraformaldehyde and measured on a 3 laser, 14 colour LSR-II flowcytometer (BD Biosciences). Analysis was performed with FlowJo software version 10 (Treestar). T-cells were gated as Singlets/Lymphocytes/Viable/CD14-CD20-/CD45+/CD3+ before CD4 and CD8 gating was applied. Any anomalies indicative of unstable signal acquisition were excluded using the time parameter. Cytokine positivity was determined by placement of cytokine gates on the medium control samples and subsequently applying the gates to the PPD or ESAT6-CFP10 fusion protein stimulated samples. A representative gating strategy is depicted in **Extended Data 4**. All samples minimally contained over 1000 CD3+ T-cell events.

Antibody ELISAs

Antibody levels in serum and BAL were determined by Enzyme Linked ImmunoSorbent Assay (ELISA). In brief, 96-well plates were coated with either 5 µg/mL PPD or *Mtb* HN828 Whole Cell lysate (BEI Resources, VA, USA) in PBS. After overnight blocking with 1% BSA, samples were added. Bound antibodies were subsequently detected with either alkaline phosphatase-conjugated anti-IgG(H+L) (ThermoFisher Scientific) for broad Ig response analysis or anti-IgA(H) (Fisher Scientific) for subtype specific analysis, and the addition of *para*-nitrophenylphosphate substrate for ELISA colour development. All samples were normalized to arbitrary units (AU) against a serial dilution of a positive reference sample which was included in all assays.

Multiplex cytokine assay

Cytokine production of stimulated PBMCs (24 hours) and BAL cells (72 hours) was assessed by custom Milliplex Luminex kits (Merck Millipore, USA). Assays were performed according to manufacturer's protocol. In short: supernatants of stimulated cells were incubated with beads coated with cytokine-specific antibodies. Bound cytokines were visualized using biotin-coupled detection antibodies and PE-labelled streptavidin. Beads were acquired on a Bioplex 200 system and cytokine levels were calculated with Bioplex Manager software version 6.1 (both Biorad, CA, USA).

Statistical analysis

Statistical analyses were performed using Graphpad Prism software version 7 and R version 3.5.1⁴⁴. Significance of differences between groups was calculated by two-sided Mann-Whitney testing of which Holm's adjusted p-values are reported. Paired observations within groups were analysed by two-sided Wilcoxon signed-rank test. Correlation statistics were generated by Spearman's rank analysis. Unless indicated otherwise in the figure legends, statistical calculations are based on n=8 observations per treatment group.



References

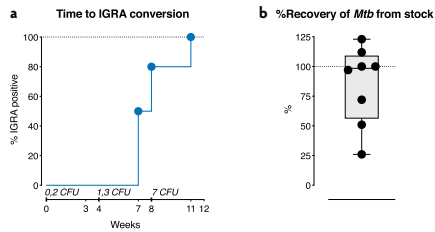
1. Geneva: World Health Organization. Global tuberculosis report 2019.
2. Kaufmann, S.H., *et al.* Progress in tuberculosis vaccine development and host-directed therapies--a state of the art review. *The Lancet. Respiratory medicine* **2**, 301-320 (2014).
3. Knight, G.M., *et al.* Impact and cost-effectiveness of new tuberculosis vaccines in low- and middle-income countries. *Proceedings of the National Academy of Sciences of the United States of America* **111**, 15520-15525 (2014).
4. Verreck, F.A.W., *et al.* Variable BCG efficacy in rhesus populations: Pulmonary BCG provides protection where standard intra-dermal vaccination fails. *Tuberculosis (Edinburgh, Scotland)* **104**, 46-57 (2017).
5. Aguilo, N., *et al.* Pulmonary but Not Subcutaneous Delivery of BCG Vaccine Confers Protection to Tuberculosis-Susceptible Mice by an Interleukin 17-Dependent Mechanism. *The Journal of infectious diseases* **213**, 831-839 (2016).
6. McShane, H. & Williams, A. A review of preclinical animal models utilised for TB vaccine evaluation in the context of recent human efficacy data. *Tuberculosis (Edinburgh, Scotland)* **94**, 105-110 (2014).
7. Hawn, T.R., *et al.* Tuberculosis vaccines and prevention of infection. *Microbiology and molecular biology reviews* : *MMBR* **78**, 650-671 (2014).
8. Roederer, M. Parsimonious Determination of the Optimal Infectious Dose of a Pathogen for Nonhuman Primate Models. *PLoS pathogens* **11**, e1005100 (2015).
9. Simmons, J.D., *et al.* Immunological mechanisms of human resistance to persistent Mycobacterium tuberculosis infection. *Nature reviews. Immunology* (2018).
10. Hessel, A.J., *et al.* Effective, low-titer antibody protection against low-dose repeated mucosal SHIV challenge in macaques. *Nature medicine* **15**, 951-954 (2009).
11. Hudgens, M.G., *et al.* Power to detect the effects of HIV vaccination in repeated low-dose challenge experiments. *The Journal of infectious diseases* **200**, 609-613 (2009).
12. White, A.G., *et al.* Analysis of 18FDG PET/CT Imaging as a Tool for Studying Mycobacterium tuberculosis Infection and Treatment in Non-human Primates. *Journal of visualized experiments* : *JoVE* (2017).
13. Rogers, P.M. A study of the blood monocytes in children with tuberculosis. *The New England journal of medicine* **198**, 740-749 (1928).
14. Naranbhai, V., *et al.* The association between the ratio of monocytes:lymphocytes at age 3 months and risk of tuberculosis (TB) in the first two years of life. *BMC medicine* **12**, 120 (2014).
15. Pitcher, C.J., *et al.* Development and homeostasis of T cell memory in rhesus macaque. *Journal of immunology (Baltimore, Md. : 1950)* **168**, 29-43 (2002).
16. Mogueche, A.O., *et al.* ICOS and Bcl6-dependent pathways maintain a CD4 T cell population with memory-like properties during tuberculosis. *The Journal of experimental medicine* **212**, 715-728 (2015).
17. Kauffman, K.D., *et al.* Defective positioning in granulomas but not lung-homing limits CD4 T-cell interactions with Mycobacterium tuberculosis-infected macrophages in rhesus macaques. *Mucosal immunology* (2017).
18. Jensen, K.H., Persson, G., Bondgaard, A.L. & Pohl, M. Development of pulmonary tuberculosis following treatment with anti-PD-1 for non-small cell lung cancer. *Acta oncologica (Stockholm, Sweden)*, 1-2 (2018).
19. Picchi, H., *et al.* Infectious complications associated with the use of immune checkpoint inhibitors in oncology: Reactivation of tuberculosis after anti PD-1 treatment. *Clinical microbiology and infection : the official publication of the European Society of Clinical Microbiology and Infectious Diseases* (2017).

20. Purwar, R., et al. Resident memory T cells (T(RM)) are abundant in human lung: diversity, function, and antigen specificity. *PLoS one* **6**, e16245 (2011).
21. Kumar, B.V., et al. Human Tissue-Resident Memory T Cells Are Defined by Core Transcriptional and Functional Signatures in Lymphoid and Mucosal Sites. *Cell reports* **20**, 2921-2934 (2017).
22. Zimmermann, N., et al. Human isotype-dependent inhibitory antibody responses against Mycobacterium tuberculosis. *EMBO molecular medicine* **8**, 1325-1339 (2016).
23. Logan, E., et al. Elevated IgG Responses in Infants Are Associated With Reduced Prevalence of Mycobacterium tuberculosis Infection. *Frontiers in Immunology* **9**(2018).
24. Chen, T., et al. Association of Human Antibodies to Arabinomannan With Enhanced Mycobacterial Opsonophagocytosis and Intracellular Growth Reduction. *The Journal of infectious diseases* **214**, 300-310 (2016).
25. Cruz, A., et al. BCG vaccination-induced long-lasting control of Mycobacterium tuberculosis correlates with the accumulation of a novel population of CD4(+)IL-17(+)TNF(+)IL-2(+) T cells. *Vaccine* **33**, 85-91 (2015).
26. Gopal, R., et al. Unexpected role for IL-17 in protective immunity against hypervirulent Mycobacterium tuberculosis HN878 infection. *PLoS pathogens* **10**, e1004099 (2014).
27. Wareham, A.S., et al. Evidence for a role for interleukin-17, Th17 cells and iron homeostasis in protective immunity against tuberculosis in cynomolgus macaques. *PLoS one* **9**, e88149 (2014).
28. Lyadova, I.V. & Panteleev, A.V. Th1 and Th17 Cells in Tuberculosis: Protection, Pathology, and Biomarkers. *Mediators of inflammation* **2015**, 854507 (2015).
29. Shen, H. & Chen, Z.W. The crucial roles of Th17-related cytokines/signal pathways in M. tuberculosis infection. *Cellular & molecular immunology* **15**, 216-225 (2018).
30. Mourik, B.C., Lubberts, E., de Steenwinkel, J.E.M., Ottenhoff, T.H.M. & Leenen, P.J.M. Interactions between Type 1 Interferons and the Th17 Response in Tuberculosis: Lessons Learned from Autoimmune Diseases. *Front Immunol* **8**, 294 (2017).
31. Scriba, T.J., et al. Sequential inflammatory processes define human progression from M. tuberculosis infection to tuberculosis disease. *PLoS pathogens* **13**, e1006687 (2017).
32. McGeachy, M.J., et al. TGF-beta and IL-6 drive the production of IL-17 and IL-10 by T cells and restrain T(H)-17 cell-mediated pathology. *Nat Immunol* **8**, 1390-1397 (2007).
33. Rakshit, S., et al. Circulating Mycobacterium tuberculosis DosR latency antigen-specific, polyfunctional, regulatory IL10(+) Th17 CD4 T-cells differentiate latent from active tuberculosis. *Sci Rep* **7**, 11948 (2017).
34. Redford, P.S., Murray, P.J. & O'Garra, A. The role of IL-10 in immune regulation during M. tuberculosis infection. *Mucosal immunology* **4**, 261-270 (2011).
35. Ottenhoff, T.H., Verreck, F.A., Hoeve, M.A. & van de Vosse, E. Control of human host immunity to mycobacteria. *Tuberculosis (Edinburgh, Scotland)* **85**, 53-64 (2005).
36. Hoft, D.F., et al. PO and ID BCG vaccination in humans induce distinct mucosal and systemic immune responses and CD4(+) T cell transcriptomal molecular signatures. *Mucosal immunology* **11**, 486-495 (2018).
37. Cadena, A.M., et al. Concurrent infection with Mycobacterium tuberculosis confers robust protection against secondary infection in macaques. *PLoS pathogens* **14**, e1007305 (2018).
38. Lee, R.S., Proulx, J.F., Menzies, D. & Behr, M.A. Progression to tuberculosis disease increases with multiple exposures. *The European respiratory journal* **48**, 1682-1689 (2016).
39. Urbanowski, M.E., et al. Repetitive Aerosol Exposure Promotes Cavitory Tuberculosis and Enables Screening for Targeted Inhibitors of Extensive Lung Destruction. *The Journal of infectious diseases* **218**, 53-63 (2018).
40. Lin, P.L., et al. Quantitative comparison of active and latent tuberculosis in the cynomolgus macaque model. *Infection and immunity* **77**, 4631-4642 (2009).
41. Talbot, E.A., Williams, D.L. & Frothingham, R. PCR identification of Mycobacterium bovis BCG. *Journal of clinical microbiology* **35**, 566-569 (1997).

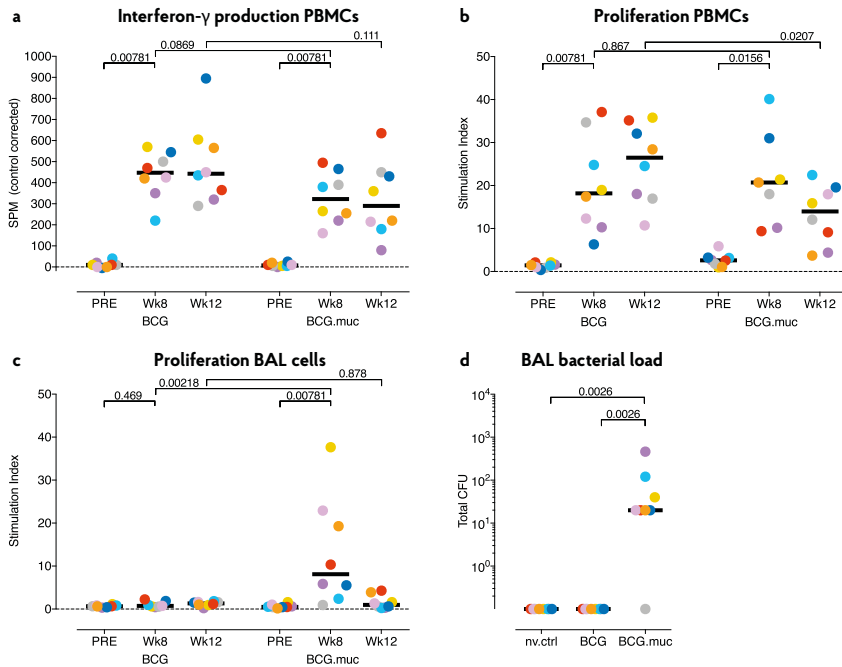


42. Franken, K.L., *et al.* Purification of his-tagged proteins by immobilized chelate affinity chromatography: the benefits from the use of organic solvent. *Protein expression and purification* **18**, 95-99 (2000).
43. Coppola, M., *et al.* New Genome-Wide Algorithm Identifies Novel In-Vivo Expressed Mycobacterium Tuberculosis Antigens Inducing Human T-Cell Responses with Classical and Unconventional Cytokine Profiles. *Sci Rep* **6**, 37793 (2016).
44. R Core Team. R: A Language and Environment for Statistical Computing. (2018).

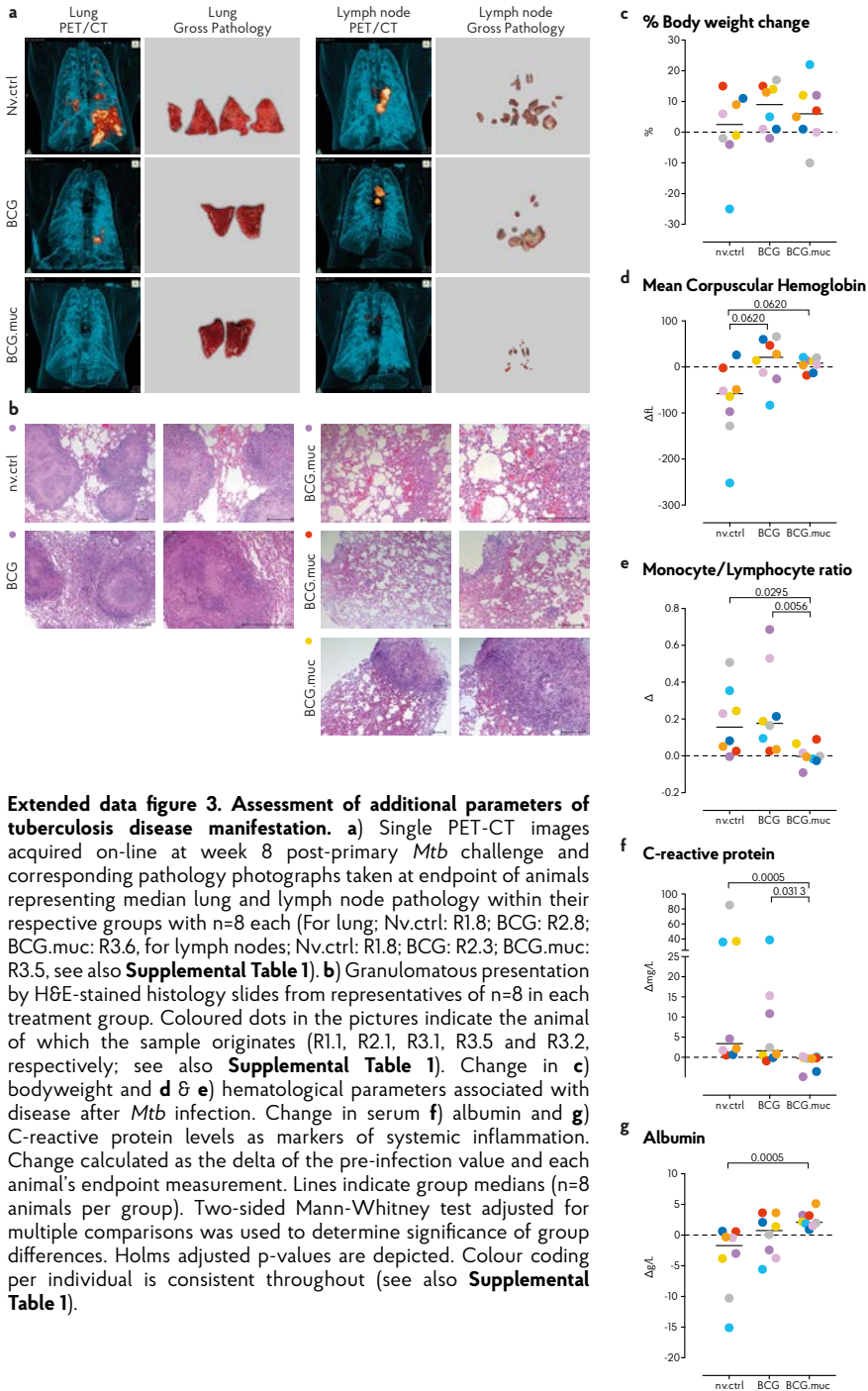
Extended / supplemental data

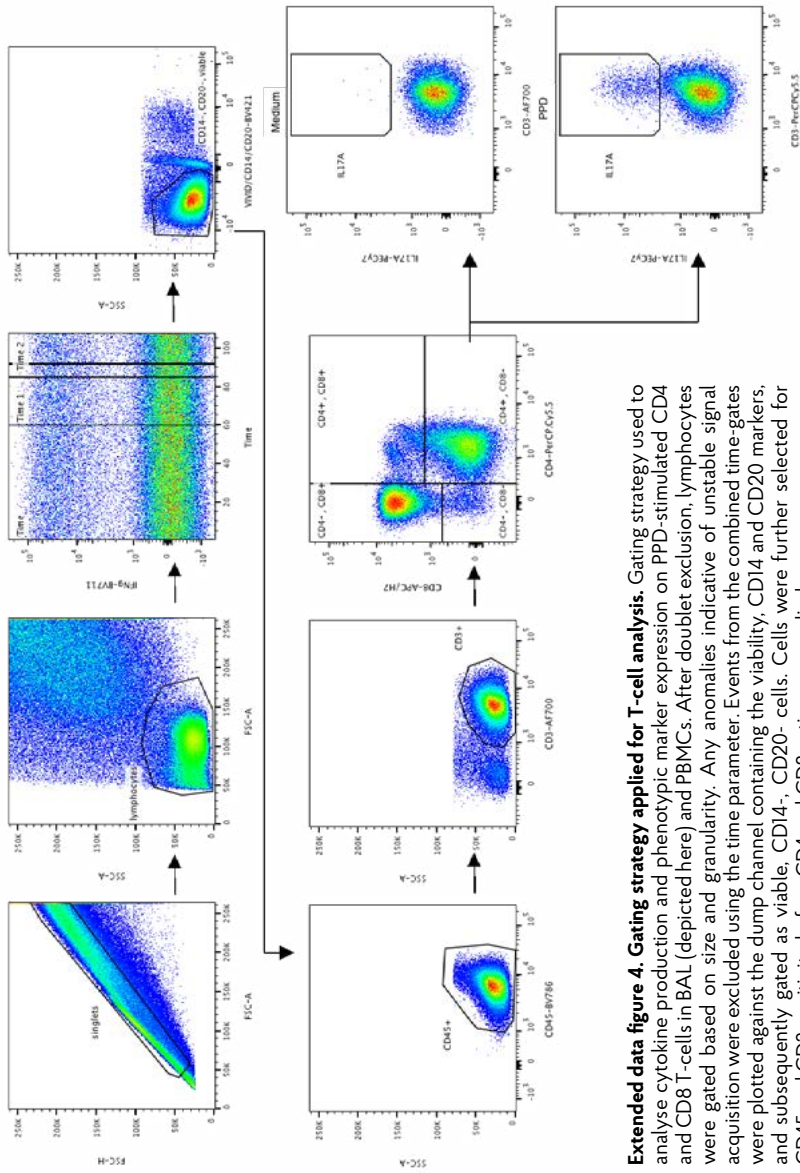


Extended data figure 1. Dose determination and quality control of *Mtb* Erdman. **a)** Kaplan-Meier plot of the IGRA conversion dynamics in 10 rhesus macaques displaying the percentage of IGRA conversion after each dose of *Mtb*. **b)** Recovery of colony forming units (CFU) from the *Mtb* Erdman stock as a percentage of expected number of CFU, as determined by plating of serial dilutions from the inoculum preparation process (n=8 independent experiments, CFU calculated from n=3 replicates). Box-whisker plot indicating 95% confidence interval (box) and range (whiskers), with the line within the box indicating the median value.



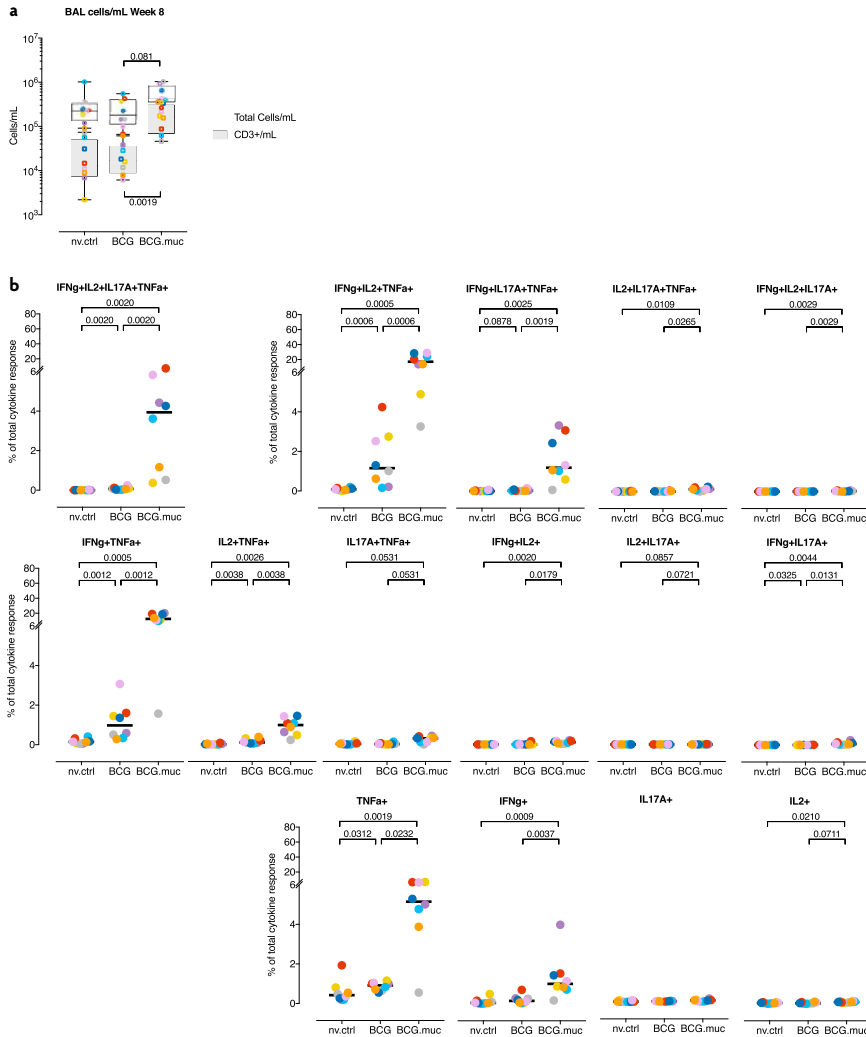
Extended data figure 2. Confirmation of BCG take in both vaccinated groups. Immune response analysis post-vaccination to confirm vaccine take in both standard BCG and pulmonary BCG (BCG.muc) vaccinated animals (n=8 animals per group, except for BCG.muc at week 8 in **b**), where n=7 animals), as demonstrated by **a)** antigen-specific IFN γ secretion in PBMCs, **b)** cell proliferation in PBMCs, and **c)** cell proliferation in BAL cells. In **a)** IFN γ secretion by ELISPOT is plotted as medium-control corrected spots per million cells (SPM). In **b)** and **c)** proliferation is depicted as stimulation index: the ratio of antigen-over medium control-stimulated values. **d)** BCG CFU cultured from BAL samples taken after BCG vaccination. BCG recovery from BAL is calculated as CFU in the total sample volume. Horizontal lines indicate group medians. Statistically significant differences within groups are determined by two-sided Wilcoxon signed-rank test; differences between groups by two sided Mann-Whitney testing. Colour coding per individual is consistent throughout (see also **Supplemental Table 1**).





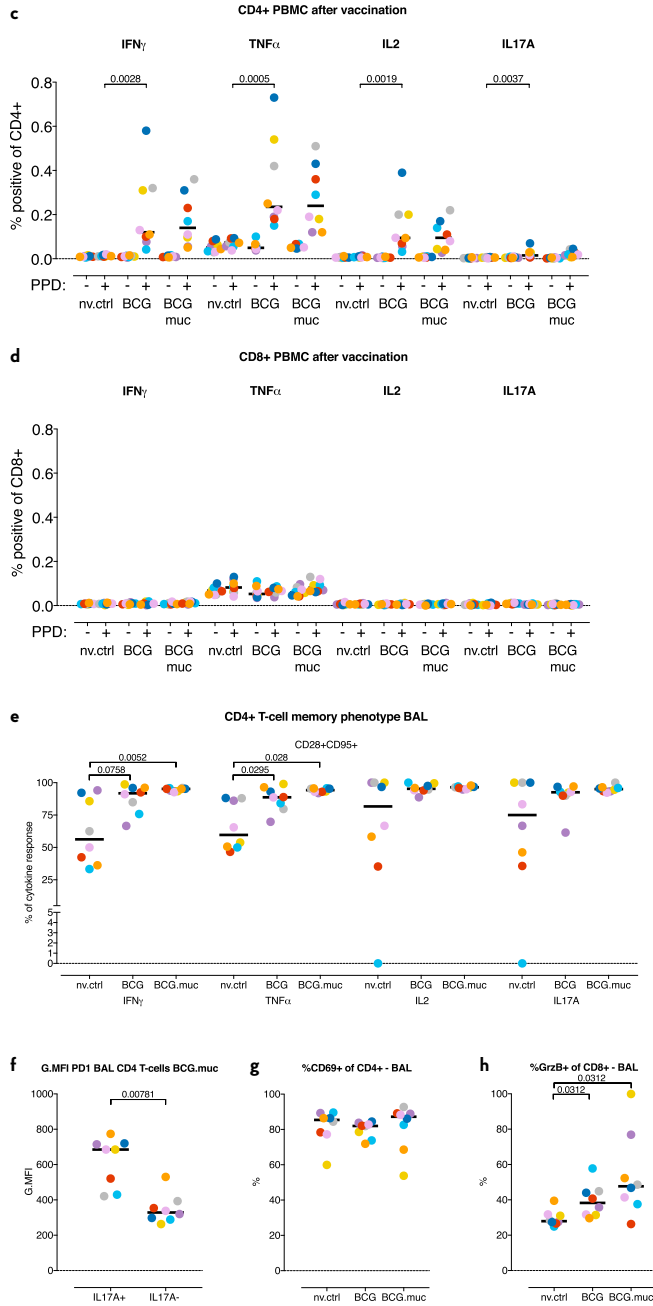
Extended data figure 4. Gating strategy applied for T-cell analysis. Gating strategy used to analyse cytokine production and phenotypic marker expression on PPD-stimulated CD4 and CD8 T-cells in BAL (depicted here) and PBMCs. After doublet exclusion, lymphocytes were gated based on size and granularity. Any anomalies indicative of unstable signal acquisition were excluded using the time parameter. Events from the combined time-gates were plotted against the dump channel containing the viability, CD14 and CD20 markers, and subsequently gated as viable, CD14⁻, CD20⁻ cells. Cells were further selected for CD45 and CD3 positivity before CD4 and CD8 gating was applied.

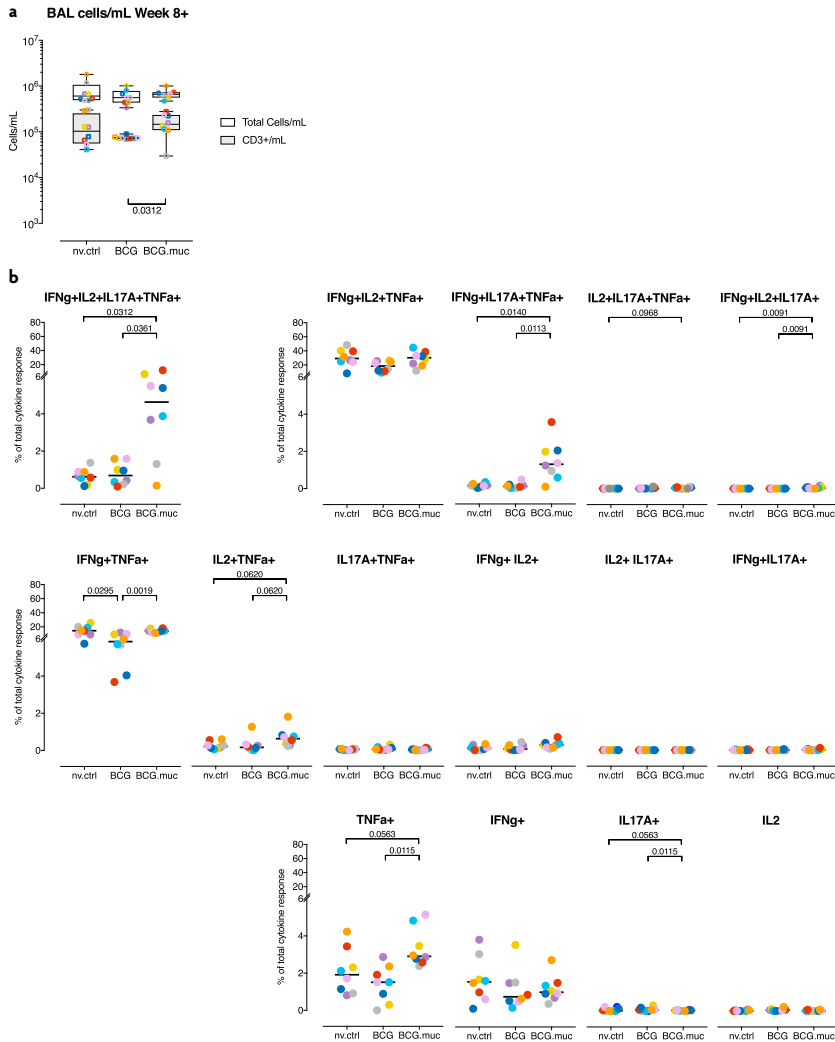




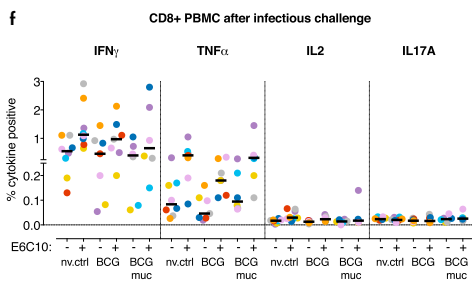
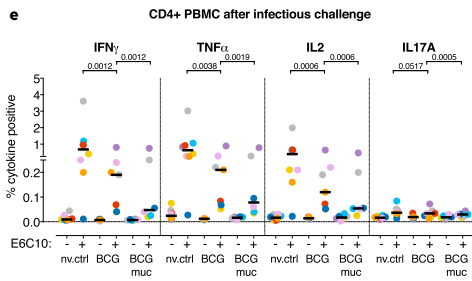
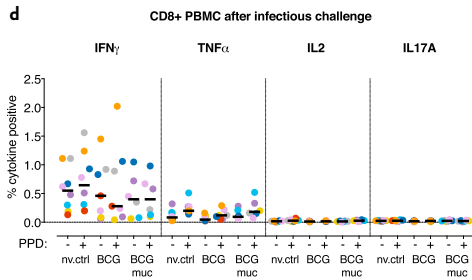
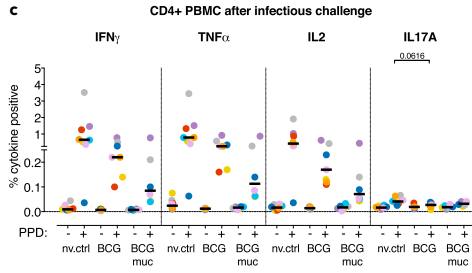
Extended data figure 5. **a)** Ex vivo enumeration of CD3+ T-cells per mL recovered BAL in relation to total BAL cellular yield and **b)** individual boolean-gated CD4+ T-cell cytokine-producing subsets in response to PPD stimulation, 8 weeks post-BCG vaccination. **c-d)** Percentage of PPD-specific cytokine responses in **c)** CD4+ and **d)** CD8+ T-cells in the periphery, 8 weeks post-BCG. **e-h)** Further characterization of mucosal response signatures. **e)** Breakdown of mucosal (from left to right) IFN γ , TNF α , IL2 and IL17A producing CD4+ T-cells in BAL per treatment group into CD28+CD95+ central memory phenotype. **f)** PD-1 expression of the cytokine producing CD4+ T-cells in BAL samples from the BCG.muc group, after stimulation with PPD. **g)** Ex vivo CD69 expression on CD4+ T-cells from BAL. **h)** Percentage of Granzyme B-expressing CD8+ T-cells in BAL.

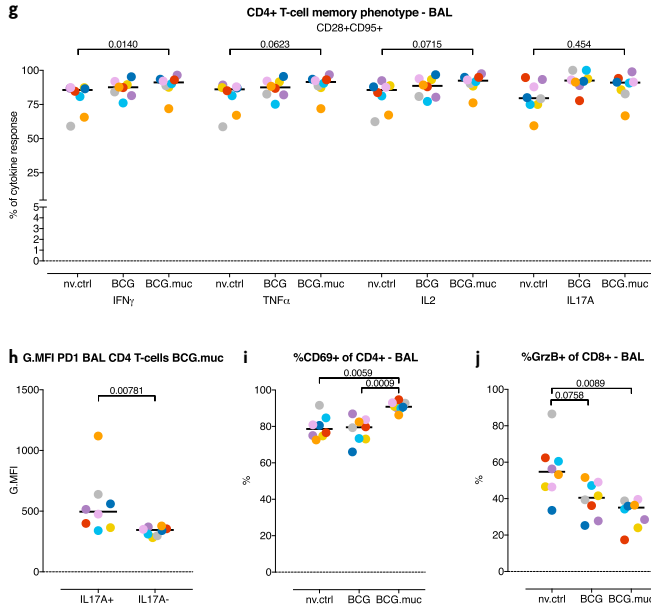
For Figure **a)** box-whisker plot indicates 95% confidence interval (box) and range (whiskers), with the line within the box indicating the median value. For Figures **b-h)** lines indicate group medians. For all figures n=8 animals per group. Two-sided Mann-Whitney test adjusted for multiple comparisons was used to determine significance of group differences. Holms adjusted p-values are depicted. Colour coding per individual is consistent throughout (see also **Supplemental Table 1**).



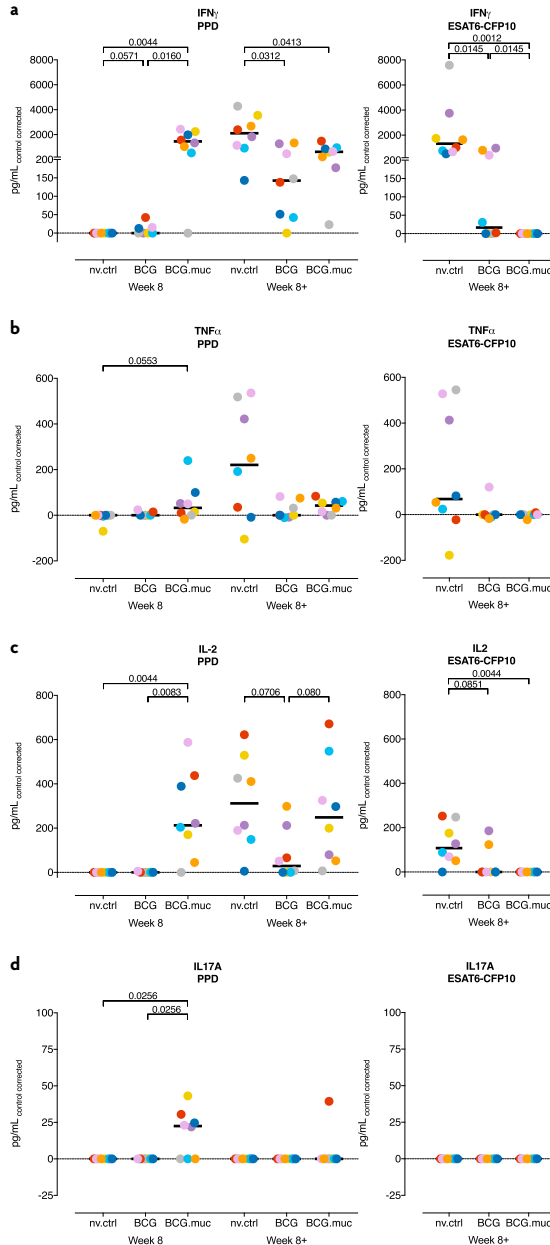


Extended data figure 6. Additional characterisation of T-cell responses after RLD *Mtb* challenge. a) *Ex vivo* enumeration of CD3+ T-cells per mL recovered BAL in relation to total BAL cellular yield, and **b)** individual boolean-gated CD4+ T-cell cytokine-producing subsets in response to PPD stimulation, 8 weeks after the first *Mtb* inoculation. Percentage of cytokine-producing T-cells in PPD stimulated **c)** CD4+ and **d)** CD8+ PBMCs and ESAT-CFP10 stimulated **e)** CD4+ and **f)** CD8+ PBMCs. Samples from 3 animals (1 from the BCG group, 2 from the BCG.muc group) were not acquired due to a technical error. The symbol “+” indicates either PPD **c & d)** or ESAT6-CFP10 **e & f)** stimulated samples; “-” indicates unstimulated, culture medium incubated samples as control.



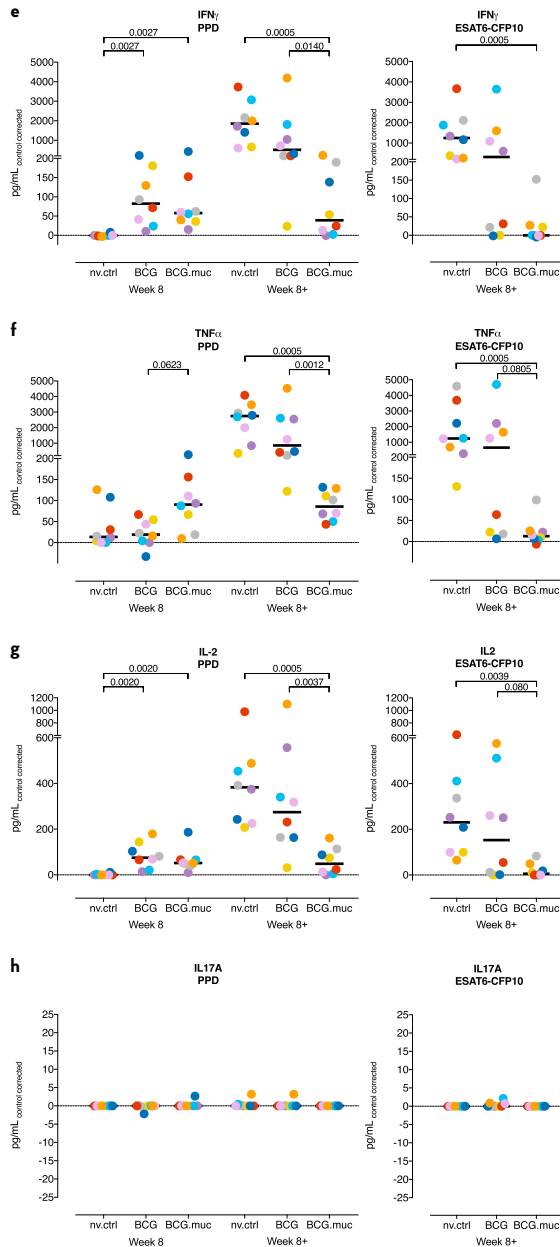


Extended data figure 6 continued. g-j) Further characterization of mucosal response signatures. **g)** Breakdown of mucosal (from left to right) IFN γ , TNF α , IL2 and IL17A producing CD4+ T-cells in BAL per treatment group into CD28+CD95+ central memory phenotype. **h)** PD-1 expression of the cytokine producing CD4+ T-cells in BAL samples from the BCG.muc group, after stimulation with PPD. **i)** *Ex vivo* CD69 expression on CD4+ T-cells from BAL. **j)** Percentage of granzyme B expressing CD8+ T-cells in BAL. For Figure **a)** box-whisker plot indicating 95% confidence interval (box) and range (whiskers), with the line within the box indicating the median value. For Figures **b-j)** horizontal lines indicate group medians. For all graphs n=8 animals per group, unless indicated otherwise. Significance of group differences determined by two-sided Mann-Whitney test adjusted for multiple comparisons. Holms adjusted p-values are depicted. Colour coding per individual is consistent throughout (see also **Supplemental Table 1**).

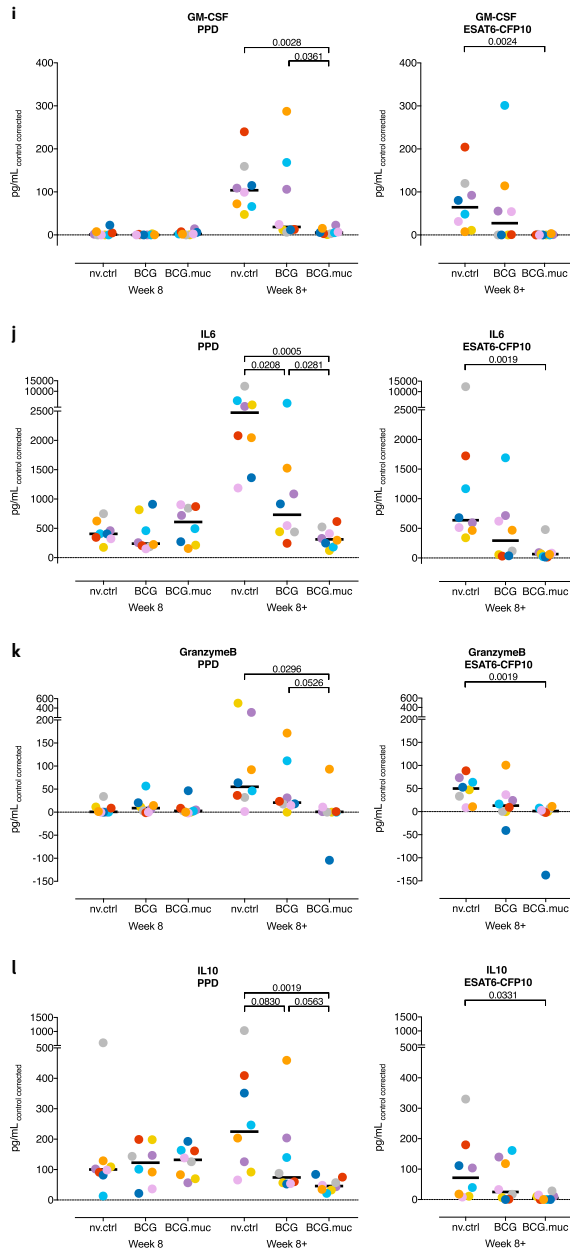


Extended data figure 7. Luminex analysis of additional cytokines. Characterisation of cytokine responses in supernatants taken after *in vitro* stimulation of **a-d**) BAL cells or **e-l**) PBMCs, either 8 weeks after vaccination with BCG (Week 8) or 8 weeks after initial RLD challenge (Week 8+). Production of **a**) IFN γ , **b**) TNF α , **c**) IL2 and **d**) IL17A by BAL cells stimulated with PPD or ESAT6-CFP10 fusion protein.


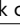




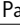




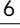



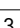
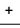






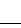




Extended data figure 7 continued. Production of **e)** IFN γ , **f)** TNF α , **g)** IL2 and **h)** IL17A, **i)** GM-CSF, **j)** IL6, **k)** granzyme B and **l)** IL10 by PBMCs stimulated with PPD or ESAT6-CFP10 fusion protein. All cytokines are plotted as medium control corrected values. Horizontal lines indicate group medians, for all graphs n=8 animals per group, except for **a-d)** where n=7 for the BCG group at week 8 post-BCG.



Extended data figure 7 continued. Significance of group differences was determined by two-sided Mann-Whitney test adjusted for multiple comparisons, of which Holms adjusted p-values are reported. Within group comparisons were tested by Wilcoxon signed-rank test. Colour coding per individual is consistent throughout (see also **Supplemental Table 1**).

	nv.ctrl							
Animal Identifier	R1.1	R1.2	R1.3	R1.4	R1.5	R1.6	R1.7	R1.8
Colour Code								
IGRA Conversion	+	+	+	+	+	+	+	+
Week of IGRA Conv.	6	6	4	4	6	7	5	5
BAL Culture	+	+	+	-	+	-	+	+
Lung Pathology	+	+	+	+	+	+	+	+
Lung CFU	+	+	+	+	+	+	+	+

	BCG							
Animal Identifier	R2.1	R2.2	R2.3	R2.4	R2.5	R2.6	R2.7	R2.8
Colour Code								
IGRA Conversion	+	+	+	+	+	+	+	+
Week of IGRA Conv.	3	9	8	3	7	9	5	4
BAL Culture	+	-	-	+	+	n.a.	+	+
Lung Pathology	+	+	+	+	+	+	+	+
Lung CFU	+	+	+	+	+	+	+	+

	BCG.muc							
Animal Identifier	R3.1	R3.2	R3.3	R3.4	R3.5	R3.6	R3.7	R3.8
Colour Code								
IGRA Conversion	-	+	+	+	-	+	-	+
Week of IGRA Conv.	n.a.	10	5	10	n.a.	5	n.a.	6
BAL Culture	-	n.a.	-	n.a.	-	-	-	-
Lung Pathology	+	+	+	-	+	+	-	+
Lung CFU	+	-	+	-	+	+	-	+

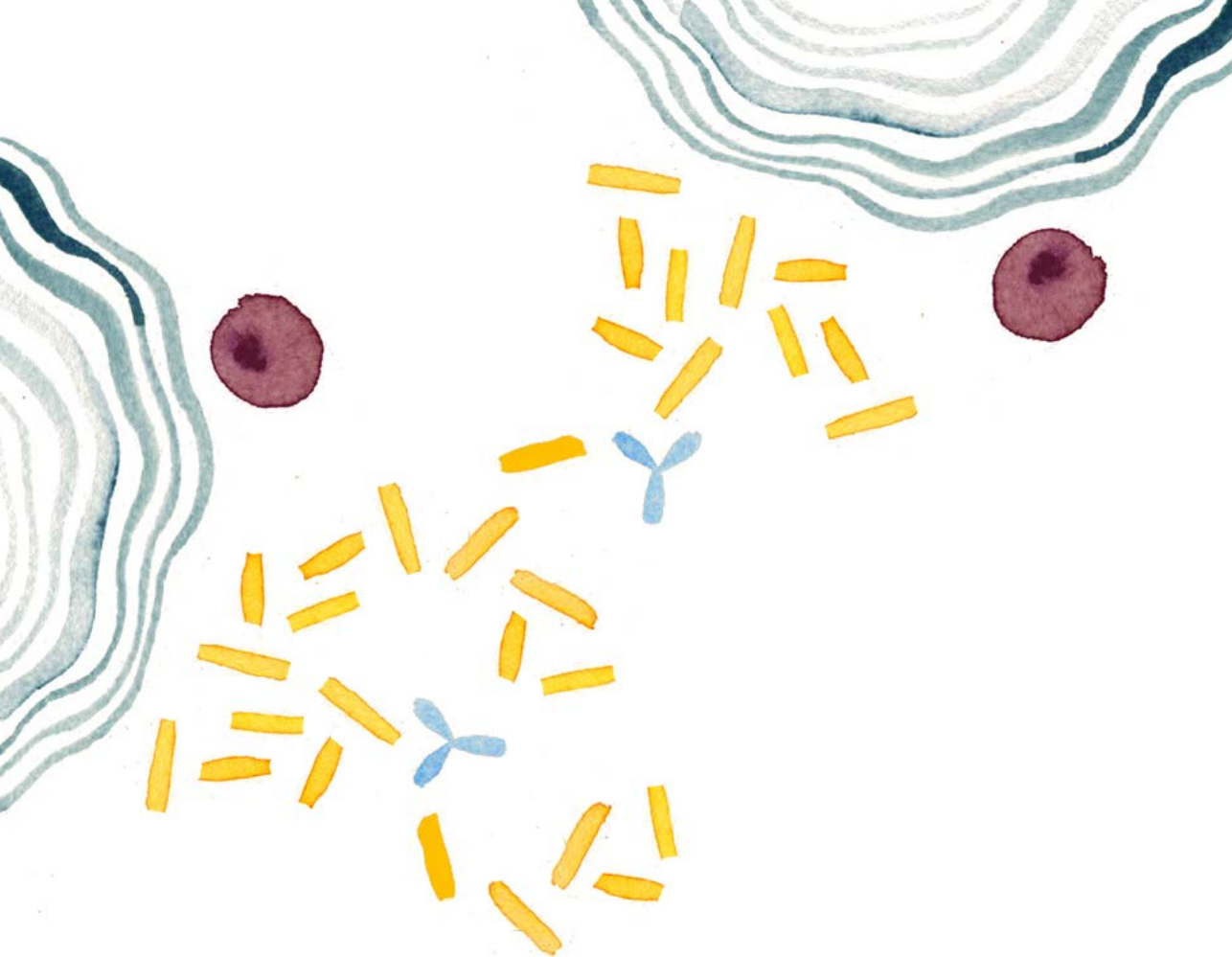
Supplemental Table 1. Summary of Mtb infection and disease measurements. Overview of the major read-outs of Mtb infection and disease per individual, showing the presence (+) or absence (-) of IGRA conversion and the week of IGRA conversion, and the presence or absence of culturable Mtb CFU from BAL samples 8 weeks after the initial challenge, lung pathology at post-mortem assessment, or culturable Mtb CFU from lung tissue samples at endpoint. "N.a." indicates: not assessable.

	Time to IGRA conversion				Pathology Score				Bacterial Load			
	Post.Vacc.		Post.Chall.		Post.Vacc.		Post.Chall.		Post.Vacc.		Post.Chall.	
Immune Parameter	rho	p	rho	p	rho	p	rho	p	rho	p	rho	p
BAL cell cytometry												
no. of CD3+ T cells	0.49	0.054	0.38	0.066	-0.56	0.023	-0.15	0.499	-0.55	0.029	-0.24	0.560
% IFN γ + CD4+ T cells	0.64	0.007	0.21	0.317	-0.59	0.015	0.00	0.984	-0.62	0.011	-0.00	0.995
% TNF α + CD4+ T cells	0.65	0.007	0.20	0.358	-0.59	0.016	0.00	0.996	-0.63	0.010	0.00	0.997
% IL2+ CD4+ T cells	0.68	0.003	0.20	0.339	-0.68	0.004	-0.01	0.949	-0.69	0.003	-0.03	0.907
% IL17A+ CD4+ T cells	0.62	0.010	0.33	0.111	-0.59	0.016	-0.47	0.020	-0.55	0.027	-0.59	0.002
% IFN γ + CD8+ T cells	0.61	0.012	-0.16	0.453	-0.52	0.037	0.33	0.114	-0.59	0.016	0.28	0.180
% TNF α + CD8+ T cells	0.39	0.133	-0.11	0.594	-0.34	0.191	0.41	0.049	-0.61	0.013	0.26	0.213
% IL2+ CD8+ T cells	0.05	0.857	-0.05	0.820	-0.05	0.865	0.29	0.177	-0.04	0.871	0.22	0.295
% IL17A+ CD8+ T cells	0.09	0.749	0.29	0.173	-0.28	0.293	0.04	0.842	-0.17	0.519	-0.08	0.724
PBMC cytometry												
% IFN γ + CD4+ T cells	0.16	0.555	-0.45	0.040	-0.17	0.520	0.65	0.001	-0.23	0.391	0.66	0.001
% TNF α + CD4+ T cells	0.02	0.943	-0.45	0.040	-0.15	0.575	0.63	0.002	-0.12	0.647	0.68	0.001
% IL2+ CD4+ T cells	0.05	0.859	-0.42	0.059	-0.13	0.640	0.63	0.002	-0.14	0.604	0.64	0.002
% IL17A+ CD4+ T cells	0.09	0.745	-0.17	0.463	-0.31	0.241	0.30	0.180	-0.21	0.442	0.41	0.065
% IFN γ + CD8+ T cells	0.07	0.801	-0.22	0.328	-0.28	0.300	0.25	0.284	-0.44	0.087	0.25	0.272
% TNF α + CD8+ T cells	0.26	0.326	-0.15	0.503	-0.42	0.107	0.32	0.163	-0.46	0.072	0.18	0.425
% IL2+ CD8+ T cells	0.23	0.393	-0.27	0.245	-0.09	0.746	0.13	0.578	-0.32	0.224	0.06	0.783
% IL17A+ CD8+ T cells	-0.32	0.220	-0.09	0.703	0.12	0.660	0.24	0.300	0.15	0.586	0.25	0.267
BAL cell secretory resp.												
IFN γ	0.60	0.018	-0.23	0.269	-0.50	0.060	0.52	0.009	-0.59	0.020	0.53	0.008
TNF α	0.41	0.132	-0.14	0.503	-0.47	0.076	0.36	0.086	-0.72	0.003	0.22	0.291
IL2	0.60	0.018	0.05	0.815	-0.51	0.050	0.13	0.560	-0.52	0.048	0.14	0.500
IL17A	0.54	0.037	0.32	0.128	-0.39	0.147	-0.24	0.254	-0.53	0.044	-0.08	0.726
IL10	0.53	0.042	0.35	0.095	-0.47	0.075	-0.17	0.439	-0.58	0.023	-0.25	0.240
GM-CSF	0.43	0.113	-0.45	0.029	-0.39	0.146	0.67	0.000	-0.40	0.141	0.68	0.000
IL6	0.42	0.115	-0.37	0.078	-0.36	0.192	0.60	0.002	-0.41	0.127	0.50	0.012
granzyme B	0.41	0.124	-0.41	0.049	-0.35	0.200	0.45	0.026	-0.45	0.090	0.39	0.059
PBMC secretory resp.												
IFN γ	0.12	0.646	-0.76	0.000	-0.21	0.432	0.82	0.000	-0.17	0.534	0.84	0.000
TNF α	0.62	0.011	-0.72	0.000	-0.54	0.030	0.72	0.000	-0.72	0.002	0.74	0.000
IL2	-0.03	0.909	-0.77	0.000	0.04	0.874	0.79	0.000	-0.04	0.888	0.78	0.000
IL17A	-0.21	0.429	-0.39	0.059	0.14	0.616	0.40	0.050	-0.15	0.569	0.34	0.101
IL10	0.01	0.978	-0.65	0.001	-0.26	0.335	0.70	0.000	-0.19	0.470	0.77	0.000
GM-CSF	0.56	0.024	-0.62	0.001	-0.63	0.008	0.63	0.001	-0.49	0.052	0.73	0.000
IL6	0.45	0.083	-0.61	0.002	-0.74	0.001	0.73	0.000	-0.39	0.133	0.87	0.000
granzyme B	-0.37	0.164	-0.45	0.029	0.07	0.796	0.66	0.000	0.30	0.261	0.78	0.000
BAL Ig levels												
pan.Ig	0.37	0.163	-0.37	0.076	-0.29	0.284	0.16	0.459	-0.38	0.151	-0.01	0.958
IgA	0.23	0.398	-0.30	0.148	-0.24	0.368	0.25	0.240	-0.32	0.220	0.00	0.992
Serum Ig levels												
pan.Ig	-0.12	0.666	-0.26	0.215	0.15	0.582	0.04	0.863	0.03	0.905	-0.05	0.799
IgA	-0.14	0.593	-0.23	0.273	0.18	0.507	0.08	0.694	0.42	0.102	0.27	0.210

Supplemental Table 2. Correlation statistics of immune response parameters and infection and disease outcome measures. Summary of non-parametric Spearman's rho correlation statistics of individual, local BAL cell and peripheral blood (PBMC) immune response characteristics as measured by flow cytometry, cytokine secretion and immunoglobulin analysis, all against the most discriminating read-outs of infection and disease in this study: time to IGRA conversion, and pathology score as well as bacterial load (CFU) from the primary targeted lung lobe. The correlation coefficients and p-values were calculated for post-vaccination responses from all vaccinees (N=16) and for post-challenge responses for all animals including the non-vaccinated controls (N=24).

Marker	Label	Clone	Manufacturer	Catalog number	Lot-numbers	Dilution
CD28	ECD	CD28.2	Beckman Coulter	6607111	6607111	1:40
CD14	BV421	M5E3	Becton Dickinson	565283	565283	1:80
CD45	BV786	D058-1283		563861	563861 7082628	1:160
CD3	AF700	SP34-2		557917	557917	1:160
CD4	PerCP.Cy5.5	L200		552838	552838	1:320
CD8	APC-H7	SK-1		641400	641400	1:80
CD69	PE	FN50		555531	6049707	1:5
GranzymeB	BV510	GB11		563388	5329695	1:80
TNF	BV650	Mab11		563418	6350858	1:20
CD20	BV421	2H7	Biolegend	302330	302330	1:320
CD95	BV605	DX2		305628	305628	1:40
PD-1	BV510	EH12.2H7		329932	212859 220454	1:20
IL-2	AF488	MQ1-17H12		500314	204521	1:10
IFN γ	BV711	4S.B3		502540	222408 201564	1:10
CD25	APC	4E3	Miltenyi	130-091-024	5171109372	1:40
CD127	PE	ebioDR5	ThermoFisher	12-1278-42	4291411	1:20
IL-17A	PE-Cy7	ebio64DEC17		25-7179-42	4291863 4312976	1:10
LIVE/DEAD Fixable Violet Dead Cell Stain	-	-		L34964		

Supplemental Table 3. Antibodies used for flowcytometric analysis of BAL and PBMC





Pulmonary vaccination with *M.tuberculosis*-derived MTBVAC induces immune responses correlating with prevention of TB infection

**K. Dijkman¹, N. Aguilo², C. Boot¹, S.O Hofman¹, C.C. Sombroek¹, R.A.W. Vervenne¹,
D. Marinova², C.H.M. Kocken³, J. Thole⁴, E. Rodríguez⁴, M.P.M Vierboom¹,
K.G. Haanstra¹, E. Puentes⁴, C. Martin², F.A.W. Verreck¹**

¹ Section of TB Research & Immunology, Biomedical Primate Research Centre (BPRC), Rijswijk, the Netherlands

² Department of Microbiology, Faculty of Medicine, University of Zaragoza, Zaragoza, Spain

³ Department of Parasitology, Biomedical Primate Research Centre (BPRC), Rijswijk, the Netherlands

⁴ Biofabri, Pontevedra, Spain

Manuscript submitted

Abstract

To combat the ongoing tuberculosis (TB) epidemic, responsible for 1.5 million deaths annually, more efficacious vaccination strategies are urgently required. In preclinical models *Mtb*-derived MTBVAC, a live attenuated candidate TB vaccine, is known to elicit protection superior to standard intradermal *Bacillus Calmette Guerin* (BCG), mediated by immunity against *Mtb*-specific antigens. Preclinical studies have also demonstrated that alternative routing to the pulmonary mucosa confers superior protection from TB compared to standard intradermal vaccination. Here, we demonstrate that pulmonary administration of MTBVAC in rhesus macaques is well tolerated and induces an immune signature previously associated with improved protection and prevention of infection by pulmonary BCG vaccination. Mucosal MTBVAC, like mucosal BCG, elicited local, antigen-specific, polyfunctional T-helper 17 cells, interleukin-10 and immunoglobulins, that disseminated throughout the lung. Additionally, pulmonary MTBVAC vaccination resulted in immune-recognition of *Mtb*-specific antigens. Beyond our previous investigations we here report that local, vaccine-induced immunoglobulins, either by BCG or MTBVAC, were able to bind *Mtb* and enhance pathogen uptake by phagocytes. Furthermore, local, antigen-specific T-cells induced by pulmonary vaccination, but not upon *Mtb* infection, expressed high levels of mucosal homing markers and displayed a tissue-residency phenotype. Our data shows that pulmonary administration of MTBVAC has the potential to enhance its protective efficacy and justifies further exploration of mucosal vaccination strategies with live attenuated TB vaccines in preclinical efficacy studies.

Introduction

Despite advances in treatment and care, tuberculosis (TB) continues to cause approximately 1.6 million deaths and an additional 10 million cases of active disease annually¹. Control of this ongoing epidemic is complicated by a lack of accurate diagnostics, lengthy treatment regimens and an increase in drug-resistant TB incidence. An effective vaccination strategy preventing TB infection or disease is therefore of critical importance in controlling the continuing tuberculosis epidemic. Unfortunately, the only prophylactic TB vaccine currently available, *Bacillus Calmette Guérin* (BCG), despite preventing dissemination of disease, is notoriously variable in protecting adults and adolescents from pulmonary TB. Pulmonary disease is the major cause of TB morbidity and mortality, and the driver of tuberculosis spread². Geographical location, prior non-tuberculous mycobacteria (NTM) exposure and over-attenuation of BCG have been implied in contributing to the variable BCG efficacy²⁻⁴. Regardless of the underlying mechanisms of this variation in efficacy, it is evident that a more reliable vaccine strategy is urgently needed.

Currently, multiple novel TB vaccines are being developed, either to replace BCG vaccination at birth or to serve as a (heterologous) booster on top of prior BCG vaccination^{5,6}. One of these new candidate-vaccines is MTBVAC, a live attenuated whole cell vaccine, designed as a potential replacement of neonatal BCG vaccination. MTBVAC was generated by genetic modification of a clinical *Mycobacterium tuberculosis* (*Mtb*) isolate and harbors deletions in two virulence genes, *phoP* and *fadD26*⁷. These deletions interfere with the transcription, synthesis and/or secretion of multiple virulence factors, including Early Secretory Antigenic Target 6 (ESAT6) and phthiocerol dimycocerosates (PDIMs). As MTBVAC is *Mtb* rather than *Mycobacterium bovis* derived, it contains regions of differences (RD) lacking from BCG and therefore has a broader antigenic repertoire⁸. Preclinical evaluation showed that MTBVAC has a safety profile comparable to BCG, but a superior capacity to protect from TB disease^{7,9}. Reactogenicity to *Mtb*-specific antigens present in MTBVAC, but absent in BCG, was found to be required for its improved protective capacity¹⁰. Although primarily designed as a BCG-replacement vaccine, revaccination with MTBVAC in BCG primed guinea pigs resulted in a further reduction of *Mtb* burden in the lung compared to BCG alone¹¹. The MTBVAC vaccine has now proceeded into clinical evaluation, and so far has been found to be safe and immunogenic in both adults and infants^{12,13}. Additional dose-finding and immunogenicity studies in neonates (NCT03536117) and Quantiferon-positive individuals (NCT02933281) are in progress.

The indicated route of administration for BCG and MTBVAC is the skin, which induces limited immune responses at the pulmonary mucosa, the primary site of infection with *Mtb*. A large body of data generated in preclinical models of TB shows that altering the route of BCG administration to the pulmonary mucosa significantly improves its protective efficacy¹⁴⁻¹⁷. In previous work, we showed that pulmonary, but not intradermal, BCG vaccination could protect highly susceptible rhesus macaques (*Macaca mulatta*) from repeated low dose *Mtb* infection and TB-associated pathology¹⁸. Macaques are considered to be a predictive model for TB vaccine development, due to their close phylogenetic relationship to man and highly similar TB disease development^{19,20}. In this repeated low dose challenge model, the protection conferred by mucosal BCG statistically correlated with the induction of polyfunctional IL17A+ CD4+ T-cells at the pulmonary mucosa and IL10 production by bronchoalveolar lavage (BAL) cells, while elevated levels of antigen-specific immunoglobulins were found in association with mucosal BCG immunization as well.

Here we investigated whether pulmonary mucosal administration of MTBVAC would induce a similar protective immune signature. We compared local and systemic immune responses of rhesus macaques vaccinated with BCG or MTBVAC, either through intradermal injection or by endobronchial instillation. As observed for BCG, pulmonary MTBVAC administration induced local IL17A producing T-cells, IL10 production and *Mtb*-specific IgA. Compared to BCG, vaccination with MTBVAC resulted in a more rapid induction of immune responses and a broader antigenic specificity. Furthermore, we identified increased expression of mucosal homing



markers of purified protein derivate (PPD)-specific T-cells from the BALs of mucosally vaccinated but not *Mtb* infected animals. Lastly, we show that vaccine-induced mucosal antibodies are functional in binding to live *Mtb* and facilitating pathogen-uptake by phagocytes.

These observations corroborate and extend beyond previous findings of improved mucosal TB vaccination and provide a rationale for exploring mucosal administration of MTBVAC with the perspective of improving our prophylaxis against TB infection and disease.

Results

Local immune signatures after mucosal MTBVAC vaccination

Compared to BCG, subcutaneous vaccination of mice with MTBVAC confers superior protection from TB pathology¹⁰. Independently, preclinical studies have shown that administration of BCG through the pulmonary mucosa, rather than the skin, induces enhanced immune responses in the lung and is more efficacious in protecting against tuberculosis pathology or even *Mtb* infection¹⁸. Thus, we hypothesize that administering MTBVAC through the lung might increase its immunogenicity and elicit immune responses associated with superior protection. We investigated this hypothesis by vaccinating rhesus macaques with MTBVAC, either through the standard intradermal route (M.id) or through endobronchial instillation (M.muc), and comparing their local and peripheral immune responses with those from animals vaccinated intradermally or mucosally with BCG (B.id and B.muc, respectively, **Figure 1a**).

Flow cytometric profiling of T-cells in BAL revealed a robust induction of PPD-specific CD4⁺ T-cells in both mucosally vaccinated groups, with MTBVAC eliciting higher responses than BCG for almost all cytokines, especially early after vaccination (**Figure 1b**). While both intradermal BCG and MTBVAC showed an increase of IFN γ , TNF α and IL2 producing T-cells in the airways in the weeks following vaccination, IL17A production was uniquely observed in the mucosally vaccinated groups (**Figure 1b**). These IL17A⁺ T-cells also produced IFN γ , TNF α and IL2, thus confirming the induction of a local, quadruple positive, CD4⁺ T-cell population, previously associated in rhesus macaques with protection from TB infection and disease (**Figure 1c**). Little PPD-specific cytokine production was observed in BAL CD8⁺ T-cells (**Supplemental Figure 1a**). Local lymphocyte proliferation was observed predominantly after mucosal vaccination (**Supplemental Figure 1b**).

While by endobronchial instillation the vaccine was targeted to the lower right lobe, we investigated whether vaccine-induced immune responses would disseminate or restricted to the targeted lobe only. At 3 and 8 weeks after vaccination, we bilaterally collected BAL for immune profiling and found that PPD-specific producing T-cells were present in both in lower right and lower left lung lobes, albeit at a somewhat lower frequency in the non-targeted lobe (**Figure 1d**). In either lobe,

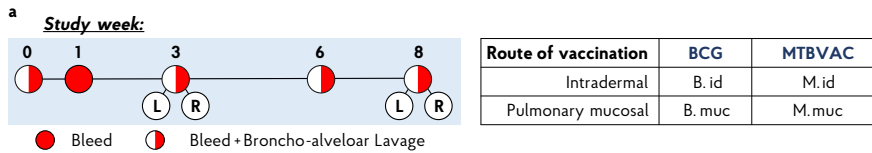


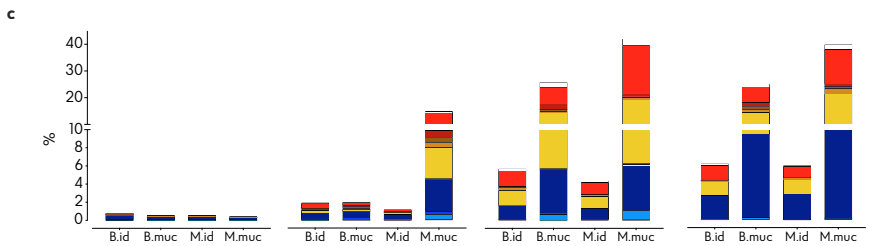
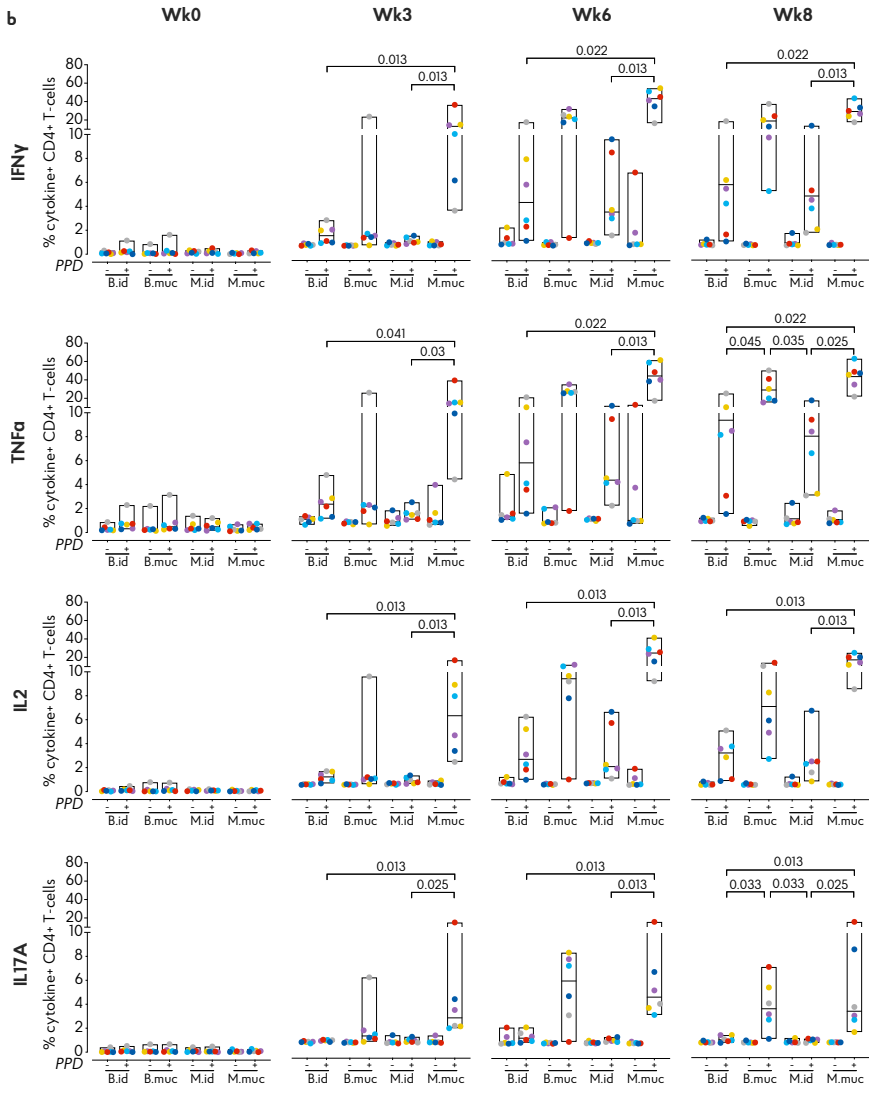
Figure 1. Pulmonary mucosal vaccination with MTBVAC induces immune signatures associated with protection. Study design and overview of BAL immune responses after either mucosal or intradermal vaccination with BCG or MTBVAC. **a)** Schematic overview of the vaccination strategies applied in the study and post-vaccination sampling of peripheral blood and BAL from the groups. Of note; only the mucosally vaccinated groups received bilateral BALs at 3 and 8 weeks post-vaccination.

MTBVAC induced earlier and higher responses compared to BCG, including polyfunctional CD4⁺ Th17 cells. We also profiled immune responses in lung-draining lymph nodes, the canonical site of T-cell priming. PPD-specific IFN γ , TNF α and IL2 production by CD4⁺ T-cells was observed most prominently after mucosal vaccination, but was also detectable after intradermal vaccination (**Supplemental Figure 1c**). Interestingly, antigen-specific IL17A⁺ CD4⁺ T-cells were not apparent in these lymph nodes (**Supplemental Figure 1c**). Either the precursor frequency of these cells was too low to be detected, or Th17 priming occurred elsewhere, for instance in tertiary lymphoid structures in the lung.

Since we previously also identified IL10 production by unfractionated BAL cells as a correlate of protection, we investigated by flow cytometric analysis whether IL10 production could be T-cell derived. Although, we confirmed high levels of PPD-specific IL10 production in stimulated BAL cell supernatants after mucosal vaccination with MTBVAC as well as BCG (**Figure 1e**), by flow cytometry very low frequencies of IL10⁺ CD4⁺ T-cells were detected in the BAL of mucosally vaccinated animals (**Figure 1f**). Thus, it seems that the high levels of IL10 are not T-cell-derived, but more likely produced by local innate immune cells (e.g. alveolar macrophages) in response to innate receptor ligation by mycobacterial compounds in the PPD preparation.

To summarize, pulmonary vaccination with MTBVAC induces, typically faster and higher, polyfunctional CD4⁺ T-cell responses and IL10 secretion signals, previously associated with protection by pulmonary BCG vaccination.





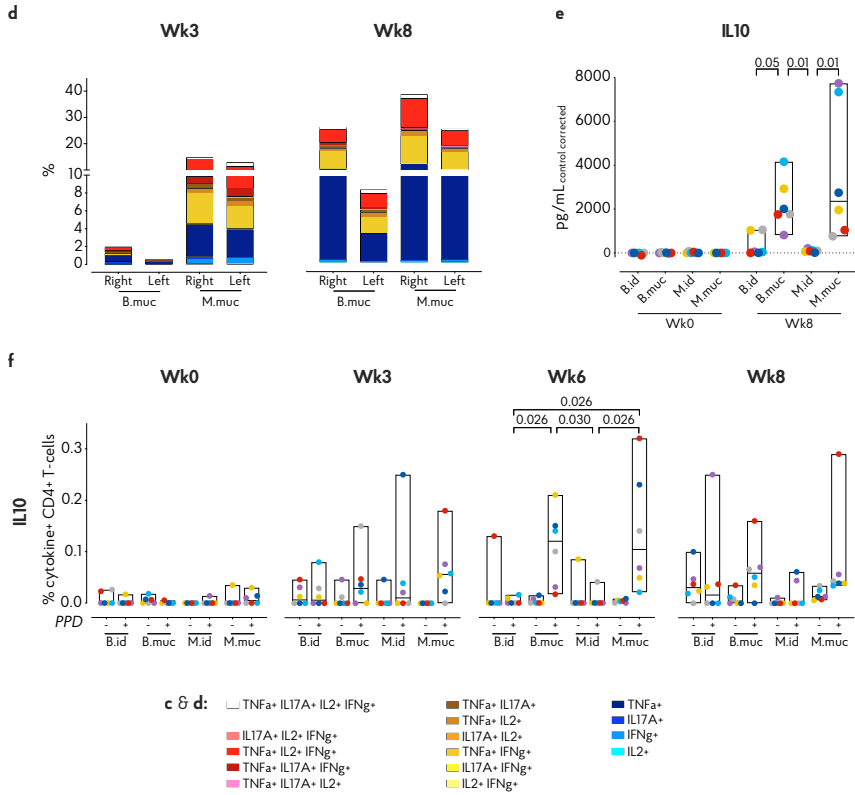
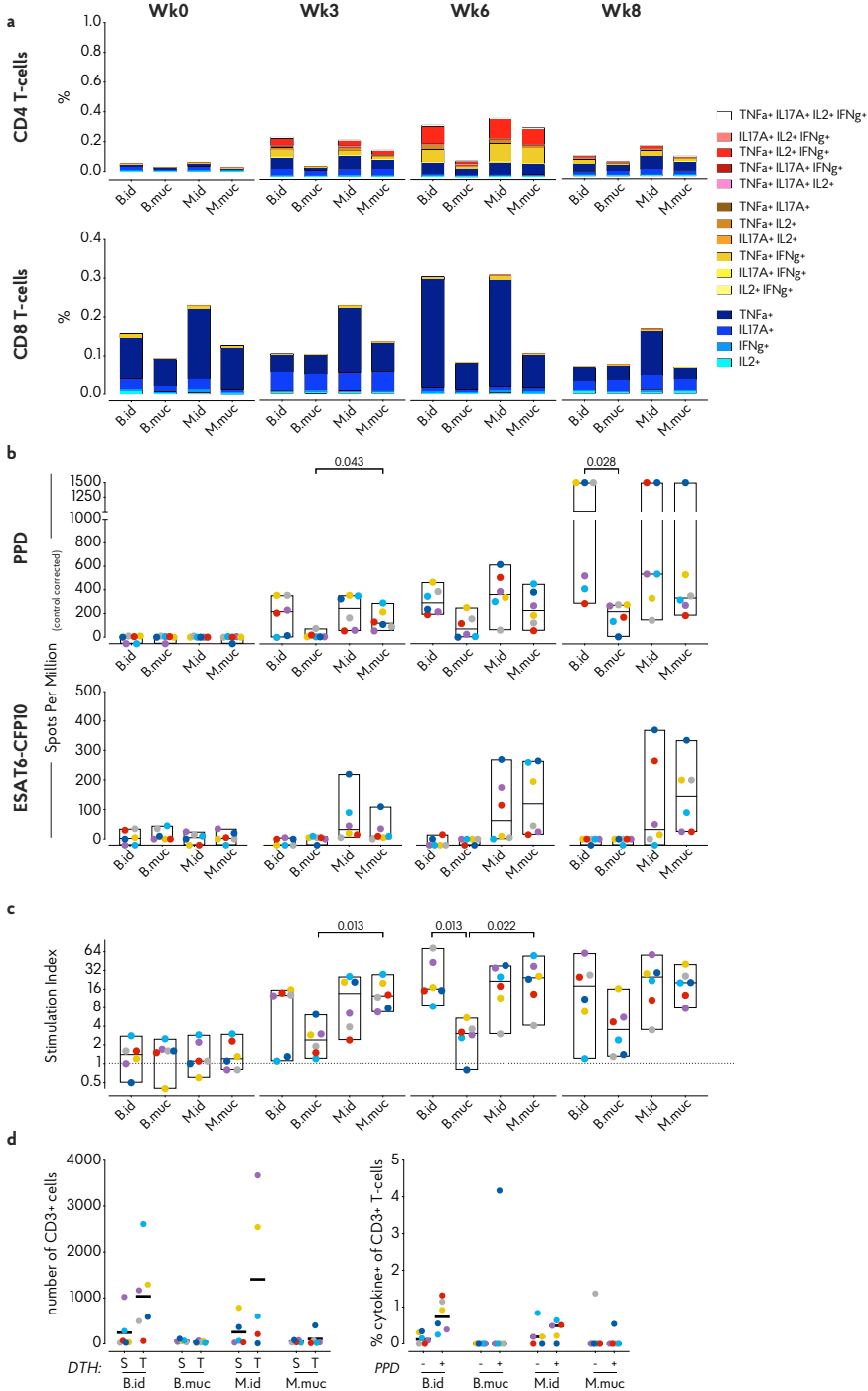


Figure 1 continued. b) Flow cytometric analysis of IFN γ , TNF α , IL2 and IL17A CD4 $^{+}$ T-cell responses after vaccination. **c)** Stacked bar graphs depicting CD4 $^{+}$ T-cell cytokine polyfunctionality after PPD stimulation by group median values. **d)** PPD-specific cytokine production of CD4 $^{+}$ T-cells in lower right and lower left lung lobe, indicating dissemination of vaccine induced immune responses. **e)** Production of IL10 by unfractionated BAL cells stimulated with PPD, plotted as culture medium control corrected values. **f)** Flow cytometric analysis of IL10 production by CD4 $^{+}$ T-cells after vaccination.

For all graphs n=6 animals per group. b & f: “+” indicates PPD stimulated samples, “-” indicates unstimulated, culture medium incubated samples as controls. Horizontal lines in bars indicate group medians. Significance of group differences was determined by two-sided Mann-Whitney test adjusted for multiple comparisons. Holms adjusted p-values ≤ 0.05 are depicted. Colour coding per individual is consistent throughout.





Peripheral immunity after pulmonary vaccination

In parallel to the pulmonary immune responses, we profiled peripheral T-cell immunity in search of potential correlates of protection with a perspective for translation to clinical settings.

However, as before, when assessing PPD-specific CD4+ and CD8+ T-cell cytokine responses by flow cytometry, no discriminating qualitative signals could be identified that distinguished the mucosally from the intradermally vaccinated animals. CD4+ T-cell cytokine production was observed from week 3 post-vaccination onward, and was most prominent in the intradermally vaccinated animals and the M.muc group (**Figure 2a** and **Supplemental Figure 2a**). A slight increase in PPD-specific CD8+ T-cell cytokine production was only apparent in the intradermally vaccinated groups at 6 weeks post-vaccination (**Figure 2a** and **Supplemental Figure 2b**). No differences in CD4+ and CD8+ T-cell polyfunctionality could be detected.

We used an IFN γ ELISPOT to assess the breadth of immune responses induced by MTBVAC in comparison to BCG. As anticipated, after stimulation with ESAT6-CFP10 fusion protein, produced by MTBVAC but not BCG, we observed higher IFN γ production by PBMCs of MTBVAC vaccinated animals compared to the BCG vaccinated groups, regardless of vaccination route (**Figure 2b**). After stimulation with PPD, which contains antigens shared by BCG and MTBVAC, intradermal MTBVAC was indistinguishable from intradermal BCG by IFN γ secretion, as observed by flow cytometry. Of note, mucosal MTBVAC appeared equally potent in inducing PPD-specific IFN γ production. Although we previously observed comparable peripheral immune responses after mucosal and intradermal BCG vaccination, here mucosal BCG vaccination appeared less potent in inducing peripheral cytokine production and proliferation (**Figure 2a-c**).

As an alternative approach, we investigated the capacity of vaccine-induced T-cells by an *in vivo* recall stimulation in a Tuberculin Skin Test (TST). To this end, eight weeks after vaccination we intradermally injected saline (S) and Old Tuberculin (T) in opposite (upper) arms of each animal and took biopsies of the injection sites 3 days later. The biopsies were subsequently processed and characterized by flow

- ◀ **Figure 2. Peripheral immune responses after vaccination.** Characterization of the height and breadth of peripheral immune responses after vaccination. **a)** Stacked bar graphs depicting CD4+ and CD8+ T-cell cytokine polyfunctionality by group median values, after PPD stimulation. **b)** PBMC IFN γ production in response to stimulation with PPD or ESAT6-CFP10 fusion protein, measured by ELISPOT. **c)** PPD-specific proliferation of PBMCs, plotted as a stimulation index: the ratio of antigen-over medium control-stimulated values. **d)** T-cell numbers in skin biopsies taken after intradermal injection of saline (S) or Old Tuberculin (T), 8 weeks after vaccination (left panel) and PPD-specific cytokine production by T-cells from Old Tuberculin skin biopsies (right panel). Dotted line in b indicates maximum limit of detection. In d, “+” indicates PPD stimulated samples, “-” indicates unstimulated, culture medium incubated samples as controls. For all graphs n=6 animals per group, except for **d)**, where n=5 animals for the B.muc, M.id and M.muc group. Horizontal lines indicate group medians. Significance of group differences was determined by two-sided Mann-Whitney test adjusted for multiple comparisons. Holms adjusted p-values ≤ 0.05 are depicted Colour coding per individual is consistent throughout.



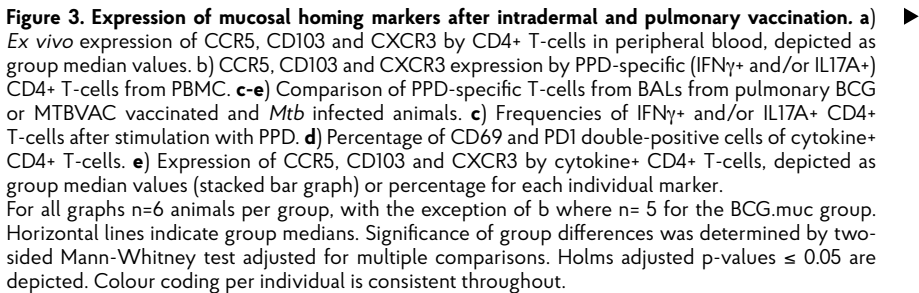
cytometry to measure the delayed type hypersensitivity response (DTH). By visual inspection of the local skin reaction, redness and swelling appeared prominently after intradermal but not mucosal vaccination (not shown). Accordingly, a tuberculin-specific influx of antigen-specific T-cells was exclusively observed in the intradermally vaccinated animals (**Figure 2d**). So, while mucosal vaccination does result in a peripheral blood response (by flow cytometry and IFN γ ELISPOT), it does not enable these cells to migrate to the site of a skin-challenge, and therefore rules out their analysis for a potential biomarker assay.

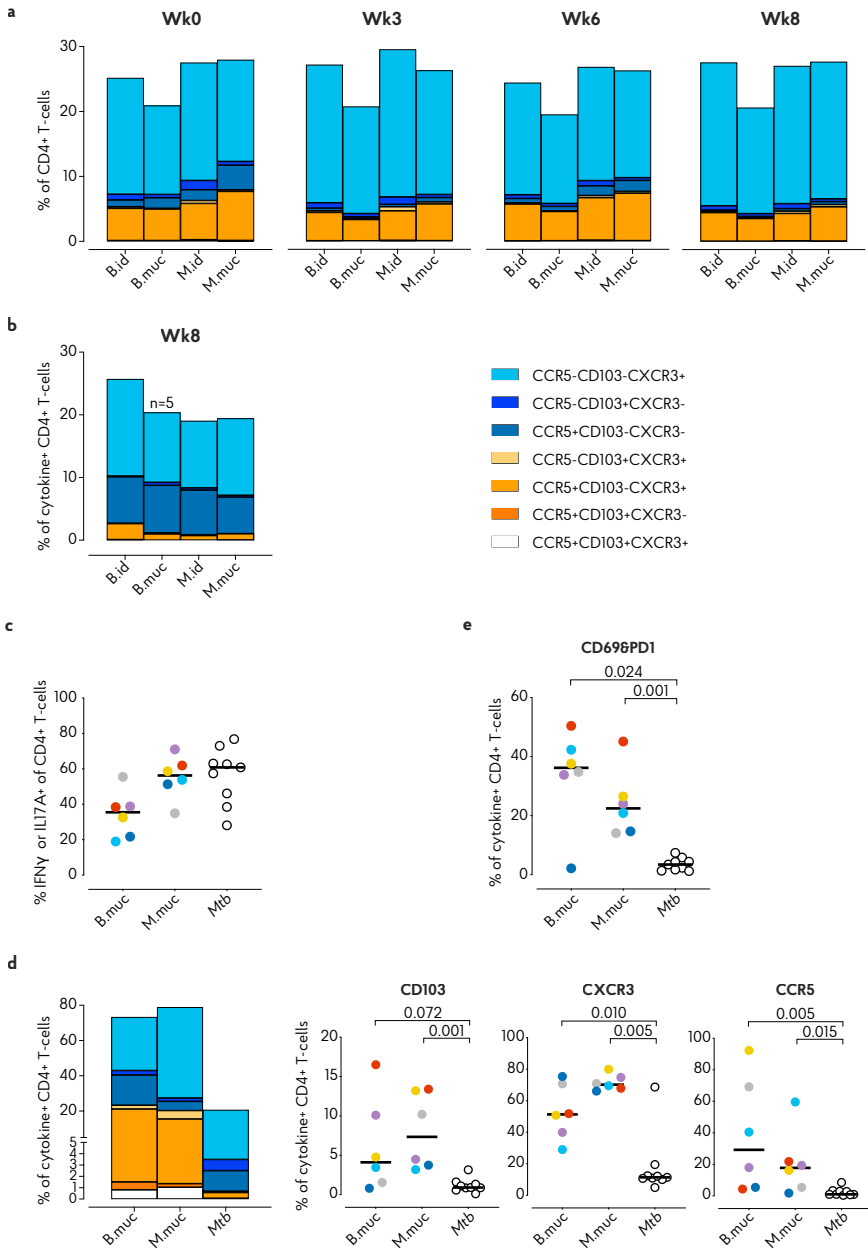
In conclusion, the superior induction of local immune responses by mucosal MTBVAC over mucosal BCG was reflected also in the periphery, and these responses appeared to cover a broader range of antigens including ESAT6. However, within the limits of our analyses, no peripheral responses discriminating between mucosal versus intradermal immunization could be identified.

Mucosal homing marker expression after vaccination

In our search for peripheral correlates of protection we also considered the possibility that pulmonary rather than intradermal vaccination would imprint peripheral T-cells with a higher expression of pulmonary mucosal homing markers. To this end, we assessed the expression of CD103, CXCR3 and CCR5, all known to be involved in homing to the pulmonary mucosa²¹, on peripheral CD4⁺ T-cells by means of flow cytometry.

Prior to vaccination, approximately 25% of circulating CD4⁺ T-cells expressed one or more of these homing markers. After vaccination, either peripherally or mucosally, this percentage did not change, nor was the pattern of homing marker co-expression notably altered in the mucosally vaccinated groups (**Figure 3a & Supplemental Figure 3a**). As only a small fraction of peripheral CD4⁺ T-cells was vaccine-specific (**Figure 2a**), we also assessed homing marker expression of cytokine (IFN γ and/or IL17A) producing CD4⁺ T-cells. However, due to the low number of cytokine-positive events in the periphery it was not possible to measure robust and reliable percentages of homing marker expression at any post-vaccination timepoint. Using a cut-off of a minimal 100 cytokine⁺ events, we only found robust frequencies 8 weeks post-vaccination. The frequency of homing markers expressed by PPD-

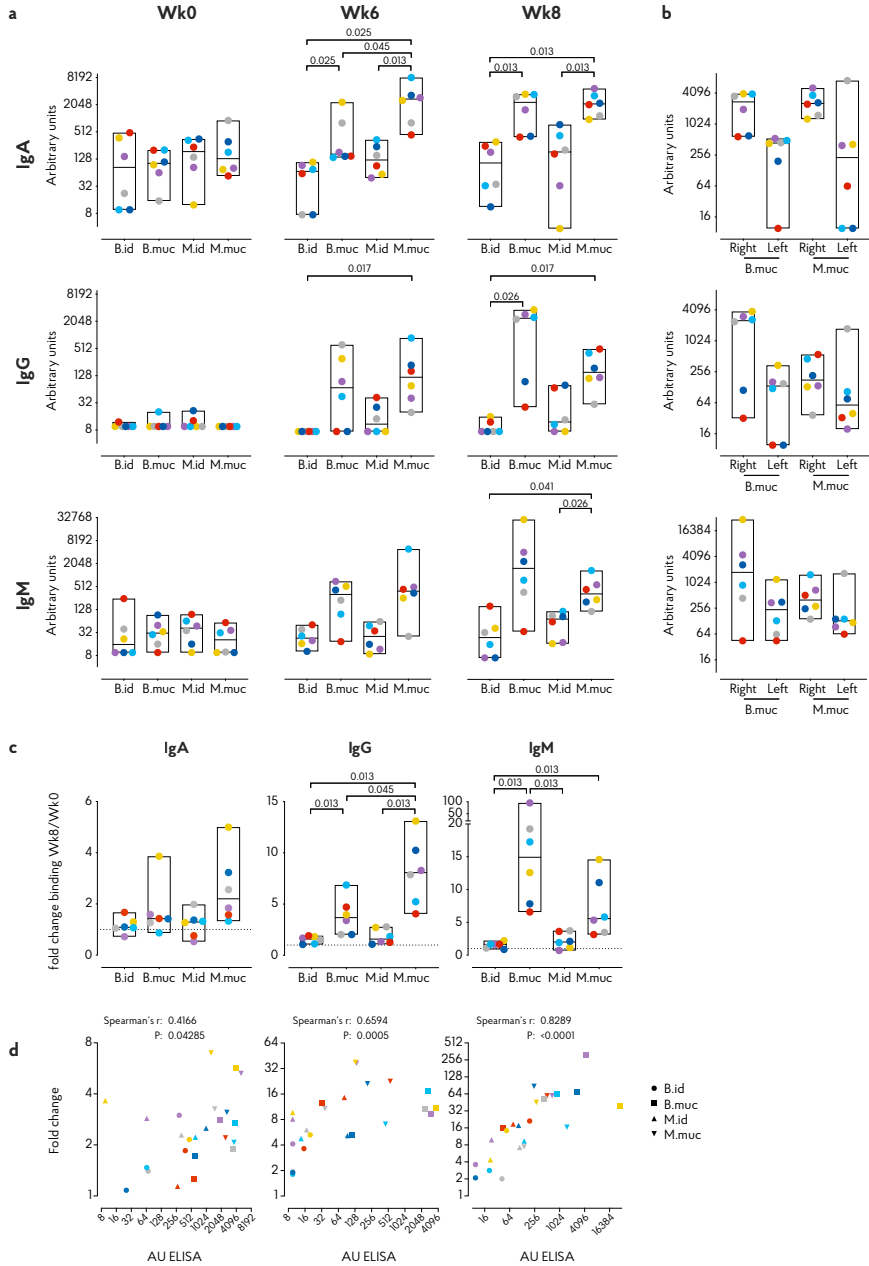
Figure 3. Expression of mucosal homing markers after intradermal and pulmonary vaccination. **a)**  *Ex vivo* expression of CCR5, CD103 and CXCR3 by CD4⁺ T-cells in peripheral blood, depicted as group median values. **b)** CCR5, CD103 and CXCR3 expression by PPD-specific (IFN γ ⁺ and/or IL17A⁺) CD4⁺ T-cells from PBMC. **c-e)** Comparison of PPD-specific T-cells from BALs from pulmonary BCG or MTBVAC vaccinated and *Mtb* infected animals. **c)** Frequencies of IFN γ ⁺ and/or IL17A⁺ CD4⁺ T-cells after stimulation with PPD. **d)** Percentage of CD69 and PD1 double-positive cells of cytokine⁺ CD4⁺ T-cells. **e)** Expression of CCR5, CD103 and CXCR3 by cytokine⁺ CD4⁺ T-cells, depicted as group median values (stacked bar graph) or percentage for each individual marker. For all graphs n=6 animals per group, with the exception of b where n=5 for the BCG.muc group. Horizontal lines indicate group medians. Significance of group differences was determined by two-sided Mann-Whitney test adjusted for multiple comparisons. Holms adjusted p-values ≤ 0.05 are depicted. Colour coding per individual is consistent throughout.



specific T-cells was comparable to that on the total CD4⁺ T-cell population, though cytokine⁺ CD4⁺ T-cells of all vaccinated groups consisted of more CCR5 single-positive cells (**Figure 3b**). When comparing homing marker expression between groups, again, no differences between the mucosally and intradermally vaccinated groups were apparent.

Although the aforementioned homing markers did not reveal a peripheral correlate either, we went on to analyze their expression on cytokine producing T-cells in the airways after mucosal vaccination as well as after experimental pulmonary *Mtb* infection (obtained from an independent low dose infection study), to characterize protective versus pathogenic BAL responses. We again analyzed the expression of CD103, CXCR3 and CCR5 of PPD-specific IFN γ and/or IL17A producing T-cells. After *Mtb* infection a high local CD4⁺ T-cell cytokine response is induced, similar to mucosal MTBVAC and significantly higher than mucosal BCG administration (**Figure 3c**). However, expression of homing markers was significantly lower in PPD-specific T-cells from the *Mtb* infected animals compared to animals vaccinated with BCG or MTBVAC mucosally (**Figure 3d**). While after *Mtb* infection approximately 20% of cytokine producing cells expressed any combination of CD103, CXCR3 and CCR5, 80% of vaccination-induced T-cells were positive for one or more of these markers (**Figure 3d**). In addition to profiling chemokine receptor expression, we also measured CD69 and PD-1 co-expression on cytokine-positive CD4⁺ T cells, as an indicator of a functional tissue-resident phenotype²². Previously, we found that CD69 expression of BAL CD4 T-cells was higher after mucosal over intradermal BCG vaccination and, separately, that IFN γ +TNF α +IL2+IL17A⁺ T-cells expressed higher levels of PD-1. When assessing co-expression of these two markers on IFN γ and/or IL17A producing CD4⁺ T-cells induced by mucosal vaccination, a substantial portion (15-50%) of these cells was found to co-express both markers. Contrarily, after *Mtb* infection, CD69 and PD1 co-expression on PPD-specific T-cells was significantly lower (typically less than 10%) (**Figure 3e**). To summarize, pulmonary vaccination, previously associated with enhanced protection, results in the presence of antigen-specific T-cells with a distinct tissue-residency & mucosal homing phenotype. The observation that *Mtb* infection does not elicit this phenotype suggests that these cells could be involved in protection.

Figure 4. Vaccine-induced humoral immune responses at the pulmonary mucosa. a) Magnitude of *Mtb* Whole Cell Lysate specific immunoglobulin (Ig) A, G and M responses in BAL. b) *Mtb* Whole Cell Lysate specific Ig levels in the lower right (vaccinated) and lower left (unvaccinated) lung lobe. Antibody levels in a and b plotted as arbitrary units, as determined by standardization against a reference sample. c) Binding of BAL immunoglobulins to live *Mtb*, depicted as the fold-change in Geometric Mean Fluorescent Intensity (GMFI) of the Ig-specific detection antibodies between week 0 and week 8 post-vaccination. d) Correlation between Ig binding to Whole Cell Lysate (in arbitrary units) and live *Mtb* (as fold change compared to control) at 8 weeks post vaccination. For all graphs n=6 animals per group. Horizontal lines indicate group medians. Colour coding per individual is consistent throughout. Significance of group differences was determined by two-sided Mann-Whitney test adjusted for multiple comparisons. Holms adjusted p-values ≤ 0.05 are depicted. Correlations in d) calculated with Spearman's rank order test.



Mucosal antibody levels and functionality

In our previously reported vaccination and RLD *Mtb* infection study, mucosal BCG vaccination resulted in pulmonary PPD-specific Ig responses. This observation, in combination with the recent interest in the role of immunoglobulins in protection from TB^{23,24}, prompted us to investigate the humoral immune response in this study in more detail.

As observed previously for BCG, also mucosal vaccination with MTBVAC resulted in a marked increase in *Mtb*-specific IgA, IgG and IgM levels in BAL fluid as detected by ELISA, and in a modest increase in some of the intradermal MTBVAC vaccinated animals (**Figure 4a**). Like the cellular immune responses, humoral immunity was found to disseminate from the vaccine-targeted lobe (**Figure 4b**).

To functionally address these humoral immune responses, we assessed the capacity of vaccination induced immunoglobulins to bind to live *Mtb* bacilli. After incubation of dsRed-expressing *Mtb* with BAL fluid, bound antibodies were subsequently detected with biotinylated detection-antibodies and PE-conjugated

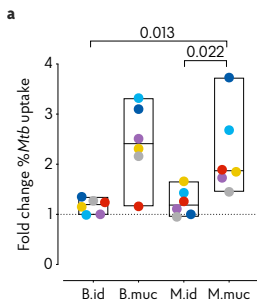
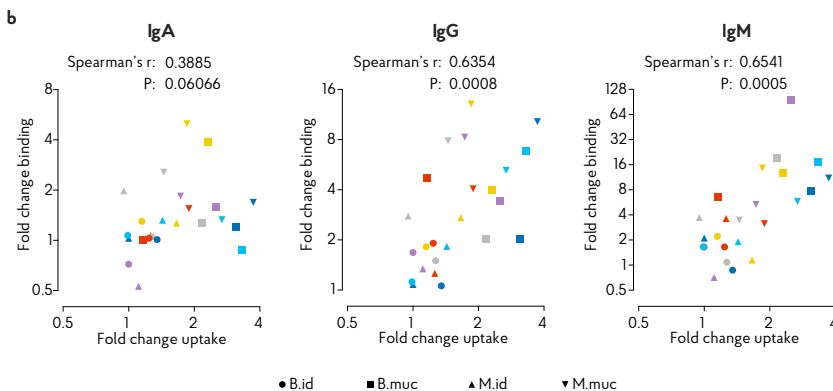


Figure 5. Vaccine-mediated uptake of *Mtb* by phagocytes.

a) Uptake of *Mtb* by PMA-activated THP1 cells after incubation with BAL fluid obtained before and 8 weeks after vaccination, depicted as the fold change in the percentage of *Mtb*+ THP1 cells. **b)** Correlation between vaccination-induced immunoglobulins capable of binding live *Mtb* and the change in *Mtb* uptake.

For all graphs n=6 animals per group. Horizontal lines indicate group medians. Colour coding per individual is consistent throughout. Significance of group differences was determined by two-sided Mann-Whitney test adjusted for multiple comparisons. Holms adjusted p-values ≤ 0.05 are depicted. Correlations in **b)** calculated with Spearman's rank order test.



streptavidin on a flow cytometer. After pulmonary but not intradermal vaccination, a distinct increase in PE fluorescence intensity, indicating increased levels of *Mtb*-binding immunoglobulins, could be observed (**Figure 4c**). Especially, *Mtb*-binding IgG and IgM were present in BAL fluid after mucosal vaccination. BAL humoral immune responses as assessed by ELISA correlated well with the amount of *Mtb*-bound antibody (**Figure 4d**).

Lastly, we investigated whether the antibodies induced by mucosal vaccination would facilitate uptake of *Mtb* by phagocytes. GFP expressing *Mtb* was incubated with BAL fluid and added to phorbol 12-myristate 13-acetate (PMA) activated THP-1 cells. After four hours, the amount of *Mtb*-GFP positive cells was assessed by flow cytometry. When comparing the amount of *Mtb*⁺ cells, an increase in uptake of *Mtb* could be observed when the bacteria were incubated with BAL fluid from mucosally, but not intradermally, vaccinated animals (**Figure 5a**). To assess the contribution of the different immunoglobulin isotypes to this uptake, we correlated the increase in uptake with the increase of *Mtb*-binding immunoglobulins induced by vaccination. Of the three isotypes assessed, the amount of vaccination-induced IgG and IgM correlated most strongly with the increase in uptake observed after vaccination (Spearman's $\rho=0.6354$, $P=0.0008$ and Spearman's $\rho=0.654$, $P=0.0005$, respectively), suggesting that these two isotypes might contribute most to the enhanced uptake of *Mtb* by phagocytes.

Discussion

In this study, pulmonary vaccination with *Mtb*-derived MTBVAC was found to induce pulmonary, PPD-specific polyfunctional Th17A cells and IL10 production, an immune signature previously found to associate with mucosal BCG-induced protection from TB infection and disease¹⁸. Compared to *Mtb* infected animals, PPD-specific T-cells in the BAL of animals vaccinated with BCG or MTBVAC through the pulmonary mucosa expressed significantly higher levels of mucosal homing markers. Pulmonary administration of either vaccine also induced immunoglobulins in the pulmonary space, of which in particular IgG and IgM isotypes (more than IgA) were able to bind live *Mtb* and enhance *Mtb* uptake by THP-1 cells. Compared to BCG, MTBVAC induced these responses more rapidly and to a higher magnitude, and, expectedly, we could demonstrate broader antigen specificity. While both mucosal vaccination strategies induced a peripheral immune response in blood, we could not demonstrate a response to an antigenic challenge in the skin, nor could we identify responses that could serve as peripheral correlates of protection.

Here, we showed that, like BCG, pulmonary administration of a live attenuated *Mtb* strain results in the presence of polyfunctional, IL17A producing T-cells. IL17A has been previously associated with protection from TB in multiple animal models²⁵⁻²⁷, though the exact mechanisms involved require further elucidation. The effector



mechanisms of IL17A are diverse, and can contribute to protection via a number of ways. For example, expression of antimicrobial β -defensin 2 by airway epithelial cells is upregulated after experimental IL17 treatment²⁸, and IL17A is also known to be involved in neutrophil recruitment to the lung, which in turn, has been implied in early protection from TB²⁹⁻³¹. Additionally, it has been demonstrated that IL17A is involved in early control of *Mtb* and the formation of protective lymphoid follicles^{25,32}. However, despite the evidence of the protective effect of IL17A in preclinical models, its precise role in human tuberculosis remains to be resolved, and is likely dependent on factors such as the time, location and magnitude of IL17A production^{33,34}.

Compared to *Mtb* infected animals, PPD-specific BAL T-cells from mucosally vaccinated animals were more frequently double-positive for CD69 and PD-1. While linked to T-cell exhaustion in chronic viral infections, PD-1 expression in TB seems to be associated with infection control, as attested by recent reports of TB reactivation after anti-PD-1 treatment^{35,36}. In mice it has been shown that, post-*Mtb*, specific PD-1+ CD4+ T-cells reside in the lung parenchyma, and adoptive transfer of these but not of PD1-negative cells conferred superior control of *Mtb* infection²². A similar PD-1^{high} lung tissue-resident T-cell population has been identified in *Mtb* infected NHP³⁷. As observed here, the protective PD-1^{high} T-cells characterized in the work of Moguche *et al.* also expressed high levels of CD69, as a marker of activation and tissue residency in lung and lymph nodes³⁸⁻⁴⁰. Of note, a recent NHP *Mtb* study reported superior protection and increased frequencies of CD69+ T-cells in the lung parenchyma after intravenous BCG vaccination compared to aerosol BCG administration⁴¹. Interestingly, endobronchial BCG vaccination also induced increased frequencies of these cells in the lung, however, these animals were not challenged with *Mtb*.

In addition to CD69 and PD1, PPD-specific T-cells induced by mucosal vaccination also more frequently expressed CD103, CXCR3 and CCR5, which are associated with mucosal homing and tissue residency. Mucosal vaccination with *Bacillus subtilis* spores expressing *Mtb* antigens boosted protection conferred by BCG and associated with the induction of CD103+CD69+ tissue-resident T-cells in mice⁴². CXCR3 has been identified as crucial for T-cell entry into the lung parenchyma⁴³. In *Mtb* infected non-human primates, CD4+ T-cells expressing CXCR3 and CCR5 were identified in granulomatous tissue, but these cells did not colocalize with *Mtb*-infected macrophages in the granuloma center and therefore seemingly unable to exert their effector function^{37,44}. Nevertheless, vaccine-induced presence of high frequencies of these cells during the early stages of infection and granuloma formation might contribute to control of *Mtb* by (alveolar) macrophages.

Both mucosal MTBVAC and BCG vaccination resulted in the presence of *Mtb*-specific immunoglobulins at the site of infection. Especially IgG and IgM in BAL were able to bind live *Mtb* and enhanced phagocytosis, while IgA showed the least amount of binding and correlation between binding and uptake by phagocytes was weak. Though not a formal correlate of protection in our previous study, evidence for the protective potential of *Mtb*-specific antibodies has been recently reported in various papers. For instance, *Mtb*-specific IgA clones isolated from TB patients were able to

restrict *Mtb* replication in a lung epithelial cell line⁴⁵. Also, elevated IgG titers to BCG have been found in association with protection against *Mtb* infection⁴⁶, and serum IgG from BCG vaccinated individuals was able to inhibit intracellular growth of mycobacteria⁴⁷. Interestingly, highly exposed individuals that remained IGRA-negative, so called resisters, exhibited enhanced antibody responses to *Mtb*⁴⁸. *Mtb*-specific antibodies could contribute to protection in various ways, including enhancement of *Mtb* phagocytosis, as observed here, activation of the inflammasome, and facilitation of antibody-dependent cell-mediated cytotoxicity (ADCC, all reviewed in ^{23,49}), and work in synergy with vaccination-elicited cellular immunity in response to *Mtb* challenge.

The protective efficacy of MTBVAC has been linked to immune-reactivity to *Mtb*-specific ESAT-6 and CFP-10 antigens, of which the induction was also observed in our study¹⁰. However, the current standard in diagnosing latent TB infection is the detection of discriminatory IFN γ responses by stimulation of peripheral blood with *Mtb*-specific antigens, including ESAT-6. Indeed, MTBVAC vaccinated neonates showed dose-dependent IGRA conversion 180 days post-vaccination, which would interfere with the diagnosis of TB¹². Further exploration of the dynamics of IGRA conversion after MTBVAC vaccination is required to assess the usefulness of the IGRA as a TB diagnostic after MTBVAC administration. Ideally, for the successful deployment of MTBVAC as a vaccine, regardless of the route of administration, new diagnostic tools, not dependent on T-cell epitopes shared by *Mtb* and MTBVAC need to be developed.

In this study, pulmonary vaccination was established through endobronchial instillation of the vaccines, a method incompatible with clinical vaccination. Other, more translatable, mucosal vaccination routes, such as aerosol, intranasal or oral administration, would need to be explored in more detail to assess whether vaccination of BCG or MTBVAC would induce similar protective immune responses. While in mice and guinea pigs aerosol/intranasal BCG vaccination showed increased efficacy compared to parenteral administration^{50,51}, data on the protective efficacy of aerosol vaccination of NHP is contradictory and so far inconclusive. Early work in macaques has shown increased protection of aerosol delivered BCG compared to intradermal BCG, on par with intravenous BCG vaccination¹⁶. Contrarily, in a recent macaque study aerosol BCG vaccination did not confer superior protection⁴¹. This discrepancy in protective efficacy could be caused by a variety of factors, including dose and viability of vaccine delivered. Studies directly comparing mucosal vaccination routes are required to identify which conditions are essential for inducing protection. In humans, aerosol vaccination with BCG has been explored in the 1960s and was found to induce dose-dependent TST conversion⁵². New studies on BCG administration by aerosol have recently been initiated, and aerosol vaccination appears to be safe and immunogenic thus far (NCT03912207, McShane, unpublished data). A study exploring endobronchial BCG instillation with the aim of developing a controlled human infection model also reported no serious adverse events⁵³. From historic data, it can be inferred that, in humans, oral BCG administration is at least as effective as



intradermal injection. Oral administration was the initial route of vaccination when BCG was deployed as a pediatric vaccine in the 1920s, and in Brazil BCG was routinely administered orally until the 1970s⁵⁴. Recent studies investigating oral BCG vaccination report no safety concerns, and, as observed here, oral administration induced *Mtb* specific mucosal IgA and CXCR3 expressing T-cells in BAL^{55,56}.

In conclusion, our data argues for further investigation of pulmonary mucosal administration of MTBVAC, already known to induce superior protection over BCG, as a potentially even more efficacious vaccination strategy to combat TB.

Acknowledgements

We thank BPRC's animal and veterinary care teams, as well as the pathology and clinical lab personnel for their outstanding contributions to this work. We thank Dr. E. Remarque for advice on statistical analysis. We thank Prof. T. Ottenhoff at the Leiden University Medical Centre for providing the *Mtb*-dsRed.

The M7 protein mix (#100768) was produced at the Centre for AIDS Reagents, NIBSC, UK, supported by EURIPRED (EC FP7 INFRASTRUCTURES-2012-INFRA-2012-1.1.5: grant number 31266, www.euripred.eu). It was provided by Dr. B. Khatri, NIBSC, as part of the EC Horizon2020 TRANSVAC2 network programme, grant agreement number 730964. The following reagent was obtained through BEI Resources, NIAID, NIH: *Mycobacterium tuberculosis*, Strain Erdman Barcode Library, NR-50781.

Material & Methods

Animals and ethics

All housing and animal care procedures were performed at the Biomedical Primate Research Centre (BPRC) in Rijswijk, the Netherlands, and in compliance with European directive 2010/63/EU, as well as the "Standard for Humane Care and Use of Laboratory Animals by Foreign Institutions" provided by the Department of Health and Human Services of the US National Institutes of Health (NIH, identification number A5539-01). The BPRC is accredited by the American Association for Accreditation of Laboratory Animal Care (AAALAC). Before the start of the study ethical approval was obtained from the independent animal ethics committee (in Dutch: Dierexperimentencommissie, DEC) as well as BPRC's institutional animal welfare body (in Dutch: Instantie voor Dierwelzijn, IvD).

Twelve female and twelve male Indian-type rhesus macaques (*Macaca mulatta*) were selected from the in-house breeding colony and stratified by gender, age and weight, into 4 groups of 6 animals. Selected animals were negative for prior exposure to mycobacteria, as assessed by tuberculin skin testing with Old Tuberculin

(Synbiotics Corporation, San Diego, CA) and an IFN γ ELISPOT against Purified Protein Derivative (PPD) from *Mycobacterium bovis*, *Mycobacterium avium* (both Fisher Scientific, USA) or *Mycobacterium tuberculosis* (Statens Serum Institute, Copenhagen, Denmark). Treatment was randomly assigned to each group.

Animals were housed pair-wise at biosafety level 3 throughout the experiment and provided with enrichment in the form of food and non-food items on a daily basis. Animal welfare was monitored daily. Animal weight was recorded prior to each blood collection event.

All animal handling and biosampling was performed under ketamine sedation (10 mg/kg, by intra-muscular injection). For endobronchial instillation ketamine sedation (5mg/kg) was supplemented with intramuscular medetomidine (0.04 mg/kg) and an analgesic applied to the larynx.

Eight weeks after vaccine administration animals were euthanized by intravenous injection of pentobarbital (200 mg/kg) under ketamine sedation. All animal caretakers and veterinary personnel were blinded to animal treatment.

Vaccines, vaccine preparation and administration

Animals were vaccinated with either Bacillus Calmette Guérin strain Sofia (InterVax Ltd., Ontario) or MTBVAC (Biofabri, Spain) via the skin or the pulmonary mucosa. The intradermally vaccinated groups received a standard, adult human dose of 1.5-6.0 $\times 10^5$ CFU BCG or 3.0-17.0 $\times 10^5$ CFU MTBVAC in 0.1 mL reconstituted vaccine in the skin (abbreviated as BCG.id or MVAC.id). The mucosally vaccinated groups were administered the same dose but in 10 mL of sterile saline solution by endobronchial instillation into the lower right lung lobe (abbreviated as BCG.muc or MVAC.muc). The vaccines, regardless of administration route, were prepared from a single pooled mix of freshly reconstituted vials immediately prior to administration. Vaccination was executed for all animals in a single session in random order within 2-3 hours from vaccine preparation.

Mtb infection

For the comparison of homing marker expression by cytokine positive pulmonary mucosal T-cells, BALs from *Mtb* infected animals were obtained 11 weeks after endobronchial administration of 3-15 CFU of *Mtb* Erdman (NR-50781, BEIResources). Infection was confirmed for all animals by the induction of *Mtb*-specific IFN γ production by PBMCs and post-mortem pathology assessment (data not shown).

Bio-sample collection and processing

Cells from the pulmonary mucosa were recovered at specific time points by broncho-alveolar lavage (BAL), targeting either the lower right or lower left lung lobe. Three volumes of 20 mL of prewarmed 0.9% saline solution were consecutively instilled and recovered. BAL fluid was harvested by centrifugation of BAL samples for 10 minutes at 400g after 100 μ m filtration. Supernatant was subsequently decanted and stored at -80°C pending further analysis. The BAL cell pellet was taken



up in RPMI supplemented with 10% fetal calf serum (FCS), glutamax and penicillin/streptomycin (from here on referred to as R10) and used in downstream assays. BAL fluid was filter-sterilized by centrifugation through 0.2 mm PVDF membrane plates (Fisher Scientific) before analysis.

Peripheral blood mononuclear cells were isolated from heparinised blood collected by venepuncture. Isolation of PBMCs was performed by density gradient centrifugation with Lymphoprep lymphocyte separation medium (Axis-Shield, UK), and PBMCs were subsequently resuspended in R10 for downstream immunological assays.

Flow cytometry

T-cell cytokine production and homing marker expression was assessed by flow cytometry. Freshly isolated PBMCs were incubated overnight with *Mtb* PPD (5 ug/mL) in the presence of GolgiPlug transport inhibitor (BD Biosciences). PMA/ionomycin stimulated samples were taken along as technical/positive controls. The next day, cells were washed and incubated with the panels listed in Supplemental Table 1. To facilitate intracellular cytokine staining, cells were permeabilized with Cytofix/Cytoperm (BD Biosciences) before addition of cytokine antibodies. After overnight fixation with 2% paraformaldehyde (PFA), samples were acquired on a 3-laser, 14-colour LSR-II flow cytometer (BD Biosciences). Analysis was performed in FlowJo version 10 (Treestar). T-cells were selected as Singlets/Lymphocytes/Viable/CD14-CD20-/CD45+/CD3+, after which further CD4 and CD8 gating was applied. Any anomalies indicative of unstable signal acquisition were excluded using the "Time" parameter. Cytokine positivity was determined by placement of cytokine gates on the medium control samples and subsequently applying the gates to the corresponding PPD stimulated samples.

Luminex

Cytokine production of BAL cells stimulated 72 hours with PPD (5 ug/mL) was assessed by custom Milliplex Luminex kits (Merck Millipore, USA). Assays were performed according to manufacturer's protocol. In short: supernatants of stimulated BAL cells were incubated with beads coated with cytokine-specific antibodies. Bound cytokines were visualized using biotin-coupled detection antibodies and PE-labelled streptavidin. Beads were acquired on a Bioplex 200 system and cytokine levels were calculated with Bioplex Manager software version 6.1 (both Biorad, CA, USA).

IFN γ ELISPOT

Non-human primate specific IFN γ ELISPOT (U-CyTech, the Netherlands) was performed on PBMCs according to manufacturer's protocol on. Briefly, 200,000 PBMCs were incubated in triplicate for 24 hours with *Mtb*-derived PPD (Statens Serum Institute, Denmark), M7 protein mix (19kDa, Ag85A, TB10.3, Ag85B, HSP20, ESAT6 & CFP7) or recombinant ESAT6-CFP10 fusion protein (provided by Kees Franken from the Ottenhoff lab, Leiden University Medical Centre). The next day cells were washed and transferred to anti-IFN γ coated membrane plates (Millipore).

After 24 hours cells were discarded and membrane-bound IFN γ was visualized using a biotinylated anti-IFN γ detector antibody, streptavidin-horseradish peroxidase conjugate and tetramethylbenzidine substrate. Spots were quantified using an automated reader (AELVIS, Hannover).

Immunoglobulin ELISA

Antibody levels in BAL were determined by Enzyme Linked ImmunoSorbent Assay (ELISA). In brief, 96-well plates were coated with either 5 μ g/mL Mtb HN828 Whole Cell lysate (BEI Resources, VA, USA) in PBS. After overnight blocking with 1% BSA, samples were added to the wells. Bound antibodies were subsequently detected with either horse radish peroxidase-conjugated anti-IgG (Rockland, PA, USA), alkaline phosphatase-conjugated anti-IgA (Fisher Scientific) or alkaline phosphatase-conjugated IgM (Sigma), and the addition of para-nitrophenylphosphate substrate for ELISA colour development. All samples were normalized to arbitrary units (AU) against a serial dilution of a positive reference sample included in all assays.

Mtb binding and phagocytosis assay

To assess *Mtb* binding of immunoglobulins present in BAL fluids, BAL fluid obtained prior to and 8 weeks after vaccination were incubated with 10^7 CFU of *Mtb* H37Rv-dsRed⁵⁷ at 37°C for 1 hour. Subsequently, each sample was divided over three vials and biotinylated detection antibodies specific for IgA, IgG or IgM (all Mabtech) were added (final dilution 1:500). After 30 minutes incubation at room temperature, streptavidin-FITC (final dilution 1:400) was added to visualize bound antibody, and samples were incubated for a further 60 minutes. Samples were fixed overnight with 2% PFA.

For the phagocytosis assay, 500.000 THP1 cells were seeded in a 24-wells plate and activated by overnight incubation with 10ng/mL PMA at 37°C. The next day, 10^7 CFU of *Mtb* H37Rv-GFP was incubated with BAL fluid as described above, and subsequently added to the activated THP-1 cells. After 4 hours cells were dissociated with trypsin-EDTA and resuspended in 2% PFA for overnight fixation. The binding assay samples were subsequently acquired on a 4 laser, FACSAriaIII system, samples from the phagocytosis assay were acquired on a 3 laser, Beckman Coulter Gallios system. For both assays, *Mtb* H37Rv-dsRed or -GFP incubated with PBS was taken along as a negative control.

Statistical analysis

Statistical analysis was performed with Graphpad Prism version 8 and R version 3.5.1⁵⁸. Significance of differences between groups was calculated by two-sided Mann-Whitney testing of which Holm's adjusted p-values are reported. Correlation statistics were generated by Spearman's rank analysis.



References

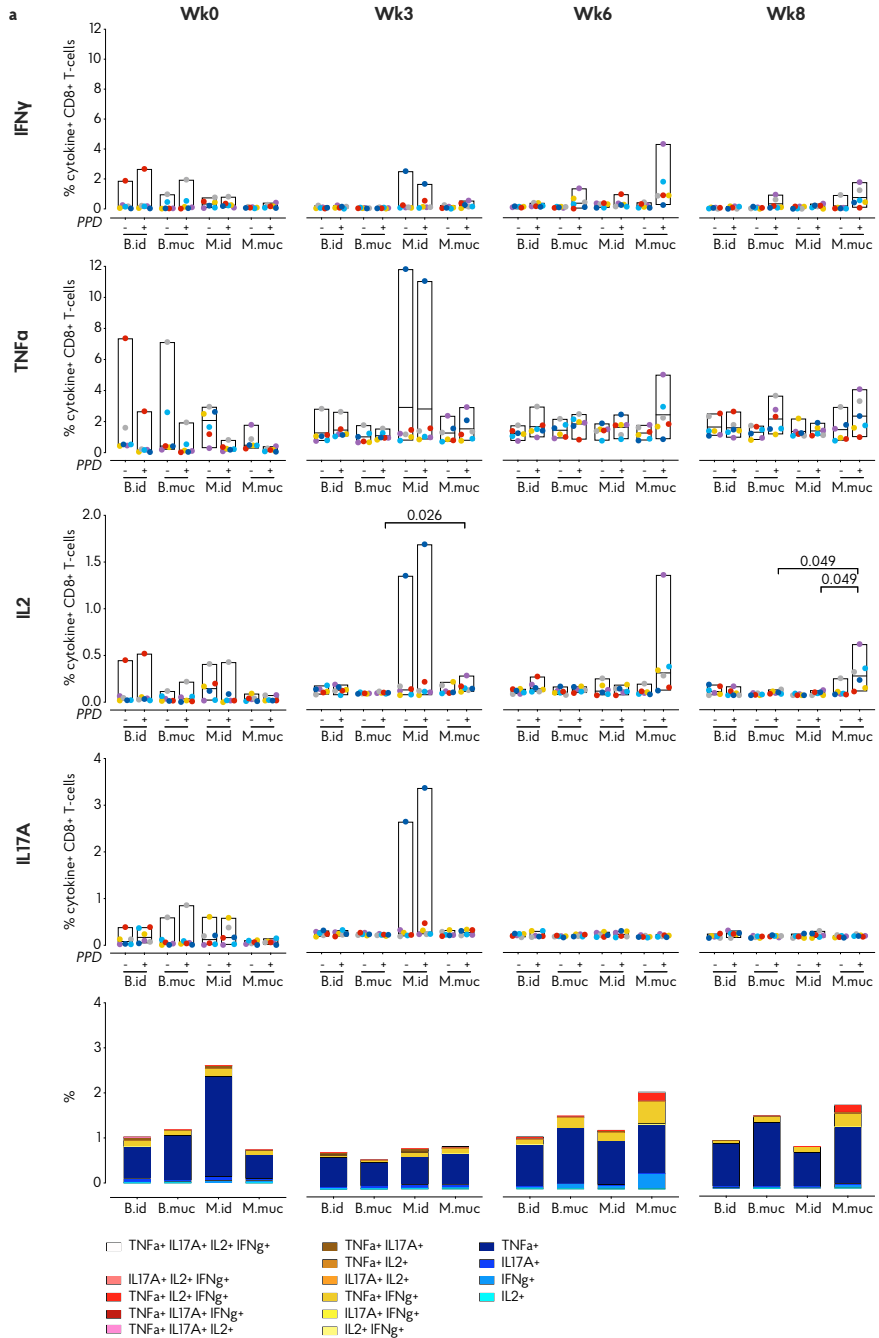
1. Geneva: World Health Organization. Global tuberculosis report 2019.
2. Mangtani, P., et al. Protection by BCG Vaccine Against Tuberculosis: A Systematic Review of Randomized Controlled Trials. *Clinical Infectious Diseases* **58**, 470-480 (2014).
3. Zhang, L., et al. Variable Virulence and Efficacy of BCG Vaccine Strains in Mice and Correlation With Genome Polymorphisms. *Mol Ther* **24**, 398-405 (2016).
4. Brandt, L., et al. Failure of the Mycobacterium bovis BCG vaccine: some species of environmental mycobacteria block multiplication of BCG and induction of protective immunity to tuberculosis. *Infection and immunity* **70**, 672-678 (2002).
5. Sable, S.B., Posey, J.E. & Scriba, T.J. Tuberculosis Vaccine Development: Progress in Clinical Evaluation. *Clinical microbiology reviews* **33**(2019).
6. Voss, G., et al. Progress and challenges in TB vaccine development. *F1000Research* **7**, 199 (2018).
7. Arbues, A., et al. Construction, characterization and preclinical evaluation of MTBVAC, the first live-attenuated M. tuberculosis-based vaccine to enter clinical trials. *Vaccine* **31**, 4867-4873 (2013).
8. Gonzalo-Asensio, J., Marinova, D., Martin, C. & Aguilo, N. MTBVAC: Attenuating the Human Pathogen of Tuberculosis (TB) Toward a Promising Vaccine against the TB Epidemic. *Frontiers in immunology* **8**, 1803-1803 (2017).
9. Aguilo, N., et al. MTBVAC vaccine is safe, immunogenic and confers protective efficacy against Mycobacterium tuberculosis in newborn mice. *Tuberculosis* **96**, 71-74 (2016).
10. Aguilo, N., et al. Reactogenicity to major tuberculosis antigens absent in BCG is linked to improved protection against Mycobacterium tuberculosis. *Nature communications* **8**, 16085 (2017).
11. Clark, S., et al. Revaccination of Guinea Pigs With the Live Attenuated Mycobacterium tuberculosis Vaccine MTBVAC Improves BCG's Protection Against Tuberculosis. *The Journal of infectious diseases* **216**, 525-533 (2017).
12. Tameris, M., et al. Live-attenuated Mycobacterium tuberculosis vaccine MTBVAC versus BCG in adults and neonates: a randomised controlled, double-blind dose-escalation trial. *The Lancet. Respiratory medicine* **7**, 757-770 (2019).
13. Spertini, F., et al. Safety of human immunisation with a live-attenuated Mycobacterium tuberculosis vaccine: a randomised, double-blind, controlled phase I trial. *The Lancet. Respiratory medicine* **3**, 953-962 (2015).
14. Verreck, F.A.W., et al. Variable BCG efficacy in rhesus populations: Pulmonary BCG provides protection where standard intra-dermal vaccination fails. *Tuberculosis (Edinburgh, Scotland)* **104**, 46-57 (2017).
15. Aguilo, N., et al. Pulmonary but Not Subcutaneous Delivery of BCG Vaccine Confers Protection to Tuberculosis-Susceptible Mice by an Interleukin 17-Dependent Mechanism. *The Journal of infectious diseases* **213**, 831-839 (2016).
16. Barclay, W.R., et al. Protection of monkeys against airborne tuberculosis by aerosol vaccination with bacillus Calmette-Guerin. *The American review of respiratory disease* **107**, 351-358 (1973).
17. Perdomo, C., et al. Mucosal BCG Vaccination Induces Protective Lung-Resident Memory T Cell Populations against Tuberculosis. *mBio* **7**(2016).
18. Dijkman, K., et al. Prevention of tuberculosis infection and disease by local BCG in repeatedly exposed rhesus macaques. *Nature medicine* (2019).
19. Cardona, P.J. & Williams, A. Experimental animal modelling for TB vaccine development. *International journal of infectious diseases : IJID : official publication of the International Society for Infectious Diseases* **56**, 268-273 (2017).

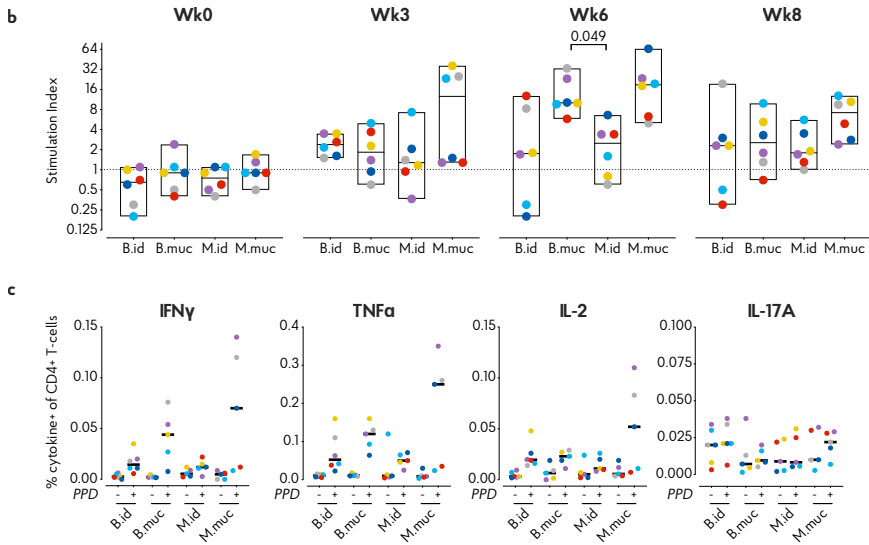
20. Hunter, R.L., et al. Pathogenesis and Animal Models of Post-Primary (Bronchogenic) Tuberculosis, A Review. *Pathogens (Basel, Switzerland)* **7**(2018).
21. Iijima, N. & Iwasaki, A. Tissue instruction for migration and retention of TRM cells. *Trends in immunology* **36**, 556-564 (2015).
22. Mogueche, A.O., et al. ICOS and Bcl6-dependent pathways maintain a CD4 T cell population with memory-like properties during tuberculosis. *The Journal of experimental medicine* **212**, 715-728 (2015).
23. Kawahara, J.Y., Irvine, E.B. & Alter, G. A Case for Antibodies as Mechanistic Correlates of Immunity in Tuberculosis. *Frontiers in Immunology* **10**(2019).
24. Tran, A.C., Kim, M.Y. & Reljic, R. Emerging Themes for the Role of Antibodies in Tuberculosis. *Immune Netw* **19**, e24 (2019).
25. Gopal, R., et al. Unexpected role for IL-17 in protective immunity against hypervirulent Mycobacterium tuberculosis HN878 infection. *PLoS pathogens* **10**, e1004099 (2014).
26. Wareham, A.S., et al. Evidence for a role for interleukin-17, Th17 cells and iron homeostasis in protective immunity against tuberculosis in cynomolgus macaques. *PLoS one* **9**, e88149 (2014).
27. Wozniak, T.M., Saunders, B.M., Ryan, A.A. & Britton, W.J. Mycobacterium bovis BCG-specific Th17 cells confer partial protection against Mycobacterium tuberculosis infection in the absence of gamma interferon. *Infection and immunity* **78**, 4187-4194 (2010).
28. Kao, C.Y., et al. IL-17 markedly up-regulates beta-defensin-2 expression in human airway epithelium via JAK and NF-kappaB signaling pathways. *Journal of immunology (Baltimore, Md. : 1950)* **173**, 3482-3491 (2004).
29. Shenoy, A.T., et al. Lung CD4+ resident memory T cells remodel epithelial responses to accelerate neutrophil recruitment during pneumonia. *Mucosal immunology* (2019).
30. J, N.H., Das, S., Tripathy, S.P. & Hanna, L.E. Role of neutrophils in tuberculosis: A bird's eye view. *Innate Immun*, 1753425919881176 (2019).
31. Miyamoto, M., et al. Endogenous IL-17 as a mediator of neutrophil recruitment caused by endotoxin exposure in mouse airways. *Journal of immunology (Baltimore, Md. : 1950)* **170**, 4665-4672 (2003).
32. Ardain, A., et al. Group 3 innate lymphoid cells mediate early protective immunity against tuberculosis. *Nature* **570**, 528-532 (2019).
33. Torrado, E. & Cooper, A.M. IL-17 and Th17 cells in tuberculosis. *Cytokine Growth Factor Rev* **21**, 455-462 (2010).
34. Shen, H. & Chen, Z.W. The crucial roles of Th17-related cytokines/signal pathways in M. tuberculosis infection. *Cellular & molecular immunology* **15**, 216-225 (2018).
35. Jensen, K.H., Persson, G., Bondgaard, A.L. & Pohl, M. Development of pulmonary tuberculosis following treatment with anti-PD-1 for non-small cell lung cancer. *Acta oncologica (Stockholm, Sweden)*, 1-2 (2018).
36. Picchi, H., et al. Infectious complications associated with the use of immune checkpoint inhibitors in oncology: Reactivation of tuberculosis after anti PD-1 treatment. *Clinical microbiology and infection : the official publication of the European Society of Clinical Microbiology and Infectious Diseases* (2017).
37. Kauffman, K.D., et al. Defective positioning in granulomas but not lung-homing limits CD4 T-cell interactions with Mycobacterium tuberculosis-infected macrophages in rhesus macaques. *Mucosal immunology* (2017).
38. Purwar, R., et al. Resident memory T cells (T(RM)) are abundant in human lung: diversity, function, and antigen specificity. *PLoS one* **6**, e16245 (2011).
39. Shioy, L.R., et al. CD69 acts downstream of interferon-alpha/beta to inhibit S1P1 and lymphocyte egress from lymphoid organs. *Nature* **440**, 540-544 (2006).
40. Kumar, B.V., et al. Human Tissue-Resident Memory T Cells Are Defined by Core Transcriptional and Functional Signatures in Lymphoid and Mucosal Sites. *Cell reports* **20**, 2921-2934 (2017).



41. Darrah, P.A., et al. Prevention of tuberculosis in macaques after intravenous BCG immunization. *Nature* **577**, 95-102 (2020).
42. Copland, A., et al. Mucosal Delivery of Fusion Proteins with *Bacillus subtilis* Spores Enhances Protection against Tuberculosis by *Bacillus Calmette-Guerin*. *Front Immunol* **9**, 346 (2018).
43. Jeyanathan, M., et al. CXCR3 Signaling Is Required for Restricted Homing of Parenteral Tuberculosis Vaccine-Induced T Cells to Both the Lung Parenchyma and Airway. *Journal of immunology (Baltimore, Md. : 1950)* **199**, 2555-2569 (2017).
44. Lin, P.L., et al. Early Events in Mycobacterium tuberculosis Infection in Cynomolgus Macaques. *Infection and immunity* **74**, 3790-3803 (2006).
45. Zimmermann, N., et al. Human isotype-dependent inhibitory antibody responses against Mycobacterium tuberculosis. *EMBO molecular medicine* **8**, 1325-1339 (2016).
46. Logan, E., et al. Elevated IgG Responses in Infants Are Associated With Reduced Prevalence of Mycobacterium tuberculosis Infection. *Frontiers in Immunology* **9**(2018).
47. Chen, T., et al. Association of Human Antibodies to Arabinomannan With Enhanced Mycobacterial Opsonophagocytosis and Intracellular Growth Reduction. *The Journal of infectious diseases* **214**, 300-310 (2016).
48. Lu, L.L., et al. IFN-gamma-independent immune markers of Mycobacterium tuberculosis exposure. *Nature medicine* **25**, 977-987 (2019).
49. Li, H. & Javid, B. Antibodies and tuberculosis: finally coming of age? *Nature reviews. Immunology* (2018).
50. Garcia-Contreras, L., et al. Immunization by a bacterial aerosol. *Proceedings of the National Academy of Sciences of the United States of America* **105**, 4656-4660 (2008).
51. Chen, L., Wang, J., Zganiacz, A. & Xing, Z. Single intranasal mucosal Mycobacterium bovis BCG vaccination confers improved protection compared to subcutaneous vaccination against pulmonary tuberculosis. *Infection and immunity* **72**, 238-246 (2004).
52. Rosenthal, S.R., McEnery, J.T. & Raisys, N. Aerogenic BCG vaccination against tuberculosis in animal and human subjects. *J Asthma Res* **5**, 309-323 (1968).
53. Davids, M., et al. A Human Lung Challenge Model to Evaluate the Safety and Immunogenicity of PPD and Live BCG. *American journal of respiratory and critical care medicine* (2019).
54. Benévolo-de-Andrade, T.C., Monteiro-Maia, R., Cosgrove, C. & Castello-Branco, L.R.R. BCG Moreau Rio de Janeiro : an oral vaccine against tuberculosis - review. *Memórias do Instituto Oswaldo Cruz* **100**, 459-465 (2005).
55. Hoft, D.F., et al. PO and ID BCG vaccination in humans induce distinct mucosal and systemic immune responses and CD4(+) T cell transcriptomal molecular signatures. *Mucosal immunology* **11**, 486-495 (2018).
56. Cosgrove, C.A., et al. Boosting of cellular immunity against Mycobacterium tuberculosis and modulation of skin cytokine responses in healthy human volunteers by Mycobacterium bovis BCG substrain Moreau Rio de Janeiro oral vaccine. *Infection and immunity* **74**, 2449-2452 (2006).
57. Korbee, C.J., et al. Combined chemical genetics and data-driven bioinformatics approach identifies receptor tyrosine kinase inhibitors as host-directed antimicrobials. *Nature communications* **9**, 358 (2018).
58. R Core Team. R: A Language and Environment for Statistical Computing. (2018).

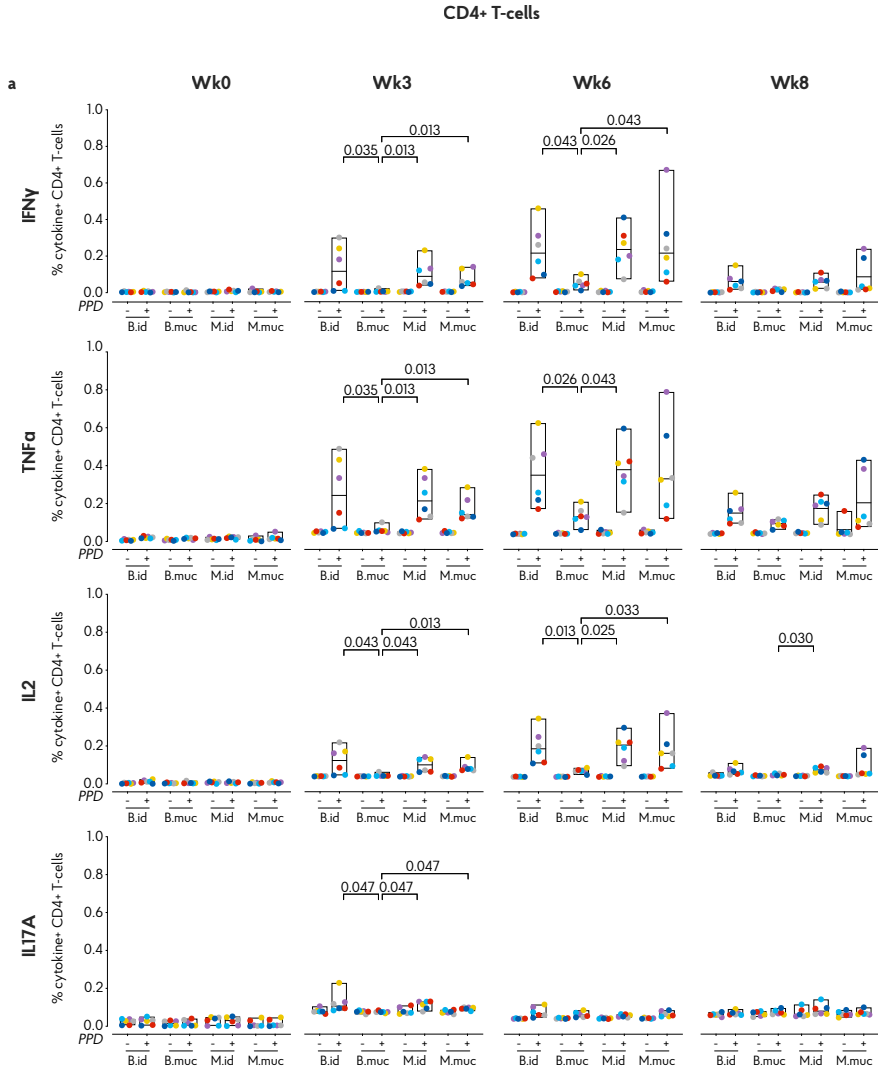
Supplemental data





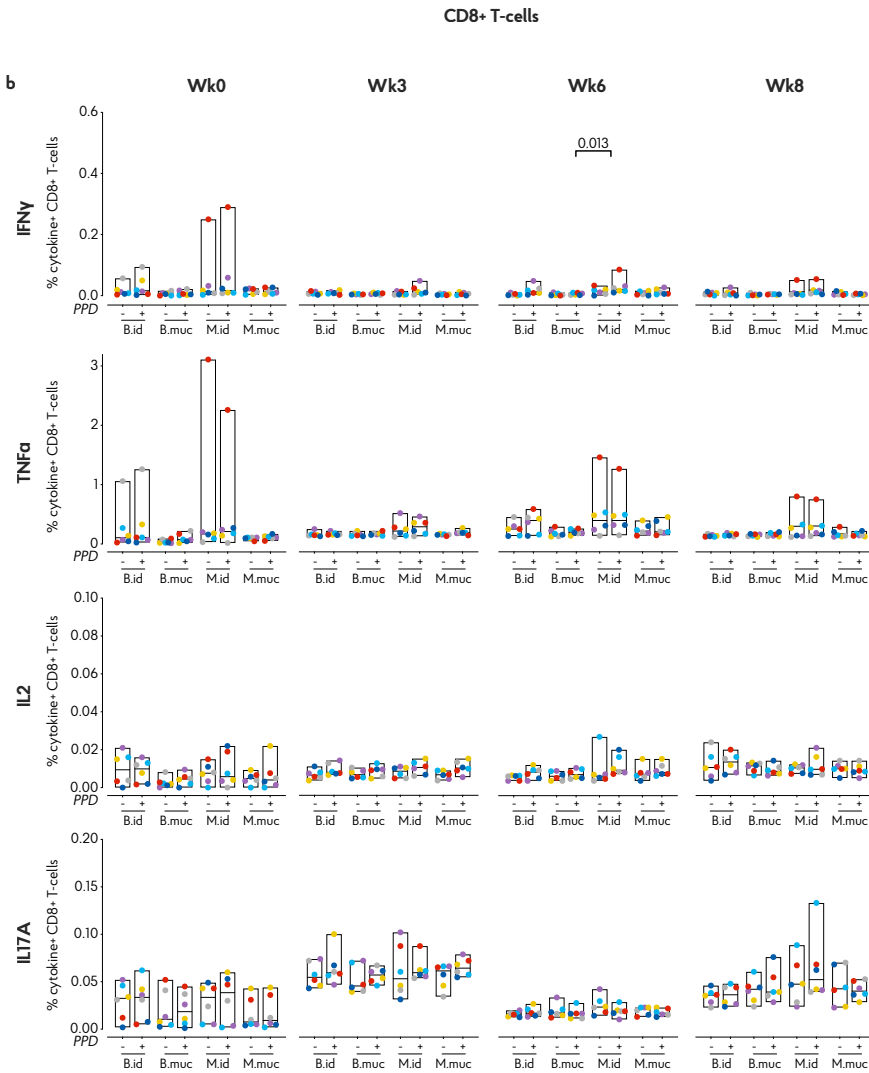
Supplemental Figure 1. BAL CD8+ T-cell responses, proliferation and lung draining lymph node T-cell cytokine production. a) Flow cytometric analysis of IFN γ , TNF α , IL2 and IL17A CD8+ T-cell responses after vaccination and stacked bar graphs depicting CD8+ T-cell cytokine polyfunctionality after PPD stimulation by group median values. b) PPD-specific proliferation of BAL cells, depicted as the stimulation index: the ratio of antigen- over medium control-stimulated values. c) Production of IFN γ , TNF α , IL2 and IL17A by CD4+ T-cells from lung draining lymph nodes in response to PPD, 8 weeks after vaccination. “+” indicates PPD stimulated samples, “-” indicates unstimulated, culture medium incubated samples as controls

For all graphs n=6 animals per group. Horizontal lines in bars indicate group medians. Significance of group differences was determined by two-sided Mann-Whitney test adjusted for multiple comparisons. Holms adjusted p-values ≤ 0.05 are depicted. Colour coding per individual is consistent throughout.

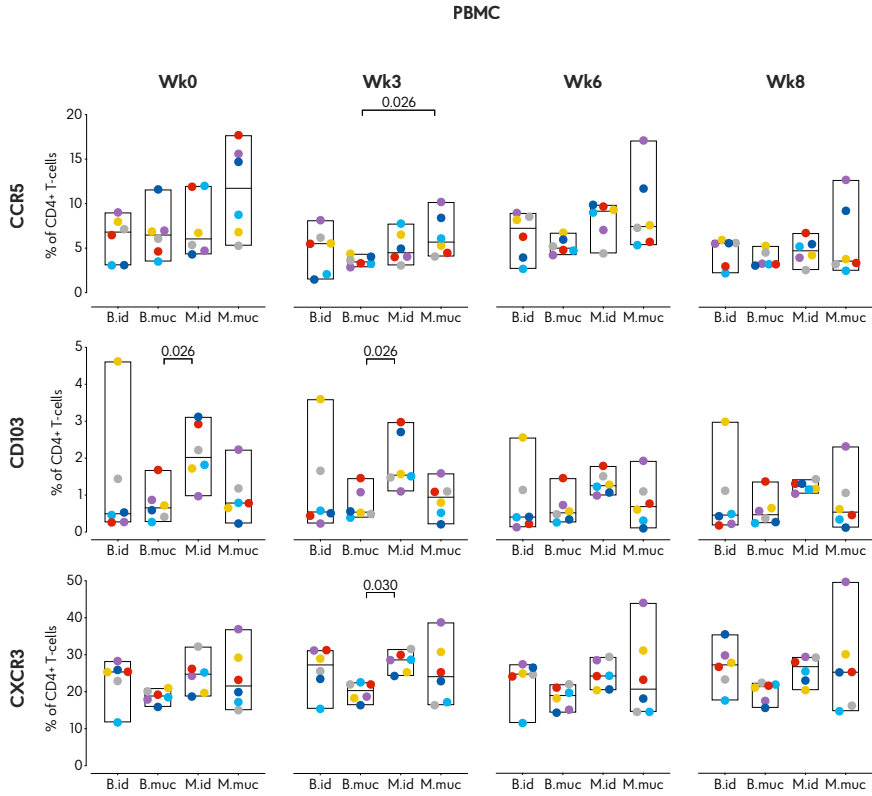


Supplemental Figure 2. Individual cytokine production by peripheral T-cells. a) Production of IFN γ , TNF α , IL2 and IL17A by a) peripheral CD4 $^{+}$ T-cells.





Supplemental Figure 2. b) peripheral CD8⁺ T-cells. “+” indicates PPD stimulated samples, “-” indicates unstimulated, culture medium incubated samples as controls. For all graphs n=6 animals per group. Horizontal lines indicate group medians. Significance of group differences was determined by two-sided Mann-Whitney test adjusted for multiple comparisons. Holms adjusted p-values ≤ 0.05 are depicted. Colour coding per individual is consistent throughout.



Supplemental figure 3. Total ex vivo homing marker expression by peripheral T-cells. Frequency of CCR5+, CD103+ and CXCR3+ CD4+ T-cells in peripheral blood. For all graphs n=6 animals per group. Horizontal lines indicate group medians. Significance of group differences was determined by two-sided Mann-Whitney test adjusted for multiple comparisons. Holms adjusted p-values ≤ 0.05 are depicted. Colour coding per individual is consistent throughout.





Systemic and pulmonary C1q as biomarker of progressive disease in experimental non-human primate tuberculosis



Karin Dijkman¹, Rosalie Lubbers², Nicole V. Borggreven³, Tom H.M. Ottenhoff⁴, Simone A. Joosten⁴, Leendert A. Trouw³, Frank A.W. Verreck¹.

¹ from the section of TB Research & Immunology, department of Parasitology, Biomedical Primate Research Centre (BPRC), Rijswijk the Netherlands, and

the departments of ² Rheumatology, ³ Immunohematology and Blood Transfusion, and ⁴Infectious Diseases, Leiden University Medical Centre (LUMC), Leiden, the Netherlands

Manuscript in press at Scientific Reports

Abstract

Tuberculosis (TB) causes 1.6 million deaths annually. Early differential diagnosis of active TB infection is essential in optimizing treatment and reducing TB mortality, but is hampered by a lack of accurate and accessible diagnostics. Previously, we reported on complement component C1q, measured in serum by ELISA, as a candidate biomarker for active tuberculosis. In this work we further examine the dynamics of C1q as a marker of progressive TB disease in non-human primates (NHP). We assessed systemic and pulmonary C1q levels after experimental infection using high or low single dose as well as repeated limiting dose *Mycobacterium tuberculosis* (*Mtb*) challenge of macaques. We show that increasing C1q levels, either peripherally or locally, correlate with progressive TB disease, assessed by PET-CT imaging or post-mortem evaluation. Upregulation of C1q did not precede detection of *Mtb* infection by a conventional interferon-gamma release assay, confirming its association with disease progression. Finally, pulmonary vaccination with Bacillus Calmette Guérin also increased local production of C1q, which might contribute to the generation of pulmonary protective immunity. Our data demonstrate that NHP modelling of TB can be utilized to study the role of C1q as a liquid biomarker in TB protection and disease, complementing findings in TB patients.

Introduction

Tuberculosis (TB) remains a highly significant burden to global health. In 2018, 6.4 million new cases of TB were officially notified to the World Health Organization (WHO)¹. However, the WHO estimates the actual number of TB cases to be 10 million¹, implying an underestimation of the true number of TB cases. Closing this gap in TB detection has the potential to prevent millions of deaths and to curb further dissemination of TB. Accordingly, the WHO has made early diagnosis of tuberculosis an integral part of their EndTB strategy.

After infection with *Mycobacterium tuberculosis* (*Mtb*), the causative agent of TB, individuals may develop latent TB infection (LTBI) or active progressive disease (although some may also clear the infection). Definitive diagnosis of active TB can only be made by detection of *Mycobacterium tuberculosis* (*Mtb*) in sputum, either by smear microscopy, culture or GeneXpert technology. These assays, however, are time-consuming, require specific (expensive) infrastructure and suffer from sampling error and low sensitivity. Immunological tests, such as Tuberculin Skin Testing (TST) or Interferon Gamma Release Assays (IGRAs) can detect exposure to mycobacteria, but are unable to differentiate between active and latent TB infection^{2,3}. These host response measures can remain positive even after treatment and clearance of infection. Accurate tests for risk of relapse after drug-treatment or risk of progression to active disease are currently unavailable. A wide range of new TB diagnostics are

currently under development, investigating the diagnostic potential of pathogen-derived components as well as host-derived biomarkers in various body fluids^{2,3}.

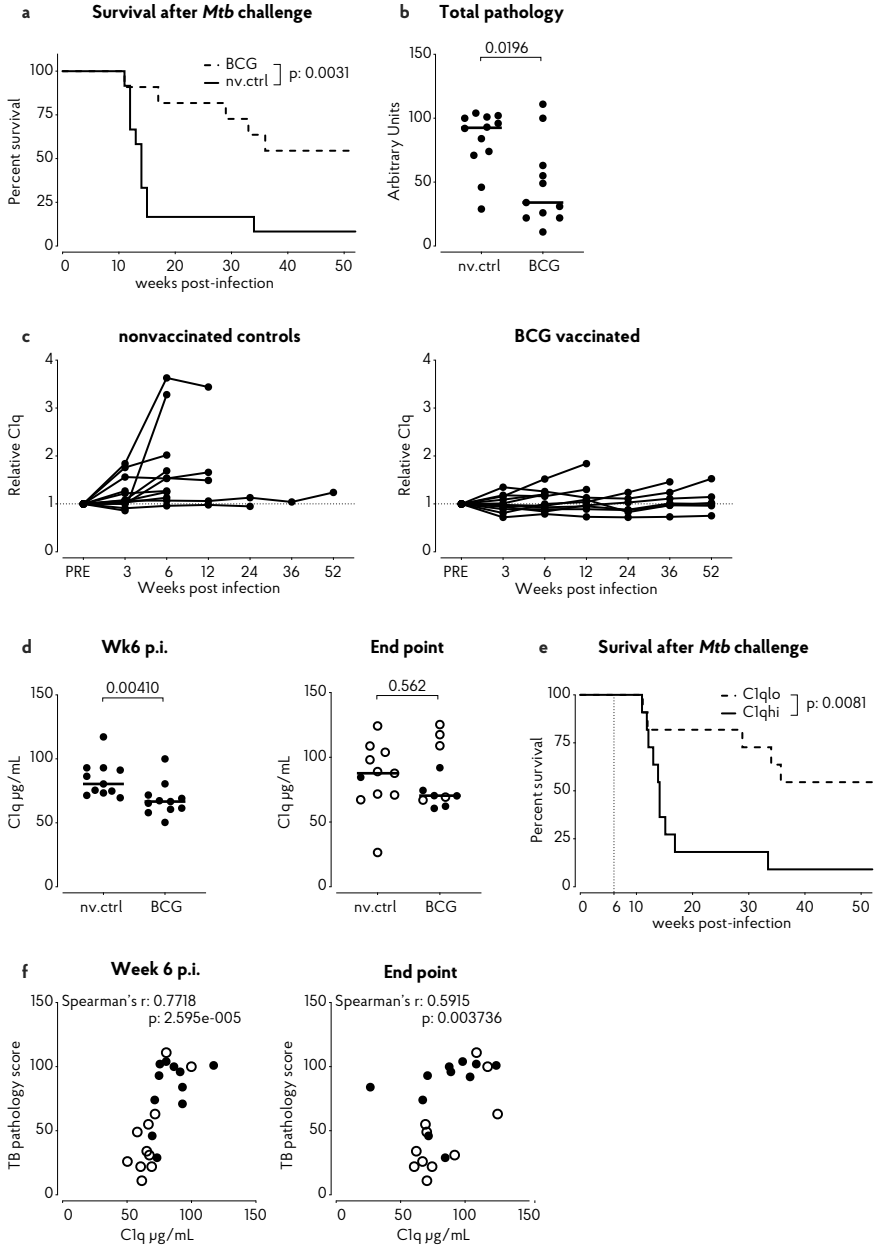
Over the last few years many host-derived candidate biomarkers of progressive TB disease have been identified, and amongst them several components of the complement system⁴⁻⁹. The complement system consists of a number of serum proteins with the capacity to recognize and neutralize invading pathogens by opsonization and lysis. One of these components, C1q, can bind to pathogen-bound C-reactive protein, IgG or IgM, thereby activating the complement cascade through its associated serine proteases C1s and C1r. This binding results in subsequent deposition of the opsonin C3b on the surface of the pathogen and, ultimately, the formation of the membrane attack complex (MAC). Additionally, C1q enhances phagocytosis and has been implied, amongst others, in tissue repair, synaptic pruning and macrophage polarization (reviewed in^{10,11}). More recently, a role for complement components in shaping innate and adaptive immune responses has been established. For instance, in a model for systemic lupus erythematosus, C1q was found to control auto-reactive CD8+ T-cell responses, by modulating the mitochondrial metabolism of these T-cells^{12,13}. C1q is mainly produced by cells of the myeloid lineage¹⁴, and especially by immature dendritic cells¹⁵, macrophages¹⁶ and mast cells¹⁷.

We and others have previously described serum C1q as a biomarker of active TB disease^{18,19}. In patients with active TB we observed significantly higher levels of serum C1q compared to individuals with latent *Mtb* infection or individuals with non-mycobacterial pneumonia. Furthermore, we showed increase of C1q after high dose TB challenge of Non-Human Primates (NHPs).

NHP and macaque species (*Macaca spp*) in particular, are considered highly relevant models for TB, due to their close phylogenetic relationship to man, outbred nature and large similarity in TB pathogenesis. Macaques are applied across the whole spectrum of TB research, both in preclinical evaluation of TB vaccines and therapeutics as well as basic research on TB disease development²⁰⁻²². Modelling in these species presents the advantage of having controlled and accurate time-response-conditions relative to infection. Depending on macaque (sub)species, *M.tuberculosis* strain and challenge dose, TB disease manifestation in macaques mimics the diversity seen in humans²³⁻²⁵.

In this work, we exploited diversity in TB disease manifestation in NHPs to examine the dynamics of C1q as a biomarker of TB disease in more detail. We assessed C1q levels in plasma and bronchoalveolar lavages (BALs) in multiple independent cohorts of *Mtb* infected macaques under varying experimental challenge conditions. By profiling circulating and pulmonary C1q levels at various timepoints after infection we show that increasing C1q levels correlate with increased TB pathology and with decreased survival following challenge with high or low dose *Mtb*. However, neither peripheral nor local upregulation of C1q preceded IGRA conversion, suggesting its association with progressive disease but not TB infection per se. Lastly, we show that pulmonary vaccination with Bacillus Calmette Guérin (BCG), which is superior in inducing protection against TB compared to standard intradermal vaccination^{23,26,27},





also results in an increase in pulmonary C1q and discuss its potential role in the generation of a protective immune responses. Our observations confirm and further support C1q as a marker of progressive TB disease.

Results

C1q is a predictive marker of disease progression in NHP TB

In addition to having described serum C1q as a biomarker of active TB in human patients, we also reported on elevated C1q levels in a preliminary analysis of serum and BAL samples from *Mtb*-infected non-human primates¹⁸. Here we set out to further investigate C1q as a marker of TB disease, under various model conditions in NHPs.

We started with retrospective measurement of C1q in serum from rhesus macaques (*Macaca mulatta*) that were either vaccinated or not with a standard human dose of intradermal BCG and subsequently challenged with a high dose (500 Colony Forming Units (CFU)) of *Mtb* strain Erdman, previously described in part in Lubbers et al (2018)¹⁸. These animals were monitored for 1 year after infectious challenge, or until reaching a humane endpoint due to progressive TB disease. In this cohort, prior BCG vaccination was efficacious and resulted in significant improvement of survival after *Mtb* challenge ($p = 0.0031$, **Figure 1a**) and reduction of TB associated pathology ($p = 0.0196$, **Figure 1b**).

Serum C1q levels did not differ between the two groups prior to infection (**Supplemental Figure 1a**). Assessing changes over time, we observed most prominent upregulation in non-vaccinated controls (nv.ctrls) already from 3 weeks after infection with *Mtb* (**Figure 1c**). In some individuals, an increase in C1q levels preceded a humane endpoint event by several weeks. By week 6 post-*Mtb* infection, group median serum C1q in non-vaccinated controls was significantly higher compared to BCG vaccinees (**Figure 1d**, left panel). Despite reducing TB pathology by prior BCG vaccination (**Figure 1b**), when comparing C1q levels at individuals' endpoints, non-vaccinated controls and BCG vaccinated animals showed no significant difference in serum C1q (**Figure 1d**, right panel).

- ◀ **Figure 1. C1q is a predictive marker of disease progression in NHP TB.** Increase in serum C1q correlates with disease manifestation after high dose *Mtb* challenge. **a**) Kaplan-Meier curves of time-to-endpoint (survival) for non-vaccinated (solid line, n=12) and BCG vaccinated (dashed line, n=11) rhesus macaques after infection with 500 CFU of *Mtb*. **b**) Total post-mortem tuberculosis pathology scores, showing reduction of TB disease by prior BCG vaccination. **c**) Serum C1q levels relative to pre-infection values of nonvaccinated controls and BCG vaccinees. **d**) Group-comparison of serum C1q concentration 6 weeks post-infection (p.i.) and at endpoint. Open symbols in right panel represent animals that reached a humane endpoint. **e**) Kaplan-Meier curves of time-to-endpoint (survival) for animals with high/above median (solid line) or low/below median C1q levels (dashed line) at 6 weeks post-infection. **f**) Correlation of serum C1q levels at 6 weeks post-infection and at endpoint, with total tuberculosis pathology scores from BCG vaccinated animals represented by open symbols.

Horizontal lines in **b**) & **d**) indicate group medians. Statistical significance of group differences determined by two sided Mann-Whitney. Statistical curve comparison in **a**) and **e**) by Mantel-Cox Log-rank test. Correlations in **f**) calculated with Spearman's rank-order test.



To determine the potential of serum C1q as a prognostic marker regardless of prophylactic treatment and prior to the incidence of humane endpoints, we divided all animals in two groups: those exhibiting week 6 C1q levels below the median value (C1q.lo) and animals with week 6 levels above the median (C1q.hi). When comparing Kaplan-Meier curves for time-to-endpoint, animals with the highest C1q levels displayed significantly reduced survival ($p = 0.0081$, **Figure 1e**). Furthermore, we found a strong statistical correlation between the total TB pathology score at necropsy and serum C1q levels at 6 weeks post-infection (Spearman's $\rho = 0.772$, $p < 0.0001$, **Figure 1f**, left panel). Individual C1q levels at endpoint correlated significantly with the total amount of pathology (Spearman's $\rho = 0.591$, $p = 0.003$, **Figure 1f**, right panel). Taken together, these observations suggest that C1q is an early marker of progressive disease after experimental infection of rhesus macaques.

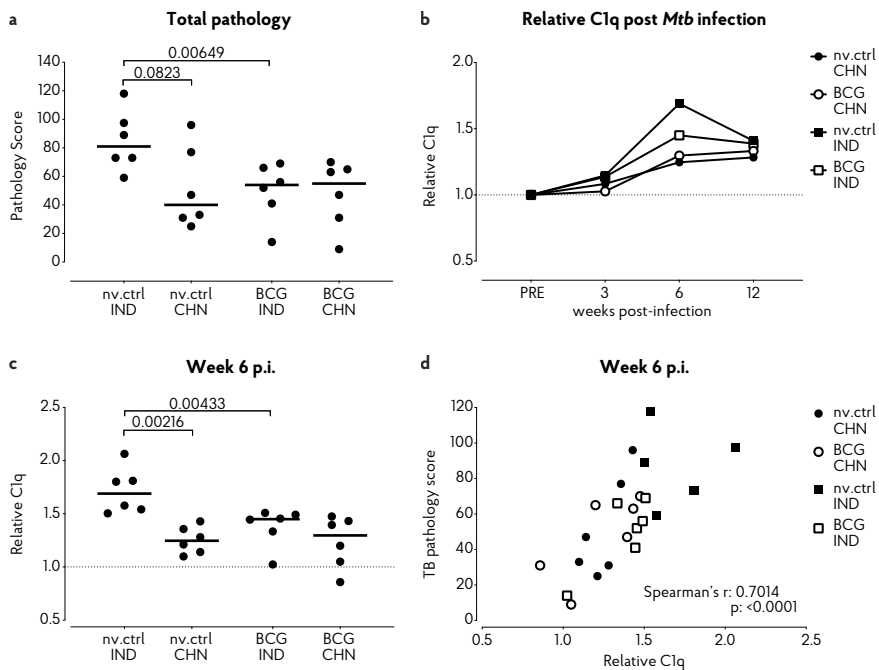


Figure 2. C1q is a marker of differential disease severity in distinctive rhesus cohorts. Serum C1q levels after *Mtb* infection of two genotypic cohorts of rhesus macaques. **a)** Total tuberculosis pathology scores after infection of unvaccinated (nv.ctrl) or BCG vaccinated rhesus macaques with 500 CFU of *Mtb*. IND: Indian genotype, CHN: Chinese genotype. N=6 per group. **b)** Group medians of relative C1q levels over the course of *Mtb* infection. **c)** Group-comparison of relative C1q levels at 6 weeks post-infection (p.i.). **d)** Correlation of relative C1q levels with total tuberculosis pathology scores.

Horizontal lines in **a)** and **c)** indicate group medians. Statistical significance of group differences determined by two sided Mann-Whitney. Correlation in **d)** calculated with Spearman's rank-order test.

C1q is a marker of differential disease severity in distinctive rhesus cohorts

We next sought to confirm the correlation of C1q upregulation with disease severity in an independent cohort of *Mtb* infected NHP. As a species, rhesus macaques can be divided into distinct subpopulations based on genetic variation that is associated with their geographical distribution²⁸. When comparing Chinese versus Indian type rhesus macaques head-to-head, we found the latter to exhibit a more severe TB disease phenotype, 12 weeks after single high dose (500 CFU) *Mtb* challenge (²³ & **Figure 2a**, non-vaccinated controls). Prior intradermal BCG vaccination reduced TB associated pathology in Indian but not Chinese type rhesus macaques. We measured C1q in serum collected at 3 weekly intervals and assessed the association of C1q levels with TB pathology.

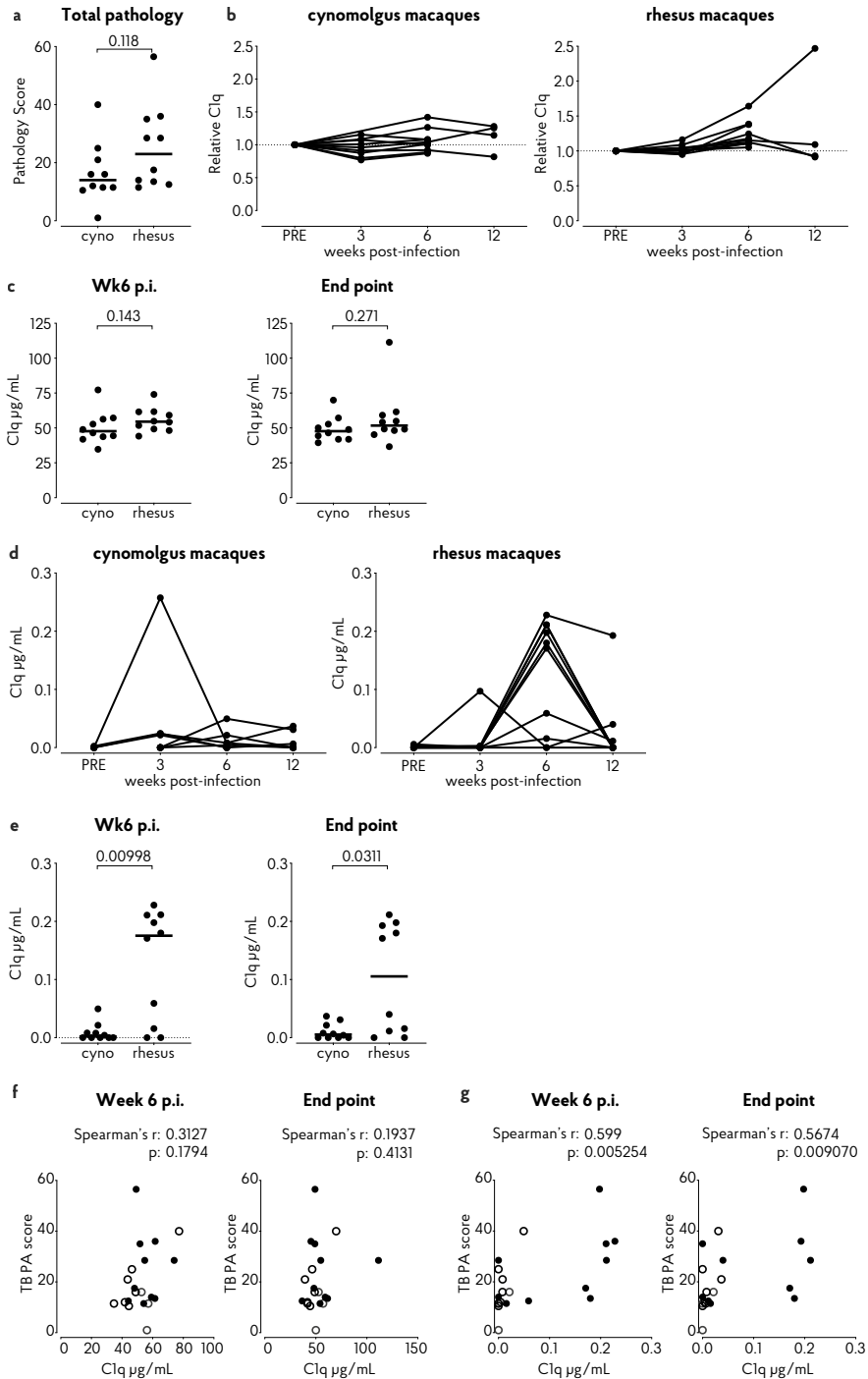
As observed previously, serum C1q levels increased during experimental infection with *Mtb*, from 3 weeks post-infection onward (**Figure 2b**). The strongest increase in serum C1q was again observed in the animals with the highest disease severity, the non-vaccinated Indian rhesus macaques (**Figure 2b**). Reduced TB pathology, as seen in Chinese type rhesus macaques or after prior BCG vaccination of Indian type rhesus macaques, is reflected in the limited upregulation of C1q in these groups (**Figure 2b**). Since we observed a trend of higher C1q levels prior to infection in BCG vaccinated Chinese rhesus macaques in particular (**Supplemental figure 1b**), we used individual fold-increase of C1q (a relative measure of C1q) in subsequent analyses. When comparing values 6 weeks post-infection, relative C1q values were significantly higher in unvaccinated Indian rhesus macaques compared to BCG vaccinated Indian rhesus macaques or unvaccinated Chinese type macaques (**Figure 2c**). Non-parametric Spearman's analysis of the relative C1q levels at week 6 versus total TB pathology scores revealed a strong correlation ($\rho = 0.7014$, $p = <0.0001$, **Figure 2d**), corroborating the association between C1q upregulation and tuberculosis disease severity.

Increased C1q is observed in the pulmonary space after *Mtb* infection

Over time we have moved away from high dose infection studies, since macaques appeared highly susceptible to infection and natural exposure to *Mtb* likely occurs at much lower doses than the 500 CFU applied in the studies described above²⁹. To investigate whether increasing serum C1q still associates with disease severity after low dose *Mtb* infection, we assessed serum C1q dynamics in a cohort consisting of rhesus and cynomolgus macaques (*Macaca mulatta* and *Macaca fascicularis*, respectively) that were infected with a low dose (<10 CFU) of *Mtb*. The two species differ in the extent of TB pathology development after experimental infection; rhesus macaques typically tend to develop more severe TB pathology (**Figure 3a**, unpublished data & ³⁰). These animals were sacrificed either 6 or 12 weeks after *Mtb* infection, and displayed significantly less TB pathology compared to the animals from the studies described in **Figure 1** and **Figure 2** (**Supplemental Figure 2**).

Baseline pre-infection levels of serum C1q did not differ between the two species (**Supplemental Figure 1c**). After infection with low dose *Mtb*, overall we observed a





modest increase in serum Clq only, most apparent between 3 and 6 weeks post-infection (with the exception of one rhesus showing a progressive increase) (**Figure 3b**). However, despite increased TB disease levels in rhesus over cynomolgus macaques, there was no significant difference in Clq levels between the two species, neither when comparing Clq levels at week 6 post-infection nor at endpoint (that is pooling endpoint values of animals sacrificed at week 6 or 12) (**Figure 3c**, left and right panel, respectively).

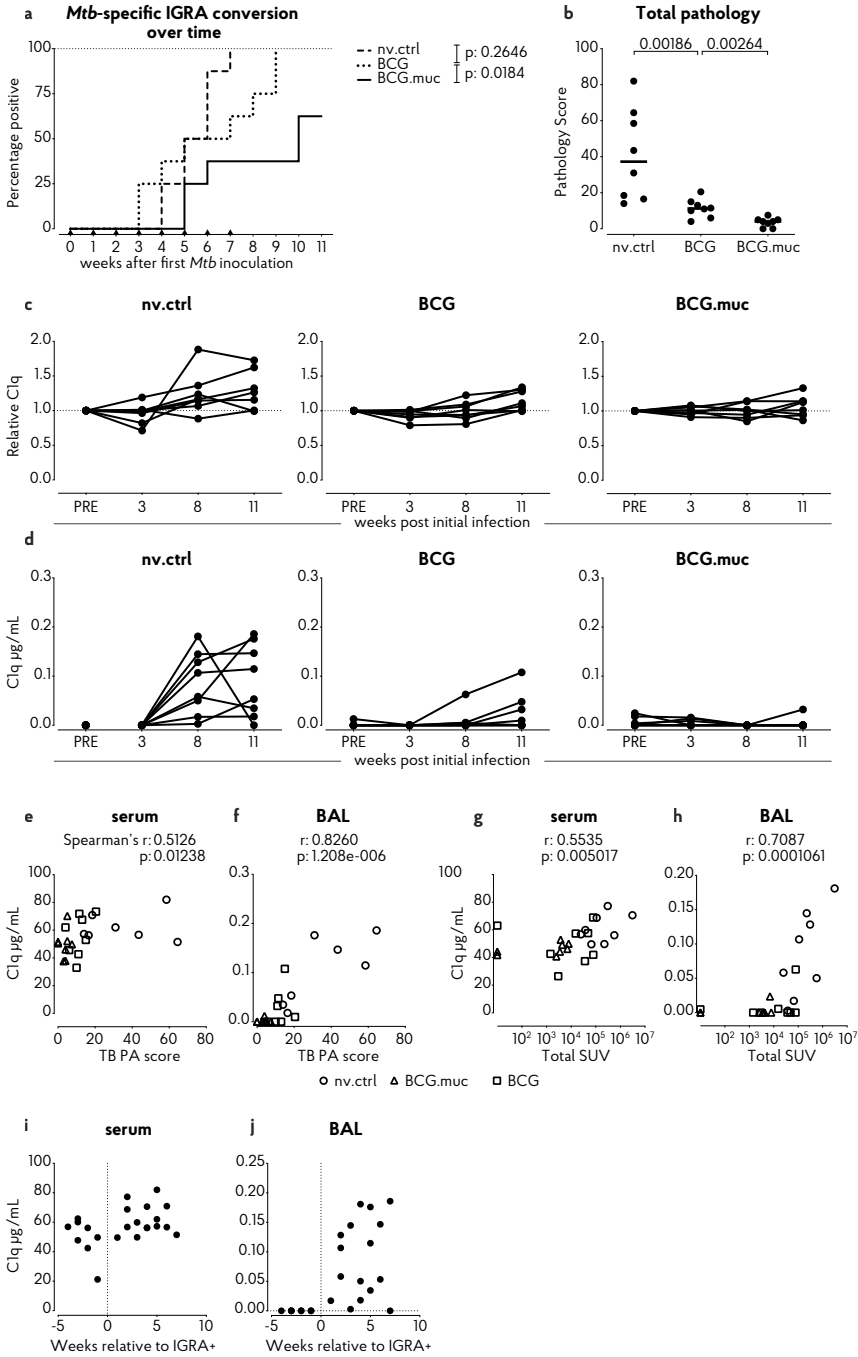
Considering the relatively low serum Clq levels in these animals after low dose *Mtb* challenge, we interrogated Clq at the site of infection by measuring Clq in BAL fluids collected at various timepoints post-infection. Prior to *Mtb* infection, Clq was virtually undetectable in BAL fluids from either species (**Supplemental Figure 1c**, right panel). However, from 3 to 6 weeks post-infection we observed a marked increase in Clq in the BALs of rhesus macaques (**Figure 3d**). In contrast, this marked increase in local Clq was absent in cynomolgus macaques (except for one animal with an (unexplained) outlier measurement at week 3). When comparing Clq values at 6 weeks post-infection and at study endpoint, increased Clq levels were observed in the rhesus but not the cynomolgus cohort (**Figure 3e**). As expected from the above findings, serum Clq levels did not correlate with TB disease scores (**Figure 3f**). But, when analyzing Clq expression in BAL 6 weeks post-challenge, we did find a statistically significant correlation with TB pathology (Spearman's rho = 0.599, $p = 0.005$, **Figure 3g**). Thus, also after low dose *Mtb* challenge and subsequent mild(er) TB disease, increasing Clq levels remain associated with disease progression and pathological involvement, albeit locally rather than peripherally.

Clq upregulation does not precede IGRA conversion

Having established that Clq is upregulated either peripherally and/or locally in association with various TB (challenge and) disease levels, we subsequently wanted to investigate if this increase in Clq could serve as a diagnostic marker of *Mtb* infection, with superior sensitivity to a conventional IFN γ Release Assay (IGRA). To address the diagnostic potential of Clq measurement, we profiled peripheral and local Clq levels in a challenge study in rhesus macaques in which we deployed a

- ◀ **Figure 3. Increase in local Clq in TB disease susceptible rhesus but not cynomolgus macaques.** Analysis of Clq levels in serum and broncho-alveolar lavage (BAL) fluid after low dose (1-7 CFU) *Mtb* challenge of rhesus and cynomolgus macaques (n=10 per species). **a**) Total tuberculosis pathology scores after *Mtb* infection of rhesus versus cynomolgus macaques. **b**) Relative levels of serum Clq over the course of *Mtb* infection for the two species. **c**) Species comparison of serum Clq concentration 6 weeks post-infection (p.i. left panel) and at endpoint, being either week 6 or week 12 post-infection by predefined study plan (right panel). **d**) BAL Clq levels over the course of *Mtb* infection for both species. **e**) Species comparison of BAL Clq levels 6 weeks post-infection (p.i) and at endpoint. Correlation of **f**) serum Clq and **g**) BAL Clq levels, both at 6 weeks post-infection and at endpoint, with total amount of tuberculosis pathology. Horizontal lines in **a**), **c**) and **e**) indicate group medians. Open symbols in **f**) and **g**) represent cynomolgus macaques; closed symbols rhesus macaques. Statistical significance of group differences determined by two sided Mann-Whitney. Correlations in **f**) and **g**) calculated with Spearman's rank-order test.





novel repeated limiting dose (RLD) *Mtb* challenge modality. In this RLD challenge model, we have demonstrated prevention of infection and disease after mucosal BCG vaccination (**Figure 4a&b**, previously published and further detailed in Dijkman et al (2019)²⁶, and depicted here only to provide relevant background).

As observed after single low dose infection, RLD *Mtb* challenge resulted in a modest increase in serum CIq over the course of the infection phase, in particular in non-vaccinated control animals, which, expectedly displayed the highest tuberculosis pathology levels at study end-point (**Figure 4c**). Animals protected from severe TB disease by prior BCG vaccination (by either standard intradermal or pulmonary mucosal route of administration) did not show any increase in relative serum CIq. Similarly, CIq is markedly increased in BAL fluids of the non-vaccinated control group, but not after prior BCG vaccination (with the exception of a few intradermally BCG vaccinated animals) (**Figure 4d**). Also in this study, we found BAL as well as serum CIq levels to statistically correlate with the level of TB pathology at endpoint, once more confirming CIq upregulation to be associated with disease development and severity rather than infection (**Figure 4e&f**). Along *Mtb* infection (rather than post mortem), disease severity can be assessed by means of PET-CT imaging, in which inflammation and metabolically active granulomas can be visualized using ¹⁸F-fluorodeoxyglucose (FDG) as a PET tracer³¹. To investigate whether CIq levels correlate with TB pathology as measured by PET-CT, we plotted summed lung and bronchoalveolar Standard Uptake Values (SUVs) obtained 8 weeks after initial challenge against CIq levels measured in serum and BAL collected at that same timepoint. Again, we found both serum and BAL fluid CIq concentrations to correlate significantly ($p < 0.05$) with PET-CT signals of TB pathology (Spearman's rho 0.554 and 0.709 respectively, **Figure 4g&h**).

We next set out to investigate if CIq upregulation preceded detection of *Mtb* infection by IGRA conversion and therefore aligned the CIq responses in the non-vaccinated control animals to their time point of IGRA conversion. As can be expected for a marker associated with progressive disease, we did not observe an increase in CIq prior to IGRA conversion, neither in serum nor in BAL (**Figure 4i&j**).

◀ **Figure 4. Infection-associated IGRA conversion precedes peripheral and local CIq increase.** Analysis of CIq levels in serum and broncho-alveolar lavage (BAL) fluid after repeated limiting dose (RLD) *Mtb* challenge of rhesus macaques that were either vaccinated by standard intradermal (BCG) or pulmonary mucosal (BCG.muc) BCG administration or left untreated (nv.ctrl). **a**) Rate of IGRA conversion after RLD *Mtb* challenge in vaccinated and non-vaccinated animals. **b**) Total tuberculosis pathology scores per treatment group after RLD *Mtb* challenge. CIq levels over the course of *Mtb* infection in **c**) serum and **d**) BAL fluid. Correlation between **e**) serum CIq and **f**) BAL CIq levels 11 weeks after the first exposure to *Mtb* and the total amount of tuberculosis pathology. Correlation between **g**) serum CIq and **h**) BAL CIq levels and total lung standard uptake values (SUV) as measured by PET-CT 8 weeks after initial *Mtb* challenge. **i**) Serum and **j**) BAL CIq levels of non-vaccinated control animals over time, aligned relative to IGRA conversion. Horizontal lines in **b**) indicate group medians. Statistical significance of group differences determined by two sided Mann-Whitney. Correlations in **e-h**) calculated with Spearman's rank-order test.



Not earlier than two weeks post-IGRA conversion local C1q levels were elevated over baseline. This observation further asserts the association of C1q with progressive, rather than latent or incipient, tuberculosis disease.

Pulmonary BCG vaccination increases local C1q production

C1q is considered to contribute to control of infection by enhancing phagocytosis of pathogens, either by opsonization and specific uptake or by activating phagocytes through engagement of C1q-binding receptors³². As we have previously found mucosal BCG to be superior over intradermal BCG in preventing TB infection and disease, we here investigated BCG's capacity to induce upregulation of C1q. We determined C1q in serum and BAL fluid from intradermal and mucosal BCG vaccinated animals from the repeated low dose challenge study described above and in **Figure 4**. Similar to what has been described for humans, BCG vaccination in rhesus macaques by either route of administration, does not lead to upregulation of serum C1q (**Figure 5a&b**). Interestingly, pulmonary, but not intradermal, BCG vaccination resulted in a marked increase in local C1q either 3 or 8 weeks after vaccination, to return to baseline levels by week 12 after vaccination (**Figure 5c&d**).

As we observed a local, but not peripheral, elevation of C1q levels, we hypothesized that local production of C1q could underlie the increase observed in the mucosally vaccinated animals. We sought to verify the possibility of local C1q production by *in vitro* stimulation of BAL cells versus Peripheral Blood Mononuclear Cells (PBMCs) from BCG vaccinated rhesus macaques (intradermal as well as mucosal), and from low dose *Mtb*-infected animals and untreated controls. Cells were incubated either with culture medium to assess *ex vivo* C1q production or with dexamethasone plus IFN γ (Dex/IFN γ), a positive control stimulus known to induce C1q release¹⁷, to assess the potency of these cells to produce C1q.

In PBMCs, a trend towards higher production by unstimulated PBMCs from vaccinated or *Mtb* infected animals (**Figure 5e**, left panel) was observed when compared to unvaccinated/ uninfected control animals. Prior BCG vaccination also seemed to potentiate C1q secretion of PBMCs, as reflected by the increase in C1q production in response to Dex/IFN γ stimulation in the vaccinees (**Figure 5e**, right panel). Locally, *ex vivo* C1q production was highest in unstimulated BAL cells of animals that were exposed to either mucosal BCG or *Mtb* (**Figure 5f**, left panel). After Dex/IFN γ stimulation, lower C1q production was observed in BCG vaccinated animals compared to non-vaccinated controls, potentially reflecting alterations in the cellular composition of the BAL (**Figure 5f**, right panel)²⁶. Collectively, our data show that pulmonary mycobacterial exposure can induce the production of local C1q, likely by resident alveolar macrophages.

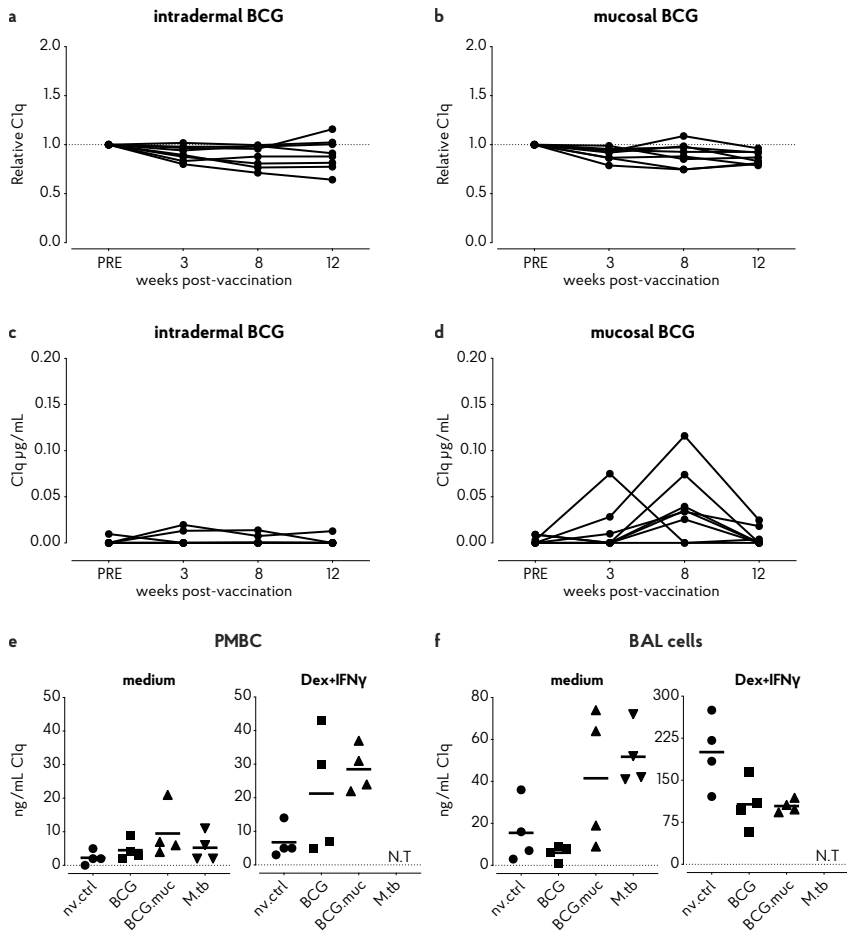


Figure 5. Pulmonary but not intradermal BCG vaccination results in upregulation of local production of CIq in rhesus macaques. a-d CIq levels in serum (a-b) and broncho-alveolar lavage (BAL) fluid (c-d) after BCG vaccination of rhesus macaques either through intradermal injection (BCG, a & c) or endobronchial instillation (BCG.muc, b & d). CIq production after stimulation with culture medium or dexamethasone plus interferon- γ (Dex+IFN γ) of e) PBMC and f) BAL cells, comparing from left to right non-vaccinated (nv.ctrl), standard BCG vaccinated, BCG.muc vaccinated, and low dose (15 CFU) *Mtb* infected rhesus macaques.

N.T = not tested. Horizontal lines in e & f indicate group medians.



Discussion

In this work, we show that increasing C1q levels in serum and BAL are associated with TB disease severity in various non-human primate TB studies. High C1q levels did not precede detection of *Mtb* infection by IGRA conversion, but did correlate with TB pathology after both high (500 CFU) and low (<10 CFU) dose *Mtb* challenge in different macaque species. Likewise, in a long-term follow up (up to 1 year) setting, we found increasing C1q levels to be associated with reduced survival. Contrarily to what has been described for serum C1q, increasing pulmonary C1q was not exclusive to infection with *Mtb*; pulmonary vaccination with BCG also resulted in a temporal increase of C1q in BAL fluid. Whether this local C1q production plays a role in protection against *Mtb* infection and disease remains to be investigated.

Our data demonstrates that, in addition to being a marker of active TB in humans, C1q can also serve as a marker of progressive disease in experimental *Mtb* infection studies in NHP. C1q levels measured after *Mtb* infection correlated with disease severity measured post-mortem, but also with disease severity measured during infection by PET-CT. As C1q can be readily measured over the course of *Mtb* infection, it could therefore be applied to monitor TB disease progression in a resource-limited setting. Especially in cynomolgus macaques, which are known to develop latent TB infection²⁴, measuring C1q at regular intervals after *Mtb* infection would be informative when assessing the occurrence and reactivation of LTBI. While the cohort of cynomolgus macaques measured in this study was not followed long enough to confirm the establishment of such a latent infection, the lack of C1q upregulation in the majority of this group might be indicative of TB latency development in these animals. As no post-infection increase in serum C1q could be observed after protective BCG vaccination, C1q can be used to assess efficacy along the infection phase when evaluating new drug or vaccine regimens in the NHP model.

Next to being a marker of progressive disease, it is tempting to speculate that C1q might also play a role in shaping the protective immune response observed after mucosal vaccination with BCG. Macrophages, including alveolar macrophages, express receptors, such as gC1qR and cC1qR (calreticulin), that can interact with either the globular head or collagen-like tail of C1q¹¹. Not only does binding of (pathogen-bound) C1q to these receptors improve pathogen uptake³², C1q-receptor interaction can also modulate macrophage inflammatory status and cytokine responses. Monocytes incubated with C1q have been described to produce higher amounts of anti-inflammatory IL-10³³, and it has been shown that C1q can polarize macrophages to an anti-inflammatory M2 phenotype, associated with the resolving of inflammation and tissue repair³⁴. After mucosal BCG vaccination we observed an increase in pulmonary C1q (**Figure 5b**), which coincides with increased PPD-specific IL-10 production by BAL cells²⁶. This increased IL-10 production in response to PPD is sustained up to several weeks after *Mtb* challenge, and might be required to counterbalance the inflammatory response induced by BCG/*Mtb*, to prevent

inflammation-induced damage³⁵. However, both IL10 production and M2 polarization have also been identified as detrimental in the context of *Mtb* infection^{36,37}, so the exact contribution of C1q to TB disease development remains to be elucidated. Lastly, C1q has the capacity to reduce production of IFN α ^{38,39}, which has been implied as detrimental in the (late phase) host immune response to *Mtb*^{40,41}. In addition to modulating innate immune responses, C1q has also been described in the regulation of adaptive immune responses, either indirectly through regulating APC function or through direct interaction with C1q-receptors expressed on T-cells. However, reports on the capacity of C1q to directly activate T-cells are contradictory and need further investigation^{42,43}. To fully appreciate the mechanistic role of C1q in shaping the protective immune response after mucosal BCG vaccination further research is required.

In summary, this work corroborates and extends on findings in human TB patients and links increased C1q levels with TB disease severity. It demonstrates that macaques can serve as informative model animals to study the role of (pulmonary) C1q in TB pathogenesis and/or protective immunity.

Acknowledgements

We would like to thank Richard Vervenne, Claudia Sombroek, Sam Hofman, Charelle Boot, and drs. Mohammed Khayum, Krista Haanstra and Michel Vierboom of BPRC's TB research group, as well as the BPRC's animal and veterinary care and pathology teams for their contributions to the studies included in this work.

Mycobacterium tuberculosis strain Erdman K01 (TMC107, NR-15404) was obtained through the NIH Biodefense and Emerging Infections Research Resources Repository, NIAID, NIH.

Non-human primate samples used in this study were banked from previous studies performed with financial support from Aeras or from the European Commission under the Framework Programme 7 project TRANSVAC, contract number 228403, governed by the European Vaccine Initiative (EVI, Heidelberg), and the Horizon2020 project TBVAC2020, contract number 643381, governed by the Tuberculosis Vaccine Initiative (TBVI, Lelystad).



Materials & Methods

Animals & Ethics

All housing and animal care procedures took place at the Biomedical Primate Research Centre (BPRC) in Rijswijk, the Netherlands. The BPRC is accredited by the American Association for Accreditation of Laboratory Animal Care (AAALAC) and is compliant with European directive 2010/63/EU as well as the “Standard for Humane Care and Use of Laboratory Animals by Foreign Institutions” provided by the Department of Health and Human Services of the US National Institutes of Health (NIH, identification number A5539-01). Before the start of each study ethical approval was obtained from the independent animal ethics committee (in Dutch: Dierexperimentencommissie, DEC), as well as BPRC’s institutional animal welfare body (in Dutch: Instantie voor Dierwelzijn, IvD).

Animals included in each study were screened negative for prior exposure to mycobacteria by means of tuberculin skin testing with Old Tuberculin (Synbiotics Corporation, San Diego, CA) and an IFN γ ELISPOT against Purified Protein Derivative (PPD) from *Mycobacterium bovis*, *Mycobacterium avium* (both Fisher Scientific, USA) or *Mycobacterium tuberculosis* (Statens Serum Institute, Copenhagen, Denmark).

For the duration of the study animals were socially housed (pair-wise) at animal biosafety level 3. Animal welfare was monitored daily. Macaques were provided with enrichment in the form of food and non-food items on a daily basis. Animal weight was recorded prior to each blood collection event. To limit possible discomfort due to severe TB disease humane endpoints were predefined. All animal handling and biosampling was performed under ketamine sedation (10 mg/kg, by intramuscular injection). When performing endobronchial challenge with *Mtb* or BAL, ketamine sedation was supplemented with intramuscular medetomidine (0.04 mg/kg) and an analgesic sprayed into the larynx. At the end of the study or when reaching a humane endpoint, animals were euthanized by intravenous injection of pentobarbital (200 mg/kg) under ketamine sedation. Veterinary staff and animal care-takers were blinded to animal treatment.

Mtb challenge

In all studies, animals were challenged with *Mycobacterium tuberculosis* Erdman K01 strain (BEI Resource, VA, USA). Every *Mtb* challenge occurred by endobronchial instillation, targeting the lower left lung lobe. All challenge events were executed in a single session within 2-3 hours from preparing the inoculum from frozen *Mtb* stock, challenging animals in random order. *Mtb* challenge dose, verified in each study by quality control plating, is indicated in the relevant results sections and figure legends.

Serum and BAL-fluid collection

Peripheral blood was collected in serum separator tubes by means of venipuncture. Tubes were spun for 10 minutes at 1000g to harvest cell-free serum, which was stored at -80°C pending further analysis. BAL was performed by targeting the lower left lung lobe by bronchoscope, followed by instillation and recovery of three times 20 mL prewarmed 0.9% saline solution. BALs were first passed over a 100 µm filter to remove mucus and debris, followed by centrifugation for 10 minutes at 400g. Supernatant was decanted and stored at -80°C pending further analysis. Serum and BAL fluid were filter-sterilized by centrifugation through 0.2 µm PVDF membrane plates (Fisher Scientific) before analysis.

Post-mortem pathology scoring

Post-mortem tuberculosis pathology was scored by a semi-quantitative grading system (adapted from⁴⁴) based on lesion size, manifestation and frequency, and lymph node involvement. Over time, from one to the other study, the scoring system has been adjusted slightly on minor details to more accurately describe disease manifestation, but the overall algorithm, as outlined in the paragraph below, has remained the same. When comparing disease severity between studies, pathology scores have been expressed as a percentage of the maximal possible score.

After euthanasia, the thoracic cavity, including the heart, ribcage, vertebrae and diaphragm were all macroscopically scored for the presence of granulomas and pleural adhesions. Lungs were isolated and lobes were separated from the trachea. Subsequently, lung lobes were cut in 5mm thick slices and scored for the amount of pathology. Lung draining lymph nodes were removed from the trachea and scored for size and extent of involvement. Extra-thoracic organs such as kidneys, spleen, pancreas and liver were macroscopically assessed for the presence of lesions. The “Total Pathology score” that is depicted throughout represents the summed score of all these organs.

C1q production by PBMC and BAL cells

To assess production of C1q by PBMC and BAL cells, freshly isolated cells were taken up in Roswell Park Memorial Institution 1640 medium (RPMI), supplemented with 10% Fetal Calf Serum (FCS), glutamine and penicillin/streptomycin. Cells were seeded at 200,000 cells per well in triplicate in 96-well round bottom plates and stimulated with 4 mg/mL dexamethasone (Merck) + 200 U/mL IFN γ (Peprotech, UK), or left untreated. Supernatants were harvested after 96 hours, pooled and filter-sterilized by centrifugation through 0.2 µm PVDF membrane plates (Fisher Scientific) before storage at -80°C and subsequent analysis by ELISA.



C1q ELISA

C1q levels in sera, BAL fluid and culture supernatants were measured using an in-house developed ELISA, as described previously¹⁸. In brief, 96-well Maxisorp plates (Nunc) were coated overnight with mouse anti-human C1q (Nephrology department, LUMC) in coating buffer (0.1 M Na₂CO₃, 0.1 M NaHCO₃, pH9.6). The next day, plates were washed with PBS/0.05% Tween and blocked with PBS/1%BSA. After subsequent washing, samples (serum diluted 1:4000, BAL fluid 1:1, culture supernatant 1:1) were added to the plates. A serially diluted pool of normal human serum (NHS) was taken along as a standard. Bound C1q was detected by incubation with rabbit anti-human C1q, followed by goat anti-rabbit HRP (both Dako) and ABTS substrate. C1q concentration is calculated in µg/mL from a human C1q standard.

Statistics

Statistical analyses were performed using Graphpad Prism, software version 7. Significance of differences between groups was calculated by two-sided Mann-Whitney testing. All correlations were calculated by Spearman's log rank testing.

References

1. World Health Organization. Global Tuberculosis report 2018 (World Health Organization, Geneva, Switzerland).
2. Walzl, G., *et al.* Tuberculosis: advances and challenges in development of new diagnostics and biomarkers. *The Lancet. Infectious diseases* **18**, e199-e210 (2018).
3. Pai, M. & Schito, M. Tuberculosis diagnostics in 2015: landscape, priorities, needs, and prospects. *The Journal of infectious diseases* **211 Suppl 2**, S21-28 (2015).
4. Scriba, T.J., *et al.* Sequential inflammatory processes define human progression from M. tuberculosis infection to tuberculosis disease. *PLoS pathogens* **13**, e1006687 (2017).
5. Cliff, J.M., *et al.* Distinct phases of blood gene expression pattern through tuberculosis treatment reflect modulation of the humoral immune response. *The Journal of infectious diseases* **207**, 18-29 (2013).
6. Jiang, T.T., *et al.* Serum amyloid A, protein Z, and C4b-binding protein beta chain as new potential biomarkers for pulmonary tuberculosis. *PLoS one* **12**, e0173304 (2017).
7. Wang, C., *et al.* Screening and identification of five serum proteins as novel potential biomarkers for cured pulmonary tuberculosis. *Sci Rep* **5**, 15615 (2015).
8. De Groote, M.A., *et al.* Discovery and Validation of a Six-Marker Serum Protein Signature for the Diagnosis of Active Pulmonary Tuberculosis. *Journal of clinical microbiology* **55**, 3057-3071 (2017).
9. Esmail, H., *et al.* Complement pathway gene activation and rising circulating immune complexes characterize early disease in HIV-associated tuberculosis. *Proceedings of the National Academy of Sciences of the United States of America* **115**, E964-e973 (2018).
10. Thielens, N.M., Tedesco, F., Bohlson, S.S., Gaboriaud, C. & Tenner, A.J. C1q: A fresh look upon an old molecule. *Molecular immunology* **89**, 73-83 (2017).
11. Bohlson, S.S., O'Conner, S.D., Hulsebus, H.J., Ho, M.M. & Fraser, D.A. Complement, c1q, and c1q-related molecules regulate macrophage polarization. *Front Immunol* **5**, 402 (2014).
12. Freeley, S., Kemper, C. & Le Friec, G. The "ins and outs" of complement-driven immune responses. *Immunological reviews* **274**, 16-32 (2016).
13. Ling, G.S., *et al.* C1q restrains autoimmunity and viral infection by regulating CD8(+) T cell metabolism. *Science (New York, N.Y.)* **360**, 558-563 (2018).
14. Lubbers, R., van Essen, M.F., van Kooten, C. & Trouw, L.A. Production of complement components by cells of the immune system. *Clin Exp Immunol* **188**, 183-194 (2017).
15. Castellano, G., *et al.* Maturation of dendritic cells abrogates C1q production in vivo and in vitro. *Blood* **103**, 3813-3820 (2004).
16. Faust, D. & Loos, M. In vitro modulation of C1q mRNA expression and secretion by interleukin-1, interleukin-6, and interferon-gamma in resident and stimulated murine peritoneal macrophages. *Immunobiology* **206**, 368-376 (2002).
17. van Schaarenburg, R.A., *et al.* The production and secretion of complement component C1q by human mast cells. *Molecular immunology* **78**, 164-170 (2016).
18. Lubbers, R., *et al.* Complement Component C1q as Serum Biomarker to Detect Active Tuberculosis. *Front Immunol* **9**, 2427 (2018).
19. Cai, Y., *et al.* Increased complement C1q level marks active disease in human tuberculosis. *PLoS one* **9**, e92340 (2014).
20. Kauffman, K.D., *et al.* Defective positioning in granulomas but not lung-homing limits CD4 T-cell interactions with Mycobacterium tuberculosis-infected macrophages in rhesus macaques. *Mucosal immunology* (2017).
21. Gautam, U.S., *et al.* In vivo inhibition of tryptophan catabolism reorganizes the tuberculoma and augments immune-mediated control of Mycobacterium tuberculosis. *Proceedings of the National Academy of Sciences of the United States of America* **115**, E62-e71 (2018).

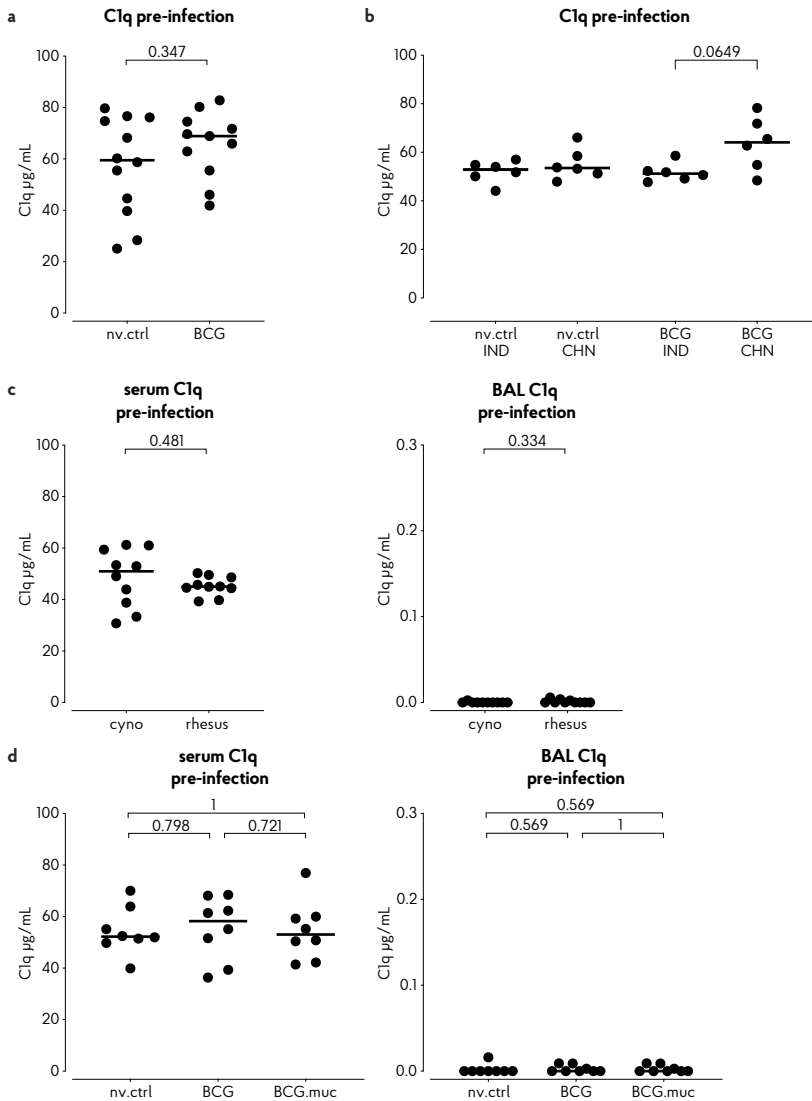


22. Hansen, S.G., *et al.* Prevention of tuberculosis in rhesus macaques by a cytomegalovirus-based vaccine. *Nature medicine* **24**, 130-143 (2018).
23. Verreck, F.A.W., *et al.* Variable BCG efficacy in rhesus populations: Pulmonary BCG provides protection where standard intra-dermal vaccination fails. *Tuberculosis (Edinburgh, Scotland)* **104**, 46-57 (2017).
24. Capuano, S.V., 3rd, *et al.* Experimental Mycobacterium tuberculosis infection of cynomolgus macaques closely resembles the various manifestations of human M. tuberculosis infection. *Infection and immunity* **71**, 5831-5844 (2003).
25. Scanga, C.A. & Flynn, J.L. Modeling tuberculosis in nonhuman primates. *Cold Spring Harbor perspectives in medicine* **4**, a018564 (2014).
26. Dijkman, K., *et al.* Prevention of tuberculosis infection and disease by local BCG in repeatedly exposed rhesus macaques. *Nature medicine* (2019).
27. Aguilo, N., *et al.* Pulmonary but Not Subcutaneous Delivery of BCG Vaccine Confers Protection to Tuberculosis-Susceptible Mice by an Interleukin 17-Dependent Mechanism. *The Journal of infectious diseases* **213**, 831-839 (2016).
28. Smith, D.G. & McDonough, J. Mitochondrial DNA variation in Chinese and Indian rhesus macaques (*Macaca mulatta*). *American journal of primatology* **65**, 1-25 (2005).
29. Fennelly, K.P., *et al.* Variability of infectious aerosols produced during coughing by patients with pulmonary tuberculosis. *American journal of respiratory and critical care medicine* **186**, 450-457 (2012).
30. Maiello, P., *et al.* Rhesus macaques are more susceptible to progressive tuberculosis than cynomolgus macaques: A quantitative comparison. *Infection and immunity* (2017).
31. White, A.G., *et al.* Analysis of 18FDG PET/CT Imaging as a Tool for Studying Mycobacterium tuberculosis Infection and Treatment in Non-human Primates. *Journal of visualized experiments : JoVE* (2017).
32. Galvan, M.D., Greenlee-Wacker, M.C. & Bohlson, S.S. Clq and phagocytosis: the perfect complement to a good meal. *Journal of leukocyte biology* **92**, 489-497 (2012).
33. Fraser, D.A., *et al.* Clq and MBL, components of the innate immune system, influence monocyte cytokine expression. *Journal of leukocyte biology* **80**, 107-116 (2006).
34. Benoit, M.E., Clarke, E.V., Morgado, P., Fraser, D.A. & Tenner, A.J. Complement protein Clq directs macrophage polarization and limits inflammasome activity during the uptake of apoptotic cells. *Journal of immunology (Baltimore, Md. : 1950)* **188**, 5682-5693 (2012).
35. Gupta, N., Agrawal, B. & Kumar, R. Controlling inflammation: a superior way to control TB. *Immunotherapy* **8**, 1157-1161 (2016).
36. Lastrucci, C., *et al.* Tuberculosis is associated with expansion of a motile, permissive and immunomodulatory CD16(+) monocyte population via the IL-10/STAT3 axis. *Cell research* **25**, 1333-1351 (2015).
37. Redford, P.S., Murray, P.J. & O'Garra, A. The role of IL-10 in immune regulation during M. tuberculosis infection. *Mucosal immunology* **4**, 261-270 (2011).
38. Lood, C., *et al.* Clq inhibits immune complex-induced interferon-alpha production in plasmacytoid dendritic cells: a novel link between Clq deficiency and systemic lupus erythematosus pathogenesis. *Arthritis and rheumatism* **60**, 3081-3090 (2009).
39. Santer, D.M., *et al.* Clq deficiency leads to the defective suppression of IFN-alpha in response to nucleoprotein containing immune complexes. *Journal of immunology (Baltimore, Md. : 1950)* **185**, 4738-4749 (2010).
40. Manca, C., *et al.* Virulence of a Mycobacterium tuberculosis clinical isolate in mice is determined by failure to induce Th1 type immunity and is associated with induction of IFN-alpha /beta. *Proceedings of the National Academy of Sciences of the United States of America* **98**, 5752-5757 (2001).
41. Stanley, S.A., Johndrow, J.E., Manzanillo, P. & Cox, J.S. The Type I IFN response to infection with Mycobacterium tuberculosis requires ESX-1-mediated secretion and contributes to pathogenesis. *Journal of immunology (Baltimore, Md. : 1950)* **178**, 3143-3152 (2007).

42. West, E.E., Kolev, M. & Kemper, C. Complement and the Regulation of T Cell Responses. *Annual review of immunology* **36**, 309-338 (2018).
43. Clarke, E.V. & Tenner, A.J. Complement modulation of T cell immune responses during homeostasis and disease. *Journal of leukocyte biology* **96**, 745-756 (2014).
44. Lin, P.L., et al. Quantitative comparison of active and latent tuberculosis in the cynomolgus macaque model. *Infection and immunity* **77**, 4631-4642 (2009).

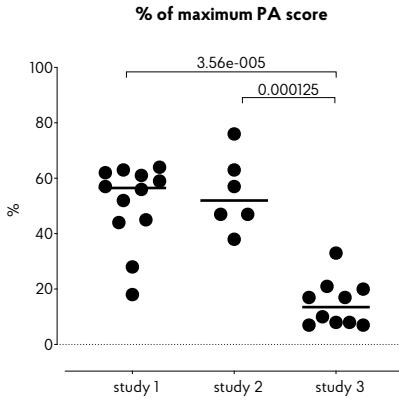


Supplemental data



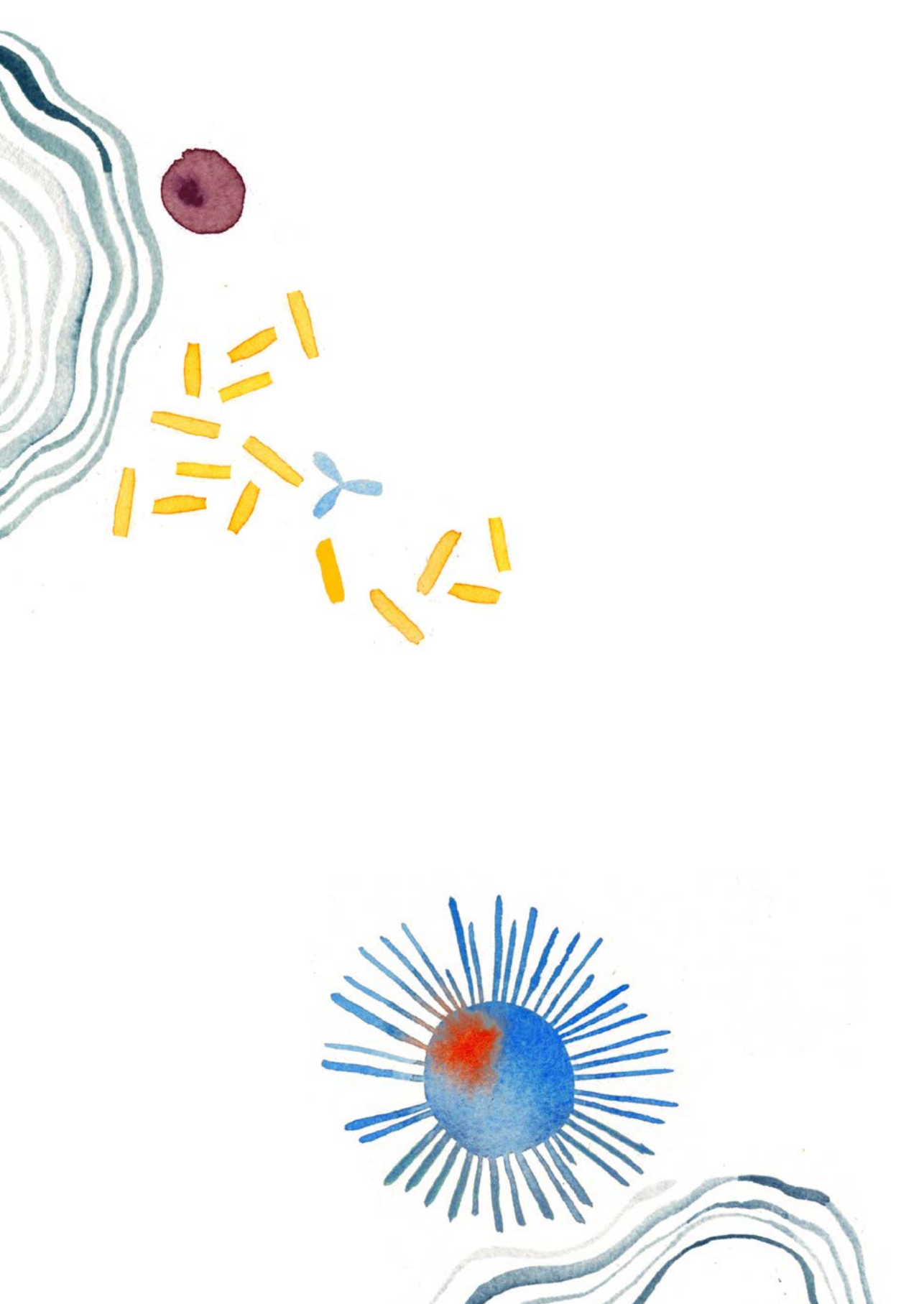
Supplemental figure 1. Pre-infection C1q levels for each study. C1q levels before infection with *Mtb* for each of the cohorts described in the main body text. **a)** Pre-infection serum C1q levels per treatment group from the high-dose *Mtb* challenge with long (1 year) follow-up described in **Figure 1.** **b)** Idem from the high-dose *Mtb* challenge study with short (3 months) follow-up described in **Figure 2.** **c)** Pre-infection serum (left panel) and BAL C1q levels (right panel) from the low dose *Mtb* challenge study described in **Figure 3.** **d)** Idem from the repeated limiting dose *Mtb* challenge study described in **Figure 4.**

Horizontal lines in a-d indicate group medians. Statistical significance of group differences determined by two sided Mann-Whitney.



Supplemental figure 2. Comparison of TB associated pathology after high and low dose *Mtb* challenge. Pathology (expressed as percentage of the maximal possible score) measured at endpoint after high dose *Mtb* challenge (500 CFU), long-term follow up (study 1), high dose, short-term follow up (study 2) and low dose (<10 CFU), short-term follow up (study 3). Horizontal lines indicate group medians. Statistical significance of group differences determined by two sided Mann-Whitney.





General discussion and future perspectives



Synopsis

To this day, tuberculosis remains a complex global health problem, the elimination of which is hindered by knowledge gaps related to protective immunity and diagnosis. In an effort to address these knowledge gaps, this thesis utilized the non-human primate model of tuberculosis to investigate protective and pathogenic immune responses after vaccination and *Mtb* infection, as well as the dynamics of a potential biomarker of active TB disease.

In **Chapter 2**, by applying a dose-escalation study design, we showed that rhesus and cynomolgus macaques are not dissimilar in their susceptibility to infection. However, also at low challenge doses, cynomolgus macaques remained more resistant to the development of TB pathology than rhesus macaques. We used this differential disease susceptibility to characterize early and local immune responses that may underlie disease development and resistance. An early, local proinflammatory innate immune response was observed in cynomolgus macaques, while rhesus macaques presented with increased expression of markers associated with immune suppression. We could not identify cellular or humoral adaptive immune responses that differed between the two species.

In **Chapter 3**, we built upon the observation from **Chapter 2** that administration of 1 CFU of *Mtb* resulted in infection in a subset of exposed animals. Intradermal or pulmonary BCG vaccinated rhesus macaques were subjected eight times to this limiting infectious dose to investigate whether we could assess vaccine-mediated prevention of infection, in addition to (partial) prevention of disease. We observed that pulmonary BCG vaccination was superior to intradermal BCG in preventing both infection and disease. This enhanced protection correlated with the induction of local, polyfunctional, IL17A producing T-cells and IL-10 production.

In **Chapter 4**, we evaluated whether the correlates of protection identified in **Chapter 3**, would also be elicited by mucosal administration of MTBVAC, a live attenuated, *Mtb*-derived TB vaccine. Like BCG, MTBVAC was found to induce local IL10 production and IL17A producing T-cells. These antigen-specific IL17A-producing T-cells were profiled more in depth, and we showed that cytokine-producing T-cells induced by vaccination display a distinct tissue-residency phenotype and express more mucosal homing markers. Cytokine producing T-cells induced by *Mtb* infection lacked this phenotype. Antibodies induced by both mucosal vaccination with BCG and MTBVAC were able to bind live *Mtb* and enhance pathogen uptake by phagocytes.

In **Chapter 5**, we utilized biosamples of the studies described in **Chapter 2** and **Chapter 3**, as well as studies performed in the past to assess the association of complement component C1q with TB disease severity. As observed in patients, C1q levels in serum were increased in animals with more TB pathology. In macaques, C1q levels correlated with the amount of pathology assessed post-mortem or by PET-CT imaging. Elevated C1q levels were detected from 6 weeks post-infection onward. An increase in C1q levels in BAL fluid and C1q production by BAL cells could be observed in *Mtb* infected, but also pulmonary BCG vaccinated animals.

New correlates of vaccine-mediated protection: dependent on time and space?

When considering vaccine-mediated protection from tuberculosis, historically, T-helper type 1 responses were thought to be sufficient for protection. However, a number of recent findings, including the work described in this thesis, have contributed to a reconsideration of this dogma¹⁻⁴. In **Chapter 3**, we specifically identified pulmonary IL-17A, IL-10 and antibodies as associated with protection from infection and disease, as conferred by mucosal BCG vaccination. In **Chapter 4**, we reconfirmed the induction of this immune signature by mucosal BCG and show that mucosal vaccination with MTBVAC elicits a similar immune-response, more rapidly and at a higher magnitude.

Interleukin-17A

Of the immune parameters profiled in **Chapter 3**, the frequency of pulmonary IL-17A+ CD4 T-cells correlated most strongly with the protection observed after mucosal BCG vaccination. These Th17A cells could still be observed in vaccinated animals after repeated *Mtb* exposure, while infection with *Mtb* on its own did not lead to the induction of significant levels of IL-17A+ CD4 T-cells, neither in the repeated limiting dose study described in **Chapter 3**, nor the dose escalation study performed in rhesus and cynomolgus macaques in **Chapter 2**. However, in both studies immune-profiling was limited to a maximum of 3 months after infection. As other NHP infection studies have reported the presence of IL-17 producing T-cells in granulomas of animals sacrificed 6 to 8 months after infection^{5,6}, it seems that while *Mtb* is capable of inducing Th17A cells, it does so at a delayed rate compared to the Th1 response.

The effector mechanisms of IL-17A are diverse, and its production could therefore contribute to protection from TB in a number of ways. Ligation of IL-17A with its receptor, expressed on a wide range of cells, including pulmonary epithelial cells and innate immune cells⁷, leads to the mounting of a proinflammatory response, by production of granulopoietic factors and recruitment of neutrophils⁸. The role of neutrophils in *Mtb* infection is dual in nature^{9,10}. By phagocytosis, secretion of antimicrobial factors and facilitation of T-cell priming, neutrophils can contribute to effective host-defense after infection with *Mtb*. Studies suggest that especially early after infection neutrophils may play a critical role in protection¹¹. Local IL-17A production might therefore facilitate protection by early recruitment of neutrophils to the site of infection. However, neutrophils have also been implicated in tissue destruction and dissemination of *Mtb*. An enhanced neutrophil response would require careful regulation, perhaps mediated by IL-10, which we find upregulated locally after protective mucosal vaccination (see **New correlates of vaccine-mediated protection: Interleukin-10**).



Additionally, there is evidence that IL-17 is involved in the establishment of protective tissue resident memory T-cells (Trm). In a mouse model of *Klebsiella pneumoniae*, pulmonary vaccination with heat-killed bacteria resulted in a population of CD4⁺ tissue resident memory T-cells, which were derived from Th17 cells and involved in bacterial clearance¹². After mucosal vaccination with BCG and MTBVAC, but not *Mtb* infection, we also observed the induction of CD4⁺ Trm (**Chapter 4**), which might similarly contribute to clearance of *Mtb*^{13,14}. Whether these Trm also arose from Th17A cells remains to be established, but it might explain the lack of Trm cell observed after *Mtb* infection. Lastly, IL-17A plays an important role in the formation of inducible bronchus-associated tissue (iBALT), which has also been associated with protection (see **The pulmonary mucosa in anti-TB immunity: iBALT section**)^{15,16}.

IL17A has been associated with protection in prior preclinical TB studies. In mice, a lack of IL-17A impaired granuloma maturation, abolished the protective effect of mucosal BCG vaccination and abrogated protection against hypervirulent *Mtb*¹⁷⁻¹⁹. Control of *Mtb* infection in cynomolgus macaques was associated with upregulation of genes related to the Th17 response²⁰. However, in a second study, granulomas of latently infected cynomolgus macaques at high risk of disease reactivation contained more IL17A producing T-cells⁶. Also in humans, the role of IL17A in protective immunity to *Mtb* remains ambiguous²¹. For example, while IL17 expressing T-cells were found to be increased in healthy, *Mtb* exposed individuals compared to TB patients, no increased *Mtb* infection or reactivation was seen in patients receiving IL17A-neutralizing antibodies for the treatment of psoriasis^{22,23}. Therefore, the precise role of IL17A in vaccine-mediated protection from TB remains to be defined.

Interleukin-10

As another correlate of protection, we identified the production of IL-10, a cytokine typically associated with immunosuppression, by BAL cells in response to PPD. In the context of *Mtb* infection and disease, immunosuppression in general is considered to be detrimental to the host. The higher frequencies of circulating CD163⁺MerTK⁺ non-conventional monocytes, known producers of IL-10²⁴, observed in disease-susceptible rhesus compared to disease-resistant cynomolgus macaques, supports this notion (**Chapter 2**). This population of monocytes has also been found to be increased in the peripheral blood and pleural effusion of TB patients, and, functionally, CD163⁺MerTK⁺ monocytes have been shown to be permissive for *Mtb* infection and less capable of stimulating T-cell responses²⁵.

As the archetypical immunosuppressive cytokine, the role of IL-10 in *Mtb* infection is generally considered to be disadvantageous. Indeed, increased levels of IL-10 are observed in the lung of and serum of TB patients^{26,27}, and knocking-out or neutralizing IL-10 signaling in experimental mouse models of infection reduced disease^{28,29}. In cynomolgus macaques, neutralization of IL-10 during the course of an 8-week *Mtb* infection, altered granuloma structure and early cytokine production. However, this

did not affect overall disease burden, though computational modelling performed on the data suggested an effect of IL-10 neutralization in bacterial control during long-term infection³⁰.

Nonetheless, IL-10 might also play a beneficial role during *Mtb* infection. Of note, we detected high levels of local, PPD-specific IL-10 production after pulmonary vaccination with live attenuated mycobacteria (**Chapter 3** and **Chapter 4**), which levels correlated positively with protection (**Chapter 3**). Though this correlation was no longer present after *Mtb* challenge, local IL-10 production remained increased in mucosal BCG vaccinated animals compared to non-vaccinated controls (**Chapter 3**).

The flow cytometric analysis in **Chapter 4** suggests that T-cells are not the major source of the IL-10 production observed after protective mucosal vaccination. Intriguingly, research in mice points to the source of IL-10 as important in *Mtb* pathogenesis; knocking-out IL-10 production by T-cells, but not monocytes/macrophages, reduced *Mtb* bacterial load³¹. Another study identified monocyte derived IL-10 as required for the induction of tissue-resident CD8⁺ T-cells by intravenous vaccination of rhesus macaques with HIV peptides³². Combining these two findings with the observation that, after mucosal vaccination with attenuated mycobacteria, tissue-resident CD4⁺ T-cells are increased (**Chapter 4**), suggests that innate IL-10 signaling might be underlying the induction of these T-cells.

Additionally, the production of IL-10 could be induced as a mechanism to limit bystander damage as a result of the pro-inflammatory Th17A cells, as described for autoimmune diseases and here induced by pulmonary vaccination³³. In the context of *Mtb* infection, limiting inflammation has been proposed as a strategy to prevent disease. Though the data in **Chapter 2** suggests that an early, local inflammatory response, as seen in disease-resistant cynomolgus macaques, is beneficial to the host, chronic inflammation due to persistent *Mtb* infection has been linked to disease progression and pathology³⁴. Fitting with that idea is the observation that TNF α acts as a double-edged sword during *Mtb* infection; important for host-protection, but pathogenic in excess quantities^{35,36}. Immunosuppression could therefore represent a host-strategy to prevent damage when elimination of the pathogen is unsuccessful³⁷. Reports of TB reactivation after treatment of cancer with checkpoint-inhibitors, such as anti-Programmed cell Death protein 1 (PD-1), in the treatment of cancer, support this notion^{38,39}.

Antibodies

Lastly, we observed the induction of antibodies in the lung after pulmonary mucosal but not intradermal vaccination. TB vaccine development has focused on the induction of a cellular immune response, as historic data on the role of the humoral immune response in TB has been conflicting⁴⁰. Also in our study, pulmonary antibody levels did not statistically correlate with the level of protection observed. However, recent studies have demonstrated a number of ways in which antibodies could contribute to vaccine-mediated protection⁴¹. In **Chapter 4** we show that



vaccine-induced antibodies in BAL fluid can bind to live *Mtb*, and that binding of IgG and IgM correlated with enhanced *Mtb* phagocytosis after incubation with BAL fluid. A similar effect of antibodies on pathogen uptake has been observed previously; incubation of BCG with serum from BCG vaccinated individuals increased phagocytosis and resulted in reduced intracellular growth⁴². IgG purified from the serum of latently infected individuals was also able to restrict intracellular growth and could promote antibody-dependent cellular cytotoxicity of PPD-pulsed cells⁴³. Furthermore, *Mtb* specific antibodies have been reported to enhance cellular immune responses⁴⁴. Observations from cohort studies further support a protective role for antibodies in *Mtb* infection^{45,46}.

However, despite this evidence of a protective role for antibodies, other reports suggest a redundant or even pathogenic role for humoral immune responses. For example, in our studies *Mtb* infection in macaques also induced pulmonary antibodies to a similar extent as mucosal vaccination (**Chapter 2** and **Chapter 3**), and monoclonal IgG, but not IgA, from TB patients has been reported to actually promote *Mtb* growth in lung epithelial cells⁴⁷.

Nevertheless, antibodies do have the potential to contribute to vaccine-mediated protection. By targeting both cellular and humoral immunity in TB vaccination a synergistic effect could be achieved, with pulmonary antibodies mediating early control of infection, for instance by enhancing phagocytosis and subsequent killing of infected macrophages, until cellular immunity has been initiated. The exact characteristics for a protective humoral immune response require further elucidation, and likely depend on antibody specificity, isotype and glycosylation pattern^{48,49}.

As discussed above, IL-17A, IL-10 and antibodies have each been linked to both protective as well as pathogenic effects in the context of *Mtb* infection, as seems to be the case with many BCG/*Mtb* induced immune responses. To which extent these immune-responses contribute to protection is therefore presumably dependent on factors such as time, spatial organization, magnitude and antigen specificity. The unravelling of these factors would require further mechanistic studies.

The pulmonary mucosa in anti-TB immunity

All new TB vaccines currently in clinical trials are administered parenterally. However, the immune-signature associated with superior protection as identified in **Chapter 3**, was specifically induced by pulmonary vaccination. The study performed in **Chapter 4** confirms this observation; while intradermal vaccination with BCG or MTBVAC did lead to a pulmonary Th1 response, though less pronounced, local IL-17A, IL-10 and IgA were either not detected or observed at a significantly lower magnitude. Together, these findings suggest a role for the pulmonary mucosa in the establishment of these immune responses as well as protection.

Alveolar macrophages

Alveolar macrophages are the predominant immune-cells populating the lung lumen⁵⁰. As sentinels of the pulmonary space, they play an essential role in tissue homeostasis by removing cellular debris and innocuous inhaled material in a tolerogenic manner^{51,52}. However, they are also capable of mounting strong proinflammatory responses when encountering pathogenic agents, as evident by the production of TNF α , IL-6 and IL-1 β by BAL cells in response to *Mtb* whole cell lysate (**Chapter 2**), and the magnitude of this proinflammatory responses appears to associate with protection from disease (**Chapter 2**).

Alveolar macrophages are typically characterized as poor antigen presenting cells⁵³, though data suggests that under proinflammatory conditions they can acquire the ability to induce lymphoproliferation⁵⁴. While we did not profile pulmonary responses early after mucosal vaccination, administration of live attenuated mycobacteria might similarly induce an inflammatory response and promote local lymphoproliferation by alveolar macrophages, potentially underlying the increase in T-cell numbers observed after mucosal BCG (**Chapter 3**).

Though the role of alveolar macrophages in priming T-cell responses in these studies needs further investigation, they are the likely source of the prominent IL-10 production observed after mucosal vaccination (**Chapter 3** and **Chapter 4**), in agreement with their role in balancing inflammation⁵². Besides preventing inflammation induced damage by mucosal vaccination, this IL-10 production might underlie the induction of tissue resident T-cells, as discussed earlier under the section **Correlates of vaccine-mediated protection – IL-10**. Complement component Iq, of which local production is observed after pulmonary BCG vaccination (**Chapter 5**), might similarly shape adaptive immune responses after vaccination, either by influencing APC function or through direct interaction with C1q-receptors expressed on T-cells^{55,56}.

Besides modulation of adaptive immune responses, alveolar macrophages might also contribute to protection directly. By epigenetic reprogramming, innate immune cells can be “trained” to more effectively exert their effector functions upon pathogen-encounter⁵⁷. A recent report shows that alveolar macrophages are also amenable to this training⁵⁸. These trained alveolar macrophages expressed higher levels of class II MHC molecules and responded more rapidly to an unrelated bacterial infection, resulting in a more favorable outcome. As peripheral BCG vaccination is known to lead to training of peripheral monocytes, mucosal BCG might similarly induce training of alveolar macrophages⁵⁹.

Upon exposure, alveolar macrophages are permissive to *Mtb* infection, and actually facilitate dissemination of infection⁶⁰. Potentiating *Mtb* control by alveolar macrophages through vaccination, either via trained immunity or early T-cell help, could represent a strategy to prevent productive *Mtb* infection. Further research, such as *in vitro* infection assays or adoptive transfer of BCG-exposed alveolar macrophages, is required to assess the contribution of alveolar macrophages in the control of *Mtb* in more detail.



Inducible Bronchoalveolar Lymphoid Tissue

The minimal IL-17A production in lung draining lymph nodes after mucosal vaccination (**Chapter 4**), could indicate that establishment of memory T-cells occurs elsewhere, potentially in vaccination induced tertiary lymphoid follicles in the lung, also known as inducible bronchus-associated lymphoid tissue (iBALT)⁶¹. Fully matured iBALT contains germinal-center (GC)-like structures, and is capable of supporting lymphocyte recruitment, priming, and proliferation^{62,63}. iBALT is not only ideally placed to initiate a rapid recall response to invading pathogens, these responses have also been described as less pathogenic⁶². While we did not assess iBALT formation after mucosal BCG vaccination, the presence of iBALT after pulmonary BCG has been reported previously⁶⁴.

The induction of iBALT has been associated with protection in experimental models of *Mtb* infection. Pulmonary vaccination of rhesus macaques with an attenuated, *Mtb* Δ sigH mutant resulted in enhanced iBALT formation compared to administration of wild-type *Mtb*, and reduced disease and bacterial burden after challenge⁶⁴. In this study, pulmonary BCG vaccination induced little iBALT formation and conferred limited protection. However, the BCG dose applied here was at least a 100-fold lower compared to the study in **Chapter 3**, and BCG CFU recovered from the lung post-vaccination remained significantly lower compared to *Mtb* Δ sigH, suggesting a role for dose in pulmonary BCG immunogenicity and the amount of protection conferred. Also in mice, by promoting early macrophage activation, lymphoid follicle formation post mucosal vaccination contributed to protection^{15,65}.

Induction of iBALT by pulmonary BCG vaccination might have similarly established a reservoir of *Mtb*-reactive T-cells, that are poised to rapidly interact with *Mtb* infected macrophages, rather than requiring recruitment from the periphery. The presence of lung tissue-resident memory T-cells after pulmonary BCG or MTBVAC administration (**Chapter 4**) seems to support this notion.

Other local factors influencing vaccine immunity

Besides alveolar macrophages, other cells present at the pulmonary mucosa could be involved in shaping the vaccination-induced immune response and protection.

While alveolar macrophages are the most prevalent phagocytes in the lung lumen, the lung interstitium is populated by interstitial macrophages, which are phenotypically and functionally distinct from alveolar macrophages⁶⁶. Though interstitial macrophages are involved in the immune response to *Mtb*⁶⁷⁻⁶⁹, they have not been extensively studied in the context of TB vaccination. An early study did observe an increase in interstitial macrophages in the lung of pulmonary BCG vaccinated mice, but these cells were found to be poor inducers of T-cell responses⁷⁰. The influence of interstitial macrophages on immunity after pulmonary vaccination would require investigation through mechanistic studies, for instance by selective depletion of these macrophages.

Recently, it has been shown that the induction of IL17A production by T-cells is dependent on cleavage of DC-derived CXCL8 by neutrophil elastase⁷¹. BCG mediated neutrophil recruitment to the pulmonary space could therefore have contributed to the induction of these pulmonary Th17 cells⁷². However, reports indicate similar neutrophil recruitment and drainage to the lymph nodes after intradermal BCG vaccination as well as lung neutrophilia after *Mtb* infection⁷³⁻⁷⁵. Why the presence of neutrophils in these circumstances does not result in the induction of Th17 responses in our model is unknown.

Another, perhaps less obvious, cell population involved in lung immunity are the alveolar epithelial cells (AECs). AECs are the major constituents of the pulmonary epithelial lining and involved in a variety of processes, such as the production of surfactants, fluid transportation and tissue repair, but also the initiation and shaping of pulmonary immune responses⁷⁶⁻⁷⁸. There are two types of AECs (Type I and Type II), but these have often been studied as a mixture in the context of BCG/*Mtb* immunity. Nevertheless, AECs have been shown to be able to phagocytose BCG, function as APCs and produce chemokines after incubation with TLR-ligands or heat-killed BCG, all suggestive of a potential immunomodulatory role after pulmonary BCG vaccination^{78,79}.

Finally, the enhanced efficacy of pulmonary BCG might not be mediated by cellular factors alone. Incubation of BCG with alveolar lining fluid prior to vaccination enhanced T-cell responses and protection, by partial removal of inhibitory cell wall components⁸⁰, a process potentially replicated during pulmonary mucosal vaccination.

Regardless of the mechanisms involved, multiple studies have demonstrated the superior potential of pulmonary over intradermal BCG vaccination to protect from TB (**Table 1**). Also, while prior NTM exposure abrogated protection conferred by intradermal BCG, it does not influence pulmonary BCG-mediated protection⁸¹. There are, however, also a number of studies where pulmonary BCG did not result in superior protection (**Table 1**), raising questions about the most appropriate way to administer live attenuated vaccines to the pulmonary mucosa, the dose delivered required for protection and the duration of protection. Head to head comparison of different mucosal delivery modalities (endobronchial, aerosol, intranasal) and vaccine doses in an experimental model of TB, such as the macaque, could help formulate the requirements for protective pulmonary vaccination and inform the design of such vaccination strategies in the clinic.



Model species	Mode of pulmonary vaccination	BCG strain & dose	Time to challenge	Protection compared to intradermal / subcutaneous BCG	Ref.
<i>Studies demonstrating superior protection by pulmonary BCG</i>					
Mouse	Intranasal	Connaught, 5×10^5 CFU	3 months	Decreased bacterial load in lung and spleen	82
Mouse	Intratracheal	Danish, 5×10^5 CFU	2 months	Decreased bacterial load in lung	13
Mouse	Intranasal	Danish, 2×10^5 CFU	6 weeks	Decreased bacterial load in lung	83
Mouse	Intranasal	Danish, 1×10^6 CFU	2 months	Decreased bacterial load in lung and spleen, increase in survival	17
Mouse	Intranasal	Pasteur, 5×10^5 CFU	2-4 months	Decreased bacterial load in lung and spleen	84
Guinea pig	Aerosol	Pasteur, 1×10^5 CFU	11 weeks	Decreased bacterial load in lung	85
Guinea pig	Aerosol	Pasteur, 1×10^5 CFU	unknown	Decreased bacterial load and pathology in lung	86
Rhesus macaques	Aerosol	unknown, 8×10^5 CFU	2 months	Decreased bacterial load and pathology in lung and lung draining lymph nodes,	87
Rhesus macaques	Endobronchial	Danish, 2.8×10^5 CFU	17 weeks	Decreased bacterial load in lung	88
Rhesus macaques	Endobronchial	Sofia, 2.8×10^5 CFU	3 months	Decreased bacterial load and pathology in lung and draining lymph nodes, delay in IGRA conversion	89
<i>Studies demonstrating no superior protective effect of pulmonary BCG</i>					
Mouse	Aerosol	CSL, 1×10^3 CFU	14 weeks	Similar numbers of bacteria in lung and spleen	90
Mouse	Intranasal	Pasteur, 1×10^5 CFU	22 weeks	Similar numbers of bacteria in lung and spleen	91
Mouse	Intranasal	Pasteur, 5×10^5 CFU	2-10 months	Similar numbers of bacteria in lung, though a decreased bacterial load in spleen	84
Rhesus macaques	Aerosol	Danish, 5×10^7 CFU	6-10 months	Similar amount of pathology and bacterial load in lung and draining lymph nodes, and extrathoracic organs	92

Table 1. Preclinical studies comparing, head to head, the protective efficacy of intradermal or subcutaneous versus pulmonary BCG vaccination after *Mtb* challenge.

The future of the macaque model in tuberculosis research

The macaque model of TB is the central pillar that supports the research in this thesis. Over the decades, modelling tuberculosis in macaques has evolved significantly, from the application of high dose challenge to experimental infection with doses as low as a single bacterium (**Chapter 2** and **Chapter 3**), and going beyond straightforward assessment of vaccine efficacy towards addressing more fundamental questions^{87,93-96}. This refinement of the macaque model, combined with promising efficacy results and several technological advancements, such as PET-CT imaging, support the use of macaques in future TB research.

Novel vaccine-mediated signals of protection in the macaque

Up until recently, vaccine-evaluation studies in rhesus macaques have demonstrated reduction of TB disease only, rather than full protection or even prevention of infection, raising the question of whether the model might be too stringent. However, two recent studies in rhesus macaques, together with the study described in **Chapter 3**, show that it is possible to elicit PoD and even Pol in this species. After subcutaneous vaccination with a cytomegalovirus vector containing nine different TB antigens, TB pathology after low dose (10-25 CFU) *Mtb* challenge could be prevented in 41% of animals⁹⁷. By applying a repeated limiting dose challenge model, we could demonstrate 25% PoD and signals of Pol after mucosal BCG vaccination; a significant delay in IGRA conversion compared to non-vaccinated controls and complete absence of disease in one of the IGRA- animals⁹⁹. Lastly, intravenous administration of BCG was able to establish complete protection from TB in 60% of vaccinated animals⁹². These encouraging findings facilitate the identification of vaccine-induced mechanisms and correlates of protection, for translation into vaccine design and efficacy-monitoring.

Back-translation of clinical findings to the macaque

In addition to these promising signals in the macaque, novel signals of protection obtained in two clinical vaccine evaluation trials offer the opportunity for back-translation into the macaque model. In a phase 2 trial, revaccination of BCG-vaccinated adolescents with BCG or H4:IC31 was shown to reduce *Mtb* infection, as measured by a reduction in sustained Quantiferon conversion⁹⁸. In a post-exposure trial, vaccination of with M72/AS01_E reduced the incidence of pulmonary tuberculosis in IGRA+ individuals by 50%⁹⁹. While other vaccination strategies have been applied as a booster to prior BCG^{100,101}, revaccination of macaques with BCG itself has not been reported so far. Similarly, to date, vaccine efficacy in macaques has always been evaluated in *Mtb* uninfected rather than IGRA+ subjects, the population in which M72/AS01_E was shown to be efficacious. Replicating these clinical trial conditions in the macaque would allow for validation of the model and interrogation of the immune system for mechanisms of protection, to an extent not readily feasible in the clinic.



In addition to informing vaccine design, in **Chapter 5** we also show the value of non-human primates in evaluating new biomarkers and diagnostics identified in human cohorts. The ability to repeatedly sample at fixed timepoints after infection make the macaque very suited to investigate the dynamics of new diagnostic modalities, and post-mortem evaluation of TB pathology allow for formal correlation of biomarkers with disease severity. Vice versa, *Mtb* infection studies in NHP have the potential to identify (very) early markers of disease, informing design of new diagnostic tools^{102,103}.

Harnessing technological advancements for the macaque model of TB

In recent years, the development of several new tools has contributed greatly to the knowledge obtained from the macaque model of TB. One technological advancement that is considered to be of particular relevance in the field of modeling TB in NHP is the application of PET-CT imaging. Previously, pathology development in *Mtb* infected NHP was a black box mostly, which could be visualized in part by means of low-resolution X-ray imaging. By combining functional PET imaging with high-resolution CT imaging, structural features of TB disease development, such as granuloma development and pneumonia, can be simultaneously assessed for their uptake of PET tracer. Currently, in macaques, only ¹⁸F-fluorodeoxyglucose (FDG) is routinely used as a functional tracer, visualizing areas of high metabolic activity indicative of inflammation, as a measure of disease severity⁹². However, many more tracers are currently under development, such as bacterium-specific compounds or radio-labelled antibodies capable of binding specific immune-cells, offering the opportunity to follow *Mtb* dissemination or recruitment of immune cells over time^{104,105}. Sequential PET-CT imaging allows for the visualization of pathology development after experimental *Mtb* infection over time, and the potential to identify subtle, temporal vaccine-effects that influence, for instance, early versus late dissemination of *Mtb*. To date, PET-CT imaging has been applied successfully to follow granuloma formation over time and to identify risk of reactivation^{6,106}.

The recently developed “barcoded” *Mtb* strains, genetically engineered strains that contain a unique molecular tag, are another powerful new tool in TB research in NHP¹⁰⁷. These barcoded strains have already been used in macaques to dissect the dynamics of granuloma spread and dissemination of *Mtb* to the lung draining lymph nodes¹⁰⁷. Additionally, by utilizing these barcoded strains in the repeated limiting dose challenge model, administering a different, predefined barcode at each challenge, the exact moment of successful infection can be determined. This represents a more accurate strategy to determine the moment of infection, compared to deriving it from the moment of IGRA conversion (as performed in **Chapter 3**), which can vary in length after successful *Mtb* infection (**Chapter 2**).

The NHP studies described in this thesis have contributed to our knowledge of protective TB immunity. By the use of a novel repeated limiting dose challenge model, we have demonstrated for the first time that, by vaccinating via the pulmonary mucosa, highly susceptible rhesus macaques can be protected from infection. The repeated limiting dose challenge model also represents a powerful new modality for the evaluation of candidate TB vaccines. In conclusion, our research demonstrates that the macaque model of tuberculosis continues to be a valuable resource to address the remaining questions surrounding TB, thereby furthering our efforts towards global elimination of the disease.



References

1. Bhatt, K., Verma, S., Ellner, J.J. & Salgame, P. Quest for correlates of protection against tuberculosis. *Clinical and vaccine immunology : CVI* **22**, 258-266 (2015).
2. Sallin, M.A., et al. Th1 Differentiation Drives the Accumulation of Intravascular, Non-protective CD4 T Cells during Tuberculosis. *Cell reports* **18**, 3091-3104 (2017).
3. Zeng, G., Zhang, G. & Chen, X. Th1 cytokines, true functional signatures for protective immunity against TB? *Cellular & molecular immunology* **15**, 206-215 (2018).
4. Lyadova, I. & Nikitina, I. Cell Differentiation Degree as a Factor Determining the Role for Different T-Helper Populations in Tuberculosis Protection. *Front Immunol* **10**, 972 (2019).
5. Gideon, H.P., et al. Variability in tuberculosis granuloma T cell responses exists, but a balance of pro- and anti-inflammatory cytokines is associated with sterilization. *PLoS pathogens* **11**, e1004603 (2015).
6. Lin, P.L., et al. PET CT Identifies Reactivation Risk in Cynomolgus Macaques with Latent M. tuberculosis. *PLoS pathogens* **12**, e1005739 (2016).
7. Gaffen, S.L. Structure and signalling in the IL-17 receptor family. *Nature reviews. Immunology* **9**, 556-567 (2009).
8. Ouyang, W., Kolls, J.K. & Zheng, Y. The biological functions of T helper 17 cell effector cytokines in inflammation. *Immunity* **28**, 454-467 (2008).
9. J, N.H., Das, S., Tripathy, S.P. & Hanna, L.E. Role of neutrophils in tuberculosis: A bird's eye view. *Innate Immun*, 1753425919881176 (2019).
10. Lyadova, I.V. Neutrophils in Tuberculosis: Heterogeneity Shapes the Way? *Mediators of inflammation* **2017**, 8619307-8619307 (2017).
11. Martineau, A.R., et al. Neutrophil-mediated innate immune resistance to mycobacteria. *The Journal of clinical investigation* **117**, 1988-1994 (2007).
12. Amezcua Vesely, M.C., et al. Effector TH17 Cells Give Rise to Long-Lived TRM Cells that Are Essential for an Immediate Response against Bacterial Infection. *Cell* **178**, 1176-1188.e1115 (2019).
13. Perdomo, C., et al. Mucosal BCG Vaccination Induces Protective Lung-Resident Memory T Cell Populations against Tuberculosis. *mBio* **7**(2016).
14. Ogongo, P., Porterfield, J.Z. & Leslie, A. Lung Tissue Resident Memory T-Cells in the Immune Response to *Mycobacterium tuberculosis*. *Front Immunol* **10**, 992 (2019).
15. Gopal, R., et al. Interleukin-17-dependent CXCL13 mediates mucosal vaccine-induced immunity against tuberculosis. *Mucosal immunology* **6**, 972-984 (2013).
16. Rangel-Moreno, J., et al. The development of inducible bronchus-associated lymphoid tissue depends on IL-17. *Nature immunology* **12**, 639-646 (2011).
17. Aguilo, N., et al. Pulmonary but Not Subcutaneous Delivery of BCG Vaccine Confers Protection to Tuberculosis-Susceptible Mice by an Interleukin 17-Dependent Mechanism. *The Journal of infectious diseases* **213**, 831-839 (2016).
18. Gopal, R., et al. Unexpected role for IL-17 in protective immunity against hypervirulent *Mycobacterium tuberculosis* HN878 infection. *PLoS pathogens* **10**, e1004099 (2014).
19. Okamoto Yoshida, Y., et al. Essential role of IL-17A in the formation of a mycobacterial infection-induced granuloma in the lung. *Journal of immunology (Baltimore, Md. : 1950)* **184**, 4414-4422 (2010).
20. Wareham, A.S., et al. Evidence for a role for interleukin-17, Th17 cells and iron homeostasis in protective immunity against tuberculosis in cynomolgus macaques. *PLoS one* **9**, e88149 (2014).
21. Lyadova, I.V. & Pantelev, A.V. Th1 and Th17 Cells in Tuberculosis: Protection, Pathology, and Biomarkers. *Mediators of inflammation* **2015**, 854507 (2015).
22. Kammuller, M., et al. Inhibition of IL-17A by secukinumab shows no evidence of increased *Mycobacterium tuberculosis* infections. *Clinical & translational immunology* **6**, e152 (2017).

23. Scriba, T.J., et al. Distinct, specific IL-17- and IL-22-producing CD4⁺ T cell subsets contribute to the human anti-mycobacterial immune response. *Journal of immunology (Baltimore, Md. : 1950)* **180**, 1962-1970 (2008).
24. Zizzo, G., Hilliard, B.A., Monestier, M. & Cohen, P.L. Efficient Clearance of Early Apoptotic Cells by Human Macrophages Requires M2c Polarization and MerTK Induction. *The Journal of Immunology* **189**, 3508 (2012).
25. Lastrucci, C., et al. Tuberculosis is associated with expansion of a motile, permissive and immunomodulatory CD16(+) monocyte population via the IL-10/STAT3 axis. *Cell research* **25**, 1333-1351 (2015).
26. Almeida, A.S., et al. Tuberculosis is associated with a down-modulatory lung immune response that impairs Th1-type immunity. *Journal of immunology (Baltimore, Md. : 1950)* **183**, 718-731 (2009).
27. Verbon, A., et al. Serum concentrations of cytokines in patients with active tuberculosis (TB) and after treatment. *Clin Exp Immunol* **115**, 110-113 (1999).
28. Redford, P.S., et al. Enhanced protection to *Mycobacterium tuberculosis* infection in IL-10-deficient mice is accompanied by early and enhanced Th1 responses in the lung. *European journal of immunology* **40**, 2200-2210 (2010).
29. Pitt, J.M., et al. Blockade of IL-10 Signaling during Bacillus Calmette-Guérin Vaccination Enhances and Sustains Th1, Th17, and Innate Lymphoid IFN- γ and IL-17 Responses and Increases Protection to *Mycobacterium tuberculosis* Infection. *The Journal of Immunology* **189**, 4079-4087 (2012).
30. Wong, E.A., et al. IL-10 Impairs Local Immune Response in Lung Granulomas and Lymph Nodes during Early *Mycobacterium tuberculosis* Infection. *Journal of immunology (Baltimore, Md. : 1950)* (2019).
31. Moreira-Teixeira, L., et al. T Cell-Derived IL-10 Impairs Host Resistance to *Mycobacterium tuberculosis* Infection. *The Journal of Immunology* **199**, 613-623 (2017).
32. Thompson, E.A., et al. Monocytes Acquire the Ability to Prime Tissue-Resident T Cells via IL-10-Mediated TGF- β Release. *Cell reports* **28**, 1127-1135.e1124 (2019).
33. McGeachy, M.J., et al. TGF- β and IL-6 drive the production of IL-17 and IL-10 by T cells and restrain T(H)-17 cell-mediated pathology. *Nat Immunol* **8**, 1390-1397 (2007).
34. Gupta, N., Agrawal, B. & Kumar, R. Controlling inflammation: a superior way to control TB. *Immunotherapy* **8**, 1157-1161 (2016).
35. Roca, Francisco J. & Ramakrishnan, L. TNF Dually Mediates Resistance and Susceptibility to Mycobacteria via Mitochondrial Reactive Oxygen Species. *Cell* **153**, 521-534 (2013).
36. Mootoo, A., Stylianou, E., Arias, M.A. & Reljic, R. TNF- α in tuberculosis: a cytokine with a split personality. *Inflammation & allergy drug targets* **8**, 53-62 (2009).
37. Divangahi, M., Khan, N. & Kaufmann, E. Beyond Killing *Mycobacterium tuberculosis*: Disease Tolerance. *Front Immunol* **9**, 2976 (2018).
38. Barber, D.L., et al. Tuberculosis following PD-1 blockade for cancer immunotherapy. *Sci Transl Med* **11**(2019).
39. Picchi, H., et al. Infectious complications associated with the use of immune checkpoint inhibitors in oncology: Reactivation of tuberculosis after anti PD-1 treatment. *Clinical microbiology and infection: the official publication of the European Society of Clinical Microbiology and Infectious Diseases* (2017).
40. Glatman-Freedman, A. & Casadevall, A. Serum Therapy for Tuberculosis Revisited: Reappraisal of the Role of Antibody-Mediated Immunity against *Mycobacterium tuberculosis*. *Clinical microbiology reviews* **11**, 514-532 (1998).
41. Kawahara, J.Y., Irvine, E.B. & Alter, G. A Case for Antibodies as Mechanistic Correlates of Immunity in Tuberculosis. *Frontiers in Immunology* **10**(2019).
42. Chen, T., et al. Association of Human Antibodies to Arabinomannan With Enhanced Mycobacterial Opsonophagocytosis and Intracellular Growth Reduction. *The Journal of infectious diseases* **214**, 300-310 (2016).



43. Lu, L.L., et al. A Functional Role for Antibodies in Tuberculosis. *Cell* **167**, 433-443.e414 (2016).
44. de Vallière, S., Abate, G., Blazevic, A., Heuertz, R.M. & Hoft, D.F. Enhancement of innate and cell-mediated immunity by antimycobacterial antibodies. *Infection and immunity* **73**, 6711-6720 (2005).
45. Logan, E., et al. Elevated IgG Responses in Infants Are Associated With Reduced Prevalence of *Mycobacterium tuberculosis* Infection. *Frontiers in Immunology* **9**(2018).
46. Coppola, M., et al. Differences in IgG responses against infection phase related *Mycobacterium tuberculosis* (Mtb) specific antigens in individuals exposed or not to Mtb correlate with control of TB infection and progression. *Tuberculosis (Edinburgh, Scotland)* **106**, 25-32 (2017).
47. Zimmermann, N., et al. Human isotype-dependent inhibitory antibody responses against *Mycobacterium tuberculosis*. *EMBO molecular medicine* **8**, 1325-1339 (2016).
48. Alter, G., Ottenhoff, T.H.M. & Joosten, S.A. Antibody glycosylation in inflammation, disease and vaccination. *Seminars in immunology* **39**, 102-110 (2018).
49. Tran, A.C., Kim, M.Y. & Reljic, R. Emerging Themes for the Role of Antibodies in Tuberculosis. *Immune Netw* **19**, e24 (2019).
50. Yu, Y.A., et al. Flow Cytometric Analysis of Myeloid Cells in Human Blood, Bronchoalveolar Lavage, and Lung Tissues. *Am J Respir Cell Mol Biol* (2015).
51. Hussell, T. & Bell, T.J. Alveolar macrophages: plasticity in a tissue-specific context. *Nature Reviews Immunology* **14**, 81-93 (2014).
52. Allard, B., Panariti, A. & Martin, J.G. Alveolar Macrophages in the Resolution of Inflammation, Tissue Repair, and Tolerance to Infection. *Front Immunol* **9**, 1777 (2018).
53. Lyons, C.R., et al. Inability of human alveolar macrophages to stimulate resting T cells correlates with decreased antigen-specific T cell-macrophage binding. *Journal of immunology (Baltimore, Md. : 1950)* **137**, 1173-1180 (1986).
54. Vecchiarelli, A., et al. Role of human alveolar macrophages as antigen-presenting cells in *Cryptococcus neoformans* infection. *Am J Respir Cell Mol Biol* **11**, 130-137 (1994).
55. West, E.E., Kolev, M. & Kemper, C. Complement and the Regulation of T Cell Responses. *Annual review of immunology* **36**, 309-338 (2018).
56. Clarke, E.V. & Tenner, A.J. Complement modulation of T cell immune responses during homeostasis and disease. *Journal of leukocyte biology* **96**, 745-756 (2014).
57. Netea, M.G., et al. Trained immunity: A program of innate immune memory in health and disease. *Science (New York, N.Y.)* **352**, aaf1098 (2016).
58. Yao, Y., et al. Induction of Autonomous Memory Alveolar Macrophages Requires T Cell Help and Is Critical to Trained Immunity. *Cell* **175**, 1634-1650.e1617 (2018).
59. Kleinnijenhuis, J., et al. Bacille Calmette-Guerin induces NOD2-dependent nonspecific protection from reinfection via epigenetic reprogramming of monocytes. *Proceedings of the National Academy of Sciences of the United States of America* **109**, 17537-17542 (2012).
60. Cohen, S.B., et al. Alveolar Macrophages Provide an Early *Mycobacterium tuberculosis* Niche and Initiate Dissemination. *Cell host & microbe* **24**, 439-446.e434 (2018).
61. Marin, N.D., Dunlap, M.D., Kaushal, D. & Khader, S.A. Friend or Foe: The Protective and Pathological Roles of Inducible Bronchus-Associated Lymphoid Tissue in Pulmonary Diseases. *Journal of immunology (Baltimore, Md. : 1950)* **202**, 2519-2526 (2019).
62. Moyron-Quiroz, J.E., et al. Role of inducible bronchus associated lymphoid tissue (iBALT) in respiratory immunity. *Nature medicine* **10**, 927-934 (2004).
63. Xu, B., et al. Lymphocyte Homing to Bronchus-associated Lymphoid Tissue (BALT) Is Mediated by L-selectin/PNAd, $\alpha 4\beta 1$ Integrin/VCAM-1, and LFA-1 Adhesion Pathways. *The Journal of experimental medicine* **197**, 1255-1267 (2003).
64. Kaushal, D., et al. Mucosal vaccination with attenuated *Mycobacterium tuberculosis* induces strong central memory responses and protects against tuberculosis. *Nature communications* **6**, 8533 (2015).

65. Slight, S.R., et al. CXCR5⁺ T helper cells mediate protective immunity against tuberculosis. *The Journal of clinical investigation* **123**, 712-726 (2013).
66. Schyns, J., Bureau, F. & Marichal, T. Lung Interstitial Macrophages: Past, Present, and Future. *Journal of immunology research* **2018**, 5160794 (2018).
67. Khan, A., Singh, V.K., Hunter, R.L. & Jagannath, C. Macrophage heterogeneity and plasticity in tuberculosis. *Journal of leukocyte biology* **106**, 275-282 (2019).
68. Huang, L., Nazarova, E.V., Tan, S., Liu, Y. & Russell, D.G. Growth of *Mycobacterium tuberculosis* in vivo segregates with host macrophage metabolism and ontogeny. *The Journal of experimental medicine* **215**, 1135-1152 (2018).
69. Samstein, M., et al. Essential yet limited role for CCR2(+) inflammatory monocytes during *Mycobacterium tuberculosis*-specific T cell priming. *Elife* **2**, e01086 (2013).
70. Lagranderie, M., et al. Dendritic cells recruited to the lung shortly after intranasal delivery of *Mycobacterium bovis* BCG drive the primary immune response towards a type 1 cytokine production. *Immunology* **108**, 352-364 (2003).
71. Souwer, Y., et al. Human TH17 cell development requires processing of dendritic cell-derived CXCL8 by neutrophil elastase. *The Journal of allergy and clinical immunology* **141**, 2286-2289. e2285 (2018).
72. Lombard, R., et al. IL-17RA in Non-Hematopoietic Cells Controls CXCL-1 and 5 Critical to Recruit Neutrophils to the Lung of *Mycobacteria*-Infected Mice during the Adaptive Immune Response. *PLoS one* **11**, e0149455 (2016).
73. Morel, C., et al. *Mycobacterium bovis* BCG-infected neutrophils and dendritic cells cooperate to induce specific T cell responses in humans and mice. *European journal of immunology* **38**, 437-447 (2008).
74. Minassian, A.M., et al. A human challenge model for *Mycobacterium tuberculosis* using *Mycobacterium bovis* bacille Calmette-Guerin. *The Journal of infectious diseases* **205**, 1035-1042 (2012).
75. Eum, S.Y., et al. Neutrophils are the predominant infected phagocytic cells in the airways of patients with active pulmonary TB. *Chest* **137**, 122-128 (2010).
76. Mason, R.J. Biology of alveolar type II cells. *Respirology* **11 Suppl.**, S12-15 (2006).
77. Matthay, M.A., Robriquet, L. & Fang, X. Alveolar epithelium: role in lung fluid balance and acute lung injury. *Proc Am Thorac Soc* **2**, 206-213 (2005).
78. Chuquimia, O.D., et al. The role of alveolar epithelial cells in initiating and shaping pulmonary immune responses: communication between innate and adaptive immune systems. *PLoS one* **7**, e32125 (2012).
79. Rizvi, Z.A., Puri, N. & Saxena, R.K. Evidence of CD1d pathway of lipid antigen presentation in mouse primary lung epithelial cells and its up-regulation upon *Mycobacterium bovis* BCG infection. *PLoS one* **13**, e0210116 (2018).
80. Moliva, J.I., et al. Exposure to human alveolar lining fluid enhances *Mycobacterium bovis* BCG vaccine efficacy against *Mycobacterium tuberculosis* infection in a CD8(+) T-cell-dependent manner. *Mucosal immunology* **11**, 968-978 (2018).
81. Price, D.N., Kusewitt, D.F., Lino, C.A., McBride, A.A. & Muttli, P. Oral Tolerance to Environmental *Mycobacteria* Interferes with Intradermal, but Not Pulmonary, Immunization against Tuberculosis. *PLoS pathogens* **12**, e1005614 (2016).
82. Chen, L., Wang, J., Zganiacz, A. & Xing, Z. Single intranasal mucosal *Mycobacterium bovis* BCG vaccination confers improved protection compared to subcutaneous vaccination against pulmonary tuberculosis. *Infection and immunity* **72**, 238-246 (2004).
83. Bull, N.C., et al. Enhanced protection conferred by mucosal BCG vaccination associates with presence of antigen-specific lung tissue-resident PD-1(+) KLRG1(-) CD4(+) T cells. *Mucosal immunology* **12**, 555-564 (2019).
84. Derrick, S.C., Kolibab, K., Yang, A. & Morris, S.L. Intranasal administration of *Mycobacterium bovis* BCG induces superior protection against aerosol infection with *Mycobacterium tuberculosis* in mice. *Clinical and vaccine immunology : CVI* **21**, 1443-1451 (2014).



85. Lagranderie, M., Murray, A., Gicquel, B., Leclerc, C. & Gheorghiu, M. Oral immunization with recombinant BCG induces cellular and humoral immune responses against the foreign antigen. *Vaccine* **11**, 1283-1290 (1993).
86. Gheorghiu, M. BCG-induced mucosal immune responses. *International journal of immunopharmacology* **16**, 435-444 (1994).
87. Barclay, W.R., et al. Protection of monkeys against airborne tuberculosis by aerosol vaccination with bacillus Calmette-Guerin. *The American review of respiratory disease* **107**, 351-358 (1973).
88. Verreck, F.A.W., et al. Variable BCG efficacy in rhesus populations: Pulmonary BCG provides protection where standard intra-dermal vaccination fails. *Tuberculosis (Edinburgh, Scotland)* **104**, 46-57 (2017).
89. Dijkman, K., et al. Prevention of tuberculosis infection and disease by local BCG in repeatedly exposed rhesus macaques. *Nature medicine* (2019).
90. Palendira, U., Bean, A.G.D., Feng, C.G. & Britton, W.J. Lymphocyte Recruitment and Protective Efficacy against Pulmonary Mycobacterial Infection Are Independent of the Route of Prior *Mycobacterium bovis* BCG Immunization. *Infection and immunity* **70**, 1410-1416 (2002).
91. Goonetilleke, N.P., et al. Enhanced immunogenicity and protective efficacy against *Mycobacterium tuberculosis* of bacille Calmette-Guerin vaccine using mucosal administration and boosting with a recombinant modified vaccinia virus Ankara. *Journal of immunology (Baltimore, Md. : 1950)* **171**, 1602-1609 (2003).
92. Darrah, P.A., et al. Prevention of tuberculosis in macaques after intravenous BCG immunization. *Nature* **577**, 95-102 (2020).
93. Langermans, J.A., et al. Divergent effect of bacillus Calmette-Guerin (BCG) vaccination on *Mycobacterium tuberculosis* infection in highly related macaque species: implications for primate models in tuberculosis vaccine research. *Proceedings of the National Academy of Sciences of the United States of America* **98**, 11497-11502 (2001).
94. Verreck, F.A., et al. MVA.85A boosting of BCG and an attenuated, phoP deficient M. tuberculosis vaccine both show protective efficacy against tuberculosis in rhesus macaques. *PLoS one* **4**, e5264 (2009).
95. Kauffman, K.D., et al. Defective positioning in granulomas but not lung-homing limits CD4 T-cell interactions with *Mycobacterium tuberculosis*-infected macrophages in rhesus macaques. *Mucosal immunology* (2017).
96. Gautam, U.S., et al. *In vivo* inhibition of tryptophan catabolism reorganizes the tuberculoma and augments immune-mediated control of *Mycobacterium tuberculosis*. *Proceedings of the National Academy of Sciences of the United States of America* **115**, E62-e71 (2018).
97. Hansen, S.G., et al. Prevention of tuberculosis in rhesus macaques by a cytomegalovirus-based vaccine. *Nature medicine* **24**, 130-143 (2018).
98. Nemes, E., et al. Prevention of M. tuberculosis Infection with H4:IC31 Vaccine or BCG Revaccination. *The New England journal of medicine* **379**, 138-149 (2018).
99. Tait, D.R., et al. Final Analysis of a Trial of M72/AS01E Vaccine to Prevent Tuberculosis. *New England Journal of Medicine* (2019).
100. Lin, P.L., et al. The multistage vaccine H56 boosts the effects of BCG to protect cynomolgus macaques against active tuberculosis and reactivation of latent *Mycobacterium tuberculosis* infection. *The Journal of clinical investigation* **122**, 303-314 (2012).
101. Darrah, P.A., et al. Boosting BCG with proteins or rAd5 does not enhance protection against tuberculosis in rhesus macaques. *NPJ Vaccines* **4**, 21 (2019).
102. Javed, S., et al. Temporal Expression of Peripheral Blood Leukocyte Biomarkers in a *Macaca fascicularis* Infection Model of Tuberculosis; Comparison with Human Datasets and Analysis with Parametric/Non-parametric Tools for Improved Diagnostic Biomarker Identification. *PLoS one* **11**, e0154320 (2016).

103. Gideon, H.P., Skinner, J.A., Baldwin, N., Flynn, J.L. & Lin, P.L. Early Whole Blood Transcriptional Signatures Are Associated with Severity of Lung Inflammation in *Cynomolgus* Macaques with *Mycobacterium tuberculosis* Infection. *Journal of immunology (Baltimore, Md. : 1950)* **197**, 4817-4828 (2016).
104. Ning, X., et al. PET imaging of bacterial infections with fluorine-18-labeled maltohexaose. *Angewandte Chemie (International ed. in English)* **53**, 14096-14101 (2014).
105. Wei, W., Jiang, D., Ehlerding, E.B., Luo, Q. & Cai, W. Noninvasive PET Imaging of T cells. *Trends Cancer* **4**, 359-373 (2018).
106. Cadena, A.M., et al. Concurrent infection with *Mycobacterium tuberculosis* confers robust protection against secondary infection in macaques. *PLoS pathogens* **14**, e1007305 (2018).
107. Martin, C.J., et al. Digitally Barcoding *Mycobacterium tuberculosis* Reveals *In Vivo* Infection Dynamics in the Macaque Model of Tuberculosis. *mBio* **8**(2017).





Appendices



Abbreviations

ADCC	antibody-dependent cell-mediated cytotoxicity
AEC	alveolar epithelial cell
APC	antigen presenting cell
ATB	active tuberculosis
AU	arbitrary units
BAL	bronchoalveolar lavage
BCG	Bacillus Calmette Guerin
CCR	C-C chemokine receptor
C1q	complement component 1q
CD	cluster of differentiation
CFP	culture filtrate protein
CFU	colony forming unit
CNS	central nervous system
CRP	C-reactive protein
CSF	cerebrospinal fluid
CT	computed tomography
CXCL	C-X-C motif ligand
CXCR	C-X-C chemokine receptor
DNA	deoxyribonucleic acid
DTH	delayed type hypersensitivity
DURT	donor unrestricted T-cells
DR	drug-resistant
ELISA	enzyme-linked immunosorbent assay
ESAT-6	early secreted antigenic target 6
FDG	fluorodeoxyglucose
GC	germinal center
HIV	human immunodeficiency virus
iBALT	inducible bronchus-associated lymphoid tissue
Ig	immunoglobulin
IFN γ	interferon-gamma
IGRA	interferon-gamma release assay
IL	interleukin
ILC	innate lymphoid cells
LAM	lipoarabinomannan
LF-LAM	lateral flow lipoarabinomannan
LTBI	latent tuberculosis infection
MAC	<i>Mycobacterium avium</i> complex
MCH	mean corpuscular hemoglobin
MDR	multidrug-resistant
MerTK	mer tyrosine kinase
MGIA	mycobacterial growth inhibition assay

MGIT	mycobacterial growth indicator tube
MHC	major histocompatibility complex
<i>MIP</i>	<i>Mycobacterium indicus pranii</i>
MRI	magnetic resonance imaging
<i>Mtb</i>	<i>Mycobacterium tuberculosis</i>
MTBC	<i>Mycobacterium tuberculosis</i> complex
NHP	non-human primates
NK	natural killer
NTM	non-tuberculous mycobacteria
OT	old tuberculin
PAMP	pathogen associated molecular pattern
PBMC	peripheral blood mononuclear cells
PD-1	programmed cell death protein 1
PDIM	phthiocerol dimycocerosates
PET	positron emission tomography
PoD	prevention of disease
PoI	prevention of infection
PoR	prevention of recurrence
PPD	purified protein derivate
PRR	pattern recognition receptors
RD	region of difference
RLD	repeated limiting dose
SIV	simian immunodeficiency virus
SUV	standard uptake value
TB	tuberculosis
TBM	tuberculosis meningitis
Th	T-helper
TNF α	tumor necrosis factor alpha
Trm	tissue resident memory T-cell
TST	tuberculin skin test
TTP	time to positivity
WCL	whole cell lysate
WHO	World Health Organization
XDR	extensively drug-resistant



Nederlandse samenvatting

Tuberculose (TB) is een infectieziekte die primair wordt veroorzaakt door de bacterie *Mycobacterium tuberculosis* (*Mtb*). Ondanks dat TB doorgaans te behandelen valt met antibiotica, sterven er op jaarbasis nog steeds ongeveer 1,5 miljoen mensen aan de gevolgen van tuberculose, wat TB tot de meest dodelijke infectieziekte maakt. Daarnaast worden er jaarlijks ook nog rond de 10 miljoen nieuwe tuberculosepatiënten gerapporteerd. De bestrijding van TB wordt gehinderd door, onder andere, een toename van antibioticaresistente stammen en een gebrek aan kennis op het gebied van diagnostiek en beschermende immuniteit.

Voorkomen is beter dan genezen, en vaccineren is een van de meest kosten-effectieve manieren om een infectieziekte te voorkomen en daarmee verdere verspreiding tegen te gaan. Als bijkomend voordeel kan door middel van vaccinatie antibioticaresistentie omzeild worden. Er is momenteel een vaccin tegen TB beschikbaar; Bacillus Calmette Guerin (BCG), een verzwakte vorm van de *Mycobacterium bovis* bacterie, verwant aan *Mtb*. Echter, intradermale vaccinatie met BCG leidt tot variabele bescherming, en is (althans in volwassenen) het minst effectief in de gebieden waar TB het meest prevalent is. Meer effectieve vaccins zijn dus dringend nodig, maar de ontwikkeling van nieuwe TB vaccins wordt bemoeilijkt door het feit dat het onduidelijk is aan welke kenmerken een immuunrespons precies moet voldoen om een individu te beschermen tegen TB. Er zijn verscheidene immuunmechanismes geïdentificeerd die van belang zijn in de afweer tegen *Mtb*, maar het induceren van deze responsen door middel van vaccinatie lijkt onvoldoende om eenduidige bescherming te leiden. Wat de situatie verder compliceert is de observatie dat, onder bepaalde omstandigheden, de responsen die van belang zijn voor bescherming juist lijken bij te dragen aan de ontwikkeling van pathologie.

Dit gebrek aan inzicht in beschermende immuniteit, gecombineerd met de kosten van grootschalige klinische studies, maken het nodig om nieuwe vaccins eerst te testen op effectiviteit in preklinische diermodellen. Dit biedt gelijk de mogelijkheid tot onderzoek naar de immuun-responsen verantwoordelijk voor bescherming en de identificatie van correlaten van bescherming die gebruikt kunnen worden in klinische studies. Tuberculose kan gemodelleerd worden in een scala aan diersoorten, waaronder niet-humane primaten (NHP). Net als de mens bezitten NHP een hoge genetische diversiteit en worden ze vanaf geboorte blootgesteld aan een verscheidenheid aan omgevings-microben. Dit laatste zorgt ervoor dat hun afweersysteem continu geprikkeld en gevormd wordt, dit in tegenstelling tot bijvoorbeeld de muis, die doorgaans onder specifiek pathogeen-vrije condities wordt gehuisvest. De twee niet-humane primate-soorten die het meest worden gebruikt in het onderzoek naar tuberculose zijn de resus makaak (*Macaca mulatta*) en de cynomolgus makaak (*Macaca fascicularis*). Na infectie met *Mtb* vertoont de ziekteontwikkeling in deze twee makaaksoorten grote gelijkenissen met het verloop

van tuberculose in de mens. Het onderzoek beschreven in dit proefschrift beoogd door middel van het makaak model van tuberculose meer inzicht te verschaffen in de immunopathogenese van TB en vaccin-gemedieerde bescherming.

Om inzicht te krijgen in vroege immuunprocessen betrokken bij de ontwikkeling van, en resistentie tegen TB, is er in **hoofdstuk 2** gebruik gemaakt van het verschil in ziekteontwikkeling na *Mtb* infectie tussen resus en cynomolgus makaken. In vergelijking met resus makaken zijn cynomolgus apen minder gevoelig voor het ontwikkelen van ziekte na experimentele infectie met *Mtb*; ze vertonen minder pathologie en zijn beter te beschermen met een BCG-vaccinatie. Een deel van de geïnfecteerde cynomolgus makaken is zelfs in staat om een (lage dosis) infectie onder controle te houden en zo een latente infectie te ontwikkelen, net als het merendeel van de *Mtb*-geïnfecteerde mensen. Welke immuunmechanismen de differentiële gevoeligheid veroorzaken en of de twee makaak soorten ook verschillen in hun gevoeligheid voor infectie is onbekend. Het doel van deze studie was dan ook driedelig: 1) het identificeren van de laagste infectieuze dosis *Mtb* voor beide soorten, doormiddel van een dosis-escalatie studiedesign, ten behoeve van het verfijnen van het model, 2) de twee soorten vergelijken qua gevoeligheid voor infectie en 3) het identificeren van immuunresponsen die mogelijk ten grondslag liggen aan het verschil in ziekteontwikkeling.

Resus en cynomolgus makaken bleken niet te verschillen in hun gevoeligheid voor *Mtb* infectie. Beide makaaksoorten zijn vatbaar voor infectie na toediening van 1 kolonievormende eenheid (KVE) *Mtb*, al leidde dit niet tot infectie in alle dieren. Dit betekent dat deze hoeveelheid de limiterende infectieuze dosis voor *Mtb* infectie in makaken vertegenwoordigt. Blootstelling aan 7 KVE *Mtb* resulteerde in infectie in alle dieren. Als eerder gerapporteerd, verschilden resus en cynomolgus makaken ook in deze studie in de mate van pathologieontwikkeling; de longen van resus makaken vertoonden meer TB pathologie en een grotere hoeveelheid *Mtb* bacteriën. In de zoektocht naar immuun-responsen die dit verschil zouden kunnen verklaren, is zowel de aangeboren als de adaptieve afweer tegen *Mtb* onderzocht vóór, en op verschillende tijdstippen ná infectie. Cellen uit de long van cynomolgus makaken bleken al voor infectie een sterkere inflammatoire response te vertonen in respons op *Mtb* dan resus makaken. Dit verschil bleef aanwezig tot 3 weken na infectie. Resus makaken daarentegen hadden op deze tijdstippen juist meer anti-inflammatoire monocytten in hun circulatie. Het verschil in ziekteontwikkeling tussen deze twee soorten lijkt dus al vroeg na infectie bepaald te worden.

In **hoofdstuk 3** is de bevinding dat 1 KVE *Mtb* al kan resulteren in infectie gebruikt om een nieuw model voor vaccin-evaluatie op te zetten, waar naast het voorkomen van ziekte, ook het voorkomen van infectie bepaald kan worden.

Door makaken meerdere keren bloot te stellen aan de limiterende infectieuze dosis van 1 KVE *Mtb* zal uiteindelijk ieder (niet-gevaccineerd) dier geïnfecteerd raken. Door deze herhaalde toediening toe te passen op gevaccineerde dieren kan



onderzocht worden of vaccinatie terugdringt op het aantal dieren wat geïnfecteerd raakt na deze herhaalde toediening, en dus de potentie heeft om infectie voorkomen. Een bijkomend voordeel is dat deze herhaalde toediening van *Mtb* de situatie in TB-endemische gebieden, waar bijvoorbeeld iemand dagelijks blootgesteld wordt aan een geïnfecteerd familielid, hoogstwaarschijnlijk beter nabootst.

Met dit nieuwe model is de beschermende werking van BCG-vaccinatie via twee verschillende routes vergeleken; vaccinatie via de standaard (klinische) route van intradermale injectie en vaccinatie via de longen door endobronchiale instillatie, waarvan uit eerder onderzoek in makaken bekend is dat het een betere bescherming tegen pathologie biedt. Vergeleken met intradermale vaccinatie, bleek pulmonaire BCG-vaccinatie in staat om het moment van infectie significant te vertragen, naast het verder verminderen van pathologie. Deze bescherming was geassocieerd met de inductie van *Mtb*-reactieve T-helper-17A cellen (Th17A), interleukine-10 (IL-10) en immuuglobuline A (IgA) in de long. Vaccinatie via de longen lijkt dus een veelbelovende strategie om TB te bestrijden.

De BCG bacil verschilt noemenswaardig van *M. tuberculosis*; het mist meerdere genomische regio's die wel aanwezig zijn in *Mtb* en als gevolg daarvan een aantal antigenen. Een van de strategieën waarmee wordt geprobeerd de effectiviteit van nieuwe TB-vaccins te verhogen, is het induceren van immuunresponsen tegen deze specifieke *Mtb* antigenen. MTBVAC, een genetische gemodificeerde *Mtb* stam met een sterk verminderde virulentie, is een dergelijk vaccin. Intradermale vaccinatie met MTBVAC resulteert, in diermodellen, in betere bescherming dan BCG, wat veroorzaakt wordt door *Mtb*-specifieke T-cel responsen. Gezien pulmonaire toediening van BCG de effectiviteit verhoogt, wat associeerde met de inductie van lokale Th17A cellen, IL-10 en IgA, is er in **hoofdstuk 4** onderzocht of pulmonaire vaccinatie met MTBVAC de potentie heeft om eenzelfde immuun-signatuur te induceren.

Zowel pulmonaire vaccinatie met MTBVAC als BCG zorgde inderdaad voor lokale productie van IL-10 en IgA en de aanwezigheid van Th17A cellen, waarbij toediening van MTBVAC leidde tot een snellere en hogere respons vergeleken met BCG. De lokale, cytokine-producerende cellen zijn in deze studie verder onderzocht op expressie van merkers geassocieerd met migratie naar de mucosa en de inductie van longweefsel-geassocieerde T-cellen. Pulmonaire *Mtb*-reactieve, cytokine-producerende T-cellen geïnduceerd na pulmonaire vaccinatie met BCG of MTBVAC brachten significant vaker één of meerdere migratie-markers tot expressie dan T-cellen geïnduceerd door infectie met *Mtb*, en lijken dus beter in staat om na infectie naar de long te migreren. Ook bleek na vaccinatie een groter percentage van deze cellen het fenotype van weefsel-geassocieerde T-cellen te hebben, wat suggereert dat er na vaccinatie, maar niet *Mtb* infectie, een lokale voorraad van *Mtb*-reactieve T-cellen in de long wordt aangelegd, die door versnelde mobilisatie mogelijk bijdraagt aan bescherming.

In **hoofdstuk 5** wordt biomateriaal gebruikt uit de studies beschreven in **hoofdstuk 2** en **hoofdstuk 3** en additionele historische studies, om de associatie van complement component 1q (C1q) met tuberculose ziekteprogressie verder te onderzoeken. Deze associatie is al eerder gevonden in humane cohortstudies, maar de NHP biedt de mogelijkheid om deze associatie verder te karakteriseren. Zoals ook geobserveerd in de mens, bevatte het serum van makaken met de meeste pathologie de hoogste hoeveelheid C1q. Een verhoging in de serum C1q waardes kon geobserveerd worden vanaf 6 weken na *Mtb* infectie, echter niet voordat infectie ook kon worden vastgesteld met behulp van een gangbare Interferon Gamma Release Assay (IGRA). Een verhoogde hoeveelheid C1q kon ook gemeten worden in de longspoeling van zowel *Mtb* geïnfecteerde dieren als pulmonair BCG gevaccineerde dieren. Zowel *Mtb* infectie als pulmonaire BCG-vaccinatie leidde tot de productie van C1q door (vermoedelijk) alveolaire macrofagen. Of dit lokale C1q een rol speelt in bescherming of pathologie in de context van *Mtb* infectie vereist verder onderzoek.

In conclusie, het onderzoek in dit proefschrift heeft bijgedragen aan de identificatie van meerdere immuunmechanismes betrokken bij bescherming tegen TB. Daarbij is voor het eerst gedemonstreerd dat vaccinatie via de longmucosa de potentie heeft om niet alleen ziekte maar ook infectie te voorkomen. Vooral de tijd en locatie van de vaccin-geïnduceerde immuunrespons lijkt van essentieel belang in het mediëren van bescherming. Pulmonaire vaccinatie in de mens wordt momenteel nog onderzocht in fase I klinische studies, maar biedt het perspectief op een verbeterde TB profylaxe. De resultaten in dit proefschrift demonstreren andermaal de toegevoegde waarde van het NHP model voor het tuberculose onderzoek, voor zowel de evaluatie van nieuwe vaccins en diagnostica als het beantwoorden van meer fundamentele vragen rondom TB infectie, pathogenese en immuniteit.



Dankwoord

*“Light is the task
where many share the toil”*

Homer

Het heeft wat meer tijd gekost dan gedacht, maar dit proefschrift is er dan toch gekomen. Mijn tijd als promotiestudent is anders gelopen dan ik initieel had voorzien, en er zijn momenten geweest waarop een goede afloop ver weg leek. Ik zal dan ook niet beweren dat het promotieonderzoek en alles wat erbij kwam kijken “licht werk” is geweest, maar ik weet wel dat de vele handen die bijgedragen hebben aan de totstandkoming van dit proefschrift het onnoemelijk veel draaglijker hebben gemaakt.

Ronald, allereerst wil ik jou bedanken voor je vertrouwen in mijn kunnen. Zonder dat vertrouwen was dit proefschrift er nooit geweest. Verder ook mijn dank voor alle tijd en moeite die je hebt gestoken in het kritisch lezen van dit proefschrift en al het regelwerk rondom de promotie.

Frank, ook jou ben ik ontzettend dankbaar voor alles wat je tijdens mijn promotietijd voor mij hebt gedaan. Je nam mij onder je vleugels op een moment waarop ik het vertrouwen in mijzelf had verloren en hebt ervoor gezorgd dat ik mij kon ontwikkelen tot de wetenschapper die ik nu ben. Je hebt mij gemotiveerd om de grenzen van mijn kunnen op te zoeken en geholpen deze te verleggen. Niet iedere begeleider geeft zijn studenten de kansen die je mij hebt gegeven, onder andere het presenteren van ons werk op de diverse congressen. Daarnaast heb je ondanks je drukke schema altijd tijd beschikbaar gemaakt voor het beantwoorden van een vraag, het doornemen van een stuk tekst, of het bespreken van de allerhande ongemakken die een promotiestudent plagen. Ik zal onze vrijdagavonddiscussies, printerpraatsessies en gezamenlijke congresbezoeken ontzettend gaan missen.

Wetenschap doe je nooit alleen, en ik ben erg dankbaar voor de inzet en gezelligheid van mijn mede-TB-groepers. De studies beschreven in dit proefschrift waren op z'n zachts gezegd logistiek uitdagend, en alleen mogelijk door het fantastische teamwork van iedereen in de groep. Allereerst mijn kamergenoten. Sam, of we nou bij de Immunobiologie of TB groep zaten, je bent een supergezellige collega en ik heb altijd enorm genoten van onze gesprekken over van alles en nog wat. Charel, jouw tomeloze inzet en behulpzaamheid hebben het onderzoek in dit proefschrift ontzettend vooruitgeholpen. Ze mogen zich daar in Utrecht in de handen wrijven dat ze er zo'n lieve collega bij hebben gekregen. Claudia, ook de vele isolaties, ELISAs, luminexen en ELISPOTS die jij over de jaren hebt uitgevoerd zijn essentieel geweest voor dit proefschrift. Ik weet niet of je het hebt geprobeerd, maar

je hebt me niet de kamer weten uit te jagen. Bedankt voor alle gezelligheid! Richard, we zijn het niet altijd meteen met elkaar eens, maar ondanks ons gekibbel heeft deze takketrol je stiekem toch altijd een fijne collega gevonden. Marieke, het is fantastisch om te zien hoe jij met je daadkracht dingen voor elkaar krijgt en hoe goed je in het team past. Bedankt voor je luisterend oor en al het advies wat je mij de afgelopen tijd hebt gegeven. Michel, wij kenden elkaar ook al van de Immunobiologie groep, het was een plezier om je ook in de TB-groep als collega te hebben, en natuurlijk mijn dank voor alle ritjes naar de NVVI. Saving the best for last; Krista, wij kennen elkaar sinds mijn eerste werkdag en of het nou aan EAE of TB was, we hebben sindsdien altijd superfijn samengewerkt. Ik heb ontzettend veel bewondering voor je toewijding en werkhouding, en ben blij dat we elkaar hebben gevonden in onze liefde voor sushi. Dank je dat jij me nu bij wil staan als paranimf!

Naast de TB-groep wil ik ook alle Parasitologie en Virologie collega's bedanken voor alle gezelligheid (en taarten, koekjes, cakes, chocolade...) in de koffiekamer en tijdens de lunch. Ook mijn andere oud-collega's van de groep Immunobiologie, Nikki, Nicole, Jacqueline, Jordan, Yolanda, Anwar en Bert, bedankt dat ik deel uit heb mogen maken van de groep, ik heb veel geleerd van deze tijd. Sandra, Jeffrey en Ella bedankt voor jullie luisterend oor door de jaren heen. Aan mijn mede-(ex)-BPRC-promotiestudenten, Saskia, Jordon, Annemarie, Astrid, Raissa, Jesse, Kinga, Aafke, Lisanne en Tina, bedankt dat ik met jullie alle perikelen rondom het promoveren kon bespreken tijdens onze PhDinners, gedeelde smart is halve smart. Een extra woordje voor jou Saskia, we hadden op het BPRC een ontzettend goede klik, en ik ben blij dat we deze we ook buiten het werk als een fijne vriendschap hebben kunnen voortzetten. Dank je voor al je steun, tips en wijsheid.

Voor alle studies beschreven in dit proefschrift is er ook "achter de schermen" een enorme berg werk verzet door de mensen van het Animal Science Department. Zonder de inzet van alle dierverzorgers, (para-)veterinair en vele anderen zou dit onderzoek niet mogelijk zijn geweest, waarvoor mijn dank. Francisca, ontzettend bedankt voor alle tijd en moeite die jij hebt gestoken in het opmaken van alle figuren en dit proefschrift en je engelengeduld als ik weer eens een punt/lijn/kopje een halve millimeter verschoven wilde zien.

I would also like to thank all the collaborators that made the research in this thesis possible and all the other wonderful scientists in the field of tuberculosis research that I had the pleasure to meet in the last couple of years. If you are one of them and happen to be reading this; thank you for making me feel welcome, it has truly been amazing to be a part of this community. Carlos, Nacho and Tricia, thank you for hosting me in your labs, I had a wonderful time. Deepak, thank you for agreeing to be part of the thesis- and defense-committee, it has always been a pleasure to meet and chat with you at conferences. Prof. Reinout van Crevel, prof. Victor Rutten en prof. Cecile van Elsen, ik wil ook jullie bedanken voor het beoordelen van mijn proefschrift. Tom, in jouw lab is het allemaal begonnen. Ik ben jou en Annemiek ontzettend



dankbaar voor alles wat jullie mij geleerd hebben, zonder deze basis zou ik niet zover zijn gekomen. Het is een eer om mijn proefschrift tegenover jou te mogen verdedigen. Ook alle (ex-)Tommies, Susan, Louis (goedemiddag!), Susanna, Edwin, Kimberly, Jan, Jolien, Kees, Krista, Simone, Marielle, Mariateresa, Matthias, Krista en meer; bedankt voor het bijdragen aan de fijne start en voortzetting van mijn wetenschappelijke carrière.

Naast fijne collega's heb ik ook het geluk gehad dat ik een kring van geweldige vrienden om mij heen heb. Linda, al is de fysieke afstand tussen ons door de jaren heen alleen maar gegroeid, onze vriendschap is steeds hechter geworden. Ik kan bij jou altijd terecht voor advies en je nuchtere kijk op de zaken heeft mij meermaals geholpen als ik met de handen in het haar zat. Ik ben superblij dat je mijn paranimf wil zijn! Misschien deelt deze life-coach in de toekomst zelfs een toetje met je.

Van soort-van-collega's naar vrienden, Bianca, als er ooit iets positiefs uit een mycoplasma-infectie is gekomen dan is het wel onze vriendschap. Superfijn dat we elkaar gevonden hebben op de gangen van D5 en dat jij en Marten nu onderdeel uitmaken van mijn vaste vriendengroep. Ties, het is ondertussen alweer 16 jaar geleden dat wij tijdens het kringzitten kennis hebben gemaakt. Astrid, wij kennen elkaar niet zò lang, maar ik ben jullie beiden ontzettend dankbaar voor alle keren dat ik welkom was bij jullie thuis, de gespeelde bordspelletjes, pubquizen en alle andere gezellige tijden die ik met jullie beleefd heb. Het waren enorm welkome afleidingen van alle beslommingen die bij het promoveren komen kijken. Floris en Ines, wat ben ik blij dat ik jullie ken en al mijn nerdy interesses met jullie kan delen, dank jullie wel voor alle vrijdagavondetentjes, bordspelletjes en DnD sessies, ook deze hebben mijn promotijd een stuk draaglijker gemaakt. Sander, je positiviteit en enthousiasme waren een inspiratie, bedankt voor alle gezelligheid bij jou en Marijke thuis, tijdens de boulder-sessies en het naborrelen. Tai, je hebt mij weten te bevrienden terwijl ik chagrijnig in een overvolle tram stond nadat alle treinen richting Rotterdam waren uitgevallen, het bewijs van je geweldige karakter. Ik ben ontzettend blij dat onze vriendschap al een immigratie heeft overleefd en ik ga ervanuit dat het ook een tweede zal doorstaan. Samantha, it is an absolute joy to have you in my life. You continue to amaze me with your unique perspective on life and how driven you are when it comes to your goals and ideals. Your cooking is pretty awesome too. Martine, jouw doorzettingsvermogen is indrukwekkend, dank je dat je tijd vrijmaakt in je drukke schema voor onze verkenning van alle Rotterdamse brunch/lunch/borrel gelegenheden en het ventileren van PhD frustraties. Petra, dank je voor al je bemoedigende woorden door de jaren heen. Jos, ik ga al onze nerdy ondernemingen missen als ik in Denemarken zit (het is nog even afwachten of dat ook gaat gelden voor je vele woordspelingen...). Ook aan alle andere Apparaatjes, Maikel, Sijmen, Rowan, Maarten, bedankt voor alle gezelligheid tijdens de vele borrels & feestjes!

Margot, zussepus, je helpt me eraan herinneren dat er meer in het leven is dan werk en wetenschap. We leiden een enorm verschillend leven, maar jij en Marilyn, en nu ook Danny en Aurely, laten mij altijd welkom en geliefd voelen bij jullie thuis. Aan mijn vader en schoonfamilie, bedankt voor alle steun door de jaren heen. Alette, nog een extra bedankje voor jou voor het ontwerpen van de prachtige omslag van dit proefschrift en het regelmatig op de katten passen zodat ik weer een congres kon bezoeken. Helaas kunnen mijn grootouders, opa en oma Nahuis, deze fase van mijn leven niet meer meemaken. In mijn jeugd was hun huis een veilige haven waar ik in alle rust mezelf kon zijn. Ik probeer hun advies om het hoofd koel en de voeten warm te houden nog steeds te volgen, zij het met wisselend succes. Ik hoop dat ze desondanks trots zouden zijn op wat ik heb bereikt.

Natan, naar goed gebruik is deze laatste alinea voor jou. Als mede-wetenschapper begrijp je als geen ander hoe zwaar een promotietraject kan zijn. De afgelopen jaren waren dan ook niet altijd even makkelijk voor ons beiden, maar we hebben ons er samen door heen geslagen. Je ambitie en zelfvertrouwen zijn tijdens mijn promotie een inspiratie voor me geweest. Dank je dat je altijd in mij hebt geloofd, en voor al je steun en liefde. Ik kan niet wachten om samen aan ons volgende avontuur te beginnen.



Curriculum Vitae

Karin Dijkman werd geboren op 5 juli 1987 te Doetinchem. In 2004 behaalde zij haar HAVO diploma aan het ISW Gasthuislaan in 's Gravenzande, en in datzelfde jaar begon zij aan de bacheloropleiding Biologische en Medische Laboratoriumwetenschappen aan de Hogeschool Rotterdam. Tijdens deze opleiding liep zij stage op de afdeling Neuroscience van het ErasmusMC, waar ze de invloed van mutaties in CaMKII op ruimtelijk leren onderzocht in het lab van prof. dr. Ype Elgersma. Haar afstudeeronderzoek, uitgevoerd op het CNCR, Vrije Universiteit, onder supervisie van dr. Edward Jacobs, en profs. drs. Sabine Spijker en Taco de Vries, behelsde het onderzoeken van de rol van een verstoord circadiaans ritme in alcoholverslaving. In 2008 studeerde Karin af aan de Hogeschool Rotterdam en begon zij aan de master Neuroscience aan de Vrije Universiteit. Het jaar daarop heeft zij deze opleiding afgebroken en gaan werken als research analist in de groep van prof. dr. Tom Ottenhoff aan het Leids Universitair Medisch Centrum. Onder supervisie van prof. dr. Annemieke Geluk onderzocht zij daar de immunogeniciteit en beschermende werking van nieuwe TB vaccin-antigenen. In 2013 begon Karin als promotiestudent in de Immunobiologie groep van prof. dr. Bert 't Hart aan het Biomedical Primate Research Centre. Na 2 jaar maakte zij de overstap naar de Tuberculose onderzoeksgroep van dr. Frank Verreck, waar ze onder zijn begeleiding gestart is met haar promotieonderzoek naar immuuncorrelaten van (vaccin-gemedieerde) bescherming in het makaak tuberculose model. Voor dit onderzoek heeft ze diverse prijzen in ontvangst mogen nemen, waaronder de Keystone Symposia Future of Science Fund beurs en de Nederlandse Vereniging voor Immunologie Bright Spark prijs. De resultaten van het promotieonderzoek staan beschreven in dit proefschrift, wat aan de Universiteit van Utrecht verdedigd zal worden met prof. dr. Ronald Bontrop als promotor.

Vanaf april 2020 is Karin werkzaam als post-doctoraal onderzoeker in de groep van dr. Rasmus Mortensen aan het Statens Serum Instituut, waar zij haar onderzoek naar een meer effectievere tuberculose vaccinatie strategie voort zal zetten.

Karin Dijkman was born on the 5th of July 1987 in Doetinchem, the Netherlands. In 2004 she finished her secondary education at ISW Gasthuislaan, 's Gravenzande and started the bachelor Biomedical Laboratory sciences at the Rotterdam University of Applied Sciences. As part of her studies, she performed an internship in the lab of prof. dr. Ype Elgersma at the department of Neuroscience at the Erasmus Medical Centre, where she assessed the influence of mutations in CaMKII on spatial learning. As second internship was carried out at the CNCR at the VU university, under the supervision of dr. Edward Jacobs and profs. drs. Sabine Spijker and Taco de Vries, where she investigated the role of a disrupted circadian rhythm on alcohol addiction. After her graduation in 2008, Karin started a master in Neuroscience at the VU university, but discontinued her studies after a year. That same year, she began working as a research technician in the group of prof. dr. Tom Ottenhoff at the Leiden University, where she assessed the immunogenicity and protective efficacy of candidate TB vaccine antigens under the supervision of prof. dr. Annemieke Geluk. In 2013, she began as a PhD-student in the group of prof. dr. Bert 't Hart at the department of Immunobiology at the Biomedical Primate Research Centre, but transitioned to the Tuberculosis research group of dr. Frank Verreck after 2 years. Under his supervision she started her PhD research on immune correlates of (vaccine-mediated) protection in the macaque model of tuberculosis. This research has been awarded with several prizes, including the Keystone Symposia Future of Science Fund scholarship and the Bright Spark award from the Dutch Society for Immunology. The results of her PhD research are collected in this thesis, which will be defended at the University of Utrecht with prof. dr. Ronald Bontrop as promotor.

From April 2020 onward, Karin will be working as a post-doctoral researcher in the group of dr. Rasmus Mortensen at the Statens Serum Institute, where she continues to work on a more effective tuberculosis vaccination strategy.



List of publications

Disparate Tuberculosis Disease Development in Macaque Species Is Associated With Innate Immunity.

Dijkman K., Vervenne R.A.W., Sombroek C.C., Boot C., Hofman S.O., van Meijgaarden K.E., Ottenhoff T.H.M., Kocken C.H.M., Haanstra K.G., Vierboom M.P.M., Verreck F.A.W.

Frontiers in Immunology. 2019 Nov 1; 10:2479.

Prevention of tuberculosis infection and disease by local BCG in repeatedly exposed rhesus macaques.

Dijkman K., Sombroek C.C., Vervenne R.A.W., Hofman S.O., Boot C., Remarque E.J., Kocken C.H.M., Ottenhoff T.H.M., Kondova I., Khayum M.A., Haanstra K.G., Vierboom M.P.M., Verreck F.A.W. *Nature Medicine* 2019 Feb; 25(2):255-262.

Systemic and pulmonary C1q as biomarker of progressive disease in experimental non-human primate tuberculosis

Dijkman K., Lubbers R., Borggreven N.V., Ottenhoff T.H.M., Joosten S.A., Trouw L.A., Verreck F.A.W. *Scientific Reports* 2020, 10:6290.

Pulmonary vaccination with *M.tuberculosis*-derived MTBVAC induces immune responses correlating with prevention of TB infection

Dijkman K., Aguilo N., Boot C., Hofman S.O., Sombroek C.C., Vervenne R.A.W., Marinova D., Kocken C.H.M., Thole J., Rodríguez E., Vierboom M.P.M., Haanstra K.G., Puentes E., Martin C., Verreck F.A.W. *Manuscript submitted*

Evaluation of heterologous prime-boost vaccination strategies using chimpanzee adenovirus and modified vaccinia virus for TB subunit vaccination in rhesus macaques.

Vierboom, M.P.M, Chenine A.L, Darrah P.A., Vervenne R.A.W., Boot C., Hofman S.O., Sombroek C.C., Dijkman K., Khayum M.A., Stammes M.A., Haanstra K.G., Hoffmann C., Schmitt D., Silvestre N., White A.G., Borish H.J., Seder R.A., Ouaked N., Leung-Theung-Long S., Inchauspé G., Anantha R., Limbach M., Evans T.G., Casimiro D., Lempicki M., Laddy D.J., Bonavia A, Verreck F.A.W. *Manuscript in press at NPJ Vaccines*

Superior trained immunity after mucosal BCG or MTBVAC vaccination

Vierboom M.P.M, Dijkman K., Sombroek C.C., Hofman S.O., Boot C., Vervenne R.A.W., Haanstra K.G., Kocken C.H.M, Verreck F.A.W., Thole J., Rodríguez E., Puentes E., Moorlag S., Andres J.D., van Crevel R., Netea M.G., Aguilo N., Martin C. *Manuscript in preparation*

Complement Component C1q as Serum Biomarker to Detect Active Tuberculosis.

Lubbers R., Sutherland J.S., Goletti D., de Paus R.A., van Moorsel C.H.M., Veltkamp M., Vestjens S.M.T., Bos W.J.W., Petrone L., Del Nonno F., Bajema I.M., Dijkman K., Verreck F.A.W., Walzl G., Gelderman K.A., Groeneveld G.H., Geluk A., Ottenhoff T.H.M., Joosten S.A., Trouw L.A. *Frontiers in Immunology*. 2018 Oct 23; 9:2427.

Exploratory urinary metabolomics of type 1 leprosy reactions.

Mayboroda O.A., van Hooij A., Derks R., van den Eeden S.J.F., Dijkman K., Khadge S., Thapa P., Kunwar C.B., Hagge D.A., Geluk A. *International Journal of Infectious Diseases* 2016 Apr; 45:46-52.

Selective blockade of CD28-mediated T cell costimulation protects rhesus monkeys against acute fatal experimental autoimmune encephalomyelitis.

Haanstra K.G., Dijkman K., Bashir N., Bauer J., Mary C., Poirier N., Baker P., Crossan C.L., Scobie L., 't Hart B.A., Vanhove B. *Journal of Immunology* 2015 Feb 15; 194(4):1454-66.

Experimental Autoimmune Encephalomyelitis in Marmosets.

Jagessar S.A., Dijkman K., Dunham J., 't Hart B.A., Kap Y.S. *Methods in Molecular Biology* 2016; 1304:171-86.

Clonal analysis of the T-cell response to *in vivo* expressed *Mycobacterium tuberculosis* protein Rv2034, using a CD154 expression based T-cell cloning method.

Commandeur S., Coppola M., Dijkman K., Friggen A.H., van Meijgaarden K.E., van den Eeden S.J.F., Wilson L., van der Ploeg-van Schip J.J., Franken K.L., Geluk A., Ottenhoff T.H.M. *PLoS One*. 2014 Jun 6; 9(6):e99203.

The *in vivo* expressed *Mycobacterium tuberculosis* (IVE-TB) antigen Rv2034 induces CD4⁺ T-cells that protect against pulmonary infection in HLA-DR transgenic mice and guinea pigs.

Commandeur S., van den Eeden S.J.F., Dijkman K., Clark S.O., van Meijgaarden K.E., Wilson L., Franken K.L., Williams A., Christensen D., Ottenhoff T.H.M., Geluk A. *Vaccine*. 2014 Jun 17; 32(29):3580-8.

Field-evaluation of a new lateral flow assay for detection of cellular and humoral immunity against *Mycobacterium leprae*.

Bobosha K., Tjon Kon Fat E.M., van den Eeden S.J.F., Bekele Y., van der Ploeg-van Schip J.J., de Dood C.J., Dijkman K., Franken K.L., Wilson L., Aseffa A., Spencer J.S., Ottenhoff T.H.M., Corstjens P.L., Geluk A. *PLoS Neglected Tropical Diseases* 2014 May 8; 8(5):e2845.



Longitudinal immune responses and gene expression profiles in type 1 leprosy reactions.

Geluk A., van Meijgaarden K.E., Wilson L., Bobosha K., van der Ploeg-van Schip J.J., van den Eeden S.J.F., Quinten E., Dijkman K., Franken K.L., Haisma E.M., Haks M.C., van Hees C.L., Ottenhoff T.H.M. *Journal of Clinical Immunology* 2014 Feb; 34(2):245-55.

An unbiased genome-wide *Mycobacterium tuberculosis* gene expression approach to discover antigens targeted by human T cells expressed during pulmonary infection.

Commandeur S., van Meijgaarden K.E., Prins C., Pichugin A.V., Dijkman K., van den Eeden S.J.F., Friggen AH., Franken K.L., Dolganov G., Kramnik I., Schoolnik G.K., Oftung F., Korsvold G.E., Geluk A., Ottenhoff T.H.M. *Journal of Immunology* 2013 Feb 15; 190(4):1659-71.

A multistage-polyepitope vaccine protects against *Mycobacterium tuberculosis* infection in HLA-DR3 transgenic mice.

Geluk A., van den Eeden S.J.F., van Meijgaarden K.E., Dijkman K., Franken K.L., Ottenhoff T.H.M. *Vaccine*. 2012 Dec 14; 30(52):7513-21.

Alternative peptide repertoire of HLA-E reveals a binding motif that is strikingly similar to HLA-A2.

Lampen M.H., Hassan C., Sluijter M., Geluk A., Dijkman K., Tjon J.M., de Ru A.H., van der Burg S.H., van Veelen P.A., van Hall T. *Molecular Immunology* 2013 Jan; 53(1-2):126-31.

ML1419c peptide immunization induces *Mycobacterium leprae*-specific HLA-A*0201-restricted CTL in vivo with potential to kill live mycobacteria.

Geluk A., van den Eeden S.J.F., Dijkman K., Wilson L., Kim H.J., Franken K.L., Spencer J.S., Pessolani M.C., Pereira G.M., Ottenhoff T.H.M. *Journal of Immunology* 2011 Aug 1; 187(3):1393-402.

